

# **The preparation and characterisation of cells and their scaffolds suitable for tissue repair applications**

Thesis submitted for the degree of  
**Doctor of Philosophy**  
in  
**Biochemical Engineering**

by  
**Leda Pittarello**  
BS MSc

The Advanced Centre for Biochemical Engineering  
Department of Biochemical Engineering  
University College London

September 2007

UMI Number: U592557

All rights reserved

INFORMATION TO ALL USERS

The quality of this reproduction is dependent upon the quality of the copy submitted.

In the unlikely event that the author did not send a complete manuscript and there are missing pages, these will be noted. Also, if material had to be removed, a note will indicate the deletion.



UMI U592557

Published by ProQuest LLC 2013. Copyright in the Dissertation held by the Author.  
Microform Edition © ProQuest LLC.

All rights reserved. This work is protected against  
unauthorized copying under Title 17, United States Code.



ProQuest LLC  
789 East Eisenhower Parkway  
P.O. Box 1346  
Ann Arbor, MI 48106-1346

To my parents, Maria and Adelmo

## Acknowledgments

First of all I would like to thank Prof. Anthony Hollander, who put trust in me and instilled me the idea of a PhD for the very first time.

I would like to thank also my supervisor Frank Baganz for his kind support and help, and my advisor Chris Mason for his encouragement during the writing of this thesis. I certainly could not have brought this hard work to completion without their input and kind help.

I wish also to thank Prof. Nigel Titchener-Hooker and Prof. Gary Lye for their special help in making all of this possible; Alethea Tabor for her comments on my data; Prof. Peter Dunnill for his extraordinary guidance during the first year of my PhD and for taking care of reviewing my data and part of this thesis. Special thanks also to Prof. Mike Hoare for giving me the possibility to work and study in the Department of Biochemical Engineering during the three years of my experimental work.

My thanks also to my colleagues for the great time I had in working with them in the lab: Julia Markusen and Emily Culme-Seymour, for the great collaboration on the alginate derivatisation work, and Spyros Gerontas for being always happy to help and discuss about our works. Many thanks also to my friend Anna Cariboni, who helped me with the staining and the photographs of my samples during the last stages of my experimental work.

I want to express my gratitude also to Prof. Tom Byers, who taught me most of all to “make no little plans”. Thanks to him I will always make of my aspirations true possibilities.

I thank Elena and Joseph as well as Samuela, Marta and Jim, Roberta, Anna, Kuna and Adrian for real friendship, and Duncan for being always so much fun and such a good mentor, anytime I need. I thank also my other best friends, who I have left in Italy a while ago, but always remain by my side: the “Pink Ladies” Dommi, Silvia and Stefania.

I thank my ex-flatmates Fabio Sormani, John Baker and Bruno Garcia for their incredible patience and for cheering me up during the most difficult moments of this journey.

Last but not least, I wish to thank my parents Maria and Adelmo, to whom I dedicate this work, for accepting my choice of doing a PhD and bearing with both my physical and psychological absence during these past years. To them as well as to my sister Sara and my lovely niece Ludovica (and to Brian!) I will always feel close even being far away.

I guess I cannot avoid thanking also the one and only person that was responsible for my moving to London five years ago – with all that much this has meant for both my career and personal life. Despite all, he opened up my view on the world and extended my horizon.

This PhD has been supported by the Department of Biochemical Engineering and the Engineering and Physical Sciences Research Council (EPSRC), and their support is gratefully acknowledged.



## Abstract

In this research, a tissue engineering approach was investigated for the fabrication of homogeneous polymer/cells scaffolds suitable for applications in the clinic, in particular for the treatment of coronary disease and atherosclerosis.

Sodium alginate chemically modified with an RGD-containing peptide promoting cell attachment was chosen as the natural polymer for the preparation of matrix/cells constructs. Several conditions were investigated to optimise the derivatisation of the biomaterial, and no major dissimilarities were identified among alginates with different guluronic/mannuronic acid compositions and viscosities during the derivatisation process. Successful incorporation of the GRGDY-pentapeptide onto the alginate was achieved. Amino acid analysis, which allowed a reliable quantification of the degree of peptide attached, demonstrated that the complete pentapeptidic sequence was present in the alginate after completion of the derivatisation procedure. However, a significant loss of the peptide's final tyrosine residue was consistently observed during derivatisation.

Studies were also performed using multipotent fibroblast-like plastic-adherent cells recovered from frozen bone marrow samples of adult patients, here defined as human "mesenchymal stem cells" (hMSCs). Prior to the cell immobilisation in the alginate matrix, the optimal conditions for cell expansion in monolayer culture were identified. Cell samples were assessed according to their percent viability at each expansion passage, doubling time, cell growth rate and specific glucose consumption rate. Overall, the highest cell growth kinetics, highest cell viabilities and lowest doubling times were observed for the combined use of serum-/bFGF-supplemented low-glucose DMEM medium and non-coated culture vessels in a 21% dissolved oxygen tension atmosphere. hMSCs expanded for four subsequent passages under these monolayer conditions proved to retain their undifferentiated state and their ability to differentiate toward multiple phenotypes.

Finally, alginate/cells beads were prepared and maintained in the optimal culture conditions identified in the monolayer studies. Constructs prepared with either hMSCs or human foreskin fibroblasts in either unmodified alginate or alginate coupled with the GRGDY-pentapeptide were analysed. After immobilisation, both cell types failed to adhere to the matrix and to acquire their characteristic elongated, spindle-shaped morphology. Lack of cell proliferation and

cell death were also observed over time for both cell types in constructs prepared with either the unmodified or the derivatised alginates.

Further studies are required to understand whether tyrosine loss is responsible for the lack of matrix-cells interactions, and to develop strategies to prevent this phenomenon.

## Table of contents

<b>Abstract</b>	<b>4</b>
Table of contents	6
<b>List of Figures</b>	<b>11</b>
<b>List of Tables</b>	<b>19</b>
<b>1 Introduction</b>	<b>23</b>
1.1 Tissue Engineering	23
1.1.1 Tissue Engineering: a new discipline	23
1.1.2 Different approaches in Regenerative Medicine	24
1.1.3 The development and the current status of Tissue Engineering	26
1.1.4 The emerging industry of Tissue Engineering	28
1.1.5 The challenges and the way forward	29
1.1.6 Vascular tissue engineering for the treatment of atherosclerosis and coronary artery disease	31
1.1.6.1 The artery wall: anatomy and function	32
1.1.6.2 Ideal mechanical and haemodynamic properties of vascular grafts	34
1.1.6.3 Tissue engineering of arterial vessel substitutes	35
1.2 Selection of a cell source for a bio-engineered tissue substitute	38
1.2.1 Autologous cells	38
1.2.2 Allogeneic cells	39
1.2.3 Xenogeneic cells	39
1.2.4 Stem cells	40
1.2.4.1 Stem cells: an alternative cell source for vascular grafts	40
1.2.4.2 Stem cells: a brief history	42
1.2.4.3 The unique properties of stem cells	42
1.2.4.4 Human stem cells and cell-based therapies	42
1.2.4.5 Obstacles limiting the promise of stem cell-based therapies	44
1.2.4.6 Embryonic and adult mesenchymal stem cells	45
1.2.4.7 Bone marrow-derived MSCs	46
1.3 Selection of a three-dimensional matrix suitable for the preparation of an engineered tissue	47
1.3.1 Synthetic materials	48
1.3.2 Natural polymers	49
1.3.3 Activation of inert supports	49
1.3.4 Sodium alginate	50
1.3.4.1 Quality of alginate	52
1.3.4.2 Alginate's biomedical and biotechnology applications	53
1.4 The role of bioactive molecules and oxygen tension in the in vitro environment	55
1.4.1 Growth medium	55
1.4.2 Serum	57
1.4.3 Growth factors	59
1.4.4 Insoluble ECM adhesion molecules	60
1.4.5 The role of oxygen in cell culture	61
1.5 The goals of the present thesis	63
<b>2. Materials and Methods</b>	<b>64</b>
2.1 Human Mesenchymal Stem Cell culture in tissue culture vessels	64
2.1.1 Isolation of human mesenchymal stem cells from frozen bone marrow samples	64
2.1.2 <i>In vitro</i> culture of human Mesenchymal Stem Cells	65

2.1.3	Cell expansion in tissue culture vessels .....	66
2.1.4	Creation of a working cell bank .....	67
2.1.5	Protocols of hMSCs culture using different basal media, different serum and fibroblast growth factor concentrations, different coatings and oxygen tensions .....	68
2.1.5.1	Basal growth medium .....	68
2.1.5.2	Serum supplementation.....	70
2.1.5.2.1	Fetal Bovine Serum concentration.....	70
2.1.5.2.2	Serum-free media experiment.....	70
2.1.5.2.3	Surface coatings of tissue culture vessels .....	72
2.1.5.2.4	Human recombinant Fibroblast Growth Factor supplementation.....	73
2.1.5.5	Dissolved oxygen tension .....	74
2.2	An alternative cell source: cell passaging protocol in tissue culture vessels for human Fibroblasts .....	74
2.3	Preparation of the alginate scaffold .....	75
2.3.1	Reconstitution of the sodium alginate matrix .....	77
2.3.2	Alginate derivatisation with GRGDY pentapeptide .....	77
2.3.2.1	Concentration of reactants .....	80
2.3.2.2	Dialysis .....	81
2.3.2.3	Lyophilisation .....	82
2.3.2.4	Alginate concentration with polyethylene Glycol (PEG) solution .....	83
2.3.2.5	Reconstitution of lyophilised alginate-GRGDY .....	83
2.4	Characterisation of the alginate matrix .....	84
2.4.1	Quantification of amino acids in the alginate-GRGDY matrix .....	84
2.4.2	Nuclear Magnetic Resonance ( <sup>1</sup> H NMR) .....	85
2.4.3	Mass spectrometry (MS).....	87
2.5	Preparation of alginate/cells constructs .....	88
2.5.1	Preparation of the cell suspension for mixing with the alginate solution.....	88
2.5.2	Cross-linking solution.....	89
2.5.3	Preparation of alginate/cells beads.....	89
2.5.4	Preparation of alginate/cells disks .....	90
2.5.5	Release of cells from matrix using trisodium citrate solution .....	92
2.6	Methods of cells and matrix/cells constructs characterisation .....	93
2.6.1	Light microscopy for visualisation of cell morphology and cell growth.....	93
2.6.2	Cell count with haemocytometer .....	93
2.6.3	Cell viability with trypan blue .....	94
2.6.4	Calculation of cell growth rates .....	95
2.6.5	Nutrient and metabolite analysis with Nova Bioprofiler .....	98
2.6.5.1	Glucose and lactate biosensors in the Nova Biomedical BioProfiler .....	98
2.6.5.2	The glucose sensor and determination of glucose consumption.....	98
2.6.5.3	Lactate production .....	100
2.6.6	Qualitative analysis of cell viability with fluorescence microscopy .....	101
2.6.7	hMSCs multipotentiality with hMSCs Functional Identification Kit.....	102
2.6.7.1	Lineage-specific differentiation.....	103
2.6.7.2	Cryosectioning of cell pellets for chondrogenesis .....	104
2.6.7.3	Immunocytochemistry .....	105
2.6.8	Cell apoptosis: Guava Nexin assay.....	106
2.6.9	Statistical analysis.....	107
2.7	MTT (3-(4,5-dimethylthiazol-2-yl)-2,5-diphenyltetrazolium bromide) assay .....	108
2.7.1	Cell standard curve .....	109

2.7.2	Cell standard curve for hMSCs immobilised in three-dimensional alginate beads .....	111
2.7.3	Determination of cell concentration in alginate beads.....	112
2.7.4	MTT protocol.....	112
2.7.4.1	MTT incubation .....	112
2.7.4.2	Solubilisation of the formazan product.....	113
2.7.4.3	Analysis of data.....	114
2.7.5	Interference of the three-dimensional alginate matrix with MTT absorbance.....	115
2.7.6	Determination of hMSCs proliferation within alginate beads .....	116
2.7.7	Interference of alginate in solution with MTT absorbance.....	116
<b>3. The derivatisation and characterisation of the alginate derived-polymer for tissue engineering applications .....</b>		<b>118</b>
3.1	Introduction .....	118
3.2	Derivatisation of the alginate with the GRGDY pentapeptide .....	119
3.2.1	Effect of preservation of alginate-derived polymer with respect to biochemistry.....	123
3.2.2	The coupling reaction .....	123
3.2.2.1	Alginate formulation.....	124
3.2.2.2	EDC and sulfo-NHS concentration employed in the coupling reaction.....	126
3.2.2.3	Use of manufacturer-prepared EDC solution .....	126
3.2.2.4	Peptide source and concentration tested for the alginate derivatisation .....	128
3.2.3	Dialysis step as purification method of the alginate-GRGDY.....	129
3.2.4	Concentration of derivatised alginate .....	131
3.2.4.1	Lyophilisation .....	131
3.2.4.2	Polyethylene glycol (PEG) concentration step .....	132
3.2.5	Freezing/no freezing step.....	134
3.2.6	Sterility of alginate-GRGDY .....	134
3.2.7	Reconstitution of the alginate-GRGDY.....	135
3.2.8	CaCl <sub>2</sub> solution as cross-linking agent .....	135
3.3	Characterisation of the alginate matrix .....	136
3.3.1	Characterisation of the alginate-GRGDY by amino acid analysis .....	136
3.3.2	Characterisation of the alginate-GRGDY by nuclear magnetic resonance .....	142
3.3.3	Nuclear magnetic resonance (NMR) and mass spectroscopy (MS) for the analysis of the GRGDY peptide before use in the derivatisation of the alginate matrix.....	149
3.4	Conclusions and discussion .....	153
<b>4. Characterisation of human mesenchymal stem cells (hMSCs) growth kinetics and metabolic activity in monolayer culture.....</b>		<b>156</b>
4.1	Growth of human mesenchymal stem cells (hMSCs) in tissue culture plastic .....	156
4.2	Single cell cloning by serial dilution .....	158
4.3	Influence of basal growth medium and Mesenchymal Stem Cell Stimulatory Supplement on hMSCs monolayer culture: preliminary conclusions .....	159
4.4	Studies on Fetal Bovine Serum .....	163
4.4.1	Effects of Fetal Bovine Serum (FBS) on hMSCs growth and metabolism in monolayer culture .....	164
4.4.2	Testing hMSCs growth under different serum-free media conditions.....	169
4.5	Influence of Fetal Bovine Serum (FBS) and basic Fibroblast Growth Factor (bFGF) on hMSCs proliferation and metabolic activity in monolayer culture .....	174
4.6	Growth kinetics and metabolic activity of hMSCs maintained in different culture vessel coatings under different serum conditions .....	181

4.7 Multipotentiality of human adult mesenchymal stem cells expanded in monolayer culture .....	192
4.8 Dissolved oxygen tension (DOT) as an important parameter for hMSCs in vitro expansion .....	199
4.8.1 Studies investigating hMSCs' proliferation and metabolic activity under different dissolved oxygen tensions.....	200
4.8.2 Combined effects of dissolved oxygen tension (DOT) and Fetal Bovine Serum (FBS) on hMSCs proliferation and metabolism .....	208
4.8.3 Combined effects of dissolved oxygen tension (DOT) and basic fibroblast growth factor (bFGF) on hMSCs proliferation and metabolism .....	216
4.8.4 Preparation of hMSCs working cell banks at 21% and 1% oxygen levels.....	222
4.9 Conclusions on MSCs monolayer culture studies .....	224
<b>5. Characterisation of alginate/cells constructs.....</b>	<b>227</b>
5.1 Alginate-GRGDY as scaffold for cell growth .....	227
5.2 Culture and characterisation of cells in alginate constructs .....	228
5.3 High and low G-content and high and low viscosity .....	229
alginates for the fabrication of hMSCs-containing beads.....	229
5.4 Fabrication of alginate-GRGDY/hMSCs beads using .....	233
alginate modified according to different derivatisation .....	233
procedures .....	233
5.5 Alginate-GRGDY/fibroblasts beads .....	237
5.6 Additional studies on alginate-GRGDY for the .....	242
immobilisation of fibroblasts .....	242
5.7 HMSCs immobilised in alginate-GRGDY disks .....	244
5.8 MTT assay: analysis of cell proliferation within alginate matrices .....	251
5.8.1 Comparison of cell numbers derived from MTT absorbance readings and from haemocytometer.....	252
5.8.2 MTT cell proliferation assay on hMSCs expanded in monolayer condition in the presence of increasing concentrations of alginate in solution.....	253
5.8.3 MTT cell proliferation assay on hMSCs expanded in monolayer culture in the presence of an increasing number of cell-free alginate beads .....	255
5.8.3.1 MTT cell proliferation assay on hMSCs immobilised in alginate beads.....	257
5.9 Conclusions and discussion .....	258
<b>6. Conclusions.....</b>	<b>261</b>
6.1 The goal of this thesis .....	261
6.2 The alginate biopolymer .....	261
6.2.1 Derivatisation of the alginate polymer.....	263
6.2.2 Alginate-GRGDY characterisation.....	264
6.3 Characterisation of human mesenchymal stem cells expanded in monolayer culture .....	266
6.3.1 Basal growth medium formulation .....	268
6.3.2 Different coating conditions for the culture vessels .....	270
6.3.3 Dissolved oxygen tension (DOT) .....	271
6.3.4 Optimal culture conditions identified for hMSCs growth in monolayer .....	272
6.4 Matrix/cells constructs .....	272
6.5 Conclusions .....	277
<b>7 Recommendations for future work .....</b>	<b>278</b>
7.1 Additional parameters to be considered for optimisation of the alginate derivatisation procedure .....	278
7.2 human Mesenchymal Stem Cells (hMSCs) characterisation .....	280

7.3 Strategies to be considered for the fabrication of functional alginate/cells constructs .....	282
<b>8. References .....</b>	<b>285</b>

## List of Figures

<b>Figure 1.1:</b> UNOS organ transplant statistics for 1990 to 1999	24
<b>Figure 1.2:</b> Different approaches in Tissue Engineering	26
<b>Figure 1.3:</b> Current research projects in tissue engineering [modified from Vacanti, 2001]	28
<b>Figure 1.4:</b> Typical location for a coronary artery bypass graft	32
<b>Figure 1.5:</b> The composition of a medium-size mature muscular artery in side view and cross section view	33
<b>Figure 1.6:</b> Scheme showing the tissues/organs constituting the potent targets for tissue regeneration by stem cell-based therapies	43
<b>Figure 1.7:</b> Examples of some materials used in bioengineered scaffolds [adapted from Sarraf <i>et al.</i> , 2002]	48
<b>Figure 1.8:</b> Chemical block structures of alginate	51
<b>Figure 1.9:</b> Cross-linking of alginate G-blocks with calcium	52
<b>Figure 2.1:</b> Schematic representation of the standard alginate derivatisation procedure for the coupling of the GRGDY pentapeptide to sodium alginate	76
<b>Fig. 2.2:</b> Overall reaction for the alginate derivatisation with GRGDY pentapeptide	79
<b>Figure 2.3:</b> Schematic flow diagram of amino acid analyser, highlighting the ion-exchange chromatography and the ninhydrin detection	85
<b>Figure 2.4:</b> Schematic representation of the fabrication of matrix/cells beads	91



<b>Figure 2.5:</b> Schematic representation of the fabrication of matrix/cells disks	92
<b>Fig. 2.6:</b> Growth phases of cells in culture [Palsson and Bhatia, 2004]	96
<b>Figure 2.7:</b> Schematic representation of the glucose membrane in the Nova Biomedical Bioprofile 400 Analyzer	99
<b>Figure 2.8:</b> Molecular structures of the MTT dye precursor and the formazan product formed upon reduction	109
<b>Figure 3.1:</b> Flow diagram representing a schematic of the alginate derivatisation with the GRGDY peptide	121
<b>Figure 3.2:</b> The mechanism of the reaction of alginate with the GRGDY peptide	127
<b>Figure 3.3:</b> Schematic of the dialysis step for the alginate-GRGDY purification using Slide-A-Lyzer Dialysis Cassettes with 3.5 kDa MWCO membranes	130
<b>Figure 3.4:</b> The weight of the dialysis cassette as monitored throughout the re-concentration of the alginate-GRGDY with the PEG concentrating solution	133
<b>Figure 3.5:</b> Chemical formula of the GRGDY peptide sequence	137
<b>Fig.3.6:</b> 1-Dimensional nuclear $^1\text{H}$ NMR spectrum for Pronova non-derivatised SLG100 alginate	144
<b>Figure 3.7:</b> 1-Dimensional nuclear $^1\text{H}$ NMR spectrum obtained for the derivatised (9X reactants, 1X peptide) SLM100 alginate	146
<b>Fig.3.8:</b> NMR spectrum recorded for Pronova SLG100 alginate coupled with 9X reactants (EDC and sulfo-NHS) and 10X GRGDY peptide	148

<b>Fig. 3.9:</b> 1-Dimensional nuclear $^1\text{H}$ magnetic resonance spectrum of the GRGDY peptide (Albachem)	151
<b>Fig. 3.10:</b> Mass spectrum of GRGDY peptide (Albachem)	152
<b>Fig. 4.1:</b> Cell growth for p4 hMSCs cultured in either MesenCult or DMEM media	161
<b>Fig. 4.2:</b> Effects of Fetal Bovine Serum on cell proliferation	165
<b>Fig. 4.3:</b> Glucose consumption and lactate production for <i>in vitro</i> expanded hMSCs maintained under different Fetal Bovine Serum culture conditions	168
<b>Fig. 4.4:</b> Impact of different Fetal Bovine Serum concentrations on hMSCs glucose consumption rate during <i>in vitro</i> expansion in tissue culture plates	168
<b>Fig. 4.5:</b> Morphology of hMSCs expanded in Knockout optimised D-MEM medium (Gibco).	173
<b>Fig. 4.6:</b> Morphology of hMSCs expanded in Ex-cell 302 CHO serum-free medium (SAFC Biosciences).	173
<b>Fig. 4.7:</b> Effects of Fetal Bovine Serum (FBS) and basic Fibroblast Growth Factor (bFGF) on hMSCs proliferative capacity	176
<b>Fig. 4.8</b> Influence of bFGF-supplementation on hMSCs metabolic activity	179
<b>Fig. 4.9:</b> Impact of bFGF-supplementation on hMSCs glucose consumption rate	179
<b>Fig. 4.10:</b> 10% serum-supplemented hMSCs expanded in non-coated plates, fibronectin-coated plates or matrigel-coated plates	182

<b>Fig. 4.11:</b> 2% serum-supplemented hMSCs cultured in non-coated plates, fibronectin-coated plates or matrigel-coated plates	183
<b>Fig. 4.12:</b> Serum-free hMSCs cultured in non-coated plates, fibronectin-coated plates or matrigel-coated plates	183
<b>Fig. 4.13:</b> Morphology of hMSCs expanded in non-coated plates in medium supplemented with 10% FBS.	186
<b>Fig. 4.14:</b> Morphology of hMSCs expanded in fibronectin-coated plates in medium supplemented with 10% FBS.	186
<b>Fig. 4.15:</b> Morphology of hMSCs expanded in Matrigel-coated plates in 10% FBS-supplemented medium.	187
<b>Fig. 4.16:</b> Effects of coatings on hMSCs metabolic activity (10% serum condition)	189
<b>Fig. 4.17:</b> Effects of coatings on hMSCs metabolic activity (2% serum condition)	190
<b>Fig. 4.18:</b> Effects of coatings on hMSCs metabolic activity (serum-free condition)	190
<b>Fig. 4.19:</b> Impact of coatings on 10% serum-supplemented hMSCs glucose consumption rate	191
<b>Fig. 4.20:</b> Effects of coatings on 2% serum-supplemented hMSCs glucose consumption rate	191
<b>Fig. 4.21:</b> Effects of coatings on serum-free hMSCs glucose consumption rate	192
<b>Fig. 4.22:</b> Adipogenic differentiation of bone marrow-derived hMSCs	194-195

<b>Fig. 4.23:</b> Mouse anti-human Osteocalcin staining for hMSCs induced for 21 days with osteogenic medium	196-197
<b>Fig. 4.24:</b> Goat anti-human Aggrecan staining for hMSCs induced for 21 days with chondrogenic supplement	198-199
<b>Fig. 4.25:</b> Effects of dissolved oxygen tension on hMSCs proliferation	202
<b>Fig. 4.26:</b> Impact of dissolved oxygen tension on hMSCs proliferation	202
<b>Fig. 4.27:</b> Morphology of hMSCs expanded in the traditional 21% Dissolved Oxygen Tension.	205
<b>Fig. 4.28:</b> Morphology of hMSCs expanded in 2% Dissolved Oxygen Tension condition.	206
<b>Fig. 4.29:</b> Impact of dissolved oxygen tension on hMSCs metabolic activity	206
<b>Fig. 4.30:</b> Effects of dissolved oxygen tension on hMSCs metabolic activity	207
<b>Fig. 4.31:</b> Effects of dissolved oxygen tension on hMSCs glucose consumption rate	207
<b>Fig. 4.32:</b> Effects of dissolved oxygen tension on hMSCs glucose consumption rate	208
<b>Fig. 4.33:</b> Effects of dissolved oxygen tension (DOT) on hMSCs proliferation in serum-free and 10% serum culture conditions	209
<b>Fig. 4.34:</b> Cell metabolic activity measured by means of the MTT Cell Proliferation assay	211

**Fig. 4.35:** Photographs taken at day 6 of culture for cells maintained at 21% DOT, with or without serum. The photographs were taken with the phase contrast microscope (**A** and **B**) and with the confocal microscopes (**C** and **D**) after treatment with the calcein AM/ethyidium homodimer dyes. 212

**Fig. 4.36:** Photographs taken at day 6 of culture for cells maintained at 1% DOT, with or without serum. The photographs were taken with the phase contrast microscope (**A** and **B**) and with the confocal microscopes (**C** and **D**) after treatment with the calcein AM/ethyidium homodimer dyes. 213

**Fig. 4.37:** Effects of dissolved oxygen tension on hMSCs metabolic activity 215

**Fig. 4.38:** Effects of dissolved oxygen tension on hMSCs metabolic activity 215

**Fig. 4.39:** Effects of dissolved oxygen tension and FBS-supplementation on hMSCs glucose consumption rate 216

**Fig. 4.40:** Growth kinetics curves obtained for hMSCs maintained under different dissolved oxygen tension (DOT) and bFGF conditions 217

**Fig. 4.41:** Effects of dissolved oxygen tension and bFGF on hMSCs metabolic activity 221

**Fig. 4.42:** Effects of dissolved oxygen tension and bFGF on hMSCs metabolic activity 221

**Fig. 4.43:** Effects of dissolved oxygen tension and bFGF-supplementation on hMSCs glucose consumption rate 222

**Fig. 5.1 A and B:** hMSCs immobilised within SLG100 alginate-GRGDY beads. The alginate was derivatised with 9X reactants and 1X peptide 231

**Fig. 5.2:** hMSCs immobilised within SLG100 alginate-GRGDY beads. The alginate was derivatised with 9X reactants and 10X peptide 236

**Fig. 5.3:** Fluorescence photograph obtained for hMSCs immobilised within SLG100 alginate-GRGDY beads stained with calcein AM/ethidium homodimer. The alginate was derivatised with 9X reactants and 10X peptide prior to the beads preparation

237

**Fig. 5.4 A and B:** Human foreskin fibroblasts immobilised within SLG100 alginate-GRGDY beads. The alginate was derivatised with 9X reactants and 10X GRGDY peptide

241

**Fig. 5.5:** Human foreskin fibroblasts immobilised in SLG100, 9X reactants, 32X GRGDY peptide alginate-GRGDY

243

**Fig. 5.6:** Fluorescence photograph obtained for human foreskin fibroblasts immobilised within SLG100 alginate-GRGDY beads stained with calcein AM/ethidium homodimer. The alginate was derivatised with 9X reactants and 32X peptide prior to the beads preparation

244

**Fig. 5.7:** Schematic of the cross-linking procedures for the preparation of alginate/cells beads (A) and layers (B)

246

**Fig 5.8 A, B and C:** hMSCs immobilised within alginate-GRGDY beads. The alginate polymer was coupled with 9X EDC and sulfo-NHS and 32X GRGDY peptide

249-250

**Fig 5.9 A and B:** hMSCs seeded on top of alginate-GRGDY disks. The alginate polymer was coupled with 9X EDC and sulfo-NHS and 32X GRGDY peptide

250-251

**Fig. 5.10:** MTT absorbance values at 600 nm detected from human MSCs (p8) cultured in monolayer

253

**Fig. 5.11:** MTT absorbance values obtained for hMSCs in microwell after 10 days in culture in the presence of an increasing concentration of alginate in solution

254

**Fig. 5.12:** MTT absorbance values measured at 600 nm for hMSCs expanded in monolayer condition in the presence of an increasing number of non-derivatised alginate beads 256

**Fig. 5.13:** MTT absorbance readings measured at 4 different time-points for an increasing number of alginate/hMSCs beads (average  $4 \times 10^3$  cells/bead) 257

## List of Tables

<b>Table 1.1:</b> Major components found in tissue-culture media [Palsson and Bhatia, 2004]	56
<b>Table 1.2:</b> Major constituents of serum [Palsson and Bhatia, 2004]	58
<b>Table 2.1:</b> Serum-free media investigated for the expansion of hMSCs in tissue culture flasks	71
<b>Table 2.2:</b> Ratios of the reactants concentrations as used by Rowley (1998) and in the present research for the alginate derivatisation procedure	81
<b>Table 2.3:</b> Serial dilution of the cell suspension for the MTT cell standard curve	110
<b>Table 2.4:</b> Serial dilution of alginate/cells beads for the MTT assay standard curve	111
<b>Table 2.5:</b> Volume of cell suspension, cell concentration, number of beads and volume of DPBSG during the MTT study	115
<b>Table 2.6:</b> Serial dilution for the testing the interference of the alginate in solution with MTT absorbance	117
<b>Table 3.1:</b> Derivatisation procedures performed in the present study for the incorporation of the GRGDY peptide in the alginate matrix	122
<b>Table 3.2:</b> Products specifications for Pronova SLG100, SLG20, SLM100 and SLM20 alginates	125
<b>Table 3.3:</b> Amino acid analysis data from alginate-GRGDY samples	138



**Table 4.1:** Population Doubling Level (PDL), Doubling Time (Td) and cell growth rate ( $\mu$ ) values calculated for the hMSCs expanded in either MesenCult medium or low-glucose DMEM 161

**Table 4.2:** Population Doubling Level (PDL), Doubling Time (Td) and cell growth rate ( $\mu$ ) values calculated for hMSCs expanded in different serum conditions 166

**Table 4.3:** Percent cell viability values obtained for hMSCs cultured in four different serum conditions 167

**Table 4.4:** Serum-free media investigated for the expansion of hMSCs in tissue culture flasks 170

**Table 4.5:** Population Doubling Level (PDL), Doubling Time (Td) and cell growth rate ( $\mu$ ) values calculated for hMSCs expanded in different FBS and bFGF conditions 177

**Table 4.6:** Percent cell viability values obtained for hMSCs expanded in the absence of bFGF under different serum conditions 178

**Table 4.7:** Population Doubling Level (PDL), Doubling Time (Td) and cell growth rate ( $\mu$ ) values calculated for hMSCs expanded in different coating conditions 185

**Table 4.8:** Percent cell viability values obtained for hMSCs expanded in different coating conditions 188

**Table 4.9:** Terminology adopted in this research to define the different oxygen levels investigated during in vitro expansion of hMSCs in monolayer culture 200

**Table 4.10:** Population Doubling Level (PDL), Doubling Time (Td) and cell growth rate ( $\mu$ ) values obtained for hMSCs expanded in different dissolved oxygen tension conditions 203

<b>Table 4.11:</b> Population Doubling Level (PDL), Doubling Time (Td) and cell growth rate ( $\mu$ ) values calculated for cells expanded in different oxygen conditions	203
<b>Table 4.12:</b> Percent cell viability values calculated for cells cultured in different dissolved oxygen tension conditions	204
<b>Table 4.13:</b> Percent cell viability values calculated for hMSCs cultured in different dissolved oxygen tension conditions	205
<b>Table 4.14:</b> Cell viability values calculated for hMSCs cultured in different oxygen and serum conditions	210
<b>Table 4.15:</b> Population Doubling Level (PDL), Doubling Time (Td) and cell growth rate ( $\mu$ ) values calculated for hMSCs expanded in different oxygen and serum conditions	214
<b>Table 4.16:</b> Percent cell viability values calculated for hMSCs cultured in different oxygen and bFGF conditions	218
<b>Table 4.17:</b> Percent cell viability values calculated for hMSCs cultured in different oxygen and bFGF conditions	219
<b>Table 4.18:</b> Influence of dissolved oxygen tension and bFGF-supplementation on hMSCs viable, early apoptotic and late apoptotic cell populations	220
<b>Table 5.1:</b> Percent cell viability and cell concentration values obtained for hMSCs immobilised in non-derivatised alginate (control beads) and alginates modified with the GRGDY peptide. All alginates were coupled with 9X sulfo-NHS and EDC and with 10X peptide concentrations	235
<b>Table 5.2:</b> Percent cell viability and cell concentration values obtained for human foreskin fibroblasts immobilised in non-derivatised alginate (control beads) and in	

alginate modified with the GRGDY peptide according to the standard derivatisation procedure. 9X sulfo-NHS and EDC and 10X peptide were used for the coupling reaction

240

# 1 Introduction

## 1.1 Tissue Engineering

### 1.1.1 Tissue Engineering: a new discipline

The loss or failure of an organ or tissue is one of the most frequent, devastating, and costly problems in healthcare [Langer and Vacanti, 1993]. Until very recently, most scientists and clinicians believed that damaged or diseased human tissue could only be replaced by donor transplants or with totally artificial parts. The main drawback of organ transplantation is that the need for donor organs far exceeds the supply. The need for substitutes to replace or repair tissues or organs because of disease, trauma, or congenital problems is indeed overwhelming, and the organ shortages for transplantation continue to worsen [Nasseri *et al.*, 2001; Tie, 2001] (figure 1.1) [UNOS, 2001]. This trend persists, as demonstrated by the fact that, in the United States alone, approximately only 23,500 people received transplants from July 2000 to July 2001, while approximately 80,000 registrations were left on the waiting list for an organ during the same period [<http://ustransplant.org>., 2002; UNOS, 2002 and UNOS, 2001].

The necessity of alternative therapies is illustrated by this ever-widening supply and demand mismatch of organs and tissues for transplantation [2000 Annual Report of the US Scientific Registry for Transplant Recipients and the Organ Procurement and Transplantation Network: Transplantation Data: 1990-1999.]. The overwhelming organ shortage has resulted in new surgical techniques, such as transplanting whole organs (e.g. kidneys) from living, related donors and splitting adult organs for transplant (e.g. a part of a liver or a lung from a parent to a child). Despite excellent results with these transplant techniques, the problem of donor scarcity remains. Alternative current treatment modalities include surgical reconstruction, use of mechanical devices, or supplementation of metabolic products. While these strategies incorporate significant advances in the field of medicine, they have a number of inherent limitations, replacing the diseased organ or tissue only imperfectly, or displaying lack of compliance of the artificial prostheses to allow growth and/or requiring immunosuppressive treatment.

A new multidisciplinary research field, tissue engineering, aims to provide vital tissues with the abilities to function, grow, repair and remodel. Langer and Vacanti (1993) defined tissue engineering as “an interdisciplinary field that applies the principles and methods of engineering and the life sciences toward the development of biological substitutes that restore, maintain, or improve tissue function” [Langer and Vacanti, 1993]. This new promising solution to tissue loss requires an interdisciplinary cooperation among developmental and cellular molecular biologists, engineers, material scientists, and physicians.

The hope is that tissue-engineered products deliver superior treatments, improving the speed, extent and duration of healing compared to conventional treatments. The most important expected outcomes are enhanced quality of life of patients and the ability to overcome organ shortage for transplantation in the long run.

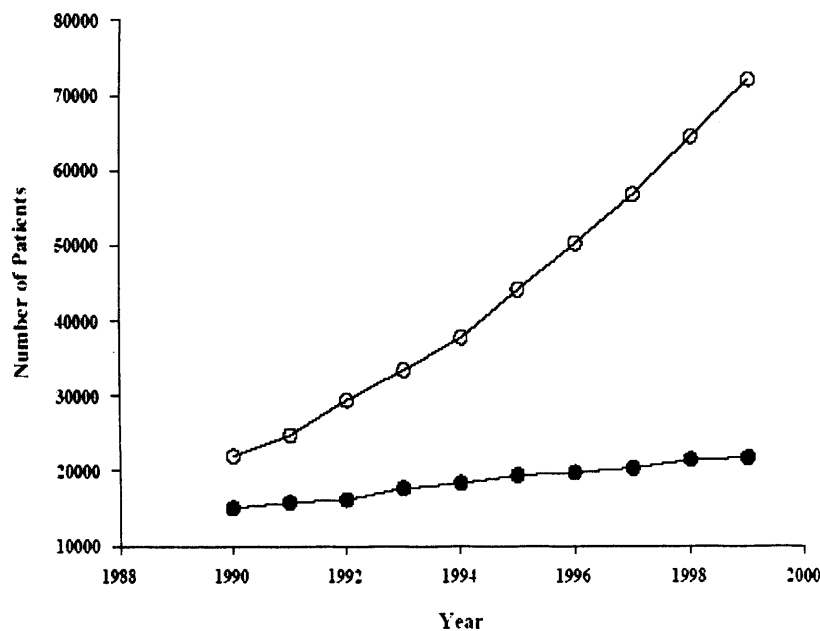


**Figure 1.1:** UNOS organ transplant statistics for 1990 to 1999 documenting the wait-listed patients (○) and transplants (●) [www.unos.org.].

### 1.1.2 Different approaches in Regenerative Medicine

One approach to regenerative medicine is simple in that it just involves injecting a bioactive substance, such as a growth factor, into the damaged tissue or organ. That

substance recruits the patient's own cells to migrate into the desired area and to encourage proliferation or differentiation to re-form new healthy tissue.

A second avenue explored in creating new tissues is the re-introduction into the body of individual cells or clusters to reproduce a specific – often enzymatic – function. It has been used successfully in pancreatic islet transplantation [White *et al.*, 2001]. A non-enzymatic example is the transplantation of myoblast cells into the area of myocardial infarction to limit the area of fibrotic scarring and restore contractile function [Menasche' *et al.*, 2001].

Another approach originally described for similar applications is the implantation of an acellular biomaterial which acts as a template for tissue regeneration and which is repopulated by native cells from adjacent uninjured tissue.

The more complex and challenging approach involves the patient receiving a three-dimensional construct that contain all of the following components – cells, scaffold or support material, and sometimes bioactive substances. The cells could be obtained from the patient or from a donor. The scaffold could be natural, artificial, biodegradable or non-biodegradable. The bioactive substances could be growth factors, hormones, peptide sequences or protein coatings to promote cell attachment. The entire 3D structure is transplanted into the damaged site where the cells proliferate and/or the patient's cells are recruited and organized into new tissue. As the tissue matures, the scaffold material could degrade, leaving only tissue [Mooney and Mikos, 1997]. Figure 1.2 illustrates the main different tissue engineering approaches explored so far.

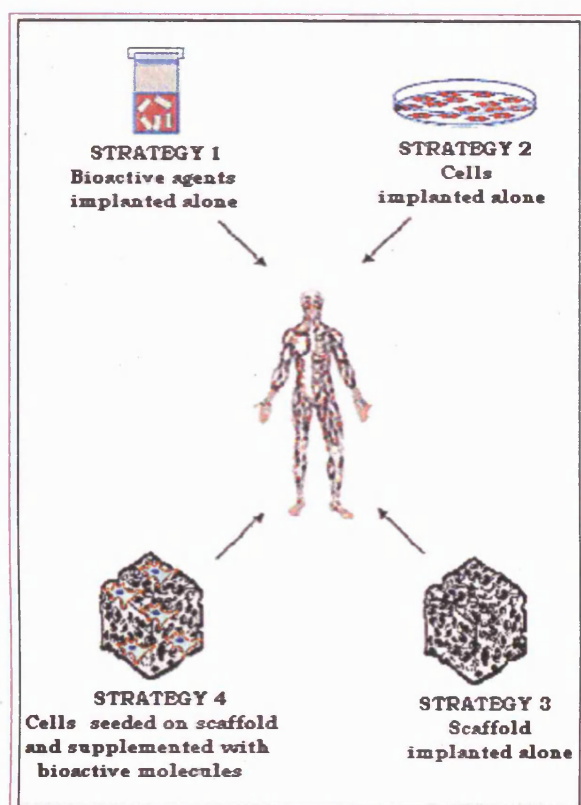


**Figure 1.2** Different approaches in Regenerative Medicine. (Picture adapted from biolab – laboratory for bioimages & bioengineering, available at <http://www.bio.dist.unige.it>).

### 1.1.3 The development and the current status of Tissue Engineering

The idea behind tissue regeneration and transplantation is not a new one. Rudimentary attempts of transplantations were already performed in the Middle Ages. Even the science itself is not brand new. The first accepted example of tissue engineering dates back 70 years to when Bisceglie (1933) wrapped mouse tumour cells in a polymer membrane and successfully transplanted them into the chick embryo peritoneum [Bisceglie, 1993]. Thirty years ago Chick *et al.* reported their results of encapsulated pancreatic islet cells in semipermeable membranes to aid glucose control in patients with diabetes [Chick *et al.*, 1975]. A few years later, Yannas *et al.* [Yannas *et al.*, 1980] designed a collagen, glucosaminoglycan scaffold, which aided in regenerating dermis for the burn patient. Later, Bell *et al.* added

fibroblasts to a contracted collagen gel to replace skin [Bell *et al.*, 1981]. Recent advances in cellular and molecular biology have provided the means to more precisely manipulate, and perhaps duplicate, tissue function. In the 1990s, tissue engineering evolved tremendously and so far no tissue or organ has been excluded from active research.

It has been projected that tissue engineering will be one of the most significant health/science employment fields of the next few centuries. In 2000, Tissue Engineer has been listed as the number one career and, interestingly, three of the other top five careers involve technologies that readily overlap with the field of tissue engineering [TIME Magazine, 2000]. However, this novel biotechnology is still in its infancy: despite the huge breadth of interest in and immense potential of this rapidly growing field, to date tissue-engineered products are available only for a few specific clinical applications. The first tissue-engineered product (cartilage-ACT product Carticel) was approved for marketing in 1996 in the USA. Since then, progress in tissue engineering has resulted in several commercialised products for skin substitution, knee cartilage repair and a few bone repair products from several companies in Europe and the USA. These products yet have to gain broad acceptance in clinical practice [JRCEC, 2003].

The table in figure 1.3 gives an overview of current research projects in tissue engineering [Vacanti, 2001].

There are also new products in the pipeline, addressing diseases for which no treatment is available today, for example in the cardiovascular area (tissue-engineered heart valves, vessel grafts and heart muscle tissue) or concerning neurodegenerative diseases (e.g. Alzheimer's and Parkinson's). These applications may also constitute future business opportunities.



Research projects: in vitro, preclinical, <sup>2</sup> or clinical			
Tissue (References)	In vitro studies	In vivo studies	Clinical studies
Bladder		X	
Blood vessels [10]		X	
Bone		X	
Cartilage for joints			X
Cartilage for urethral sphincter			X
Ear		X	
Eye	X		
Genitals		X	
Heart muscle		X	
Heart valves		X	
Intestine		X	
Joints		X	
Kidney		X	
Liver		X	
Meniscus		X	
Oral mucosa		X	
Nerves (peripheral)		X	
Pancreas		X	
Salivary gland		X	
Skin			X
Spinal cord		X	
Trachea		X	
Ureter		X	
Urethra		X	

<sup>2</sup>Preclinical studies are in vivo animal studies.

**Figure 1.3:** Current research projects in tissue engineering [modified from Vacanti, 2001].

#### 1.1.4 The emerging industry of Tissue Engineering

In a little over a decade, more than \$3.5 billion has been invested in worldwide research and development in tissue engineering. Over 90% of this financial investment has been from the private sector [Lysaght and Reyes; 2001]. A recent study identified a total of 113 companies active in the field of tissue engineering in Europe, 54 companies belonging to the core tissue-engineering category [JRCEC, 2003]. From this study emerged that the European market is characterised by young, small, research-based and technology-oriented companies, most of them SMEs with less than 50 employees. Comparable results have been obtained for the USA market from a survey made in 2001 [Lysaght and Reyes, 2001]. The United States gave birth to the field of tissue engineering through pioneering efforts in cell therapy and biomaterials engineering, aided by the presence of a strong private and entrepreneurial spirit. Growth in the U.S. biotechnology industry led to establishment

of several of the first cellular tissue engineering and cell therapy companies around mid- to late-1980s [McIntire *et al.*, 2002]. According to both the European and the USA surveys, tissue-engineering firms have increased spending at a compound annual rate of 16% since 1990 [JRCEC, 2003; Lysaght and Reyes, 2001]. About two dozens of the companies are listed on the stock exchanges (representing 35% of the workforce employed) [JRCEC, 2003]. However, as stated earlier (previous section) no profitable tissue-engineered product seems to be yet on the market.

At the end of 2002, ten tissue-engineered products were in various stages of clinical trials; however, six products had failed or were abandoned [Lysaght and Hazlehurst, 2004]. The industry leaders, Organogenesis and Advanced Tissue Sciences, filed for Chapter 11 and reorganised under new organisations (Novartis and Smith and Nephew, respectively) in late 2002 due to financial challenges of development, manufacture, testing distribution and poor market acceptance [www.yahoo.com, 2002]. Both Organogenesis and Advanced Tissue Sciences faced significant difficulties including slow regulatory approval, competitors entering the market, and highly laborious and expensive manufacturing processes prone to introduction of microbial contaminations [Stone, 2003].

### **1.1.5 The challenges and the way forward**

Important scientific and technical problems still need to be solved for the development of more complex tissues (e.g. comprehensive understanding of cell and tissue growth and behaviour, large-scale production and storage). The lack of a specific European regulatory framework for tissue-engineered products is currently hampering market growth in Europe. Only products that respond to large, long-term clinical trials testing their quality, safety and efficacy can gain approval from the regulatory bodies and ensure profits to the manufacturing firms. The small biotech companies involved in the manufacturing of tissue-engineering products do not have the resources for such trials to provide information on the cost-effectiveness of their products compared to conventional alternatives. In the USA, the Food and Drug Administration has been working toward a comprehensive regulatory scheme for tissue-engineered products since early 1997, and only very recently it has developed a

guideline covering the rules requirements for human cells, tissues, and cellular and tissue-based products [Federal Register, November 24, 2004].

Certainly tissue engineering is “a new commercial biotechnology sector in Europe” [“European Commission focuses on human tissue engineering potential”, Brussels, 22 January 2004, IP/04/85]. Even though still in its infant phase, tissue engineering is expanding very quickly and, by providing the health sector with new opportunities and challenges, it is initiating a revolution in health care and biomedical research, and it is setting the stage for a new era in transplantation.

The next 5 to 10 year will be critical for the maturation of tissue engineering and its pivotal role in clinical medicine [McIntire *et al.*, 2002]. Filling the gap areas in basic science and engineering will be crucial for the development of actual products. The free movement of tissue-engineered products will be aided by the establishment of a uniform regulatory framework, and the creation of important alliances as well as mergers and acquisitions will help in reaching critical mass, rendering the companies more effective in both the discovery and the commercialisation processes [Pangarkar *et al.*, 2003]. In addition, a highly automated development of new tissue-engineering products will permit biotech companies to utilize their existing equipment and GMP facilities, and this may ultimately decrease time to market, facilitating success of the resulting products [Mason, 2003a, Mason, 2003b; Naughton, 2002].

Ultimately, the perceived potential of stem cells to impact this area has already dramatically stimulated research activity in cellular tissue-engineering and cell therapy. The recent advances in these fields have created a window of opportunity for the successful application of tissue-engineering products in clinical practice. The use of autologous stem cells (isolated from the same patient) promise to overcome the ethical concerns surrounding embryonic stem cells, together with the immunological and safety considerations encountered when using allogeneic (derived from a donor of the same species) or xenogeneic (animal-derived) cells.

### **1.1.6 Vascular tissue engineering for the treatment of atherosclerosis and coronary artery disease**

Among all the possible tissue engineering applications, cardiovascular tissue engineering has two key advantages in that it is both a life-saving or limb-saving treatment and targets a very large patient population [L'Heureux *et al.*, 2007]. The need for arterial substitutes in the clinic is unfortunately increasing, due to the ever-growing occurrence of vascular disease and atherosclerosis in recent years. Atherosclerotic vascular disease, including peripheral vascular and coronary artery disease, is the major cause of mortality and morbidity in the United States, Europe, and other western nations [Niklason *et al.*, 1999]. The development of arterial atherosclerosis occurs when deposits of cholesterol and plaque accumulate at a tear in the inner lining of an artery. As the deposits harden and occlude the arterial lumen, blood flow to distant tissues decreases and a clot may become lodged, completely blocking the artery. Current surgical therapy for diseased vessels less than 6 mm in diameter involves bypass grafting with autologous blood vessels such as saphenous vein or, for coronary artery grafting, the internal mammary artery [Niklason *et al.*, 1999; Darling *et al.*, 1972]. Coronary artery bypass grafting procedures are performed approximately 600,000 times annually in the United States alone [Edelman, 1999; [www.americanheart.org](http://www.americanheart.org)]. Figure 1.4 illustrates the vessels involved in the coronary artery bypass grafting surgical procedure. Although common surgical practice, vascular grafting is usually associated with dysfunction or inflammatory responses and thrombotic complications. Allografts are problematic because of a high rate of rejection. Synthetic materials are excessively thrombotic when used to by-pass arteries less than 6 mm in diameter, with thrombosis rates higher than 40% after 6 months [Edelman, 1999]. As a result, the need for a tissue-engineered vessel of small calibre composed of biological materials and autologous cells has arisen and has been an area of active investigation for more than 15 years [Edelman, 1999].

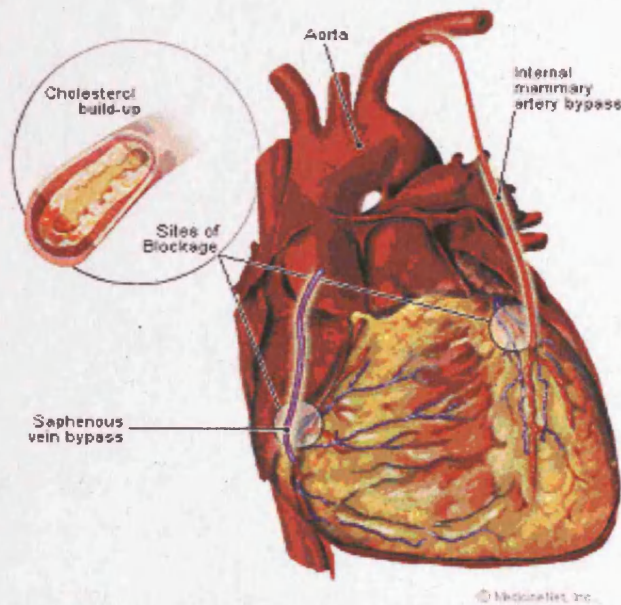


**Figure 1.4:** Typical location for a coronary artery bypass graft. The most commonly used bypass vessel is the saphenous vein from the leg. Bypass grafting involves sewing the graft vessels to the coronary arteries beyond the narrowing or blockage. The other end of this vein is attached to the aorta. Over the past 10 to 15 years, chest wall arteries, particularly the left internal mammary artery, have been increasingly used as bypass grafts. (The picture was sourced from MedicineNet, available at: <http://intensivecare.hsnet.nsw.gov.au>).

#### 1.1.6.1 The artery wall: anatomy and function

The wall structure of the blood vessels is composed of three distinct and well-defined layers: the tunica *intima*, tunica *media*, and tunica *adventitia* (figure 1.5).

The innermost layer or *intima*, directly bordering the vessel lumen, typically consists of a monolayer of endothelial cells and an underlying thin (approx. 80 nm) basal lamina. Endothelial cells are usually flat and elongated in the direction of blood flow. The internal elastic lamina, which separates the *intima* and *media*, is essentially a fenestrated “sheet” of elastin that allows the transport of H<sub>2</sub>O, nutrients, and electrolytes across the wall. An important role of the endothelium is to act as a non-thrombogenic lining that separates the wall contents from the flowing blood. It allows transport of substances to and from the bloodstream, and it must be considered as a selective barrier.

The *media* layer contains spindle-shaped smooth muscle cells that are embedded in an extracellular plexus of elastin and collagen (primarily types I, III, and V), as



well as an aqueous ground substance matrix containing proteoglycans. The primary roles of the contraction of vascular smooth muscle are to modify the distensibility of the large arteries or to regulate the luminal diameter in medium and small arteries [Milnor, 1990]. The connective tissue augments the structural integrity of the wall and its ability to generate force, and acts as a scaffolding on which the cells can adhere or move on.

Finally, the *adventitia*, or outermost layer of the wall, consists primarily of a dense network of type I collagen fibers with admixed elastin and fibroblasts. The collagenous adventitia is thought to limit acute overdistension in the vessel and may serve primarily as a protective sheath, similar to the epicardium of the heart. Moreover, the presence of nerves within the adventitia also allows innervation of smooth muscle in the outer media, while the *vasa vasorum*, an intramural network of arterioles, capillaries, and venules allows sufficient transport of  $O_2$ ,  $CO_2$ , nutrients, and metabolites to the outer portion of the wall in thick arteries.

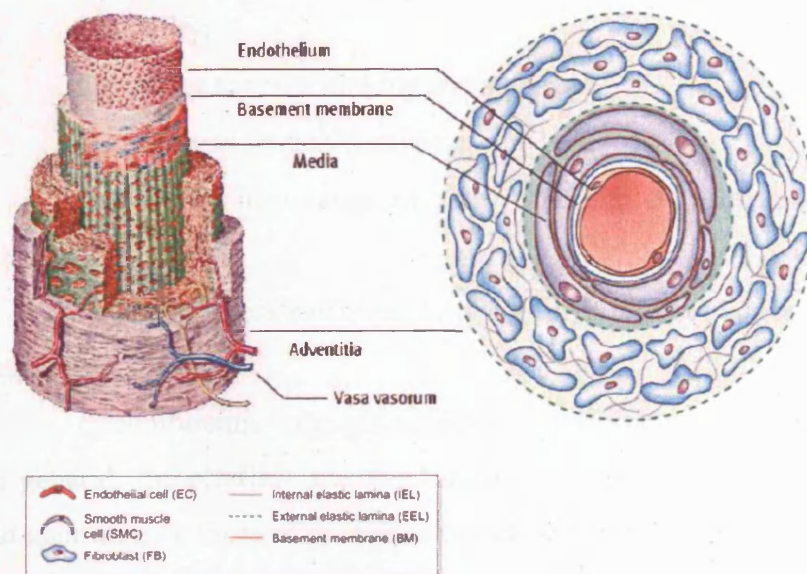


**Figure 1.5:** The composition of a medium-size mature muscular artery in side view and cross section view. Pictures adapted from Hansen and Jain, 2003.

### **1.1.6.2 Ideal mechanical and haemodynamic properties of vascular grafts**

Tissue-engineering techniques may employ different types of materials, often after colonization by the selected cell type, to achieve a *live* prosthesis with the capacity to take part in the tissue-repair process. This represents a promising experimental approach to the *in vitro* creation of live autologous vascular substitutes with an ability for growth, repair and remodelling [Bujan *et al.*, 2004].

The physical and mechanical properties of commercially available grafts vary widely, but a number of characteristics common to all successful vascular prostheses may be identified. These include [Greenwald and Berry, 2000]:

- biocompatibility;
- lack of chemical reactivity;
- very low thrombogenicity;
- porosity;
- sterility.

Moreover, to guarantee simple insertion and long-term success of a graft, the following properties are also essential [Greenwald and Berry, 2000]:

- flexibility;
- the ability to resist kinking and squashing;
- the ability to stretch/elasticity;
- availability in a range of sizes to match the dimensions of the native vessels;
- tensile stiffness sufficient to resist fraying at cut edges and tearing out of sutures;
- circumferential strength sufficient to withstand arterial pressures.

In general, the physical and mechanical properties of successful vascular grafts should approximate those of the native vessels to which they are attached.

In the last 40 years, as techniques and materials have improved, the success rate of vascular prostheses with diameter greater than 6 mm has risen steadily, 5-year survival rates exceeding 95% in most centres [Nugent and Edelman, 2003]. Modern materials meet many of the above-listed requirements, permitting high success rates of the implantation procedure and long-term patency of large grafts. However, with smaller grafts no comparable improvement has occurred, the majority failing within 5

years [Pevec *et al.*, 1992]. This is mainly caused by intimal hyperplasia and, ultimately, atherosclerosis, developing in and around the downstream anastomosis [Bos *et al.*, 1998]. Thus, in most cases the long-term success rate of grafts with a diameter of less than 6 mm is far from satisfactory and falls steadily as the diameter becomes smaller [Greenwald and Berry, 2000]. Recently, a variety of materials including Nylon, Teflon, Orlon, Dacron, polyurethane and PTFE have been tested, and other materials are currently being investigated. However, these biomaterials lack the ability to grow and consequently do not achieve adequate remodelling, giving rise to post-implant complications such as thrombosis, stenosis or aneurismal dilation. More research is needed to determine the effectiveness of possible successful approaches in the treatment of compromised small vessels.

#### **1.1.6.3 Tissue engineering of arterial vessel substitutes**

The vascular wall, with its complicated architecture and distinctive mechanical properties, presents an enormous challenge to tissue engineering. The search for a perfect model, and perhaps the birth of vascular tissue engineering, can be tracked back to 1986 when Weinberg and Bell constructed an *in vitro* tissue-engineered blood vessel composed of natural materials [Weinberg and Bell, 1986]. They mimicked the adventitial and medial layers of native artery using culture derived collagen/fibroblast gel sheets and a similar collagen/smooth muscle cell (SMC) sheet wrapped over each other to form a tubular construct. These were then lined by an endothelial cell monolayer. This artificial artery represented a major advance in conduit technology. The endothelial lining of this blood vessel model functioned like a normal endothelium in several respects. To maximize the burst strength, Winberg and Bell optimized several parameters including the collagen concentration, initial cell density, and time elapsed after casting, and thus they produced a model with a burst strength of 323 +/- 31 mmHg. However, the tensile strength of such constructs was woefully inadequate for physiological use and required external support from a Dacron<sup>TM</sup> framework, which inevitably introduced limitations to the biological adaptation and/or vasoactivity. Additional limitations of this model were lack of elastin in the matrix mixture and incorrect orientation and low density of the smooth muscle cells and collagen fibers.



A vascular graft formed without the use of a scaffold support was later developed by L'Heureux and colleagues [L'Heureux *et al.*, 1998]. Human vascular smooth muscle cells were used to mimic the media layer in this system, and fibroblasts were then wrapped around the media to serve as the adventitia. This tissue-engineered vessel exhibited a well-defined organisation and had a burst strength of more than 2000 mmHg, comparable to human vessels. One week after implantation into canine femoral arteries these structures remained patent in 50% of cases. However, it was unclear whether the material exhibited the normal viscoelastic response under physiological loading, or whether it would experience compliance mismatch on implantation.

Another interesting approach was followed by Niklason *et al.*, who used a scaffold made of a biodegradable polyglycolic acid (PGA) mesh and seeded it with porcine aortic smooth muscle cells [Niklason *et al.*, 1999]. The constructs were cultured for several weeks under pulsatile radial stresses in a parallel flow system. Following an 8-week period of *in vitro* maturation, porcine endothelial cells were seeded onto the lumen of the constructs to form a confluent monolayer. Culture medium containing growth factors and supplements (e.g. 20% fetal bovine serum, ascorbic acid, copper sulphate, and amino acids) was used to ensure that the proper biochemical signalling was available for cells to produce and cross-link matrix proteins. The resulting constructs exhibited burst pressures greater than 2000 mmHg and desirable histological characteristics. When cultured under pulsatile conditions, these engineered vessels were also able to contract in response to known vasoactive substances, such as serotonin and endothelin-1. However, the engineered vessels did not demonstrate a full vasoactive response when compared with native blood vessels.

More recently, in the first clinical use of a vascular construct produced *in vitro*, Shin'oka *et al.* were able to regenerate a low-pressure pulmonary outflow tract in pediatric patients with cyanotic congenital defects [Shin'oka *et al.*, 2001; Shin'oka *et al.*, 2005]. Shin'oka seeded autologous bone marrow cells into tubes of a copolymer of L-lactide and  $\epsilon$ -caprolactone reinforced with a polyglycolic acid sleeve. Unfortunately, following implantation, these grafts were not suitable for the high-pressure nonpulmonary circulation.

Interestingly, L'Heureux and colleagues have recently developed a completely autologous approach whereby dermal fibroblasts obtained from skin biopsies were grown in conditions that promote the production of extracellular matrix proteins

[L'Heureux *et al.*, 2006]. Following 6-10 weeks in culture, sheets of dermal fibroblasts were detached from the culture substrate and fused into a homogeneous tissue, which resulted in multilayer vessels with burst pressures in excess of 3000 mmHg. Prior to implantation these vessels were seeded with autologous endothelial cells taken from the patients. Despite being time-consuming, this approach is showing encouraging results from the follow-up on ongoing clinical trials. With this approach graft failure appears unlikely to be life or limb-threatening, and all grafts seem to demonstrate excellent surgical handling characteristics [L'Heureux *et al.*, 2007].

In conclusions, over the past twenty years several approaches to creating tissue engineered blood vessels have been investigated, and research has moved toward engineering a completely natural vessel composed of smooth muscle cells and endothelial cells that is grown under biological conditions [Riha *et al.*, 2005]. However, so far only two techniques (i.e. Shin'oka's and L'Heureux's) have been translated to clinical use. Early clinical trials results for both techniques seem encouraging; however, significant clinical (i.e. long production time) and regulatory challenges (i.e. lack of a harmonised European regulatory framework for advanced medicinal therapeutics) remain to be overcome before vascular tissue engineering can develop satisfactory small artery prosthesis for clinical use [L'Heureux *et al.*, 2007].

## **1.2 Selection of a cell source for a bio-engineered tissue substitute**

The source of the cells is a key element enabling or prohibiting potential tissue-engineering application. There are a variety of choices, depending on the clinical procedure:

1. autologous cells
2. allogeneic cells
3. xenogeneic cells
4. stem cells, either autologous (adult derived) or allogeneic (embryonic, fetal or adult derived).

The urgency or lack of urgency of the clinical application will determine how the cells will be selected, obtained, cultivated, and manipulated. For instance, cells required for blood vessel repair could be isolated from the patient's own body, if the cell cultivation procedure is performed in advance. In contrast, nerve repair must occur within several hours/days from the initial damage in order to be successful, and therefore in this case the use of pre-cultivated cells and cells that can be expanded *in vitro* in sufficient quantity in culture are required. The source of the cells influences the culture requirements, delivery strategies and many other design parameters [Young *et al*, 1997].

### **1.2.1 Autologous cells**

Autologous cells are derived from the specific individual into which they will be later reimplanted. The use of autologous cells obviates the problem of host's immune rejection and, due to the reduced safety and regulatory requirements compared to the use of allogeneic and xenogeneic cells, they are often seen as the most obvious route to clinical application of tissue-engineered products. Cultured autologous cells were in fact the first to be used in clinical application of cellular tissue engineering: Gallico and colleagues cultured *in vitro* autologous keratinocytes and employed the resulting grafts in burn patients [Gallico *et al.*, 1984]. Due to the long time required to harvest the cells, expand them in culture, and construct the implant, autologous cells are not

the best choice for implants to be used in emergency clinical procedures. Moreover, the use of autologous cells does not necessarily imply minimal manipulation and maximum safety for the host, as culture protocols and reagents, if not screened and validated, can introduce adventitious agents and alter cell populations regardless of their origin.

Tissue availability, inherent variability and limitations on expansion in culture are the major drawbacks to the use of autologous cells.

### **1.2.2 Allogeneic cells**

Allogeneic cells are derived from an individual of the same species other than the recipient. Unlike autologous cells, allogeneic cells can be cultured and cryopreserved in sufficient quantity ready for immediate use. However, the use of allogeneic sources presents unique immunological and safety considerations. Allograft rejection is primarily a T cell mediated immune response. Endothelial cells, leukocytes and other cell populations are strongly allostimulatory. By contrast, there is now substantial accumulated clinical experience regarding the lack of immunogenicity of other cell types such as keratinocytes, fibroblasts, and smooth muscle cells [Falanga *et al.*, 1998; Laning *et al.*, 1999; Young *et al.*, 1997]. The inability of these cells to stimulate naïve T cells presents the possibility of using allogeneic skin constructs containing only human epidermal keratinocytes and dermal fibroblasts for tissue engineering applications [Wilkins *et al.*, 1994]. In summary, allogeneic cells may represent a valid alternative to the use of autologous cells when the degree of immunoreactivity of the resulting graft is reasonably low.

### **1.2.3 Xenogeneic cells**

Xenogeneic cells are derived from a species different to that of the recipient. The use of xenogeneic cells obviously requires additional safety assessment in order to ensure that pathogenic viruses and prions are not introduced into the human population. Gel encapsulation of cell aggregates, cell microencapsulation, conformational coating of cell clusters, genetic manipulation and other technologies

are currently being developed to block rejection and enable the use of xenogeneic tissue [Uludag *et al.*, 2000].

#### **1.2.4 Stem cells**

Stem cells have the potential to revolutionize cell therapy and tissue engineering. The peculiar biological properties of these cells make their clinical exploitation both feasible and attractive. Human embryonic stem cells, which are isolated from a blastocyst, are pluripotent and can give rise to virtually any cell type in the body [Department of Health and Human Services, June 2001]. Adult stem cells, existing in most, if not all, tissues, have also been shown to differentiate into numerous specialized, functional cells [Pittenger *et al.*, 1999]. For this reason the use of stem cells has opened the door to the possible generation of almost limitless cell sources for a variety of tissues, and stem cells are considered an attractive “raw material” for multiple biotechnological applications. However, stem cells’ potential is limited, to date, by researchers’ rudimentary ability to control their proliferation and differentiation. The stability of Mesenchymal Stem Cells’ phenotype remains a concern and the ability to control or direct cell response is still one of the most limiting but important aspects of cellular tissue engineering. Aside from scientific and technical hurdles, the use of embryonic stem cells can provoke strong ethical reactions. This field is just beginning to be understood and obviously there are several significant scientific challenges and ethical issues to overcome prior to the feasibility of use for a repair aid. Stem cells’ properties, their potential applications and the obstacles hampering their use in clinic are briefly described in the next sections.

##### **1.2.4.1 Stem cells: an alternative cell source for vascular grafts**

The source of cells to be seeded onto or into synthetic grafts for blood vessel repair is not yet unequivocally established [Nerem, 2004]. With regard to clinical applications, several vascular human cell sources have been investigated [Schnell *et al.*, 2001]. However, the proliferative capacity of many adult tissue-specific cells is very limited, making their expansion *in vitro* difficult in the preparation for scaffold

seeding. Long-term *in vitro* cultivation also reduces their functional quality. As far as the engineering of small-calibre arteries for bypass surgery is concerned, smooth muscle cells -which are the main cellular component of these vessels- divide a finite number of times before undergoing growth arrest in a state known as senescence. This is largely due to the progressive erosion of chromosome-capping telomeres with each cell division, which ultimately leads to a critically short telomere length that signals senescence [Bierman E.L., 1978]. Smooth muscle cells must proliferate for at least 45-60 population doublings (PDs) to produce a mechanically robust artery *in vitro*. Bovine, porcine and human fetal and neonatal cells have long telomeres, and correspondingly divide extensively in culture [Kozik *et al.*, 1998]; long enough, in fact, to form arteries *in vitro*. However, non-neonatal human smooth muscle cells that would be used clinically for tissue engineering can proliferate *in vitro* for only 10-30 PDs before undergoing senescence [Bierman, 1978]. The limited life-span of non-neonatal smooth muscle cells may therefore be the rate-limiting step in constructing autologous human arteries *in vitro*. An important attempt at extending the life-span of non-neonatal human smooth muscle cells by inducing telomerase expression in these cells has been recently investigated [McKee *et al.*, 2003].

However, as an alternative to this approach, attention has started shifting from seeding scaffolds with tissue-specific cells to the use of stem cells or progenitor cells. Recent *in vitro* studies conducted by Kadner and colleagues have shown that constructs seeded with bone marrow stromal progenitors cells develop a matrix composition similar to that of constructs seeded with vascular cells [Kadner *et al.*, 2002]. In contrast to vascular cells, these cells can be obtained without the need to disrupt intact vessels, representing an easy-to-access cell source in a possible routine clinical scenario. Due to their good proliferation and progenitor potential, these cells are expected to be an attractive alternative for cardiovascular tissue engineering application. Moreover, adult bone marrow cells (including mesenchymal stem cells), endothelial cells, vascular smooth muscle cells and fibroblasts all derive from the mesodermal germ layer. This close embryonic relationship further justifies studies focused on guiding differentiation of adult mesenchymal stem cells into vascular cells [Department of Health and Human Services, June 2001].

#### **1.2.4.2 Stem cells: a brief history**

Mesenchymal Stem Cells (MSCs) were first identified in the pioneering studies of Friedenstein, who isolated bone-forming progenitor cells from rat marrow [Friedenstein *et al.*, 1966]. However, the new stem cell biology era began only in 1998, when James Thomson and his colleagues reported methods for deriving and maintaining human embryonic stem cells from the inner cell mass of human blastocysts that were produced through *in vitro* fertilization (IVF) and donated for research purposes [Thomson *et al.*, 1995]. Since then, several research teams have tried to characterize many of the molecular characteristics of these cells and to improve the methods for culturing them.

#### **1.2.4.3 The unique properties of stem cells**

It is nowadays generally accepted that all stem cells –regardless of their source– exhibit three general and unique properties: they are capable of dividing and renewing themselves for long periods; they are unspecialized; and they can give rise to specialized cell types [Department of Health and Human Services, June 2001]. Furthermore, a stem cell can be considered totipotent, pluripotent, or multipotent [Vats *et al.*, 2002]. A totipotent stem cell can form all cells/tissues that contribute to the formation of an organism (e.g. the fertilized egg or zygote); a pluripotent stem cell can form most (but not all) cells/tissues of an organism (e.g. embryonic stem cells and embryonic germ layers); and a multipotent stem cell can form a small number of cells/tissues that are usually restricted to a particular germ layer origin (e.g. bone marrow stromal or mesenchymal stem cells) [Kuo and Tuan, 2003]. Stem cells' long-term self-renewal and their pluri/multi-potentiality are what make them particularly attractive for clinical applications in the innovative field of tissue engineering.

#### **1.2.4.4 Human stem cells and cell-based therapies**

Perhaps the most important potential application of human stem cells is the generation of cells and tissues that could be used for cell-based therapies. Today, donated organs and tissues are often used to replace ailing or destroyed tissue, but the need for transplantable tissues and organs far outweighs the available supply. Stem cells, directed to differentiate into specific cell types, offer the possibility of a

renewable cell source for the replacement of compromised tissues and organs. Among the disorders that might benefit from stem cell-based therapy are brain damages and disorders, acute liver and heart failures, vision disorders, arthritis, skin disorders and diabetes (see figure 1.8) [Orlic *et al.*, 2001; Soria *et al.*, 2000; Guettier, 2005; Lindvall *et al.*, 2004].

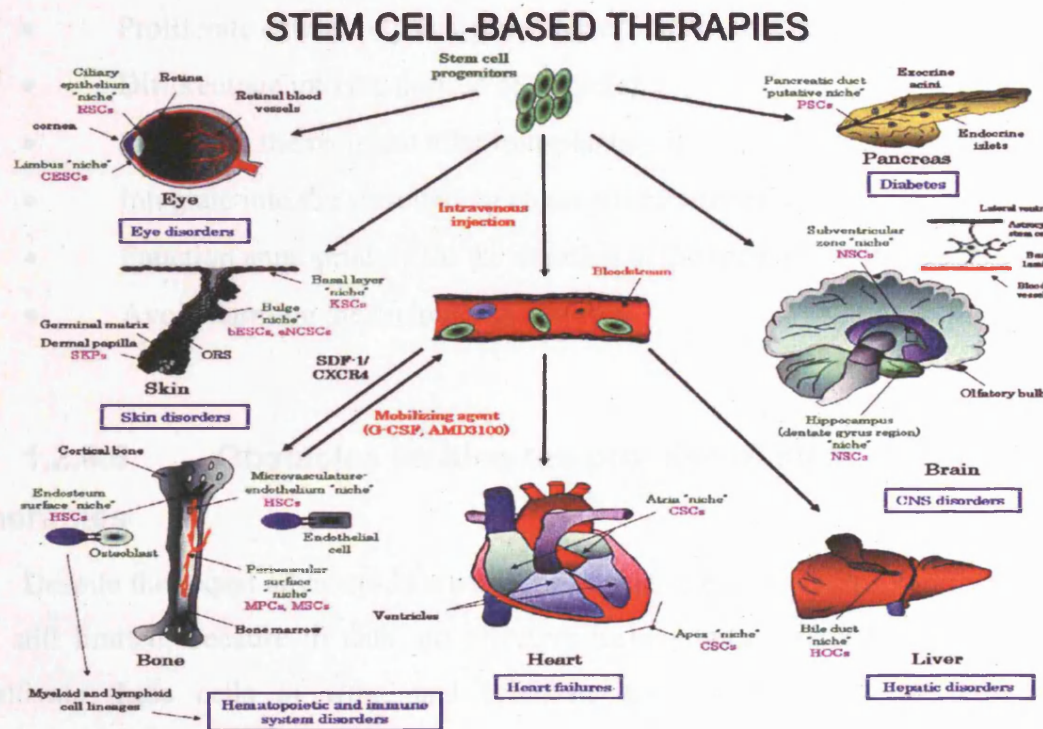


**Figure 1.6.** Scheme showing the tissues/organs constituting the potent targets for tissue regeneration by stem cell-based therapies. The localization of tissue-specific stem cells and their niches is shown. The tissue-specific degenerating disorders and diseases that might be treated by the transplantation of stem cell progenitors derived from embryonic stem cells, fetal stem cells, umbilical cord blood, and adult tissues/organs, including bone marrow (BM), are also indicated. The possibility of the mobilization of BM stem cells and their progenitors in the bloodstream by using the mobilizing agents is also shown. Abbreviations: bESC, bulge epithelial stem cell; CESC, corneal epithelial stem cell; CNS, central nervous system; CSC, cardiac stem cell; CXCR, CXC-chemokine receptor; eNCSC, epidermal neural crest stem cell; G-CSF, granulocyte colony-stimulating factor; HOC, hepatic oval cell; HSC, hematopoietic stem cell; KSC, keratinocyte stem cell; MPC, mesodermal progenitor cell; MSC, mechenchymal stem cell; NSC, neural stem cell; PSC, pancreatic stem cell; RSC, retinal stem cell; SDF, stromal-derived precursor [Mimeault and Batra, 2006].



However, to realize the promise of novel cell-based therapies for such pervasive and debilitating diseases, it will be essential to find a way to easily and reproducibly manipulate stem cells so that they possess the necessary characteristics for successful differentiation, transplantation and engraftment. The following is a list of steps in successful cell-based treatments that will be necessary to learn to precisely control to bring such treatments to the clinic.

To be useful for transplant purposes, stem cells must be reproducibly made to:

- Proliferate extensively and generate sufficient quantities of tissue.
- Differentiate into the desired cell type(s).
- Survive in the recipient after transplantation.
- Integrate into the surrounding tissue after transplantation.
- Function appropriately for the duration of the recipient's life.
- Avoid harming the recipient in any way.

#### **1.2.4.5 Obstacles limiting the promise of stem cell-based therapies**

Despite the recent advances in stem cell research, the clinical utility of these cells is still limited, because to date, no effective technological methodologies exist to cultivate these cells *in vitro*, and scientists are just beginning to direct the differentiation of the human pluripotent stem cells and to identify the functional capabilities of the resulting specialized cells. In addition, the defining parameters required to maintain and expand the stem cell pool *in vitro*, and the mechanisms regulating their differentiation are still poorly defined [Zandstra and Nagy, 2001].

Mesenchymal stem cells' definition itself is still unclear. Mesenchymal stem cell (MSC) is the designation commonly applied to the plastic-adherent cells isolated from the bone marrow; however, this heterogeneous population is recognized, among leading investigators, to be too "crude" to be considered all mesenchymal stem cells, and there are no convincing data to support the "stemness" of these cells [Horwitz and Keating, 2000]. In order to address the inconsistency between nomenclature and biological properties, it has been recently proposed to term multipotent "mesenchymal stromal cells" the fibroblast-like plastic-adherent cells, regardless of the tissue from which they are isolated, while reserving the term "mesenchymal stem

cells” (for which the acronym MSC remains unchanged) for cells that meet specified stem cell criteria [Horwitz *et al.*, 2005]. This proposed solution is still the object of debate among scientists worldwide, and clearly the confusion over stem cells’ terminology is a reflection of the need for thorough characterization of these cells [Kuo and Tuan, 2003].

In order to avoid this issue, the mixed population of bone marrow derived progenitor cells used in this research will be referred to as multipotent “mesenchymal stem cells”, as this was the accepted term at the beginning of this research.

#### **1.2.4.6 Embryonic and adult mesenchymal stem cells**

The embryonic stem cell is defined by its origin –that is from one of the earliest stages of the development of the embryo, called the blastocyst. Human embryonic stem cells can be cultured by isolating a blastocyst, removing the outer cell wall, placing into culture with a layer of mouse feeder cells, and adding selected differentiation factors after colonies of embryonic stem cells have been formed [Pedersen, 1997]. Pluripotency –that is the ability to give rise to differentiated cell types that are derived from all three primary germ layers of the embryo, endoderm, mesoderm, and ectoderm- is what makes ES cells unique. Despite the potential of ES cells, legal and ethical issues surrounding their use have turned much attention to the use of adult stem cells. Relative to embryonic stem cells, adult stem cells have also reduced tumorigenicity and thus are preferable for therapeutic purposes because they are considered safer for implantation. Besides, the use of autologous adult stem cells avoids triggering of immune rejection.

Adult stem cells are undifferentiated (unspecialized) cells that reside in small numbers among differentiated (specialized) cells in many adult mammalian normal tissues/organs, including bone marrow, heart, kidneys, brain, skin, eyes, gastrointestinal tract, liver, pancreas, lungs, breast, ovaries, prostate, and testis [Department of Health and Human Services, June 2001; Muschler *et al.*, 2003; Muschler *et al.*, 2002]. Bone marrow-derived MSCs for example, represent a very small fraction, 0.001-0.01%, of the total population of nucleated cells in marrow [Pittenger *et al.*, 1999]. Numerous studies have revealed that a population of adult stem cells resides within specific areas designated as niches in most of the above-mentioned tissues or organs [Heissig *et al.*, 2005]. Adult stem cells appear to persist

in their specialized niches where they remain quiescent (resting or not actively proliferating/dividing) for many years until they are activated by disease or tissue injury. Although adult stem cells share with embryonic stem cells the ability to renew themselves and to generate differentiated cell progenitors of different lineages [Caplan, 1991; Pittenger *et al.*, 1999], they generally show a more restricted differentiation potential and give rise to a more limited number of distinct cell progenitors. However, due to the potential advantages listed above, adult stem cells are the object of intense and active investigations in the emerging fields of cell-based therapy and tissue engineering.

#### **1.2.4.7 Bone marrow-derived MSCs**

Adult bone marrow is one of the most widely used sources of adult stem cells. Bone marrow contains at least two, and likely more discernable stem cell populations [Jiang *et al.*, 2002; Mazurier *et al.*, 2003]. Besides the hematopoietic stem cell (HSC), which renew circulating blood elements, a cell type termed mesenchymal or marrow stromal (MSC) also exists in marrow [Majumdar *et al.*, 1998]. This cell provides support for hematopoietic and other cells within the marrow, and contribute to the regeneration of mesenchymal tissues such as bone, cartilage, muscle, ligament, tendon, adipose, and stroma [Kuznetsov *et al.* 1997; Friedenstein *et al.*, 1987; Haynesworth *et al.*, 1992]. Both HSCs and MSCs can be isolated from the mononuclear fraction of bone marrow aspirates. Unlike hematopoietic stem cells, which can be identified and isolated on the basis of characteristic surface markers, there is not currently a well-established, unique profile of surface markers to identify MSCs [Minguell *et al.*, 2001; Fibbe, 2002]. As a result, mesenchymal stem cells are most commonly identified by their tendency to adhere to tissue culture plastic. In fact, one of the most common techniques used to isolate and culture expand *in vitro* the multipotent human MSCs is aspiration from bone marrow followed by density gradient fractionation and direct plating [Pittenger *et al.* 1999]. Other techniques utilized for MSCs' identification are based on their expansion potential and their capacity to undergo all three differentiation pathways of osteogenesis, chondrogenesis, and adipogenesis in culture with appropriate combination of growth factors and supplements [Pittenger *et al.*, 1999].

Recent studies have demonstrated the existence of bone marrow-derived endothelial progenitor cells that contribute to vasculogenesis and angiogenesis [Takahashi *et al.*, 1999] and experiments have proved endothelialization of artificial grafts using bone marrow cells (BMCs) [Noishiki *et al.*, 1996]. Bone marrow cells (BMCs) have also been seeded onto a biodegradable scaffold to establish tissue-engineered vascular autografts successfully implanted *in vivo* both in animal and human models [Matsumura *et al.*, 2003a; Matsumura *et al.*, 2003b]. More recently, a specific subpopulation of human bone marrow-derived MSCs has demonstrated the potential to differentiate into endothelial-like cells *in vitro* [Oswald *et al.*, 2004] making it an attractive candidate for the development of engineered vessels as well as for the vascularization of engineered tissues. These findings may support the development of tissue-engineered vascular grafts based on autologous bone marrow-derived MSCs, although clinical studies will have to establish whether these cells have enough potential for expansion to be practically useful and to display significant positive effects in patients with small vessel diseases.

To summarise, the promise of stem cell therapies is an exciting one, but significant technical hurdles remain that will only be overcome through years of intensive research. Like many expanding fields of scientific inquiry, research on stem cells raises scientific questions as rapidly as it generates new discoveries. However, stem cells remain one of the most fascinating areas of biology today, and research in this emerging field of science is showing the first promising results, indicating that Regenerative or Reparative Medicine, that is treatment of disease through cell-based therapies, is most likely to become a real possibility in the near future.

### ***1.3 Selection of a three-dimensional matrix suitable for the preparation of an engineered tissue***

Most tissue-derived cells are anchorage dependent and require attachment to a solid surface for viability and growth. Biomaterials are used to promote cell adhesion, spreading and migration, to guide the organization, growth and differentiation of cells in the process of forming functional tissue and provide both physical and chemical cues.

Scaffold materials for tissue engineering applications must at minimum satisfy a number of design criteria to function appropriately and promote new tissue formation. These criteria include classical parameters such as structural and mechanical properties as well as biological performance parameters like biocompatibility and suitability for cell adhesion [Chen *et al.*, 2002].

Both synthetic and natural materials have been designed to meet nutritional and biological needs for the specific cell population involved and to guide the development of new tissues. A list of some materials used as bioengineered scaffolds is presented in the table in figure 1.7.

---

Synthetic polymers used as scaffolds in tissue engineering
Poly beta-hydroxybutrate
Polyglycolic acid
Polylactic acid
Polyglycolic acid-poly L lactic acid co polymer
Polyethylene
Polyethylene oxide
Carrier materials of natural origin used as scaffolds in tissue engineering
Collagen sponges
Collagen gel
Alginate
Fibrin
Hyaluronic acid
Gelatin
Collagen-glycosaminoglycan matrices

---

**Figure 1.7:** Examples of some materials used in bioengineered scaffolds [adapted from Sarraf *et al.*, 2002].

### 1.3.1 Synthetic materials

A variety of synthetic materials, both degradable and non-degradable, have been used to fabricate tissue engineering matrices. Two main structural types are fiber-based and sponge-based scaffolds. Currently, polyglycolic acid and poly-L-lactic acid, which are biodegradable materials, are mainly used in this field, and the hydrolytically degradable poly(lactide-co-glycolide) PLG polymers have been approved by the FDA for use in the body [Thomson *et al.*, 1995; Wong and Mooney,

1997]. Such synthetic polymers are well suited for the delivery of a large number of cells because of their high porosity and extensive surface area. Their porosity also allows for the vascularization and structural integration of the new tissue with surrounding native tissue after implantation. Synthetic polymers can be readily processed into the devices of varying sizes and shapes and have chemical and mechanical properties that can be accurately controlled and manipulated.

### **1.3.2 Natural polymers**

Natural polymers include both extracellular matrix (ECM) proteins and derivatives (including collagen, fibrin, gelatin, hyaluronic acid) and materials derived from plants and seaweed (such as alginate). A variety of naturally derived hydrogel forming polymers, a class of highly hydrated polymer materials (water content  $\geq 30\%$  by weight) [Park and Lakes, 1992] are being employed as scaffold materials because they are either components of or have macromolecular properties similar to the natural ECM. These materials have been shown to interact in a favourable manner *in vivo* and thus have been utilized as hydrogel scaffold materials for tissue engineering [Lee and Mooney, 2001].

### **1.3.3 Activation of inert supports**

In order to promote cell attachment and cell growth, polymers can be modified at their surface.

Tissue-culture vessels, for example, are usually made of polystyrene, which can be treated by radiofrequency plasma deposition or exposure to sulphuric acid in order to increase the number of charged groups at its surface. Alternatively, polymer surfaces can be treated with purified protein solutions (such as fibronectin, laminin, collagen and other extracellular matrix proteins) that permit cell adhesion. The optimal surface for cell adhesion has an intermediate wettability and high surface free energy, which allows cell adhesion proteins to adsorb to the surface.

With the exception of collagen, which is a natural ECM protein, most hydrogel forming polymers do not normally permit cell adhesion. Furthermore, because of the hydrophilic nature of hydrogels, ECM proteins such as laminin, fibronectin and vitronectin typically do not readily adsorb to the gel surface [West and Hubbell,

1997]. A common approach to design a highly specific adhesive surface requires covalently bonding synthetic peptides or incorporating small biologically active functional groups of the ECM to the graft polymer [West and Hubbell, 1997]. These peptidic sequences and functional groups are based on the receptor-binding domains of cell adhesion proteins. Most cell types synthesize and express on their surface specific proteins, known as integrins, which are able to recognize these cell binding peptidic sequences. The most common peptide used in this approach is the amino acid sequence arginine-glycine-aspartic acid (RGD) derived from numerous ECM proteins including fibronectin, laminin, vitronectin and collagen [West and Hubbell, 1997]. The proteins that contain the RGD sequence, together with their specific integrin cell receptors, constitute a major recognition system for cell adhesion. The RGD peptide, the major cell binding sequence, is critical for the interaction of the ECM proteins with the adhesion receptors [Ruoslahti and Pierschbacher, 1987; Ruoslahti, 1996]. Other common peptides used in this approach include arginine-glutamic acid-aspartic acid-valine (REDV) (from fibronectin), tyrosine-isoleucine-glycine-serine-arginine (YIGSR) (from laminin) and isoleucine-lysine-valine-alanine-valine (IKVAV) (from laminin) [West and Hubbell, 1997].

Mooney and colleagues at the University of Michigan, for example, have been tailoring and modifying alginate with the RGD peptide to promote cellular adhesion [Alsberg *et al.*, 2001; Rowley *et al.*, 1999], ultimately permitting optimal performance of the alginate in tissue-engineering applications (see also section 1.4.4.2).

#### **1.3.4 Sodium alginate**

Alginate is a naturally derived polysaccharide and one of the most versatile biopolymers with a wide range of pharmaceutical and biomedical applications.

Alginate is a common term for a family of natural non-branched binary copolymers of 1-4 glycosidically linked  $\beta$ -D-mannuronic acid (M) and  $\alpha$ -L-guluronic acid residues (G).

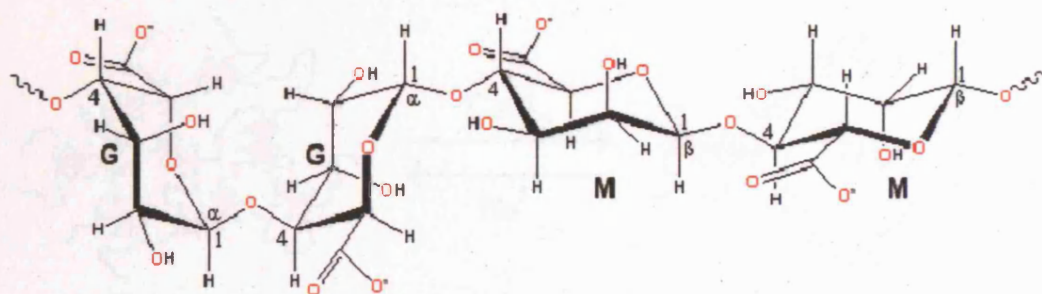


**Figure 1.8:** Chemical block structures of alginate. Picture adapted from Mulder, 2002.

All current industrial manufacture of alginate is based on extraction of the polymer from brown algae. The seaweed grows naturally mainly in the temperate zone, but large amounts are also cultivated in the Far East, on the coast of China and Japan in particular. The ratio of the M and G subunits and their sequential arrangement will vary from one species of brown algae to another. Similar variations are also found in the seaweed during the growth season, and between different parts of the plant.

The functional properties of alginate mostly utilized are the viscoelastic ones, as a gelling agent through cross-linking with calcium, and as a viscosifier in aqueous solutions. Solubility, swellability and film-forming properties are other capabilities utilized in biomedical and pharmaceutical applications. The gelling properties of alginate are a function of the M/G composition and the sequential structure of M and G along the alginate chain. Divalent cations cooperatively bind between the G-blocks of adjacent alginate chains, creating ionic interchain bridges which cause gelling of aqueous alginate solutions. A solution of calcium chloride is most commonly used to donate the calcium ions, which compete for the sodium ion position on the hydroxyl groups of adjacent blocks of G subunits. The gel formation can be reversed by addition of excess sodium ions [Martinsen *et al.*, 1989] (Figure 1.9).



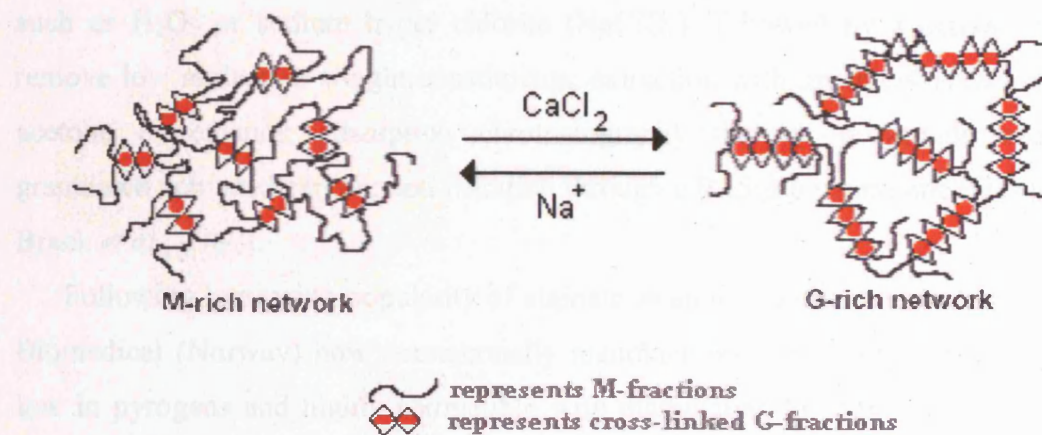


**Figure 1.9:** Cross-linking of alginate G-blocks with calcium [Melvik *et al.*, Pronova Biomedical].

Injectable, *in vivo* gelling forms of alginate [Marler *et al.*, 2000; Alsberg *et al.*, 2001] have been successfully combined with cells and/or bioactive molecules and delivered in a minimally invasive manner.

#### 1.3.4.1 Quality of alginate

In order to be used for transplantation, matrix components of a tissue engineered product must be non-toxic, non-immunogenic and pyrogen free (not contain components such as proteins, complex carbohydrates, and nucleotides from micro-organisms) [Skjak-Braek *et al.*, 1989]. Natural, non-animal derived matrices are the most desirable from a regulatory standpoint. Plant derived materials, such as alginate, are ideal because they do not contain human pathogens. However, potential contaminants typically found in alginate include hazardous and cytotoxic components, like endotoxins, heavy metals and polyphenols, which need to be removed [Zimmermann *et al.*, 2001]. These are present in alginates in various amounts according to their source and type. The phenolic compounds can be detected by fluorescence spectroscopy in concentrations lower than 1 ppm [Skjak-Braek *et al.*, 1987]. The contaminants can be reduced by selection of the original alginate material with low initial polyphenols. Alternatively, various purification protocols can be employed to remove mitogenic and cytotoxic impurities and other contaminants from the alginate. These include treatment with specific enzymes, or with bleaching agents

such as H<sub>2</sub>O<sub>2</sub> or sodium hyper chlorite (NaClO<sub>2</sub>); followed by a dialysis step to remove low molecular weight constituents; extraction with organic solvents, such as acetone or ethanol; adsorption chromatography through polyamide beads or granulated activated carbon; and filtration through a 0.45 µm membrane filter [Skjak-Braek *et al.*, 1987].

Following increasing popularity of alginate as an immobilization matrix, Pronova Biomedical (Norway) now commercially manufactures ultra-pure alginates that are low in pyrogens and highly compatible with mammalian biological systems. These alginates have been shown to support tissue and vascular in-growth with minimal inflammatory response and capsule formation in *in vivo* animal models [Halberstadt *et al.*, 2002].

#### **1.3.4.2 Alginate's biomedical and biotechnology applications**

Alginates have been used for decades as helping agents in various human-health applications, including in traditional wound dressings, in dental impression material, and in some formulations preventing gastric reflux. However, due to its increasing popularity as an immobilization matrix in various biotechnological processes, alginate's applications now include other and more advanced technical domains in addition to its traditional uses. Alginate hydrogels are for example currently extensively used in enzyme and cell encapsulation and in tissue engineering applications.

Perhaps the most exciting prospect for alginate gel immobilized cells remains their potential use in cell transplantation. Here, the main purpose of the gel is to act as a barrier between the transplant and the immune system of the host [Draget *et al.*, 2005]. Different cells have been suggested for gel immobilization, including dopamine-producing adrenal chromaffin cells for treatment of Parkinson's disease [Aebischer *et al.*, 1993]. However, major interest has been focused on insulin-producing cells for treatment of Type I diabetes. Alginate/poly-L-lysine capsules containing pancreatic Langerhans islets have been shown to reverse diabetes in large animals and currently are being clinically tested in humans [Soon-Shiong *et al.*, 1993; Soon-Shiong *et al.*, 1994].

Entrapment of cells within calcium-alginate spheres has also become the most widely used technique for the immobilization of living cells [Smidsrod and Skjak-Braek, 1990].

Mooney and co-workers have studied alginate that contain covalently bound the adhesion RGD peptide sequence as a substrate for growth of a variety of cell types *in vitro* [Rowley and Mooney, 2002]. Mooney's group also successfully transplanted calvarial osteoblasts [Alsberg *et al.*, 2001], pre-adipocytes [Halberstadt *et al.*, 2002], fibroblasts [Marler *et al.*, 2000] and cotransplants of calvarial osteoblasts and chondrocytes [Alsberg *et al.*, 2002] immobilised within the modified gel *in vivo* using modified alginate scaffolds. Other studies reported data retention of cell function and differentiation using alginate as a matrix. In addition, chondrocytes have been shown to maintain a stable differentiated phenotype when cultured in alginate as compared to 2-D cultures [Hauselmann *et al.*, 1994].

Peptide modified alginates have been also employed as potential scaffolds for skeletal muscle engineering [Rowley and Mooney, 2002]. Alginate hydrogels have also shown potential as Schwann cell matrices in the area of nerve grafting [Mosahebi *et al.*, 2001] and as scaffolds to promote hepatocyte function and synthesis of liver specific proteins [Glicklis *et al.*, 2000]. A recent study [Wang *et al.*, 2003] has demonstrated that purified, unmodified alginate gels with a high guluronic acid content are able to support proliferation of rat marrow cells and their differentiation along the osteoblastic lineage. However, in two separate studies, both rat neonatal cardiac cells and human MSCs were shown not to proliferate after immobilization in unmodified alginate scaffolds [Dar *et al.*, 2002; Ma *et al.*, 2003].

There are still several important issues that need to be addressed prior to the feasibility of using alginate scaffold materials for tissue engineering applications in a clinical setting. These include tailoring the alginate's micro-architecture in a way that permits vascularization of the newly formed tissue; controlling the alginate's decomposition and degradation and its clearance from the body, and ensuring its biocompatibility through purification techniques that remove immune response invoking impurities.

However, in many cases, alginate has already demonstrated the potential to act as an optimal scaffold material for different cell transplantation and tissue-engineering applications, in particular for structural tissues such as soft tissue, cartilage,

myocardium, bone and liver. These encouraging results, together with the lack of studies demonstrating the suitability of the alginate as scaffold material for the preparation of tissue engineered vascular grafts, justify and drive interest on studies investigating alginate in this particular field.

### ***1.4 The role of bioactive molecules and oxygen tension in the in vitro environment***

As already mentioned (see section 1.1.2), tissue engineering principles are based on the utilization of three primary components: the biomaterial, the cells and the biomolecules, which serve to integrate and to functionally regulate the behaviour of the first two. Biomolecules are regulatory molecules that function as mediators of cell communication and can exert multiple biological functions by interaction with specific cell surface receptors. Bioactive molecules include agents with a large diversity of functions that are key to either the assembly and structural integrity of tissue engineered constructs or to the functional parameters of these constructs.

This chapter describes the roles of the animal serum and the soluble growth factors that are normally added to the basal medium in which the cells are grown in routine culture techniques. In addition, a brief description of the role of some insoluble ECM macromolecules that can be used as additional supplements in the medium formulation or can be coated to the surface of the culture vessels or added to the scaffold material in cell culture applications is provided. Finally, the effects of the oxygen tension and oxidative stress on cell proliferation potential are presented.

#### **1.4.1 Growth medium**

All isolated cells cultured *in vitro* need an artificial environment that allows growth and proliferation. Cell cultures must be maintained regularly to prevent overgrowth, accelerated cell death from exhausted medium, and to promote the growth of the next generation of cells [Palsson and Bhatia, 2004]. The liquid or “medium” in which cells are grown and expanded in culture provides inorganic salts, amino acids, carbohydrates, vitamins and other nutrients important for cell

maintenance *in vitro*. Table 1.1 lists major components found in commercially available tissue-culture media. Medium formulation is typically tailored for each cell type – some aspects mimic the physiological environment (pH, osmolarity), others are supra-physiologic (hormones, nutrients), and some are non-physiologic (indicator dyes, antibiotics) [Berthiaume, 1998].

Medium components	Amount	Physiological range	Purpose
Sodium chloride	6-8 g/L	5.55 – 6.14 g/L	Adjusts osmotic pressure
Inorganic salts	0.8-1 g/L	NA	Provide electrolyte balance similar to blood
Sodium bicarbonate	2-3 g/L	1.85-2.52 g/L	Provides buffering capacity, with appropriate CO <sub>2</sub> level in the gas phase, maintains pH at 7.4
D-glucose	1 g/L	0.81-1.04 g/L	Source of energy, carbon
Amino acids	1 g/L	NA	Sources of nitrogen for protein synthesis
Vitamins	0.01 g/L	NA	Cofactors in various intracellular biochemical reactions
Phenol red	0.01 g/L	NA	Visual pH indicator
Serum (see fig.1.13)	1-20 % v/v	NA	Provides cell growth, attachment factors, hormones, carrier proteins
Growth factors, hormones	1-10 microg/L	NA	Stimulate growth, functions
Antibiotics	1-50 microg/L	NA	Prevent contamination by microorganisms

**Table 1.1:** Major components found in tissue-culture media [Palsson and Bhatia, 2004].

Typically, a synthetic basal medium is chosen to meet the environmental and nutritional requirements of a given cell line. However, basal media formulations normally will not support cell growth alone, but must be further supplemented with animal serum.

### **1.4.2 Serum**

Serum is a fraction of whole blood. Plasma is the non-cellular fraction of blood, whereas serum is the liquid that remains after plasma is allowed to clot. Sera are typically added to culture medium in a proportion of approximately 1 to 20 % by volume. Common tissue culture sera are newborn calf (NCS), fetal bovine (FBS), horse (equine), pig (porcine), and human. Fetal bovine serum (FBS) has been adopted as the standard supplement because of its rich content of growth factors and its low gamma globulin content [<http://www.cellgro.com> Mediatech, Inc. Cell Culture Reference Guide]. Historically, medium containing fetal bovine serum has been used for culture of a wide range of cell types.

As seen in table 1.2 [Palsson and Bhatia, 2004], sera are very complex supplements containing mostly proteins but also important growth factors, adhesion factors, minerals, lipids, enzymes and hormones that can be key to successful tissue culture.

Constituent	Effect on cells
Albumin, globulins, transferrin	Carriers for fatty acids, iron, etc.
Fibronectin, fetuin	Attachment factors
Alfa2-macroglobulin	Inhibits proteases
Growth factors and growth hormones	Promote cell proliferation
Hormones (e.g. insulin and corticosteroids)	Stimulate uptake of glucose and amino acids; alter growth rate
Carbon and nitrogen sources	Nutrients
Minerals and trace elements	Essential for the activity of metalloenzymes
Inhibitors	Inhibit cell proliferation

**Table 1.2:** Main constituents of serum [Palsson and Bhatia, 2004].

Despite the beneficial effects, the use of sera has some significant disadvantages, including batch-to-batch variability, the presence of adventitious agents, product availability, interference with detection of cell products, and potential regulatory hurdles. Moreover, sera contain a wide range of minor components that may potentially affect cell growth. These minor undefined components, including nutrients such as amino acids, nucleosides and sugars, are inherent to sera and may affect various parameters of particular importance [<http://www.cellgro.com> Mediatech, Inc. Cell Culture Reference Guide]. In order to minimize these variables there has been a move towards the use of serum-free media.

Removal of bovine serum from organ culture medium is necessary also because of the potential risk of infection. Bovine serum is the usual supplement in the medium for expanding human cells, however transmission of bovine diseases might be inevitable when such cells are introduced into the patient for tissue engineering applications. In addition, bovine serum proteins attach to the surface of the cells and the biomaterial. It is possible that transferring bovine serum proteins into patients elicits an unfavourable immune reaction [Yamamoto *et al.*, 2003]. Nowadays there is both a moral and legal imperative (European Directive 86/609/EEC as amended by

Directive 2003/65/EC) for scientists to use alternatives to animals in research wherever possible. To avoid all the above mentioned unfavourable possibilities, leading companies are supplying researchers with serum substitutes and serum-free media, which are used to support the maintenance and expansion of many cell types, including hematopoietic stem cells and other progenitor cells.

For instance, serum-free culture has been explored for human nasal epithelial cells (HUNEC) [Mattinger *et al.*, 2002], human corneal endothelial cells [Bednarz *et al.*, 2001] but, most importantly, for rhesus monkey and human embryonic stem cells ([Pei *et al.*, 2003; Amit *et al.*, 2003] respectively). A culture system for the growth and assay of human bone marrow stromal precursors under serum-deprived conditions has also been developed [Gronthos and Simmons, 1995]. As an alternative to serum-deprived conditions, human chondrocytes have been cultured in a medium supplemented with autologous serum, and then transplanted into the patient's cartilage defects [Brittberg *et al.*, 1994]. Moreover, the effects of human serum on the *in vitro* differentiation of human bone marrow fibroblasts into adipogenic and osteogenic cells have been investigated [Oreffo *et al.*, 1997]. Human bone marrow derived MSCs have also been cultured in human and rabbit sera [Kuznestov *et al.*, 2000] or in autologous serum [Yamamoto *et al.*, 2003] to test the hypothesis that these cells can be successfully expanded *ex vivo* without losing their potentiality for osteoblastic differentiation even in an FBS-free culture system.

All these studies represent important prerequisites for future investigations on the role of serum in the regulation of cell proliferation, differentiation and development.

### **1.4.3 Growth factors**

To enhance cell proliferation, growth factors and other bioactive soluble macromolecules can be added directly to the growth medium or can be incorporated into the scaffold material. Growth factors play important regulatory roles in the control of the immune response, inflammatory reactions, cell proliferation and tumour growth [Yarden *et al.*, 1991]. They can stimulate or inhibit cell division, differentiation, migration and apoptosis, and they are involved in the regulation of several cellular processes such as gene expression, DNA and protein synthesis, and autocrine and paracrine factor release.



Some growth factors have demonstrated the ability to induce division of the endothelial cells and smooth muscle cells that represent the main cellular constituents of large blood vessels. These growth factors include:

- a) basic fibroblast growth factor (bFGF) – both endothelial and smooth muscle
- b) vascular endothelial cell growth factor (VEGF) – endothelial cells
- c) platelet-derived growth factor (PDGF) - smooth muscle cells
- d) epidermal growth factor (EGF) – smooth muscle cells
- e) endothelin-1 (ET-1) - smooth muscle cells

Each of these growth factors can interact with one another in an additive, cooperative, synergistic or antagonistic manner, and thus must be studied individually. For tissue engineering purposes, whether the cells are quiescent or activated, and whether they are in a two or three-dimensional culture environments, will influence the production of endogenous growth factor and consequently will also affect the response to exogenously applied bio-molecules.

#### **1.4.4 Insoluble ECM adhesion molecules**

The extracellular matrix (ECM) contains a number of proteins that contribute to both organizing the matrix and helping cells attach to it. Not surprisingly then, the composition and geometry of the ECM have both been shown to play a role in cell function. Due to the important effects of the ECM on cell behaviour, insoluble ECM molecules, such as fibronectin, laminin, or collagen, have been used to promote tissue regeneration in tissue engineering applications. These cue materials, together with the soluble factors such as growth factors or hormones normally added to the medium of culture, can be utilized to promote cell development and function [Gooch *et al.*, 1998].

Cell-ECM interactions can be controlled by modification of the solid substrate on which cells are grown. Polystyrene and other polymers normally employed in the preparation of tissue culture vessels can be improved just by coating the surface with ECM molecules such as collagen or fibronectin. Many tissue culture plates are currently treated with these molecules to improve cell binding.

As already mentioned (see section 1.3.3), biomaterial scaffolds can also be treated with the RGD and other short peptide sequences derived from cell binding regions of ECM proteins in order to achieve biospecific cell adhesion [Gooch *et al.*, 1998].

Culture surfaces modified with fibronectin are currently investigated for cell culture by several groups. Fibronectin, a large glycoprotein found in all vertebrates, was the first non-collagen ECM proteins to be well characterized [Alberts *et al.*, 1994]. Human fibronectin (HFN) sometimes serves as a general cell adhesion molecule through its central-binding domain RGD sequence. The apparent function of fibronectin is to mediate cell attachment by interacting with cell surface receptors and extracellular matrix components ([Hynes, 1985]; [Rouslahti, 1988]). HFN is not only used as a substrate to promote cell attachment; it is involved in many other cellular processes, including cellular migration during wound healing, tissue repair and development, embryogenesis, blood clotting, and haemostasis/thrombosis.

Also Matrigel, a solubilized basement membrane preparation commercially available, is currently used for several cell culture applications. According to the manufacturer's (Becton-Dickinson Biosciences, Oxford, UK) specifications, ordinary matrigel contains (as a proportion of protein by weight) 56% laminin, 31% type IV collagen, 8% entactin, 5% heparan sulfate proteoglycans.

Both fibronectin and matrigel are used as substrates for growth and differentiation of different cell types.

#### **1.4.5 The role of oxygen in cell culture**

Metabolically active cells are also consuming and producing dissolved gases (oxygen and carbon dioxide). Cell viability and function are in fact dependent upon both nutrient supply and oxygenation. As a consequence, the *in vitro* growth characteristics of cells are subject to dissolved oxygen tension, among many other culture-related factors, such as the already described media formulation and growth factors supplementation [Parrinello *et al.*, 2003].

Oxygen consumption can be a critical variable for certain cell types (for example hepatocytes consume five- to ten-fold more oxygen than other cells). Oxygen delivery in culture is different than oxygen delivery *in vivo* because of the lack of red blood cells (with haemoglobin) as oxygen carriers. Therefore, in culture, oxygen delivery is

limited by two factors: 1) the relatively low solubility of oxygen in media at body temperature (1.19  $\mu\text{M/mm Hg}$ ) and 2) transport of oxygen from gas phase to cell surface [Palsson and Bhatia, 2004].

Standard culture conditions use dissolved oxygen tension levels (20%-21%) that are hyper-physiologic for many cell types, including articular chondrocytes and bone-marrow derived MSCs, which are adapted to relatively low oxygen levels ( $< 10\%$ ) *in vivo* [Scott, 1992]. This suggests that excessive oxidative stress may limit the growth potential of cells under standard conditions. Indeed, it has been shown that MSCs cultured in low oxygen outgrow their high oxygen counterparts by at least 2-fold [Moussavi-Harami *et al.*, 2004], suggesting that high oxygen levels are stressful to MSCs and limit their *in vitro* growth by inducing senescence. Culture-induced stress is probably an important factor affecting the *in vitro* growth of MSCs, and it is possible that preventing oxidative stress might help in overcoming this barrier. Lowering incubator oxygen levels may represent an effective and simple means to that end, but other modifications of standard conditions, such as the addition of antioxidants to the culture medium, might confer additional protection against oxidative damage. Moreover, even routine cell culture procedures such as initial cell isolation and trypsinization are potential sources of oxidative stress. Such occasional stress exposures might impact growth even in cultures exposed most of the time to low oxygen conditions.

The attenuation of growth imposed by culture-related stress seriously restricts cell yields and may have a negative impact on subsequent differentiation of MSCs and chondrocytes.

Recent studies [Moussavi-Harami *et al.*, 2004] have proved that low oxygen culture is an effective means to control oxidative stress and to increase the proliferative potential of MSCs and chondrocytes destined for grafting procedures. Other investigations have demonstrated that a low oxygen atmosphere significantly affects rat marrow MSCs' proliferation, differentiation and mobilization into the peripheral blood [Lennon *et al.*, 2001; Rochefort *et al.*, 2006;]. Hypoxic conditions have also proved to be necessary to maintain full pluripotency of human embryonic cells [Ezashi *et al.*, 2005].

However, additional studies will be needed to determine what are likely to be diverse phenotypic effects of oxidative damage on human marrow-derived MSCs.

### ***1.5 The goals of the present thesis***

The driver for this research stems from the ability to create viable three-dimensional alginate/hMSCs constructs and to define the optimal culture conditions where the cells display the ability to proliferate while retaining their original undifferentiated status and multipotentiality.

In order to accomplish this, the investigations of this research have been carried out at three levels.

Firstly, studies on the alginate matrix itself were conducted with the intention of optimising the carbodiimide coupling reaction between alginate and peptide, in order to enhance the efficiency of the derivatisation chemistry and to prepare a three-dimensional alginate matrix that permits cell adhesion and cell proliferation. In addition, NMR methods and amino acid analysis were performed to help characterising the resulting matrix and to quantify the degree of peptide attachment.

Secondly, the effects of some important culture parameters on MSCs' viability, proliferation and metabolism were investigated in a two-dimensional culture environment (tissue culture plates). In particular, attention was focused on changing medium composition in respect of serum concentration and FGF-supplementation, on modifying the plastic surface of the vessels through coating with different biomolecules, and on testing different oxygen tensions.

Finally, the cells were combined with the GRGDY-modified alginate matrix and the optimal parameters identified in the two-dimensional environment were applied to the resulting three-dimensional constructs. Investigations were performed on the constructs in order to evaluate the cells ability to retain their initial viability and original undifferentiated status, and to determine the degree of cell proliferation.

## **2. Materials and Methods**

### **2.1 Human Mesenchymal Stem Cell culture in tissue culture vessels**

#### **2.1.1 Isolation of human mesenchymal stem cells from frozen bone marrow samples**

The multipotent Mesenchymal Stem Cells (MSCs) used in this study were isolated from frozen human bone marrow samples received from the Department of Haematology, UCLH. The use of human clinical samples had been approved by the University College London Hospital Ethics of Human Research Committee (project reference number 03/0136). The mononuclear cells were isolated from frozen bone marrow samples stored in a liquid nitrogen container (Biostore 10) deploying a Ficoll gradient.

This procedure is described for a total volume of thawed diluted sample of 120 mL (typically the amount of the original sample after thawing was around 125-150 mL, the sample was diluted 1:2 and however only 120 mL of the total diluted sample was used).

First of all, 120 mL of the original thawed bone marrow sample was filtered through a 40µm nylon cell strainer (Falcon, Bibby Sterilin, Stone, UK). 100 mL of the resulting material was transferred in a 250 mL sterile bottle (Nalgene/Fisher) and was then rinsed with an equal volume (100 mL) of Dulbecco's phosphate buffered saline without calcium and magnesium (PBS, Biowhittaker, Walkersville, MD, USA). 6x20 mL aliquots of sterile Ficoll (density 1.077g/mL, Ficoll-Paque Plus, Stem Cell Technologies Inc., Vancouver BC) was poured into 6x50 mL centrifuge tubes (Corning, Acton, MA, USA) and 20 mL of the diluted bone marrow sample was then very slowly added to the edge of each tube such that the sample remained above the Ficoll surface. During this procedure the centrifuge tube was held at a sharp, slanted angle in order to increase the surface area on the top of the liquid and to create a clear phase separation between the Ficoll layer (at the bottom of the tube) and the sample (at the top of the Ficoll phase), avoiding mixing of the two layers.

A 30 minutes centrifugation at 650g, room temperature (20°C), and with no brake applied (5810R Centrifuge, Eppendorf AG, Hamburg, Germany) was performed in order to fractionate most of the red blood cells to the bottom of the tube, while maintaining the mononuclear cells at the interface of the Ficoll liquid. After centrifugation, the mononuclear cells were carefully removed from the tube without disturbing the Ficoll interface.

Approximately 5-6mL was collected (maximum of 10mL) from each tube and transferred into a new 50mL centrifuge tube. The cells were rinsed with approximately 40mL of PBS per tube and then centrifuged at 650g for 15 minutes, at room temperature (20°C), using a low brake setting. After discarding the supernatants, the cell pellets were gently resuspended and pooled together with a total growth medium volume of 12mL, and the cell suspension was equally divided into 3 vented T150 flasks (Corning, 150cm<sup>2</sup>) already filled with 26mL complete growth medium (total volume within each flask was approximately 30mL). The flasks were then placed at 37°C in a 5% CO<sub>2</sub> humidified incubator (HeraCell150, Kendro Laboratory Products GmbH, Langenselbold, Germany or Galaxy S, RS Biotech Laboratory Equipment Ltd., Irvine, Scotland) for 2 days to allow the hMSCs to attach to the plastic surface. The spent medium containing non-adherent cells was then removed and replaced with fresh complete medium of culture. While waiting for the hMSCs to become visible (ca. 7 days) and ready for passaging (ca. 2-3 weeks), fresh complete growth medium was added every 4-5 days. After reaching approximately 70-80% confluency, the cells were trypsinised, counted with an haemocytometer and split into the required number of new vented T75 or T150 flasks in order to have an initial cell seeding density (ICD) of  $5 \times 10^3$  cells/cm<sup>2</sup> (see sections 2.1.3 and 2.6.2). The flasks were labelled as passage 2 (p2) and incubated at 37°C in an atmosphere of 5% CO<sub>2</sub>. When the resulting second passage cells were 70-80% confluent, they were either passaged again at the same ICD and labelled as passage 3 cells, or frozen in liquid nitrogen.

### **2.1.2 *In vitro* culture of human Mesenchymal Stem Cells**

The *in vitro* expansion of hMSCs was performed in sterile, polystyrene T150 tissue culture flasks (150cm<sup>2</sup>) (Corning Life Science, Corning, New York) with 30mL

complete growth medium/ flask ( $0.2\text{mL}/\text{cm}^2$ ). The flasks were factory treated with a plasma charge, which introduces a hydrophobic, negatively charged surface. The cultures were maintained in a 5%  $\text{CO}_2$ ,  $37^\circ\text{C}$  humidified incubator and the cells were expanded in culture at 70-80% confluence (as described in section 2.1.3) and plated in new T150 flasks at the initial cell density of  $5 \times 10^3$  cells/ $\text{cm}^2$  ( $7.5 \times 10^5$  cells/flask). The culture medium was removed from the flasks and replaced with fresh and pre-warmed ( $37^\circ\text{C}$ ) medium ( $30\text{mL}/\text{flask} = 0.2\text{mL}/\text{cm}^2$ ) every 3-4 days of culture to provide the cells with the necessary nutrients and growth factors and to remove metabolic products.

Different culture conditions were compared and evaluated in this research, as described in section 2.1.5.

### **2.1.3 Cell expansion in tissue culture vessels**

Human MSCs were harvested from their T150 tissue culture flasks with a trypsin/EDTA solution.

After removing the spent medium, each flask was rinsed with 20mL PBS without calcium and magnesium ( $0.1\text{mL}/\text{cm}^2$ ) (BioWhittaker) to remove residual serum proteins that reduce trypsin activity. Each flask was treated with 6mL ( $0.04\text{mL}/\text{cm}^2$ ) of 0.25% trypsin/0.02% EDTA (Sigma-Aldrich, LTD, Irvine, Ayrshire, UK). The enzymatic solution was spread over the whole growth surface and was left in action for 5-7 minutes at room temperature ( $20^\circ\text{C}$ ). The flasks were then gently tapped against the palm of the hand in order to completely detach the hMSCs from the surface of the culture vessel. Trypsin activity was then quenched with 12mL ( $0.08\text{mL}/\text{cm}^2$ ) of complete cell growth medium per flask. Since trypsin is a non-specific protease that could permeate the cell membrane, the cells were never exposed to the trypsin solution for periods longer than 10 minutes. The cell suspensions from all individual flasks were combined together and gently mixed with a sterile pipet to ensure homogeneity of the final cell suspension. A 0.5mL volume sample was used for the determination of cell density with haemocytometer and for the cell viability assay with trypan blue dye (section 2.1.3, 2.6.2 and 2.6.3). The cell suspension was then centrifuged within a 50mL centrifuge tube at 100g for 5 minutes. After discarding the supernatant, the cell pellet was resuspended with the necessary volume

of complete cell growth medium. The resulting cell suspension was transferred within new T150 tissue culture flasks so that the initial seeding density ICD was  $5 \times 10^3$  cells/cm<sup>2</sup> ( $7.5 \times 10^5$  cells/flask). The volume of cell suspension within each flask was adjusted to a final value of 30mL ( $0.2 \text{ mL/cm}^2$ ) by addition of the necessary amount of complete growth medium, pre-warmed at 37°C. The flasks were incubated and re-fed with complete cell growth medium as previously described (section 2.1.2).

#### **2.1.4 Creation of a working cell bank**

In order to create a supply of low-passage cells for future experiments, a working cell bank of fourth passage (p4) hMSCs was created from cells isolated from a frozen bone marrow sample.

Five vented T150s of 80-90% confluent cells were harvested and trypsinised as described in section 2.1.3. The cells were treated with 6mL of 0.25%trypsin/0.02%EDTA (Sigma) per flask until the cells had completely detached from the cell growth surface (approximately 5 minutes). Complete DMEM medium (12mL/flask) was added to quench trypsin activity and the resulting cell suspensions were removed from the flasks, pulled together and equally divided into two 50mL centrifuge tubes. A 0.5mL volume sample was taken from each tube and used for the determination of the cell density with haemocytometer and for the cell viability with trypan blue dye, as described in sections 2.6.2 and 2.6.3. The cell suspensions were centrifuged at 160g for 5 minutes. After discarding the supernatants, the two cell pellets were combined together and resuspended in 4mL of complete DMEM medium. Another cell count was performed after centrifugation to confirm the cell concentration and ensure that no significant cell loss had occurred during the centrifugation step.

3.6mL of complete DMEM medium were added to the resulting cell suspension. Finally 1.9mL (20%) of cryopreservation medium containing 75% fetal bovine serum (FBS, Biowhittaker) and 25% DMSO (Sigma) were slowly added to the cell suspension (final cell concentration =  $1 \times 10^6$  cells/mL). The total cell suspension (approximately 9.5mL) was equally aliquoted into 9 cryopreservation vials (Nalgene, 1mL cell suspension/vial), which were then placed overnight in the -80°C freezer within a controlled rate freezer container (Nalgene TM Cryo 1°C Freezing Container,



-1°C/min=rate of cooling) before transfer into liquid nitrogen (-196°C) for long-term storage.

### **2.1.5 Protocols of hMSCs culture using different basal media, different serum and fibroblast growth factor concentrations, different coatings and oxygen tensions**

Taking into account the lack of a uniform approach for hMSC isolation and expansion between laboratories, various culture conditions were compared in this research with the purpose of first identifying an optimal laboratory protocol for hMSCs expansion with a view to later large-scale production, while maintaining their multipotency.

Several culture parameters, including the quality of fetal calf serum, basal medium, glucose concentration, bone marrow mononuclear cell plating density, hMSC passaging density, and surface characteristics of the tissue culture vessels are known to affect the final outcome [Sotiropoulou *et al.*, 2006]. Also the use of basic fibroblast growth factor (FGF), the most common growth supplement in hMSC culture media, importantly influences cell proliferation and differentiation potential [Pitaru *et al.*, 1993; Savion *et al.* 1996; Majors and Muschler, 1996].

In this study attention was focused on the following parameters:

- Basal cell growth medium
- Fetal bovine serum (FBS) concentration
- Surface coating of tissue culture vessels
- basic Fibroblast Growth Factor (bFGF) supplementation
- Oxygen tension

#### **2.1.5.1 Basal growth medium**

Two different growth media were compared for the *in vitro* expansion of hMSCs.

Complete MesenCult medium, obtained supplementing the basal MesenCult medium (Stem Cell Technologies Inc., Vancouver, British Columbia, Canada) with 10% (v/v) Mesenchymal Stem Cell Stimulatory Supplement (Stem Cell Technologies

Inc.), 100U penicillin/mL, 100 $\mu$ L streptomycin/mL (both from BioWhittaker, Walkersville, MD, USA) and 1ng/mL recombinant human fibroblast growth factor (rhFGF) (R&D Systems, Minneapolis Minnesota, USA); and low-glucose (1 g/L) Dulbecco's Modified Eagles Medium DMEM (Biowhittaker), which was supplemented with the same reagents (Mesenchymal Stem Cell Stimulatory Supplement, penicillin, streptomycin and recombinant human fibroblast growth factor (rhFGF)) added in the same concentrations as for the MesenCult medium.

Fourth passage (p4) bone marrow-derived hMSCs were expanded in 12-well tissue culture plates with either complete MesenCult medium or complete DMEM medium, formulated as described above. In addition, these media were used for the cell expansion also in their serum-free formulation, or after addition of only 2% (v/v) serum. The Mesenchymal Stem Cell Stimulatory Supplement from StemCell Technologies Inc., which was found to consist only of Fetal Bovine Serum supplemented with l-glutamine, was used for the serum-supplementation of both the MesenCult and the DMEM media. The cultures were maintained at 5% CO<sub>2</sub>, 37°C for a 12-day period. During the course of the culture, the plates were re-fed every 2-3 days in order to provide the cells with the necessary nutrients and growth factors and to remove metabolic products. The cells were trypsinised at 4 different time-points during the culture for the evaluation of the cell density and viability, as measured with haemocytometer and trypan blue dye. This experiment was repeated twice, always with p4 MSCs; the results of these studies are discussed in section 4.3.

After a few preliminary studies, the basal low-glucose DMEM medium was supplemented with 10% (v/v) Fetal Bovine Serum (FBS) screened for hMSCs (Stem Cell Technologies Inc.), 2mM l-glutamine, 100U penicillin/mL and 100 $\mu$ L streptomycin/mL (both from BioWhittaker) and 1ng/mL recombinant human fibroblast growth factor (rhFGF) (R&D Systems). This was the standard formulation for the DMEM medium, which was subsequently adopted for the expansion of the hMSCs used in this research, and it will be referred to as "complete DMEM" for the remainder of this thesis.

## **2.1.5.2 Serum supplementation**

### **2.1.5.2.1 Fetal Bovine Serum concentration**

The standard 10% FBS-supplemented complete DMEM formulation was compared to DMEM growth medium equally supplemented with l-glutamine, penicillin, streptomycin and recombinant human fibroblast growth factor, but supplemented with different (0%, 2% and 15%) FBS concentrations. The serum used in this research was fetal bovine serum (FBS) specifically selected by the manufacturer (Stem Cell Technologies) for optimal hMSCs growth.

The cells were plated in 24-well plates ( $ICD=5 \times 10^3$  cells/cm<sup>2</sup> or  $9.5 \times 10^4$  cells/well) and cultured with the different media formulations. The cells were harvested at different time-points over the 13-15 days culture period. At each time-point the cell density and viability were determined with haemocytometer and trypan blue (see sections 2.6.2 and 2.6.3.) and the cell metabolism was evaluated with the Nova Biomedical Bioprofile Analyzer (see section 2.6.5). The experiment was performed twice and the results obtained for the serum studies are presented in section 4.4.1.

### **2.1.5.2.2 Serum-free media experiment**

A preliminary qualitative experiment was performed where hMSCs were cultured in different serum-free media, in order to see whether any of these formulations permitted, promoted or halted cell growth. The following commercially available serum-free media were tested:

No.	Medium	Manufacturer	Cat. no.
1	CD Hybridoma Medium without L-glutamine	Gibco	11279-023
2	Stem Pro-34 SFM without L-glutamine without antibiotics	Gibco	10640-019
3	Protein free Hybridoma Medium PFHM II (1X)	Gibco	12040-051
4	Hybridoma-SFM serum-free Hybridoma Medium	BioWhittaker	12045-084
5	Ultraculture medium	BioWhittaker	BW12-725F
6	UltraDOMA Hybridoma serum-free growth Medium, defined 1X	BioWhittaker	BW12-723B
7	Knockout D-MEM optimised D-MEM Medium for ES cells	Gibco	10829-018
8	Ex-cell 325 PF CHO serum-free Medium, protein-free	SAFC Biosciences	14340C
9	Ex-cell 302 CHO serum-free Medium	SAFC Biosciences	14324C
10	Ex-cell 620-HSF hybridoma serum-free Medium	SAFC Biosciences	14621C
11	Ex-cell CD CHO serum-free Medium, chemically defined	SAFC Biosciences	14361C

**Table 2.1:** Serum-free media investigated for the expansion of hMSCs in tissue culture flasks. Following the manufacturer's suggestion, the Knockout D-MEM medium (medium number 7 on the table) was supplemented with 15% Knockout Serum Replacement (Gibco, Cat. No.=10828).

The cells used for this experiment were obtained from a third passage (p3) working cell bank. Cryopreservation vials of hMSCs were removed from liquid nitrogen storage and were thawed within a 37°C water-bath for exactly two minutes and then transferred to T25 tissue culture flasks (Corning, 25cm<sup>2</sup>). The cells were expanded at the standard culture conditions (complete DMEM medium, 5% CO<sub>2</sub>,

37°C and 21% oxygen) for two passages before reaching the desired cell number. [The cell banking and passaging protocols are described in detail in section 2.1.4 and 2.1.3 respectively.] The sequential adaptation protocol here described was then followed for each one of the 11 serum-free media under investigation and listed in table 2.1. Actively dividing, high (> 90%) viability cells were used. Sixth passage (p6) cells were inoculated at double the normal seeding density ( $10 \times 10^3$  cells/cm<sup>2</sup>) in a 50:50 (v/v) mixture of traditional serum-supplemented DMEM : one of the serum-free media investigated. The cultures were monitored until the confluency reached approximately 80%. The cells were then sub-cultured into a 10:90 (v/v) mixture of serum-supplemented DMEM : serum-free medium. When 80% confluency was reached again the cells were sub-cultured into 100% serum-free medium. Two T25 control flasks were maintained in the standard complete DMEM medium formulation throughout the whole experiment. At each expansion passage the cells were split in 1:2 ratio without performing any cell count with haemocytometer, as the present was purely a preliminary exercise performed to obtain information on cell survival and to monitor significant cell morphology changes in the different serum-free culture media tested.

Light microscopy was used for the qualitative assessment of cell growth, proliferation and morphology. In particular, significant change in cell density and cell morphology were observed. These results are presented in section 4.4.2.

#### **2.1.5.2.3 Surface coatings of tissue culture vessels**

The effects of different surface coatings on the hMSCs proliferation and expansion potential were evaluated by comparing the culture within 24-well uncoated tissue culture plates (353047, Falcon, Becton Dickinson Labware Franklin Lakes, NJ, USA) with the culture of the same cells maintained in 24-well tissue culture plates coated by the supplier with either human fibronectin or with a thin Matrigel basement membrane matrix layer (Becton Dickinson Labware, Bedford, MA). The cells were seeded at an ICD of  $5 \times 10^3$  cells/cm<sup>2</sup> ( $9.5 \times 10^4$  cells/well) and fed with 1mL complete DMEM/well. The three different coating conditions described were also tested using rhFGF-free or serum-free DMEM formulations, or with DMEM medium supplemented with different serum concentrations. The cells were harvested at different time-points over the 13-15 days culture period. At each time-

point the cell density and viability were determined with haemocytometer and trypan blue (see sections 2.6.2 and 2.6.3) and the cell metabolism was evaluated with the Nova Biomedical Bioprofile Analyzer (see section 2.6.5). The experiment was repeated twice and the results obtained for the coating studies are presented in chapter 4.

#### **2.1.5.2.4 Human recombinant Fibroblast Growth Factor supplementation**

The standard formulation of the complete DMEM culture medium included supplementation with 1ng/mL human recombinant basic Fibroblast Growth Factor (bFGF).

To investigate the effects of bFGF-supplementation on the growth potential of human MSCs, p4 hMSCs were plated at the usual ICD ( $5 \times 10^3$  cells/cm<sup>2</sup>) in non-coated 24-well tissue culture plates and cultured for a 13-day period. The cells were expanded in low-glucose (1g/L) DMEM medium in standard culture conditions (10 % v/v FBS and 1 ng/mL bFGF supplementation). In addition, hMSCs were cultured in the plain basal (serum-free and bFGF-free) low-glucose DMEM medium, and in the same medium supplemented with increasing serum concentrations (2%, 10% or 15%). For each serum concentration, both the bFGF-free and the bFGF-supplemented conditions were tested. As usual, the cells were re-fed every 2-3 days over the 13-day period of culture, thus ensuring the provision of nutrients and growth factors together with the removal of metabolic products. The cells were harvested as previously described (section 2.1.3) at day 3, day 7, day 10 and day 13 of culture, i.e. when the 80% cell confluence was reached on the surface of the well plates. At each time-point the cells were harvested and assessed for cell count and cell viability as previously described (sections 2.6.2 and 2.6.3 respectively), and for each serum and bFGF condition a sample of the spent medium was recovered and assessed with the Nova Biomedical BioProfiler for the analysis of the cells metabolic activity, following the protocol elucidated in section 2.6.5.

The experiment was performed twice and the results obtained for the bFGF studies are presented in section 4.5.

#### **2.1.5.5 5 Dissolved oxygen tension**

Where it is not otherwise specified, the humidified incubator for the culture of hMSCs was maintained at 5% CO<sub>2</sub>, 37°C and 21% O<sub>2</sub>. 21% oxygen levels are normally used in standard incubators and standard culture conditions, as they permit optimal growth of fibroblasts. However, MSCs live at relatively low oxygen levels *in vivo* [Grant and Smith, 1963; Ishiwaka and Ito, 1998; Harrison *et al.*, 2002; Grigoryan *et al.*, 2005], and the hyperoxic conditions employed in standard incubators can cause sufficient oxidative stress to induce premature senescence in MSCs, limiting their *in vitro* proliferation potential [Moussavi-Harami *et al.* 2004]. Modifying the oxygen tension is thought to have important effects on MSC growth and proliferation. For the purpose of evaluating the effects of oxygen tension on hMSCs proliferation rate and metabolism, the above-mentioned standard culture conditions were compared to low-oxygen (1% or 2%) and intermediate-oxygen (10%) culture conditions. The cells were cultured in 24-well plates and tested for cell proliferation and cell metabolism at different time-points in a similar way as for the previous culture conditions examined (sections 2.1.5.2, 2.1.5.3 and 2.1.5.4). Each experiment was performed twice and the results obtained for the studies on different oxygen tensions are presented in chapter 4.

### **2.2. An alternative cell source: cell passaging protocol in tissue culture vessels for human Fibroblasts**

The human foreskin fibroblasts used in this study (Karocell, Stockholm) were kindly provided by Dr. Stephen Minger, Wolfson Centre for Age-Related Diseases, King's College London. The cell growth medium was Iscove's modified Dulbecco's medium (IMDM) which had been supplemented by the manufacturer (Invitrogen, Paisley, UK) with 4mM glutamine and 25mM HEPES, and then further supplemented with 10% heat inactivated foetal bovine serum (Invitrogen, Paisley, UK) and 100U/mL penicillin/streptomycin (BioWhittaker, Walkersville, MD).

As for hMSCs, the fibroblasts were cultured in tissue culture flasks specifically treated by the manufacturer in order to encourage cell attachment to the plastic surface. The cells were cultured with 30mL medium/T150 flask (0.2mL/cm<sup>2</sup>) and

were usually expanded at a 1:3 split ratio, following the trypsinisation procedure already described (see section 2.1.3). Human fibroblasts were maintained in culture at 37°C and 5%CO<sub>2</sub> in a humidified incubator.

### **2.3 Preparation of the alginate scaffold**

The matrix used in this research for the three-dimensional studies with alginate/cells constructs consisted of sterile GRGDY-derivatised alginate. Alginate constructs have been extensively used in cell therapy and tissue engineering applications, mainly with secretory cells (e.g. islet cells) or transformed producer-cell lines that normally are expanded in suspension cultures [Read *et al.*, 1999; Mullen *et al.*, 2000; Tobias *et al.*, 2001]. However, mesenchymal stem cells are anchorage-dependent cells that need to interact with a substrate or biomaterial to survive [Saltzman, 2000]. Alginate and other hydrogels are unable to specifically interact with mammalian cells, due to their hydrophilic nature [Smentana, 1993]. It was therefore necessary to chemically modify the alginate hydrogel by covalently binding the pentapeptide cell adhesion ligand glycine-arginine-glycine-aspartic acid-tyrosine (GRGDY) containing the specific RGD sequence, which has shown to promote cellular anchorage and interaction with hydrogels [Rowley *et al.*, 1999; Chung *et al.*, 2002].

This section describes the preparation of alginate-GRGDY matrices. The preparation of alginate constructs including cells is described in section 2.5. A schematic representation of the standard alginate derivatisation method used in the present research is shown in figure 2.1.



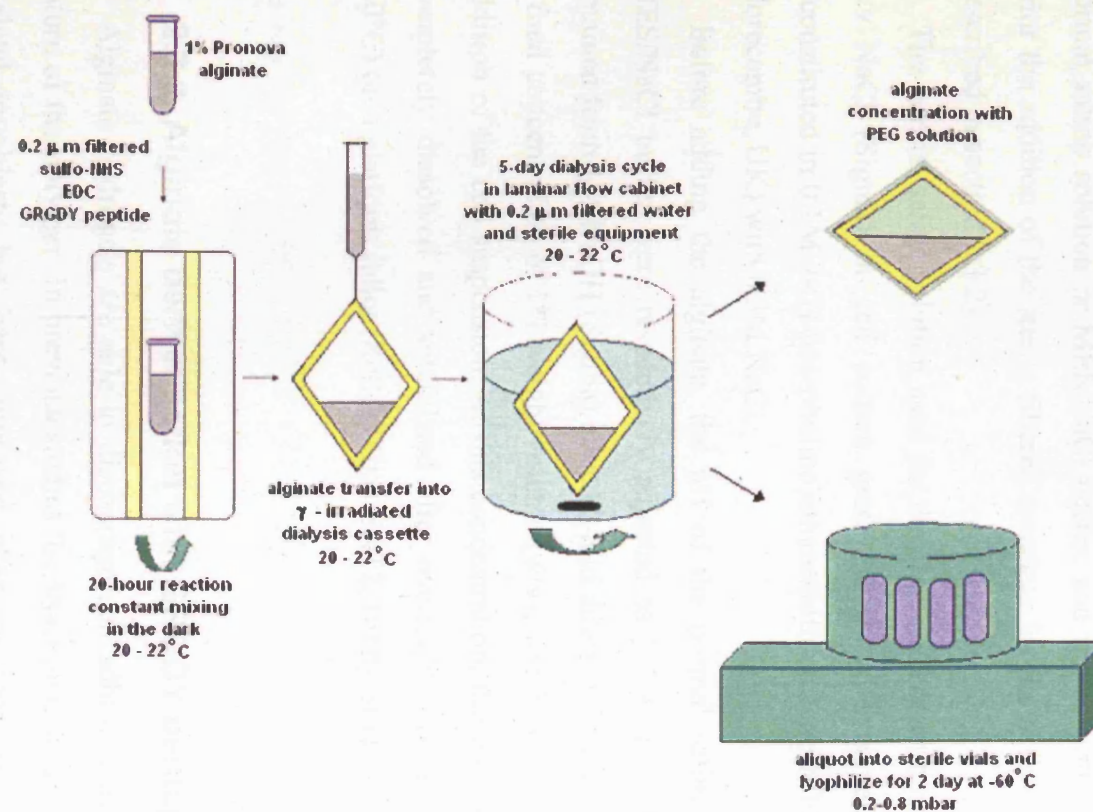


**Fig.2.1:** Schematic representation of the standard alginate derivatisation procedure for the coupling of the GRGDY pentapeptide to sodium alginate.

### **2.3.1 Reconstitution of the sodium alginate matrix**

Sodium alginate (please see section 1.3.4) was the scaffold material investigated in the present research.

The alginates used in this research were supplied as sterile freeze-dried products by NovaMatrix FMC BioPolymer AS, (Drammen, Norway). Different Pronova alginates were tested; the defining characteristics of these biomaterials, such as the guluronic acid content and molecular weight, were provided by the manufacturer (see table 3.2).

Vials of each sterile alginate were reconstituted as required with sterile filtered normal saline solution or MES/NaCl buffer, and mixed until visibly homogeneous prior the addition of the sterile filtered reactants for the derivatisation procedure (as described in section 2.3.2).

The normal saline solution used for the alginate reconstitution consisted of 0.9% w/v NaCl (Sigma) in cell culture grade water. Alternatively, the alginate was reconstituted in 0.1M 2-(N-Morpholino)ethanesulfonic acid (MES) buffer (Lancaster, Morecambe, UK) with 0.3M NaCl.

Before adding the alginate, the pH of the normal saline and the pH of the MES/NaCl buffer were respectively adjusted to 7-7.4 and 6.5 with 0.1M NaOH obtained from 1M NaOH (Sigma) after 10-fold dilution. The alginate was prepared at a final concentration of 1% weight/volume (w/v), which was isotonic for subsequent addition of the cell suspension. At this concentration, the water-soluble alginate was completely dissolved and solubilised after overnight mixing at room temperature (20°C) on a platform roller (Roller Mixer SRT2, Bibby Stuart Scientific, Stone, UK).

### **2.3.2 Alginate derivatisation with GRGDY pentapeptide**

Alginate hydrogels are able to discourage cell adhesion due to the hydrophilic nature of the polymer. In previous studies the attachment and proliferation of mouse skeletal myoblasts has been improved after incorporation of the pentapeptide GRGDY onto the polysaccharide chain of the alginate [Rowley *et al.*, 1999; Rowley and Mooney, 2002]. In this research, sodium alginate was covalently modified

utilizing aqueous carbodiimide chemistry in order to incorporate the pentapeptidic GRGDY sequence. The GRGDY pentapeptide was conjugated to the alginate's carboxylic acid groups on the uronic acid units of the polymer backbone through the terminal amine of the peptide, as it is schematically represented in Figure 2.2.

A water-soluble carbodiimide, 1-ethyl-(dimethylaminopropyl) carbodiimide (EDC), (Sigma-Aldrich Co., Ltd., Gillingham, Dorset, UK), was used to form amide linkages between amine containing molecules and the carboxylate moieties on the alginate polymer backbone. The amine-reactive O-acylisourea intermediate formed is prone to hydrolysis and thus will regenerate its carboxyl group, unless it encounters an amine. The co-reactant N-hydroxy-sulfosuccinimide (sulfo-NHS), (Pierce, Rockford, IL) was therefore added to stabilise the reactive EDC-intermediate against the competing hydrolysis reaction, raising the efficiency of amide bond formation. The amine-reactive intermediate was this way converted to a sulfo-NHS (N-hydroxysulfosuccinimide) ester, which then reacted with the amino terminus of the peptide. The EDC was converted to urea.

The peptide used in this research was supplied by two different suppliers, Neosystem Groupe SNPE, Strasbourg, France and Albachem, Edinburgh, and the whole procedure was performed in totally aseptic conditions, thus optimising the potential for the final derivatised product being sterile. A total of 12 derivatisation experiments, investigating different alginate types and alternative derivatisation procedures, were performed throughout the research.

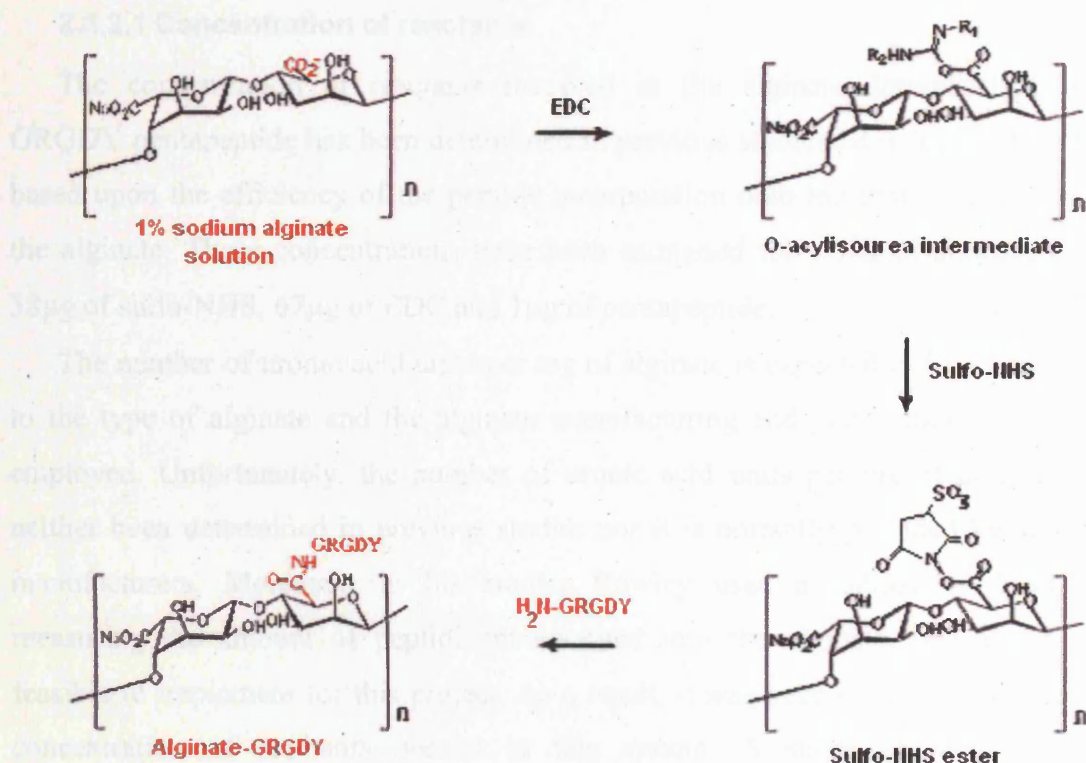


**Fig. 2.2:** Overall reaction for the alginate derivatisation with GRGDY pentapeptide. Amide bond formation is mediated by the carbodiimide through the carboxyl group on the uronic acid units of the alginate and the N-terminal amine of the pentapeptide. Adapted from Rowley, 1999.

The reaction was carried out in a 50mL sterile tube (Bibby Sterilin Ltd, Stone, UK) on a platform roller (Roller Mixer SRT2, Bibby Stuart Scientific, Stone, UK) in the dark, to avoid potential denaturation of the reactants involved in the reaction.

Particular care was taken in maintaining the temperature constant at room temperature (approximately 20-22°C) throughout the whole alginate derivatisation procedure. This was necessary because the temperature can significantly affect the carbodiimide reaction by modifying the reaction rates, the molecular mixing and the diffusion of molecules across the dialysis membrane [Markusen, 2005]. First, the sulfo-NHS was added to the alginate solution and mixed for 5 minutes; the EDC carbodiimide was then added to the solution and allowed to react on the roller for 30 minutes. Finally, the GRGDY pentapeptide was added to the tube and the resulting solution was mixed for a predetermined time period, typically 20 hours.

### 2.3.2.1 Concentration of reactants

The concentration of reactants involved in the alginate derivatisation with GRGDY pentapeptide has been determined in previous studies [Rowley *et al.*, 1999] based upon the efficiency of the peptide incorporation onto the uronic acid units of the alginate. These concentrations have been estimated for 1 mg of alginate to be 38µg of sulfo-NHS, 67µg of EDC and 1µg of pentapeptide.

The number of uronic acid units per mg of alginate is expected to vary according to the type of alginate and the alginate manufacturing and purification procedures employed. Unfortunately, the number of uronic acid units per mg of alginate has neither been determined in previous studies nor it is normally provided by alginate manufacturers. Moreover, in his studies Rowley used a radioactive label for measuring the amount of peptide incorporated into the alginate, which was not feasible to implement for this project. As a result, it was necessary to determine the concentration of reactants needed in this system. A series of range finding experiments has been previously performed in order to test several reactant concentrations for the carbodiimide reaction [Markusen, 2005]. In the present research, attention was focused on the use of highly purified alginate (Pronova SLG100), with high (approximately 148mPa·s) viscosity. In her studies [Markusen, 2005] Markusen showed that 9X and 12X were optimal reactants concentrations to achieve successful peptide incorporation onto the Pronova SLG100 alginate polymer. These concentrations were multiple of those defined by Rowley [Rowley *et al.*, 1999], more specifically 9X and 12X corresponded respectively to nine times and twelve times the reactants for 1mg of alginate (please see table 2.2). The reactants used for the carbodiimide reaction (sulfo-NHS, EDC and GRGDY peptide) were individually weighed and dissolved in a small volume (500µL) of water for cell culture applications (WFI, BioWhittaker) to the desired concentrations. The dissolved reactants were then filtered through 13mm syringe filters (0.2µm pore size) and finally added to the 1% w/v alginate solution (typical alginate volumes were 3-12 mL) in the reaction vessel as described in section 2.4.2. The sulfo-NHS and EDC were filtered using a low binding polytetrafluoroethylene (PTFE) membrane (Millex-LG, Millipore) whereas a low binding polyvinylidene fluoride (PVDF) membrane (Durapore, Millex-GV, MilliporeCorp., Bedford, Massachusetts, USA) was used for the filtration of the GRGDY peptide.

<b>Reactants' ratio</b>	<b>EDC concentration (µg)</b>	<b>Sulfo-NHS concentration (µg)</b>	<b>GRGDY concentration (µg)</b>
<b>1X (Rowley's)</b>	67	38	1
<b>9X</b>	603	342	9
<b>12X</b>	804	456	12

**Table 2.2:** Ratios of the reactants concentrations as used by Rowley (1998) and in the present research (9X and 12X) for the alginate derivatisation procedure. The values are expressed per mg of alginate.

### 2.3.2.2 Dialysis

After completion of the 20-hour reaction, a dialysis cycle was performed in order to reduce the levels of residual cell-toxic reactants, such as EDC, leftover from the carbodiimide reaction. The alginate-GRGDY was therefore dialysed for 5 days in Reverse Osmosis (RO) purified water (MilliQ Synthesis A10, Millipore, Molsheim, France) filtered through a UV irradiated 0.22 µm filter (Acropak 500 capsule, Pall, Ann Arbor, Michigan) using gamma-irradiated dialysis cassettes (Slide-A-Lyzer, Pierce, Rockford, Illinois) with a molecular weight cut-off (MWCO) of 3.5 kDaltons. The alginate was injected into the pre-wetted dialysis cassettes using a 20mL Leur-lock syringe with a 21 gauge needle (Becton Dickinson UK Ltd., Cowley, UK). The dialysis process deployed 5 litres beakers (Azlon, bibby Sterilin Ltd., Stone, UK) filled with 5 litres of RO purified and filtered water. The water was constantly mixed at low speed (approximately 80-120 rpm) and was changed every 12 hours, and the whole procedure was performed avoiding direct light exposure, at 20°-22°C, within a laminar floor hood (LFH). All aseptic operations were conducted using sterilized equipment.



### 2.3.2.3 Lyophilisation

During the 5-day dialysis cycle a significant influx of water into the dialysis cassette was observed. As a result, the final alginate-GRGDY appeared to be over-diluted. It was therefore necessary to increase the resulting alginate concentration to reach the desired 1% w/v final concentration, in order to allow addition of the cell suspension. Previous solutions to this problem were investigated [Markusen, 2005] including the re-suspension of the cells in a very small volume of culture medium (e.g. 100 $\mu$ L) before addition to the alginate, and the utilisation of solid polyethylene glycol (PEG) crystals (Sigma P-2139; Fluka Chemie no.94646) or Sterile Slide-A-Lyzer® concentrating solution (Pierce, identity of which was proprietary) to concentrate the alginate-GRGDY inside the dialysis cassette after completion of the dialysis process. However, these methods had important limitations, leading either to the formation of hydrogels with low strength and amorphous shape, or requiring excessive handling and non-aseptic manipulations. For this reason lyophilisation, which requires reduced aseptic manipulations, was adopted as the method for the concentration of the alginate-GRGDY, even though a long lyophilisation procedure (typically 2 days) was required in order to increase the alginate's concentration to the desired 1% w/v final concentration required. After the 5-day dialysis procedure, the alginate-GRGDY was removed from the dialysis cassette using a 50mL Luer-Lok syringe with a 21 gauge needle (Becton Dickinson), while air was injected into the cassette to prevent damage to the dialysis membranes. The alginate-GRGDY was aliquoted into 75x25mm sterilised soda glass vials (Samco, LIG Supplies Ltd., March, UK) which were then covered with sterilised aluminium foil, loaded onto a tube rack and submerged in liquid nitrogen for 10 minutes. Particular care was taken during the freezing step in order to prevent entering of the nitrogen into the vials. The vials of frozen alginate were then placed onto the freeze drier chamber (Edwards Freeze Dryer) pre-cooled at -60°C. The aluminium foil was removed from the vials and the chamber was sealed with the cover containing a thin layer of vacuum grease (Dow Corning high vacuum grease, Dow Corning Corp, Midland, Michigan, USA). In order to prevent an increase in temperature above -60°C within the vials, the vacuum pump for the chamber was immediately turned on and set up at an initial vacuum of approximately 0.2-0.4 mbar. The lyophilisation was carried out for two days, after which the vacuum pressure had decreased to 0.6-0.8 mbar, indicating that

the alginate was completely dry. The vacuum was then shut off and the chamber was slowly vented through a 0.2µm PTFE filter (Midisart, Sartorius AG, Goettingen, Germany). The vials were then removed from the chamber, covered with autoclaved aluminium foil, transferred to the laminar flow cabinet and covered with sterilised caps. The resulting freeze-dried alginate-GRGDY was either stored at -20°C in the dark until use, or immediately reconstituted and used for the preparation of cells/alginate-GRGDY three-dimensional constructs.

#### **2.3.2.4 Alginate concentration with polyethylene Glycol (PEG) solution**

Concentration of the alginate-GRGDY with PEG Slide-A-Lyzer concentrating solution (Pierce) was investigated as an alternative method to the lyophilisation procedure described in the previous section. This alternative concentration procedure was performed on a small amount of SLG100 alginate-GRGDY (9X reactants 10X peptide) that was left inside the dialysis cassette after completion of the 5-day dialysis cycle. The concentration of the resulting alginate-GRGDY solution was calculated by measuring the total volume inside the cassette and by weighing the cassette containing the alginate-GRGDY throughout the whole procedure. The cassette was placed in a sterile plastic bag containing the PEG solution and the weight was monitored at small intervals, making it possible to estimate when the concentration of the alginate-GRGDY had reached 1% w/v. The cassette was then removed from the PEG concentrating solution, and the alginate-GRGDY solution was extracted from the cassette with a 50 mL syringe fitted with a sterile 21 gauge needle. The resulting alginate-GRGDY solution was then either immediately used for the preparation of cells/alginate three-dimensional beads (as described in section 2.5.3), or frozen and stored at -20°C, covered with aluminium foil, for subsequent use (see flow chart in chapter 3).

#### **2.3.2.5 Reconstitution of lyophilised alginate-GRGDY**

After lyophilisation, the derivatised alginate was typically reconstituted in normal saline solution (0.9% NaCl in cell culture grade water), in order to achieve a final 1% w/v alginate concentration, which was isotonic for subsequent addition of the cell suspension. The extensive dialysis cycle (5 days) caused removal of the majority of



the sodium ions and subsequently protonation of the carboxyl groups on the GRGDY-derivatised alginate polymers, converting the alginate into water-insoluble alginic acid (Doumeche, 2004). To help the dissolution of the resulting alginic acid, the necessary amount of 1M NaOH (Sigma) was added to the normal saline solution used for the alginate reconstitution. Typically 0.75-1.0mL of normal saline supplemented with 35-50 $\mu$ L of 1M NaOH were used to reconstitute each individual vial of the lyophilised alginate.

After reconstitution with normal saline solution the alginate-GRGDY solution was stored in the dark at +4°C until use.

## **2.4 Characterisation of the alginate matrix**

Amino acid analysis and Nuclear Magnetic Resonance (NMR) were employed for the characterisation of the alginate matrix prepared as described in section 2.3. Mass Spectrometry and ultraviolet (UV)/visible spectroscopy were performed on the GRGDY peptide supplied by Albachem Limited in order to measure the amount of peptide added to the reaction vessel during the alginate derivatisation. These characterisation studies on the alginate matrix were carried out in collaboration with Emily Culme-Seymour (Department of Chemistry, UCL) and the results obtained are presented in chapter 3.

### **2.4.1 Quantification of amino acids in the alginate-GRGDY matrix**

Amino acid analysis is a useful tool for analysing any amino acid containing compound, and provides a quantitative result of exactly how much of which amino acid is present. The diagram in Figure 2.3 describes how the analysis is carried out.

The intact protein is firstly hydrolysed with 6 M HCl for 1 to 4 days at 110°C, producing a solution of the component amino acids. These amino acids are then separated by ion exchange chromatography: the amino acids are applied at pH 3 to a column made of sulfonated polystyrene (a cation exchanger), onto which they all bind, and subsequently they are eluted off the column in sequence via increasing the pH.

First off are the acidic amino acids (e.g. D), then neutral (e.g. G), then aromatic, due to additional hydrophobic interactions with the aromatic ring (e.g. Y), and finally basic (e.g. R). After being eluted off the column, each amino acid is visualised by reaction with ninhydrin: the adducts that are produced in the reaction coil can be detected by a spectrophotometer ( $\lambda_{\text{max}} = 570 \text{ nm}$ ), and ultimately quantified by comparison with a calibration mixture of amino acids.

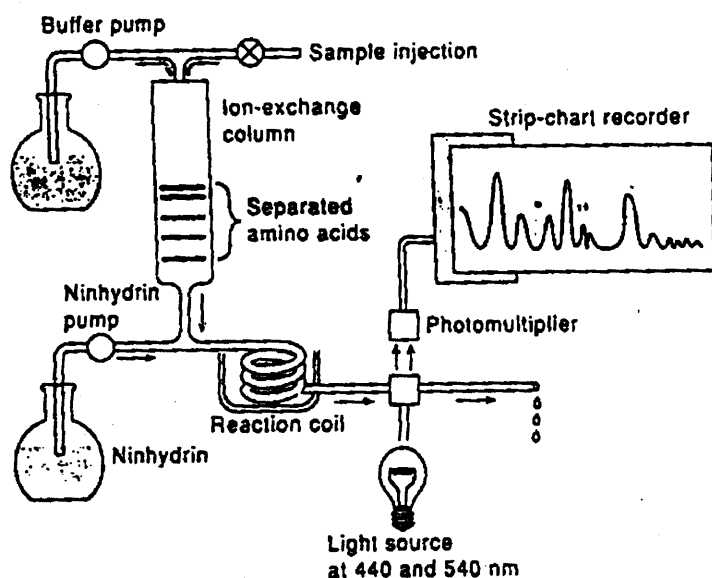


**Figure 2.3:** Schematic flow diagram of amino acid analyser, highlighting the ion-exchange chromatography and the ninhydrin detection. (Picture sourced from <http://www.altabioscience.bham.ac.uk>).

Amino acid analysis was employed in this project to evaluate the degree of the peptide attachment on the alginate polymeric chain after completion of the coupling reaction described in section 2.3. The analysis was performed by Alta Bioscience at the University of Birmingham. Unopened vials of sterile alginate-GRGDY from storage after lyophilisation were submitted for analysis.

## 2.4.2 Nuclear Magnetic Resonance ( $^1\text{H}$ NMR)

Nuclear Magnetic Resonance ( $^1\text{H}$  NMR) was performed to characterise the alginate matrix.

NMR is a procedure that, taking advantage of the magnetic properties of nuclei, allows for the identification of each atom and each functional group in a pure

molecule. It shows how many atoms of each type and what atom environments exist within the sample under analysis.

All the protons surrounding the five carbons on the ring of either the G- or M-unit in alginate are detectable by NMR spectroscopy. However, the signals from the protons on four of the carbons overlap largely, due to the similarities between their respective environments. The only signal that is visible derives from the anomeric protons on both of the units at position C-1. These are the only protons that are directly adjacent to two oxygen atoms, electronegative atoms that shift the signal from the anomeric proton slightly downfields, away from the bulk signal from the alginate, thus making the signal visible. The size of the shift of the anomeric protons depends on their environment regarding both the particular unit it is from, as well as the neighbouring unit. A proton on a G-unit positioned next to a M-unit will be in a different environment (and so a different shift) than a proton on a G-unit positioned next to another G-unit.

The block structure and molecular weights of a range of sodium alginates has previously been analysed via a range of techniques, resulting in information about the M-unit to G-unit ratio and the distribution of the uronic acid residues [Johnson *et al.*, 1997]. One major problem of the alginate is its high viscosity and large molecular weight, resulting in a broad NMR signal. Johnson and colleagues (1997) thus adapted a method to reduce the viscosity of the alginate before NMR analysis from the work of Haug *et al.* 1966 and Grasdalen *et al.* 1979, to produce a visibly more refined alginate signal.

The protocol utilised in the work presented here was adapted from the method described by Johnson *et al.*, 1997. Firstly, acid hydrolysis was performed on the alginate sample: the alginate was dissolved in distilled water and the pH was adjusted in two steps to the final value of 3.6 by dropwise addition of 1M HCl, followed by addition of 0.05M H<sub>2</sub>SO<sub>4</sub>. The hydrolysis was performed within an oil bath at 120°C under reflux. The solution was then cooled to room temperature prior to the freezing in liquid nitrogen, and the resulting material was lyophilised overnight.

<sup>1</sup>H NMR was performed on Pronova sodium alginate samples as follows: the alginate sample (approximately 12 mg) was dissolved in 2 mL of deuterated water (D<sub>2</sub>O) and filtered through cotton wool. The alginate solution was brought to 358°K within a NMR glass tube over a 15 minutes period, and the proton spectrum of the

solution was recorded using a Bruker AMX 400 spectrometer (Bruker Spectrospin), with a 30° pulse sequence and with water suppression.

In order to determine the optimal NMR protocol, giving spectra with clear signals and allowing to gain accurate integral values of the alginate and tyrosine peaks, a series of experiments were performed with partially hydrolysed alginate and tyrosine. The same technique described above was performed on the alginate dissolved in deuterated water (D<sub>2</sub>O) after addition of a tyrosine solution in D<sub>2</sub>O. The <sup>1</sup>H NMR spectrum was recorded as described above.

<sup>1</sup>H NMR was performed following the same procedure also on the alginate resulting after derivatisation with the GRGDY pentapeptide. In order to aid dissolution, deuterated sodium hydroxide (NaOD) was added to the alginate-GRGDY solution under Argon atmosphere. The material was then sonicated, heated and filtered through cotton wool and was then ready for the acquisition of the spectrum, which was recorded as described above.

### **2.4.3 Mass spectrometry (MS)**

Mass Spectrometry (MS) is an analytical tool used for measuring the molecular mass of a sample. It is most generally used to find the composition of a physical sample by generating a mass spectrum representing the masses of sample components. MS can have many different applications, including amino acid sequencing and analysis of proteins, peptides and oligonucleotides. As such, it can be employed to obtain sequence confirmation or *de novo* characterisation of peptides, or to obtain accurate molecular weight measurement in order to determine the purity of a sample and to verify amino acid substitutions in the sample.

Structural information can be obtained by analysing the sample's mass spectrum, which is measured by a mass spectrometer.

In this research Mass Spectrometry was performed to obtain information on the chemical structure and amino acid composition of the GRGDY peptide supplied by Albachem Limited. Mass spectra were obtained through the UCL Mass Spectrometry Department, and the results obtained are presented in section 3.3.1.1.

## **2.5 Preparation of alginate/cells constructs**

This section describes the preparation of the cells/matrix three-dimensional constructs. Alginate coupled with the GRGDY pentapeptide and prepared as described in section 2.3 was used as scaffold biomaterial.

The selected cells were harvested from their culture in tissue culture flasks and counted as described in sections 2.1.3 and 2.6.2 prior to the addition to the alginate matrix.

Non-derivatised alginate (alginate which had not been reacted with the GRGDY peptide) was used for the preparation of cells/non-derivatised alginate constructs serving as controls.

### **2.5.1 Preparation of the cell suspension for mixing with the alginate solution**

The cells used for the preparation of three-dimensional constructs with the alginate-GRGDY matrix were harvested from their tissue culture flasks and trypsinised as described in section 2.1.3.

After trypsinisation, the cell suspensions from individual flasks were combined together in 50mL centrifuge tubes. A small sample was removed from the cell suspension and analysed with a haemocytometer for the determination of the cell density. The cells were then centrifuged at 100-160g for 5 minutes. After removal of the supernatant, the cell pellet was resuspended with cell growth medium to the desired concentration. At this stage of the procedure it was necessary to completely remove the trypsin/EDTA solution from the centrifuge tube, in order to prevent chelation of divalent ions such as calcium by residual EDTA present in the trypsinised cell suspension. Such chelation would have caused a reduction of the ratio of divalent/monovalent ions, consequently resulting in the undesirable dissolution of the alginate hydrogel. When particularly small working volumes were used, a second centrifugation was performed in order to resuspend the cells in a larger volume (e.g. 5-7mL) of culture medium to further dilute the residual trypsin/EDTA solution. After this second centrifugation step, the supernatant was removed and discarded and the

cell pellet was finally resuspended in the required small volume of culture medium prior to being mixed into the matrix solution.

### **2.5.2 Cross-linking solution**

A 1% w/v calcium chloride (Sigma) solution in normal saline solution was used to cross-link the alginate matrix during the fabrication of three-dimensional cells/alginate beads or sheets. 0.1M NaOH was used to adjust the pH of the  $\text{CaCl}_2$  solution to 6.5-7. The resulting solution was sterile-filtered through a 0.22  $\mu\text{m}$  cellulose acetate membrane (Nalgene) prior to use.

### **2.5.3 Preparation of alginate/cells beads**

The selected cells were combined with the alginate matrix in three-dimensional spherical-shaped beads with a final diameter of approximately 2-2.5 mm. Typical combined matrix/cells working volumes were 0.2-1.2mL. The final matrix/cells beads consisted for 25% v/v of the resuspended cell pellet and the remaining 75% v/v was the matrix solution.

The fabrication of beads was preferred to the preparation of other three-dimensional constructs, such as tubes or sheets [Markusen, 2005]. The preparation of small spherical beads proved to be an easier and more rapid method to produce high numbers of multiple individual units usable for the evaluation of the cell growth and viability at micro-scale level. After trypsinisation the cells were homogeneously resuspended and mixed with the alginate to the final alginate concentration of 1% w/v and final cell concentrations ranging from  $2 \times 10^6$  to  $1 \times 10^7$  viable cells/mL. The alginate/cells mixture was drawn into a 1mL syringe and then very slowly syringed through a sterile 0.1mm diameter blunt needle. During this process small beads/droplets were dripped into the  $\text{CaCl}_2$  cross-linking solution. The beads were left in the cross-linking solution for 15-20 minutes and were then collected by pouring the  $\text{CaCl}_2$  cross-linking solution into a previously autoclaved metal strainer. The beads were then rinsed with culture medium within a Petri dish in order to reduce the residual  $\text{CaCl}_2$  levels. Finally the beads were carefully transferred into the microwells

(1 bead/well) of 24-well ultra-low attachment plates (Costar, Corning Life Sciences, Corning, New York). The beads were cultured at required conditions (selected medium of culture, tissue culture plates, temperature and CO<sub>2</sub>), depending on the particular cell type under investigation and were re-fed every 3 to 4 days with fresh growth medium (1mL/well). Each alginate/cells beads experiment was repeated twice, and the results of these studies are described in chapter 5.

A schematic of the beads fabrication is shown in figure 2.4.

#### **2.5.4 Preparation of alginate/cells disks**

The preparation of three-dimensional alginate/hMSCs disks (or layers) was performed with the purpose of investigating the possible detrimental effects of the high molar concentration of the cross-linking solution on the cells after instantaneous immobilisation within the alginate matrix. The fabrication of alginate disks involves a two-step process, which makes it possible to de-couple the alginate preparation and the cell seeding. Firstly, the alginate is layered on top of Millipore Millicell transwells, which are placed in the wells of tissue culture plates pre-loaded with the CaCl<sub>2</sub> solution. After formation of the alginate disks (approximately 1 hour), the cell suspension is added on top of the alginate layer and the cross-linking solution is replaced with growth medium. The preparation of alginate/cells disks is represented in figure 2.5.

Disks were prepared with either plain Pronova SLG100 alginate or SLG100 alginate derivatised following the standard procedure (see section 2.3.2) with 9X reactants and 32X peptide (see table 2.1). Two different types of transwells were used: Millipore Millicell-PCF 3µm membrane, 12mm diameter (small sheets), cultured in 24-well ultra-low attachment tissue culture plates (Costar, Corning Life Sciences, Corning, New York), and Millipore Millicell-CM transwells 0.4µm membrane and 30mm diameter (big sheets), cultured in 6-well ultra-low attachment tissue culture plates (Costar, Corning).

100µL and 250µL of alginate were added to each well respectively. After trypsinisation, p5 hMSCs were counted with an haemocytometer as previously described (see section 2.6.2), resuspended in growth medium and seeded on top of the alginate layers within the transwells. Initial seeding densities were  $5 \times 10^4$  cells/cm<sup>2</sup>

(corresponding to  $9 \times 10^4$  cells/transwell) for the small disks, and  $3.3 \times 10^4$  cells/cm<sup>2</sup> (corresponding to  $3.12 \times 10^5$  cells/transwell) for the bigger transwells. The resulting hMSCs/alginate disks were cultured at 37°C and 5% CO<sub>2</sub> with 1 mL and 3 mL of complete DMEM respectively. The growth medium was replaced with fresh complete DMEM every 3-4 days. Each alginate/cells disks experiment was repeated twice, and the results obtained from these studies are presented in chapter 5.

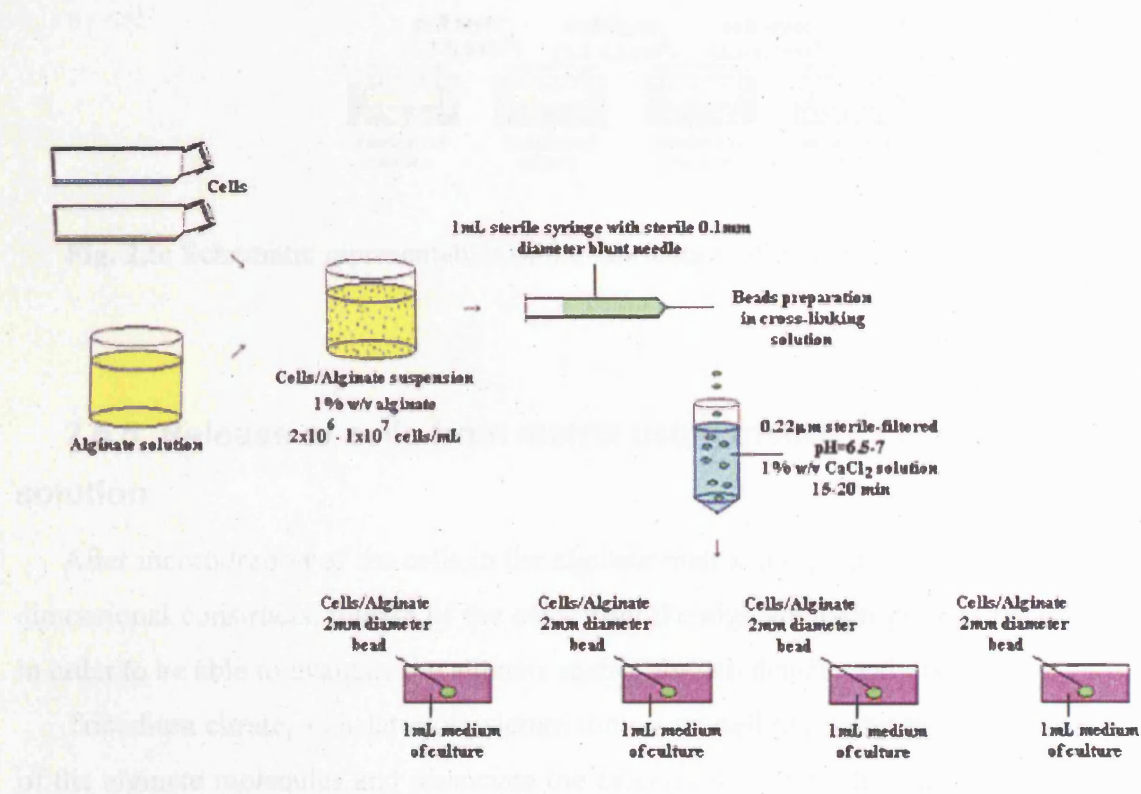


**Fig. 2.4:** Schematic representation of the fabrication of matrix/cells beads.



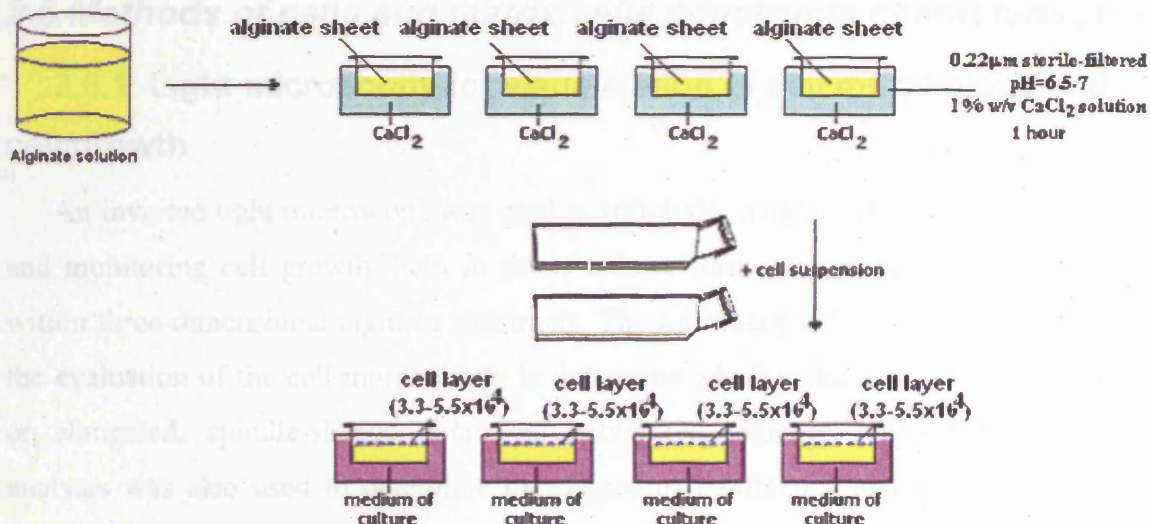


**Fig. 2.5:** Schematic representation of the fabrication of matrix/cells disks.

### 2.5.5 Release of cells from matrix using trisodium citrate solution

After incorporation of the cells in the alginate matrix and preparation of the three-dimensional constructs, release of the cells from the alginate hydrogel was necessary in order to be able to evaluate the alginate matrix for cell density and viability.

Trisodium citrate, a chelator of calcium ions, was used to reverse the cross-linking of the alginate molecules and dissociate the calcium ions from the alginate hydrogel [Read, 2001]. Previous studies have shown that the cell viability is not affected by cell exposure to a 0.1M trisodium citrate solution in complete DMEM [Markusen, 2005]. Such a solution was therefore prepared for the dissociation of the cells/alginate constructs. The samples were incubated with the chelating solution for 10-15 minutes at room temperature and the resulting cells/alginate suspensions were thoroughly mixed to ensure homogeneous single cell suspension prior to the assessment of the cell density and viability with haemocytometer and trypan blue dye.

## **2.6 Methods of cells and matrix/cells constructs characterisation**

### **2.6.1 Light microscopy for visualisation of cell morphology and cell growth**

An inverted light microscope was used at 100-400X magnification for visualising and monitoring cell growth, both in tissue culture flasks, tissue culture plates and within three-dimensional alginate constructs. The microscopical observation allowed the evaluation of the cell morphology, to determine whether the cells were rounded, or elongated, spindle-shaped, and well networked together. The microscopical analysis was also used to determine the degree of confluency and to evaluate the presence of actively dividing cells, indicating cultures in exponential growth phase. Finally, the microscopic evaluation of the culture samples permitted to detect the presence of cellular debris, indicating cell death in the medium of culture.

The cells usually grow over time increasing in number and spreading throughout the plastic surface of the tissue culture vessel. Harvesting and trypsinisation of the cells was performed at 70-80% confluency in order to avoid formation of cell aggregates and to facilitate the detachment of single cells from the cell growth surface.

The colour of the spent medium was observed as an index of the healthy state of the cultures. The medium of culture appeared orange/red (basic) when healthy respiring cells released CO<sub>2</sub> and metabolic waste products such as ammonium ions. On the other hand, the medium of culture appeared red/purple when cell growth was poor and cell density low. Finally, a yellow (acidic) and turbid spent medium suggested the presence of eventual micro-organisms contaminating the culture.

### **2.6.2 Cell count with haemocytometer**

A cell count with haemocytometer was performed to determine the density of the cell suspension at each passage. For this purpose, after trypsinization and quenching with complete medium, a small sample of the cell suspension (typically 0.5mL) was removed and diluted 1:2 with trypan blue dye (BioWhittaker, Walkersville, MD, USA). To improve the accuracy of the cell count the diluted cell suspension was gently pipetted until complete homogeneous mixing. Typically 20µL of sample were

placed under a cover slip on the haemocytometer. The cells were counted in the grid that was etched onto the surface of the haemocytometer. The cell count was performed three times for each sample and the average value was used for the calculation. The total number of cells/mL was determined by multiplying the total cells counted in 10 squares by 1000 times the trypan blue dilution factor (2), as summarised in the equation:

$$\text{Average number of cells in 10 squares} \times 1000 \times \text{Dilution factor (2)} = \text{Number of cells/mL}$$

The multiplication factor of 1000 was obtained from the volume of  $1\text{mm}^3$  contained in the counting grid (10 squares  $\times$  1mm  $\times$  1mm  $\times$  0.1mm) and converted to mL ( $1\text{mm}^3 = 0.001\text{mL}$ ) for the original sample.

The homogeneity of the cell suspension affected the accuracy of the cell count. Thorough pipetting was performed to ensure homogeneity of the cell suspension prior cell enumeration. However, the presence of occasional aggregates within the cell suspension may have led to lower results than actual numbers, as ultimately this procedure was dependent on the age of the culture, effective trypsinisation and the operator's technique. In order to decrease statistical error due to small sample size, between 100-200 cells were normally counted over the 10 squares of the haemocytometer grid for each replicate.

### **2.6.3 Cell viability with trypan blue**

The exclusion assay with trypan blue dye was performed for the assessment of the cell viability. This technique is one of the most common methods used to assess cell viability [Patterson, 1979]. Trypan blue is a small molecular weight dye that stains the cells in their cytoplasmic region. At each harvesting step during cell expansion, a 0.5 mL sample of the cell suspension was removed after trypsinisation and quenching with complete medium, and then diluted 1:2 with trypan blue dye for the determination of cell viability. When the cell suspension was diluted with the dye, the live cells with an intact cell membrane excluded the dye (unstained, bright cells),

whereas the dead cells with a permeable membrane allowed the dye to enter and colour the cells (stained, blue cells).

The efficacy of the assay is time-dependent, since after 15 minutes the dye can permeate live cells together with the dead ones [Veckeneer *et al.*, 2001]. For this reason the cell count was always performed immediately after addition of the dye to the cell suspension. The viability of the cell suspension was determined by the equation:

$$\text{Percentage of viable cells} = (\text{Number of live cells} / \text{Total number of cells}) \times 100$$

#### **2.6.4 Calculation of cell growth rates**

Cell growth typically exhibits a characteristic growth curve, as seen in figure 2.6. Cells progress through a consistent pattern comprising four main phases, including an initial lag phase, where the cells become accustomed to the new environment, a period of logarithmic growth in which the number of cells increases exponentially, a stationary phase (the plateau phase) in which the rate of cell proliferation slows down, and a final decline phase, characterised by cell death caused by depletion of essential nutrients or by the toxic metabolic by-products built-up in the culture medium.

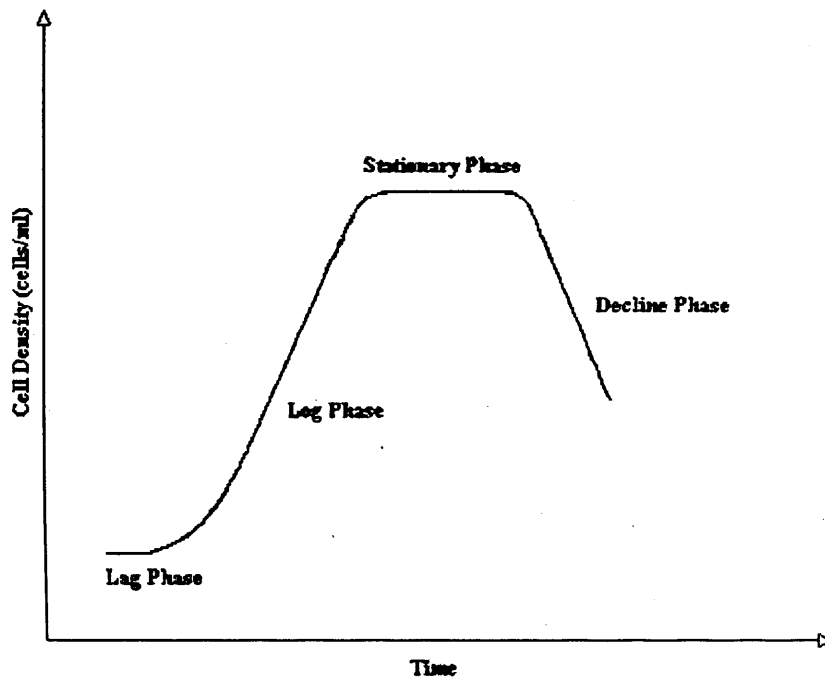


**Fig. 2.6:** Growth phases of cells in culture [Palsson and Bhatia, 2004].

The cells were trypsinised and counted using a haemocytometer according to the standard protocol described in section 2.6.2 in order to determine the initial and final cell densities ( $X_0$  and  $X$ ).

The population doubling level (PDL) and the doubling time  $T_d$  (hours) of the cells were then calculated as follows:

$$\text{PDL} = \log_{10}(X / X_0) / \log_{10}(2)$$

$$T_d = T / \text{PDL},$$

where  $T$  (hours) is the total length of the culture.

For cells maintained in a closed system, such as the tissue culture flasks or plates used in this research, the cell growth can be described as:

$$dX / dt = \mu X$$

which, integrating for the initial concentration  $X = X_0$  at  $t = 0$  becomes:

$$X = X_0 \exp (\mu t).$$

When the cell population increases from  $X_0$  to  $2X_0$  in the doubling time  $T_d$ , the equation becomes:

$$2X_0 = X_0 \exp (\mu T_d)$$

which can also be written in the following form:

$$T_d = \ln(2) / \mu \quad (\text{Doran, 1995; Butler, 2004}).$$

The cells growth rate  $\mu$  ( $\text{hours}^{-1}$ ) was calculated using the following equation:

$$\mu = \ln (2) / T_d \quad (\text{Doran, 1995; Butler, 2004}).$$

which can also be expressed as follows:

$$\mu = 2.3 * \log_{10} (X / X_0) / T$$

The growth rate  $\mu$ , the PDL and the doubling time  $T_d$  were calculated as described in this section for the characterisation of the hMSCs cultured in this research in monolayer, under the different culture conditions described in section 2.1.5. All these parameters were determined at selected time points over a total culture period of 13-15 days. In addition, in order to provide a more complete cell characterisation, the cell metabolism was evaluated from the spent medium recovered from the wells of the tissue culture plates. The spent medium was analysed with the Nova Biomedical Profile Analyzer, and the exact volume of the medium recovered at each time point was used as a correction factor for the calculation of the glucose consumption and lactate production (as described in section 2.6.5). The results obtained from the hMSCs growth and metabolic studies are presented in chapter 4.

## **2.6.5 Nutrient and metabolite analysis with Nova Bioprofiler**

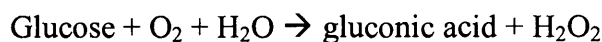
The growth medium recovered at different time-points during cell culture was analysed, immediately after removal from the tissue culture plates, with the Nova Biomedical BioProfile 400 analyzer. Samples of growth medium were taken during the experiment and the glucose and lactate concentrations were measured afterwards with the BioProfiler's sensors and used for the determination of glucose consumption, lactate production and specific glucose consumption rate. Only one sample per condition was taken and measured with the BioProfile analyzer for the metabolic analysis data sets presented in chapter 4.

### **2.6.5.1 Glucose and lactate biosensors in the Nova Biomedical BioProfiler**

Potentiometric-based electrodes measure charged ions and have a sensing membrane that is selective to the ionic species being measured. They develop a voltage proportional to the concentration of the measured ionic activity. The basic amperometric electrode is the oxygen electrode, which consists of an oxygen-permeable membrane covering a platinum cathode. The Nova Biomedical BioProfiler's glucose and lactate biosensors are amperometric electrodes that have immobilized enzymes in their membranes. They develop a current proportional to the substrate being measured, and can therefore be used to quantitate the metabolite concentration.

### **2.6.5.2 The glucose sensor and determination of glucose consumption**

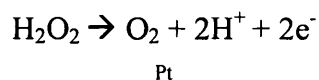
Glucose oxidase is bonded to a polymeric membrane substrate in the BioProfiler's glucose sensor. The enzyme catalyses the oxidation of  $\beta$ -D-glucose to gluconic acid and hydrogen peroxide, as described in the reaction below:



glucose oxidase

Glucose diffuses from the sample through the membrane to the immobilized enzyme layer where oxidation occurs. The hydrogen peroxide produced is then oxidized at the platinum electrode.

The platinum electrode, which is maintained at an applied voltage, detects the hydrogen peroxide produced:



The current generated is linearly related to the concentration of hydrogen peroxide  $[\text{H}_2\text{O}_2]$  and this is related to the concentration of glucose  $[\text{Glu}]$  in the sample:

$$[\text{Glu}] = J [\text{H}_2\text{O}_2]$$

where  $J$  is a constant set during calibration.

The measured current  $i$  is related to the concentration of glucose as follows:

$$i = KJC$$

where  $K$  is a constant which includes electrode geometry, overall diffusion coefficients and reaction rates, and  $C$  is the glucose concentration.

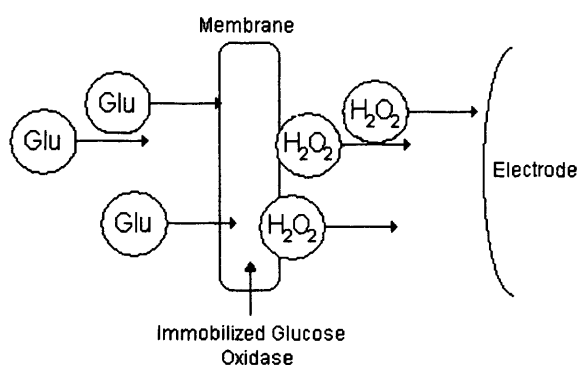


**Figure 2.7:** Schematic representation of the glucose membrane in the Nova Biomedical Bioprofile 400 Analyzer. (Picture sourced from the Nova Biomedical BioProfile 400 instruction manual).



Glucose is the primary energy source. The rate at which cells consume glucose during *in vitro* expansion can be used as an indication of cell proliferation [Ozturk *et al.*, 1997].

Glucose concentration was measured using the Nova Bioprofiler at selected time-points just prior to trypsinisation. The specific glucose consumption rate GCR (g/cell/hour) was then determined using the following equation:

$$GCR = \frac{G_c V}{\int_0^t X_s ds} = \frac{G_c V}{[A \exp(kt) - A] t / 2} = \frac{G_c V}{(X_t - X_0) T / 2}$$

Where  $G_c$  = glucose consumed during the selected culture period (g/L)

$V$  = volume of growth medium analysed (L/cm<sup>2</sup>)

$X_s$  = change in cell density for the culture length (hr/cells/cm<sup>2</sup>)

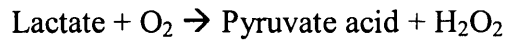
$T$  = total culture time (hours)

$X_0$  = cell density at  $t = 0$

$X_t$  = cell density at the time  $t$

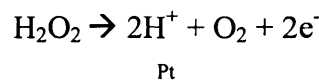
### 2.6.5.3 Lactate production

Lactate is produced during metabolism of glutamine. Together with glucose consumption, lactate production can be determined as an indication of the cell metabolism. The Nova Biomedical Profile Analyzer measures the lactate concentration based on the level of H<sub>2</sub>O<sub>2</sub> produced during the enzymatic reaction between lactate and oxygen molecules in the presence of the lactate oxidase enzyme:



lactate oxidase

At a constant potential of 0.70 volts, electroactive H<sub>2</sub>O<sub>2</sub> is oxidized at the surface of the platinum anode as follows:



The current generated by the flow of electrons at the surface of the platinum electrode is proportional to the lactate concentration of the sample.

The lactate concentration (g/L) was measured in the spent growth medium at selected time-points during culture with the Nova Biomedical Bioprofiler. The lactate values were then plotted over the desired culture period (expressed in days) and a linear curve was fit to the data.

### **2.6.6 Qualitative analysis of cell viability with fluorescence microscopy**

The Live/Dead Viability/Cytotoxicity Assay (Molecular Probes, Inc, Eugene, Oregon, USA) was used to study and confirm the cell viability data obtained from the trypan blue dye exclusion assay. This qualitative assay utilises two fluorescent dyes to discriminate between live and dead cells, measuring recognized parameters of cell viability, intracellular esterase activity and plasma membrane integrity. Calcein-AM is a non-fluorescent cell-permeable substance (calcein acetoxy-methyl ester), which is intracellularly converted to the green fluorescent calcein by esterase activity in viable cells. The polyanionic calcein is well retained within live cells, producing an intense uniform green (excitation/emission approximately 495nm/515nm) fluorescence. Ethidium homodimer-1 (EthD-1), a red DNA dye non-permeable to viable cells, stains nucleic acids by intercalating between the base pairs. EthD-1 enters cells with damaged membranes and undergoes a forty times enhancement of its fluorescence on binding to nucleic acids, thereby producing a bright red (excitation/emission approximately 495nm/635nm) fluorescence in dead cells. This assay was performed on both cells cultured in monolayer and on three-dimensional cells/alginate beads.

For the assessment of cell viability in monolayer, the cells were cultured on sterile 13mm diameter glass coverslips (BDH) placed within the transwells of 24-well tissue culture plates ( $ICD=5 \times 10^3$  cells/cm<sup>2</sup>). The cells were washed with PBS (200  $\mu$ L/coverslip) prior to the assay, in order to remove or dilute serum esterase activity generally present in serum-supplemented growth media. Serum esterase activity could in fact cause some increase in extracellular fluorescence by hydrolyzing calcein AM.

The 2mM EthD-1 and the 4mM calcein-AM stock solutions were diluted with PBS to a 6.6 $\mu$ M and 3.2 $\mu$ M working solutions respectively. Each coverslip was

treated with an equal amount (66 $\mu$ L) of EthD-1 working solution, calcein-AM working solution and PBS, so that the final concentrations used were 2.2 $\mu$ M for the EthD-1 and 1.06 $\mu$ M for the calcein AM. The samples were incubated with the dyes for 30-40 minutes at 37°C. Using fine-tipped forceps, the coverslips were then carefully inverted and mounted on glass microscope slides (BDH). To prevent evaporation, the coverslips were sealed to the glass slides with clear fingernail polish, and were then visualised on a fluorescence microscope with optimal excitation/emission wavelengths of approx. 495/515nm for calcein AM and 495/635nm for EthD-1.

To assess the cytotoxicity of the cells immobilised within alginate beads, each construct was thoroughly washed with PBS (300 $\mu$ L/bead) and then incubated with an equal amount (165 $\mu$ L) of EthD-1 working solution, calcein-AM working solution and PBS, so that the final concentrations used were 2.2 $\mu$ M for the EthD-1 and 1.06 $\mu$ M for the calcein AM. After 30-40 minutes incubation at 37°C, the beads were washed with PBS (300 $\mu$ L/bead) and carefully transferred on the cavities of microscope glass slides (Fisher, 1 bead/cavity). In order to prevent movement or loss of the beads, new untreated coverslips (Chance Propper Ltd, West Mids, England) were mounted and sealed with clear fingernail polish on top of the glass slides. The resulting samples were finally observed on the fluorescence microscope with excitation/emission wavelengths indicated above.

### **2.6.7 hMSCs multipotentiality with hMSCs Functional Identification Kit**

The Human Mesenchymal Stem Cell Functional Identification Kit (R&D Systems, Inc, Minneapolis, USA) was used to measure the cells' ability to differentiate into multiple mesenchymal lineages. hMSCs isolated from frozen bone marrow samples (as described in section 2.1.1) were cultured for 19-21 days under conditions that were favourable for adipogenic, chondrogenic, or osteogenic differentiation (section 2.6.7.1). The cells were then fixed and stained with specific antibodies included in the kit, normally used to define the mature phenotypes of

adipocytes, chondrocytes and osteocytes (section 2.6.7.3). This experiment was performed twice, and the results for these studies are presented in chapter 4.

#### **2.6.7.1 Lineage-specific differentiation**

Initially, adipogenic/osteogenic basal medium was prepared by supplementing  $\alpha$  Minimum Essential Medium ( $\alpha$ MEM) (Gibco) with 10% Fetal Bovine Serum (Gibco) and 1% 100X Penicillin-Streptomycin-Glutamine (Gibco) [100U/mL Penicillin, 100 $\mu$ g/mL Streptomycin, 2mM L-glutamine].

Chondrogenic basal medium was prepared by supplementing DMEM/F12 medium (Gibco) with 1% ITS supplement (R&D Systems) and 1% 100X Penicillin-Streptomycin-Glutamine (Gibco) [100U/mL Penicillin, 100 $\mu$ g/mL Streptomycin, 2mM L-glutamine].

The cells were harvested and counted following the standard protocol previously described. For adipogenic and osteogenic differentiations, fourth passage (p4) the cells were resuspended in  $\alpha$  Minimum Essential Medium basal medium (0.5mL/well) and cultured until 80-90% confluent (approximately 2-3 days) on top of sterile 13mm diameter glass coverslips (BDH), within 24-well tissue culture plates, at  $2.1 \times 10^4$  cells/cm<sup>2</sup> and  $4.2 \times 10^3$  cells/cm<sup>2</sup> respectively. In order to avoid cell detachment, which can occur during osteogenic differentiation, the cells undergoing osteogenic differentiation were seeded on coverslips which had been previously coated (24-30 hours at 37°C) with 1 $\mu$ g/mL human fibronectin (R&D Systems). Once the cells had reached 80-90% confluence, the basal medium was replaced with  $\alpha$ MEM supplemented respectively with 10X Adipogenic Supplement (1:100 dilution) and 10X Osteogenic Supplement (1:20 dilution). The cultures were maintained for 19-21 days at 37°C and 5%CO<sub>2</sub> and re-fed every 3-4 days with  $\alpha$ MEM freshly supplemented with the respective differentiation supplements.

For chondrogenic differentiation, six-eight  $2.5 \times 10^5$  fourth passage (p4) cells aliquots were transferred to six-eight 15mL conical tubes. The tubes were centrifuged at 200g for 5 minutes at room temperature, the supernatant was removed from each tube and each pellet was resuspended with 1mL of DMEM/F12 basal medium. The pellets were centrifuged a second time at 200g for 5 minutes at room temperature, the supernatants were discarded and the pellets were resuspended with 0.5mL of DMEM/F12 basal medium previously supplemented with 20X chondrogenic supplement (1:100 dilution). The samples were centrifuged again at 200g for 5

minutes at room temperature and the resulting pellets were left in their tubes with the chondrogenic differentiation medium and incubated at 37°C and 5%CO<sub>2</sub>. The caps of the tubes were left loose throughout the culture to allow gas exchange and the growth medium was replaced every 3-4 days with freshly supplemented chondrogenic differentiation medium.

After 19-21 days in lineage-specific culture conditions, both coverslips and pellets were washed with PBS and fixed with 4% paraformaldehyde (TAAB Laboratories, England, UK) in PBS (BioWhittaker) for 20 minutes at room temperature. Using a fine-tipped forceps, the coverslips for adipogenic and osteogenic differentiation were carefully removed from the tissue culture plates, inverted and mounted on polished glass microscope slides (BDH) and were then immediately processed for immunocytochemistry (see section 2.6.7.3). Whereas the pellets for chondrogenic differentiation were frozen in optimum cutting temperature O.C.T. freezing compound (BDH) and liquid nitrogen and stored at -80°C until processing (see section 2.6.7.2).

#### **2.6.7.2 Cryosectioning of cell pellets for chondrogenesis**

After fixation with 4% paraformaldehyde, the cell pellets were transferred from their tubes to 7 mm x 7 mm x 5 mm disposable vinyl plastic base moulds (Fisher) and embedded in optimum cutting temperature (O.C.T.) freezing compound (BDH). Each sample was frozen in liquid nitrogen to form a block that could be cryosectioned and kept at -80°C for long-term storage. The frozen pellets were cut into 5-7µm sections using standard cryosectioning methods (Cryostat Bright Otf Model, Serial no. 95037/4676, Bright Instruments Co.).

The specimens were collected directly on clean SuperFrost Plus glass slides (VWR International, Leuven). Usually no more than three sections, each spaced well apart, were placed per slide. A circle was drawn with a liquid barrier marker pen (Dako) around each section on the slides in order to prevent reagent mixing between samples. The sections were left to air-dry at room temperature for 2-3 hours and the slides were then carefully wrapped in aluminium foil and store at -20°C overnight.

### 2.6.7.3 Immunocytochemistry

Both the coverslips from adipogenesis and osteogenesis culture and the cryo-sections obtained from the cell pellets maintained in chondrogenic conditions were placed in a humidified chamber and processed for immunocytochemistry. Firstly, the samples were permeabilised and blocked with 0.3% Triton X-100, 1% BSA and 10% normal donkey serum in PBS in order to prevent non-specific binding. The blocking step was performed at room temperature for 45 minutes. The samples were then incubated with the appropriate antibody working solution overnight at 2-8°C. The coverslips for adipogenic differentiation were treated with 1µg/100µL goat anti-mouse FABP-4. 1µg/100µL mouse anti-human osteocalcin was used for coverslips cultured with osteogenic differentiation medium whereas the cell pellets for chondrogenic differentiation were incubated with 1µg/100µL goat anti-human Aggrecan (all primary antibodies from R&D Systems). After overnight incubation, the samples were washed three times with PBS containing 1% BSA for 5 minutes. The samples were then incubated with the appropriate secondary antibody solution prepared in PBS containing 1% BSA. The incubation was maintained for 60 minutes at room temperature in the dark. Rhodamine Red-conjugated donkey anti-goat antibody (Jackson ImmunoResearch Lab. Inc., West Grove, PA, USA; Fluorophore/Protein absorbance ratio: A550/A280=0.71) was used for the reaction with adipo-induced coverslips and the chondro-induced pellets, whereas the coverslips that had been maintained in osteogenic differentiation medium were treated with Rhodamine Red-conjugated donkey anti-mouse antibody (Jackson ImmunoResearch Lab. Inc.; Fluorophore/Protein absorbance ratio: A570/A280=1.3). After incubation with the secondary antibodies, the samples were washed with 1% BSA in PBS for 5 minutes and then with distilled water. Using a fine-tipped forceps, the coverslips for adipogenic and osteogenic differentiation were carefully inverted and mounted on glass microscope slides. New untreated glass coverslips (Chance Propper Ltd, West Mids, England) were mounted on top of the cell sections obtained from the pellets for the chondrogenic differentiation. The resulting samples were then observed on the fluorescence microscope.

Negative controls were assessed in order to test for the specificity of the antibodies involved: three samples per each condition were tested following exactly the procedure described above but omitting the primary antibody incubation. These

negative controls were instead incubated over-night with PBS containing 1% BSA and 10% normal donkey serum.

### **2.6.8 Cell apoptosis: Guava Nexin assay**

Apoptosis, or programme cell death, is an important regulatory pathway of cell growth and proliferation. This phenomenon is characterised by intracellular processes that result in typical physiological changes, including: externalisation of phosphatidyl serine (PS) to the cell surface, cleavage and degradation of specific cellular proteins, compaction and fragmentation of nuclear chromatin, and, at later stages, loss of membrane integrity [Kerr *et al.*, 1972; Wyllie, 1993].

A fluorescence-based assay was performed in order to measure apoptosis based upon the Guava EasyCyte system, a blue laser 96-well microcapillary flow cytometry instrument (Guava EasyCyte). This simple assay uses a combination of dyes to identify and distinguish apoptotic cells from dead cells and debris.

Annexin V is a calcium-dependent phospholipid binding protein with high affinity for phosphatidyl serine (PS) [van Heerde *et al.*, 1995], a membrane component normally localised to the internal surface of the cell membrane. In early apoptotic cells, molecules of PS are translocated to the outer surface of the cell membrane where Annexin V can readily bind them [Fadok *et al.*, 1992; van Engeland *et al.*, 1996]. The Annexin V-PE provided with the Guava PCA-96 Nexin kit (Guava Technologies Inc. Hayward, CA; cat. no. 4500-0160) detects PS on the external membrane of apoptotic cells.

A cell-impermeant DNA intercalator, 7-aminoactinomycin (7-AAD), is the second dye included in the kit. This dye is excluded from live, healthy cells and early apoptotic cells, and is therefore used to monitor cell membrane permeability changes commonly observed later in apoptosis as well as in necrotic cells.

Three cell populations can be distinguished simultaneously in this assay: non-apoptotic Annexin V (-) and 7-AAD (-) cells, early apoptotic Annexin V (+) and 7-AAD (-) cells and late stage apoptotic and dead cells, which stain positively for both dyes.

Using both these dyes in a single assay not only allows the monitoring of cellular events leading to physiological changes typically involved in cell apoptosis, but also

enables users to distinguish between cellular processes occurring at different stages of this phenomenon.

The cells were harvested and counted as previously described (section 2.1.3 and section 2.6.2). The cell suspension was equally divided in 1mL capacity microcentrifuge tubes (Eppendorf), so that the final cell concentration was between  $1 \times 10^4$  and  $5 \times 10^4$  cells/tube. The tubes were centrifuged at 360g, +4°C for 5 minutes.

After complete removal of the supernatant, each cell pellet was resuspended in 40µL 1X Nexin buffer, obtained by diluting 10X Nexin Buffer with purified deionised water. 5µL Annexin V-PE and 5µL Nexin 7-AAD were added to each tube and the staining reactions were then incubated shielded from light for 20 minutes at +4°C. After incubation, each sample was diluted by addition of 150µL 1X Nexin Buffer, so that both the Annexin V-PE and the Nexin 7-AAD concentrations in the final 200µL working solution were 2.5%. The resulting samples were transferred into individual wells of a 96-well microplate (Corning Incorporated, Costar, NY, USA) and were then immediately assessed on the Guava PCA-96 system using the ExpressPlus application software within CytoSoft.

The Nexin assay was performed on bFGF-free and bFGF-supplemented hMSCs cultured in different oxygen conditions, in order to evaluate the effects of both bFGF supplementation and oxygen tension on cell apoptosis. The results are described in section 4.8.3.

### **2.6.9 Statistical analysis**

For the cell proliferation and cell viability analysis, three replicates for each condition were performed and assessed. The mean and standard error of the mean (S.E.) of the three measurements were calculated for each condition, whereby the standard error was given by the formula:

$$\text{Standard Error (S.E.)} = \frac{\sigma}{\sqrt{n}}$$



where  $\sigma$  is the sample standard deviation (i.e. the sample based estimate of the standard deviation of the population), and  $n$  is the population size (number of replicates) of the sample.

The statistical significance of results was assessed using the single factor analysis of variance (one-way ANOVA) program from Microsoft Excel 2002. The single factor ANOVA analysis tool performed a simple analysis of variance, testing the hypothesis that the means from two or more samples were equal (drawn from populations with the same mean). Analysis of the groups of data that produced a p-value  $>0.05$  indicated that the means were not statistically different (to the 95% confidence level); whereas a p-value  $<0.05$  indicated one or more of the samples did not have the same mean.

## **2.7 MTT (3-(4,5-dimethylthiazol-2-yl)-2,5-diphenyltetrazolium bromide) assay**

Several methods have been developed to study cell viability and proliferation in cell populations. The most common method for the determination of the growth and proliferation of anchorage-dependent cells involves harvesting of the cells with a 0.25% trypsin/0.02% EDTA solution, followed by cell staining and cell enumeration using a haemocytometer and microscope (section 2.6.2 and 2.6.3). However, this cell count method may be considered time consuming, labour intensive and dependent on the operator's technique. For this reason in this research an alternative method, the MTT assay, was investigated for the cell quantification.

This assay has been demonstrated as a sensitive, precise, rapid and reliable test method by many studies [Ferrera *et al.*, 1993]. Moreover, results from MTT studies have shown a good correlation and consistency with direct cell counting and other *in vitro* proliferation assays [Zund *et al.* 1999; Markusen *et al.*, 2006; Ciapetti *et al.*, 1993].

The MTT (3-(4,5-dimethylthiazol-2-yl)-2,5-diphenyltetrazolium bromide) is a tetrazolium salt which is widely used to quantitate cell proliferation and cytotoxicity. The MTT Cell Proliferation assay has been developed based on the metabolic activity of viable cells. Because the original tetrazolium salt is reduced to a coloured, water-

insoluble formazan product only by metabolically active cells, this assay detects viable cells exclusively. After it is solubilized, the formazan formed can easily and rapidly be quantitated in a conventional ELISA plate reader at 550-600 nm (maximum absorbance). Because this technique needs no additional cell washing or cell harvesting steps, the complete assay from the start of the microculture to data analysis in an ELISA plate reader can be performed in the same microplate. In addition, the ELISA plate reader is linked with a computer allowing rapid and automated data processing. In the present research, the whole assay was performed in a 96-well microplate format. This miniaturization allowed many samples to be analysed rapidly and simultaneously.

The MTT assay performed in this study was utilised for the quantification of both cells grown in adherent cultures in tissue culture vessels and of cells immobilised within three-dimensional alginate beads. The assay method used was adapted from Mosmann's protocol (1983) Markusen's revised version (2005).

The molecular structures of the MTT salt and its formazan product are shown in figure 2.8.

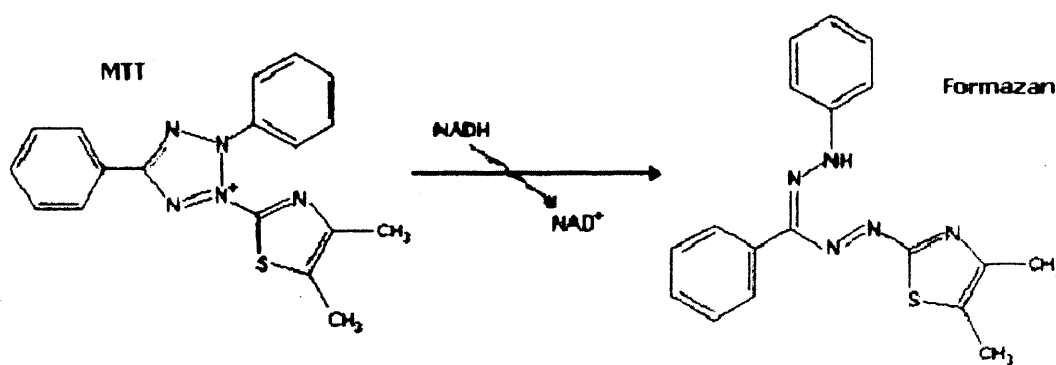


**Fig. 2.8:** Molecular structures of the dye precursor 3-(4,5-dimethylthiazol-2-yl)-2,5-diphenyltetrazolium bromide (MTT) and the purple formazan product formed upon reduction. (Picture adapted from biosynth chemistry and biology, available at <http://www.biosynth.com>).

### 2.7.1 Cell standard curve

First of all, a cell standard curve was created from a serial dilution of the cell suspension. hMSCs were harvested with a 0.25% trypsin/0.02% EDTA solution as described in section 2.1.3. A small sample (500μL) of the cell suspension was used for the determination of the cell count using a haemocytometer, as described in

section 2.6.2. After centrifugation and removal of the supernatant, the cell pellet was resuspended with Dulbecco's phosphate buffered saline with 1g/L D-glucose and 36mg/L sodium pyruvate (DPBSG, Biowhittaker, Cambrex, Verviers, Belgium) to a final concentration of  $2 \times 10^6$  viable cells/mL. A small aliquot of this cell suspension was used for an additional cell count after dilution with DPBSG, in order to confirm the cell concentration in the pellet sample. The cell suspension was serially diluted with DPBSG in a 96 well microplate; the final working volume in each well was 100 $\mu$ L. The serial dilution was performed in duplicate with cell concentrations ranging from 0 to  $20 \times 10^4$  viable cells/well (table 2.3). The MTT protocol was performed as described in section 2.7.4.

Volume of cell suspension ( $\mu$ L)	Number of viable cells/well	Volume of DPBSG ( $\mu$ L)
100	$20 \times 10^4$	0
75	$15 \times 10^4$	25
50	$10 \times 10^4$	50
25	$5 \times 10^4$	75
12	$2.4 \times 10^4$	88
The cells were diluted 1:12 with DPBSG and a further serial dilution was performed as follows		
50	$1.2 \times 10^4$	50
30	$0.72 \times 10^4$	70
10	$0.24 \times 10^4$	90
control	0	100

**Table 2.3:** Serial dilution of the cell suspension for the MTT cell standard curve.

### 2.7.2 Cell standard curve for hMSCs immobilised in three-dimensional alginate beads

Prior to the performance of the MTT assay on the cells/alginate beads, it was necessary to remove from the beads the residual culture medium containing phenol red that would interfere with the absorbance reading. For this reason, the beads were first transferred into a 10cm Petri dish (Sterilin, Bibby Sterilin, Stone, UK) and washed with DPBSG. After this washing step, the beads were removed from the Petri dish and placed into a 96-well microplate. In order to assess the linearity of each MTT assay, a serial dilution of beads was performed, as shown in table 2.4. The serial dilution was performed in duplicate with number of beads per well ranging from 0 (for a background control) to 3. A cell standard curve was in this way created for hMSCs immobilised in the beads, since the number of cells/well would be a multiple of the number of beads. For the determination of the number of cells/well, additional beads were dissolved and used for the cell enumeration using a haemocytometer, as described in section 2.7.3. Afterwards, the final working volume in each well was equalised with DPBSG to a total volume of 100 $\mu$ L/well, and the MTT assay was performed as described in section 2.7.4.

Number of beads per well	Volume of DPBSG ( $\mu$ L)	Total (average) number of cells/well
0	100	control
1	100	1X
2	100	2X
3	100	3X

**Table 2.4:** Serial dilution of alginate/cells beads for the MTT assay standard curve. Additional beads were dissolved and used for the cell count with a haemocytometer, in order to determine the total number of cells/well for each experiment. In order to calculate the remaining total number of cells/well, the average number of cells/beads, denoted as 1X, was multiplied by 2 (2X) and by 3 (3X).

### **2.7.3 Determination of cell concentration in alginate beads**

For the determination of the cell concentration in the beads, 1-3 beads were dissolved for 15 minutes in a 0.3M trisodium citrate (Sigma) and 10X trypsin/EDTA in saline (BioWhittaker). Typically 100µL citrate and 10µL trypsin/EDTA were used for each bead. The dissolved beads were then mixed and homogeneously resuspended into a single cell suspension. A small sample of the resulting cell suspension was used for the determination of the cell count with a haemocytometer (section 2.6.2) and for the assessment of the cell viability using the exclusion assay with trypan blue dye (section 2.6.3). The total volume of each sample was carefully monitored with a graduated pipette and the total cell concentration and the average cell concentration for each bead were subsequently calculated as follows:

$$\text{Total cell concentration} = (\text{cell concentration/mL}) \times (\text{total volume})$$

$$\text{Average cell concentration/bead} = \text{total cell concentration} / \text{number of beads dissolved}$$

The number of beads dissolved in each experiment varied depending upon the size of the bead and the original cell concentration in the bead.

### **2.7.4 MTT protocol**

#### **2.7.4.1 MTT incubation**

A 5mg/mL MTT (Sigma) solution in Dulbeccos's phosphate buffered saline with 1g/L D-glucose and 36mg/L sodium pyruvate (DPBSG, Biowhittaker, Cambrex, Verviers, Belgium) was added to each sample well and left in action for 1-3 hours, at 37°C in a humidified 5% CO<sub>2</sub> incubator (HeraCell150, Kendro Laboratory Products GmbH, Langenselbold, Germany or Galaxy S, RS Biotech Laboratory Equipment Ltd., Irvine, Scotland). Typically 100µL DPBS and 10µL MTT were added to each well. During incubation with the MTT solution the microplate was covered with plastic film in order to minimize evaporation. After diffusion into the cells, the water

soluble yellow MTT salt was converted by the mitochondrial dehydrogenase enzyme of viable cells into an insoluble purple formazan product.

In the case of cells/alginate beads, it was necessary to add a 0.3 M trisodium citrate (Sigma) solution in distilled water (BioWhittaker) in order to dissolve the alginate within the beads. The citrate solution (40 $\mu$ L/well) was left in action at 37°C for an additional hour and the microplate was then centrifuged (5810R, Eppendorf AG, Hamburg, Germany) at 100g for 5 minutes. The supernatant was carefully removed from each well in order to eliminate any volume inconsistencies that may have arisen from the initial DPBSG or alginate beads, and to eliminate the majority of the alginate solution from the well. Mixing of the cell suspensions resulting from the dissolution with trisodium citrate was avoided in order to reduce loss of cells adhering to the inner surface of the pipette. Particular attention was also taken in removing the supernatant from the microplate wells after centrifugation, in order to ensure that the cell pellet at the bottom of the well was not disturbed during the procedure.

The hMSCs cultured in monolayer (without the alginate matrix) were incubated with the MTT solution following the same procedure, even though in this case the addition of the trisodium citrate solution was not necessary. An MTT procedure identical to the one outlined above for the cells/alginate beads was followed in order to mimic the contents of the residual alginate in the wells containing beads.

#### **2.7.4.2 Solubilisation of the formazan product**

After centrifugation and removal of the supernatant, the microplates were either immediately treated for the dissolution of the formazan product, or wrapped in foil and frozen at -80°C. The freezing step allowed to perform the procedure more conveniently in two separate steps. The frozen plates from each time point were usually thawed and completely processed (e.g. dissolved and read) on the same day. Microplates containing only cell pellets (and no cells/alginate beads) were treated immediately after centrifugation (or after the freezing-thawing step) with a solution of isopropanol (Sigma) containing 0.1N HCl (Fluka), in order to dissolve the formazan product after permeabilisation of the cells.

Whilst the cells/alginate beads resulting from centrifugation (or from the freezing-thawing step) were reconstituted with DPBSG (50 $\mu$ L/bead) supplemented with 10X

trypsin/EDTA in saline (20 $\mu$ L/bead), prior the addition of the isopropanol/HCl solution. Treatment with 10X trypsin/EDTA was necessary to release the single cells from the alginate-GRGDY matrix and to obtain a homogeneous cell suspension. After addition of 10X trypsin/EDTA in saline, the microplates were wrapped in plastic film and incubated at room temperature for approximately 30 minutes. The bead/s in each well sample was/were then thoroughly mixed with a micropipette to a final single cell suspension prior addition of the isopropanol/HCl solution.

The microplates were covered with plastic film in order to minimize evaporation and were incubated at room temperature with the isopropanol/HCl solution (100 $\mu$ L/well) for 20 minutes. The cell pellet in each well was then thoroughly mixed to maintain the homogeneity of the cell suspension and the microplates were subsequently incubated at room temperature for additional 20 minutes. Finally, the cell suspension in each well was mixed again just before reading the absorbance of the samples.

#### **2.7.4.3 Analysis of data**

After addition of the isopropanol/HCl solution, the 96 well microplates were read on a spectrophotometer (Packard Bioscience Spectracount<sup>TM</sup>, Packard-Becker BV, Groningen, The Netherlands) using an absorbance value of 600nm.

In most cases when isopropanol is used to dissolve the formazan final product, the absorbance is measured at 570nm with background subtraction (reference wavelength) at 630nm [Mosmann, 1983; Wang, 2003; Yang, 2003]. Sometimes the data are read at 620nm [Carrier *et al.*, 1999]. In the present research, the Packard Bioscience microplate spectrophotometer used did not contain a 570nm filter, therefore the reading was always performed at 600nm which was the closest filter available in the instrument. As previously demonstrated, the utilisation of a different wavelength did not affect the results of the MTT assay [Markusen, 2005].

### 2.7.5 Interference of the three-dimensional alginate matrix with MTT absorbance

In this research the MTT assay was performed on three-dimensional beads containing only alginate (without cells), in order to evaluate the possible interference of the residual alginate with the final MTT results. For this purpose, beads consisting of complete MesenCult medium (25% v/v) and 1% w/v Pronova SLG100 alginate solution (75% v/v) were prepared as described in section 2.5.3, and then tested with the MTT assay according to the procedure that follows. For this experiment, a 96 well microplate was seeded with a constant cell concentration and an increasing number of “cell-free” alginate beads in each well. Typically 12 $\mu$ L of cell suspension were seeded in each individual well, corresponding to a cell concentration of  $2.05 \times 10^4$  cells/well. Table 2.5 shows the volumes of cell suspensions and of DPBSG and the number of alginate beads loaded to each well in the present experiment.

Volume of cell suspension ( $\mu$ L)	Cell concentration n/well	Number of beads/well	Volume of DPBSG ( $\mu$ L)
0 (control)	0	0	100
12	$2.05 \times 10^4$	0	88
12	$2.05 \times 10^4$	1	88
12	$2.05 \times 10^4$	2	88
12	$2.05 \times 10^4$	3	88
12	$2.05 \times 10^4$	4	88

**Table 2.5:** Volume of cell suspension, cell concentration, number of beads and volume of DPBSG loaded into each individual well of a 96 well microplate for the testing of the alginate interference with MTT absorbance. Each well was loaded with the same cell concentration and an increasing number of cell-free alginate beads.



The microplates were incubated with the MTT solution and then immediately treated for the dissolution of the beads with trisodium citrate, according to the procedure outlined in section 2.7.4. No freezing-step was performed for the present experiment. These results are discussed in chapter 5.

### **2.7.6 Determination of hMSCs proliferation within alginate beads**

In order to evaluate the hMSCs growth within three-dimensional alginate beads over a time course, the MTT assay was performed at different time-points over a 14-day culture period on cells entrapped within alginate beads. Concurrently, a serial dilution was performed in duplicate, with 0, 2, 4 and 6 beads per well to confirm the linear correlation between the number of cells/well and the number of beads tested. The beads were prepared with 25% v/v cell suspension and 75% v/v Pronova SLG100 alginate-GRGDY.

In a similar study, the effects of the freezing-step were also evaluated by comparing the absorbance values obtained for plates frozen after MTT incubation with those measured for plates immediately processed for the dissolution of the formazan product. These results are discussed in chapter 5.

### **2.7.7 Interference of alginate in solution with MTT absorbance**

The MTT assay was also performed on both hMSCs and rSMCs cultured in monolayer in the presence of alginate in solution, in order to evaluate the possible interference of the alginate in solution with the final MTT absorbance values. For this purpose, hMSCs or rSMCs were resuspended in complete growth medium and seeded on 96-well plates at the initial seeding density of  $6 \times 10^3$  cells/cm<sup>2</sup>. After 24 hours in culture, the medium was replaced from each well with the alginate solution. A serial dilution was performed in duplicate with alginate concentrations ranging from 0 to

1mL/well. The culture was regularly evaluated microscopically for possible morphological changes, or eventual cell death, occurring over time.

The MTT assay was performed for both the rSMCs and hMSCs culture after 10 days in culture, according to the procedure already described. These results are described in chapter 5.

The table below shows the cell concentration, the volumes of growth medium and of alginate in solution loaded into each individual well of a 96-well plate in the present experiment.

Cell concentration /cm <sup>2</sup>	Cell concentration /well	Volume of medium( $\mu$ L) /well	Volume of alginate( $\mu$ L)/ well
(Control) $6 \times 10^3$	$1.14 \times 10^4$	1000	0
$6 \times 10^3$	$1.14 \times 10^4$	990	10
$6 \times 10^3$	$1.14 \times 10^4$	980	20
$6 \times 10^3$	$1.14 \times 10^4$	970	30
$6 \times 10^3$	$1.14 \times 10^4$	960	40
$6 \times 10^3$	$1.14 \times 10^4$	950	50
$6 \times 10^3$	$1.14 \times 10^4$	940	60
$6 \times 10^3$	$1.14 \times 10^4$	930	70
$6 \times 10^3$	$1.14 \times 10^4$	920	80
$6 \times 10^3$	$1.14 \times 10^4$	910	90
$6 \times 10^3$	$1.14 \times 10^4$	900	100
$6 \times 10^3$	$1.14 \times 10^4$	500	500
$6 \times 10^3$	$1.14 \times 10^4$	0	1000

**Table 2.6:** Serial dilution performed into a 96 well microplate for the testing the interference of the alginate in solution with MTT absorbance. Each well was loaded with the same cell concentration and a solution with increasing concentration of the alginate in solution.

### **3. The derivatisation and characterisation of the alginate derived-polymer for tissue engineering applications**

This chapter focuses on the derivatisation of the alginate polymer with the Gly-Arg-Gly-Asp-Tyr (GRGDY) pentapeptide and on the characterisation of the resulting alginate-GRGDY, prior to its addition to the cells and its deployment as scaffold for the fabrication of tissue engineered constructs. The results obtained from the studies performed for the characterisation of these alginate constructs containing cells are presented in chapter 5.

#### **3.1 Introduction**

The aim of this research was the fabrication of alginate/cells constructs for future deployment in tissue engineering applications. Such tissue-engineered constructs could for instance be employed as living blood vessel substitutes for use in cardiac bypass surgery for coronary artery disease. Current methodologies using cells or veins or foreign materials for the treatment of these conditions are unsatisfactory [Edelman, 1999; Darling *et al.*, 1972; Niklason *et al.*, 1999]. As a result, there is a urgent need for alternatives, and tissue engineering was the approach investigated in this research.

The focus was on the use of a completely biological scaffold, one that would allow the fabrication of vascular grafts that are biocompatible and have adequate mechanical strength, durability and compliance comparable to the existing vessels [Nerem, 2000; Teebken and Haverich, 2002]. Because of their gentle gelling properties, alginates are widely used as materials for the encapsulation and immobilisation of a variety of cells *in vitro* [Fremond *et al.*, 1993] and *in vivo* [Chang *et al.*, 2001] and for several tissue engineering applications [Hauselmann *et al.*, 1996; Atala *et al.*, 1994]. Cross-linked alginate hydrogels are utilised in various biomedical applications [Draget *et al.*, 1997] and recent studies suggest that different approaches can be used to control and manipulate the physical properties of these biomaterials in a way that permits the development of cell transplantation vehicles desirable for various biomedical applications [Kong *et al.*, 2004; Kong *et al.*, 2004]. In addition, in

previous studies conducted with human cells, cell function and differentiation have been reported using alginate as a matrix [Rowley and Mooney, 2002; Wang *et al.*, 2003]. Furthermore, the alginate used in these studies (Pronova Biomedical, Oslo, Norway) has shown to support tissue and vascular ingrowth with minimal inflammatory response and capsule formation surrounding the implants when injected in the subcutaneous space of adult sheep [Halberstadt *et al.*, 2002]. Given these advantages and encouraging results, alginate was the material of choice in this work.

Ultra-pure alginates, which contain only low levels of pyrogens, were used as scaffold materials for the preparation of alginate/cells constructs. In addition, in order to reduce potential contaminants (e.g. heavy metals and polyphenols) that could be present in the commercial biomaterial, dialysis was performed on the original alginate samples prior to its addition to the cell suspension.

In order to permit and improve cell binding to the biomaterial, the GRGDY peptide, containing the specific RGD cell adhesion sequence, was immobilised onto the alginate polymeric chain. The resulting alginate-GRGDY was then used to grow adherent cells (i.e. human mesenchymal stem cells and human foreskin fibroblasts).

The results obtained from the studies investigating the alginate derivatisation procedure with the GRGDY pentapeptide are presented in section 3.2, whereas the data obtained from the characterisation studies on the resulting alginate-GRGDY matrix are described in section 3.3.

### ***3.2 Derivatisation of the alginate with the GRGDY pentapeptide***

A detailed description of the protocols employed for the preparation of the derivatised alginate-GRGDY is given in section 2.3.2. The final derivatisation procedure adopted in the present research was the result of a series of optimisation studies conducted at the beginning of this research in collaboration with Julia Markusen [Markusen, 2005].

The first step for the derivatisation of the alginate was the 20-hour reaction incorporating the GRGDY pentapeptide on the alginate, resulting in the derivatised

alginate, which displays the –GRGDY-COOH sequence bound to the carboxylic groups of the guluronic acid units recurring along the polymeric chain. Different alginate types (please see section 3.2.2.1) and reactants (EDC and sulfo-NHS) concentrations (section 3.2.2.2) were tested for the reaction. In addition, different peptide concentrations were investigated, as described in section 3.2.2.4. EDC, sulfo-NHS and the GRGDY peptide were all filtered through 0.2 µm filters prior to their addition to the reaction vessel, thus ensuring all the reagents were free from microbial contamination.

After completion of the coupling reaction a 5-day dialysis step was performed on the reaction mixture in order to remove the cell toxic reactants left over from the carbodiimide reaction (i.e. EDC and sulfo-NHS) and the heavy metals and polyphenols from the commercial alginate (please see section 3.2.3). The temperature was carefully monitored and maintained constant at 20-22°C during both the carbodiimide reaction and the dialysis cycle. Significant temperature changes would have otherwise affected the reaction, due to changes in reaction rates and molecular mixing, and the diffusion of molecules across the dialysis membrane. The whole procedure was conducted in the dark because the reactants are known to be light-sensitive.

The diagram presented in Figure 3.1 gives an overview of the derivatisation procedure employed for the attachment of the GRGDY peptide onto the alginate matrix. The different alginate types and the different reactants and peptide concentrations used in this work are shown, together with the alternative routes tested for the aseptic preparation of the final sterile alginate-GRGDY.

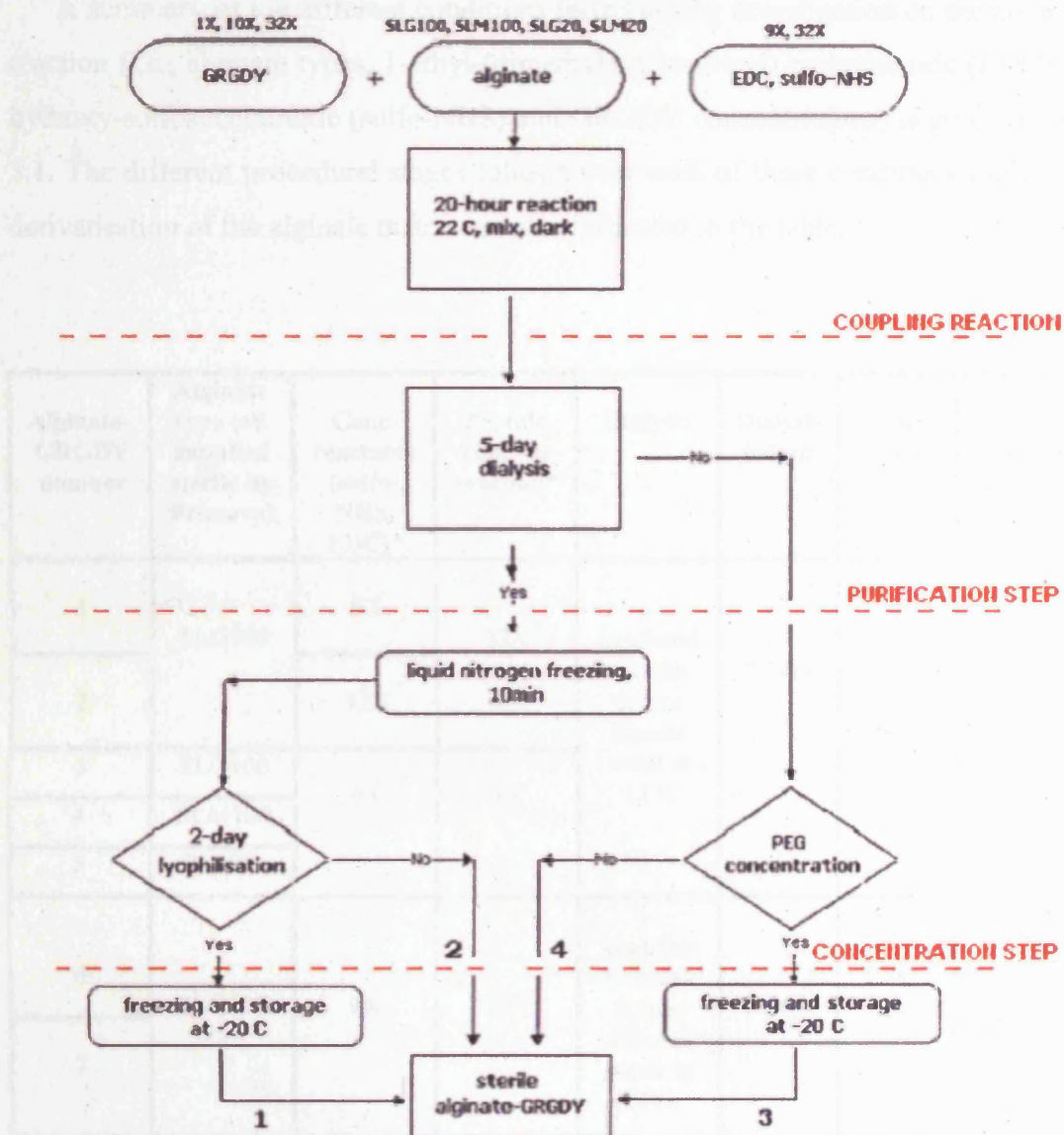


**Figure 3.1:** Flow diagram representing a schematic of the alginate derivatisation with the GRGDY peptide. The diagram shows the different factors investigated and the alternative methods employed for the preparation of the final alginate-GRGDY product:

- 1 Performing 2-day lyophilisation followed by freezing step (procedure no. 1);
- 2 Avoiding freezing step after lyophilisation (procedure no. 2);
- 3 Performing polyethylene glycol (PEG) concentration as an alternative to lyophilisation, followed by freezing step (procedure no. 3);
- 4 Avoiding freezing step after PEG concentration (procedure no. 4).

A summary of the different conditions tested during investigation on the coupling reaction (i.e., alginate types, 1-ethyl-(dimethylaminopropyl) carbodiimide (EDC), N-hydroxy-sulfosuccinimide (sulfo-NHS) and GRGDY concentrations) is given in table 3.1. The different procedural stages followed for each of these conditions during the derivatisation of the alginate matrix are also indicated in the table.

Alginate-GRGDY number	Alginate type (all supplied sterile by Pronova)	Conc. reactants (sulfo-NHS, EDC)*	Peptide conc. in reaction*	Dialysis	Dialysis length	Conc. step	Freeze-storage (-20°C)
1	SLG100	9X	32X	$\gamma$ -irradiated cassettes, 0.2 $\mu$ m filtered water in LFH	5 days	2 days lyo.	Yes
2		12X					
3	SLG100	9X	1X				
4	SLM100						
5	SLM20						
6	SLG100	9X	10X	$\gamma$ -irradiated cassettes, 0.2 $\mu$ m filtered water in LFH	5 days	2 days lyo.	Yes
7							No
8	SLG100	9X	10X	$\gamma$ -irradiated cassettes, 0.2 $\mu$ m filtered water in LFH	5 days	PEG conc.	Yes
9						(approx. 3 hours)	No
10	SLG100	9X liquid EDC	32X	$\gamma$ -irradiated cassettes, 0.2 $\mu$ m filtered water in LFH	5 days	2 days lyo.	Yes
11	SLG20						

**Table 3.1:** Derivatisation procedures performed in the present study for the incorporation of the GRGDY peptide in the alginate matrix. \*1X reactants' concentrations correspond to 1mg of alginate containing 38  $\mu$ g of sulfo-NHS, 67  $\mu$ g of EDC and 1  $\mu$ g of peptide, as defined by Rowley (1999). All reactants and peptide



were sterile filtered through a 0.2µm filter prior to derivatisation. Alginates-GRGDY no. 1, no.2, no.6 and no.10 (highlighted in yellow) were also assessed by means of amino acid analysis (data presented in table 3.3).

### **3.2.1 Effect of preservation of alginate-derived polymer with respect to biochemistry**

The 5-day dialysis step was followed by the alternative concentration procedures listed below (please see diagram in figure 3.1):

1. Performing 2-day lyophilisation followed by freezing step (procedure no. 1);
2. Avoiding freezing step after lyophilisation (procedure no. 2);
3. Performing polyethylene glycol (PEG) concentration as an alternative to lyophilisation, followed by freezing step (procedure no. 3);
4. Avoiding freezing step after PEG concentration (procedure no. 4).

The alginates resulting from these four different procedures were compared with respect to their effect on the gel strength during the preparation of alginate/cells beads and on cell behaviour. These results are described in chapter 5.

The following sections describe in more details the parameters investigated during the initial coupling reaction and subsequent dialysis and re-concentration steps of the derivatisation process.

### **3.2.2 The coupling reaction**

The carbodiimide chemistry for the alginate derivatisation was performed according to the method reported by Rowley and colleagues [Rowley *et al.*, 1999]. The H<sub>2</sub>N-GRGDY-COOH pentapeptide was incorporated onto the alginate through the carboxylic acid groups on the guluronic acid monomers of the polysaccharide chain, as already described in section 2.3.2 (please see figure 2.2 for the scheme of the reaction). The reaction involves the use of ethyl-(dimethylaminopropyl)carbodiimide (EDC) acting as a cross-linking agent and coupling the carboxyl groups on the polysaccharide to primary amines (through their N-terminal). The EDC first reacts with the alginate, by removing a proton from the



carboxyl acid groups on the uronic acid monomers. The resulting protonated EDC then reacts with the O<sup>-</sup> on the carboxylic acid group to form the intermediate (O-acylisourea), which then reacts with the sulfo-NHS to form a reactive sulfo-NHS ester. This then reacts with the N-terminal of the GRGDY pentapeptide, eliminating urea.

The reactants were added in a specific order, which was essential for the right reaction to result. The sulfo-NHS, followed by the EDC, had to be added to the alginate first, allowing enough time for them to disperse homogeneously throughout the alginate solution. This then ensured that the peptide reacted with an EDC molecule (according to the reaction shown in figure 2.2) immediately after addition to the reaction vessel. As a result, the probability that the unstable O-acylisourea intermediate would come straight into contact with a sulfo-NHS molecule was very high, thus immediately forming the amine-reactive sulfo-NHS ester.

### **3.2.2.1 Alginate formulation**

The aim of this work was to produce a scaffold suitable for addition to the cell suspension and for the fabrication of alginate/cells constructs where cell viability was maintained over time. For this purpose, the sterility of the alginate-GRGDY resulting from the alginate derivatisation with the GRGDY peptide was an essential requirement.

Preliminary studies investigating various alginate types concluded that the use of sterile Pronova sodium alginate was the best way to ensure the preparation of a final sterile product, thus enabling it to be used for cell culture work [Markusen, 2005]. The use of a sterile alginate permits to by-pass any extra sterilisation step that would otherwise result necessary after the alginate itself has been derivatised. This reduces handling of the alginate-GRGDY and allows maintaining high sterility in the final product. As a result, the alginate used in this research was supplied by the manufacturer as sterile product (NovaMatrix FMC BioPolymer, Norway). For this reason it was not necessary to perform autoclaving, which would reduce the length of the alginate chain, the alginate viscosity and molecular weight [Leo *et al.*, 1990; Vandenbossche and Remon, 1993; Zoro, 2005] and would denature the peptide, or filtration. Both these methods proved to be ineffective sterilisation techniques, hence the necessity and choice to use alginate supplied as sterile product.

In the present study the use of different Pronova ultra-pure sodium alginates was investigated. Pronova's alginate is available with either high guluronic acid (SLG) or high mannuronic acid (SLM) concentration, and with either high viscosity (SLG100, SLM100) or low viscosity (SLG20, SLM20). Four alginate types (SLG100, SLG20, SLM100 and SLM20) were investigated, and the products specifications for these alginates were provided by the manufacturer (please see table 3.2).

	SLG20	SLG100	SLM20	SLM100
Apparent viscosity (mPA s)	20-100	>100	20-100	>100
Molecular weight (kDa)	75-180	160-250	75-180	160-250
pH	5.5-8.5			
Guluronic acid (%)	>60		Unknown	
Mannuronic acid (%)	Unknown		>50	
Protein (%)	<0.3			
Endotoxins (EU/gram)	<100			
Heavy metals (ppm)	<40			
Pb (ppm)	<10			
Hg (ppm)	<1			
Microbiological purity	sterile			

**Table 3.2:** Products specifications for Pronova SLG100, SLG20, SLM100 and SLM20 alginates (provided by the manufacturer, NovaMatrix FMC BioPolymer, Norway).

The alginate was dissolved in normal-saline solution (0.9% NaCl in water for cell culture applications, pH=7-7.4) or MES/NaCl buffer as described in section 2.3.1. Preliminary investigations had shown this was the best option since when alginate mixed with water for injection was used for the preparation of alginate/cells constructs, low cell viability and cell lysis due to the non-physiological conditions (e.g. low pH and osmolarity) were observed. In addition, reconstitution of the alginate

with buffered saline solutions (e.g. PBS phosphate buffered saline without) caused precipitation of undesirable insoluble calcium phosphate after addition of the  $\text{CaCl}_2$  cross-linking solution.

### **3.2.2.2 EDC and sulfo-NHS concentration employed in the coupling reaction**

Different reactants (EDC and sulfo-NHS) concentrations were tested for the coupling of the GRGDY peptide onto alginate. The range of reactants' concentrations used in this procedure (e.g. 9X and 12X) were multiples of the 1X reactants' concentrations described by Rowley (1999), where 1X reactants correspond to 1mg of alginate containing 38  $\mu\text{g}$  of sulfo-NHS, 67  $\mu\text{g}$  of EDC and 1  $\mu\text{g}$  of peptide. 9X and 12X were respectively 9 and 12 times the reactants' concentration, as defined by Rowley (please see table 2.2). Range finding experiments conducted to optimise the alginate derivatisation procedure proved that 9X and 12X were the best reactants (EDC and sulfo-NHS) concentrations for the derivatisation of Pronova ultrapure SLG100 alginate, permitting cell attachment and cell elongation after immobilisation of the cells within the three-dimensional alginate-GRGDY/cells constructs. Higher reactants concentrations (27X and 50X) led to the dissociation of the alginate beads within 24 hours (possibly because the higher incorporation of the pentapeptide onto the alginate prevented the binding of sufficient calcium ions, which is necessary to hold the beads in shape).

Amino acid analysis was performed to ascertain the degree of derivatisation on the alginate-GRGDY obtained from the coupling reaction involving either 9X or 12X reactants concentrations. The results of these studies are described in section 3.3.1.

### **3.2.2.3 Use of manufacturer-prepared EDC solution**

1-Ethyl-3-(3-dimethylaminopropyl)-carbodiimide (EDC) is a water-soluble derivative of carbodiimide, which catalyzes the formation of amide bonds between carboxylic acids and amines by activating carboxyl to form an O-urea derivative. This derivative then reacts readily with nucleophiles. Carbodiimide has been used in this work for the coupling reaction of the alginate with the GRGDY peptide as the water-soluble derivative EDC.HCl, as it is represented in figure 3.2.

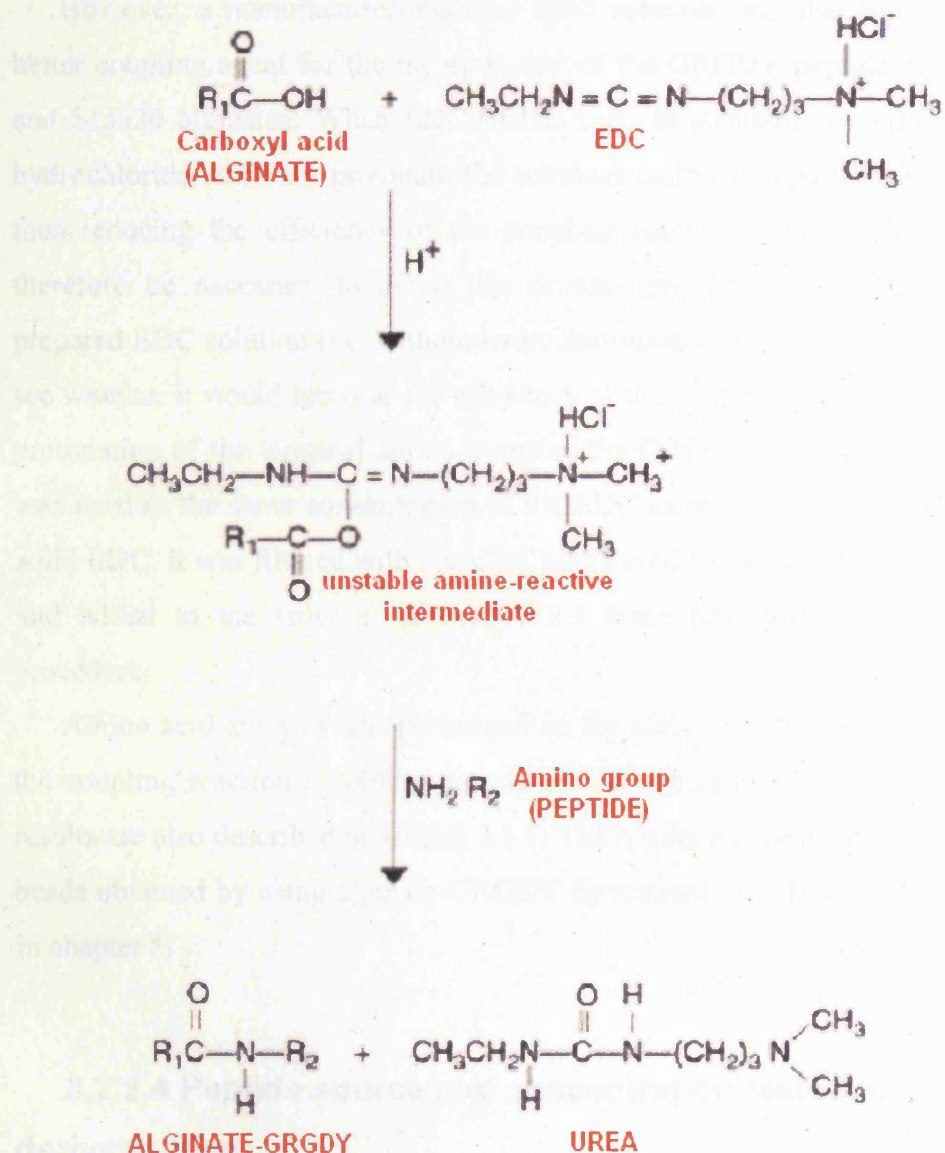


**Figure 3.2:** The mechanism of the reaction of alginate with peptide, highlighting the role of the water-soluble 1-ethyl-3-(3-dimethylaminopropyl)-carbodiimide (EDC) as coupling agent. The schematic shows the carboxyl group (-COOH) of the guluronic acid units of the alginate polymer involved in the reaction. The amino group (-NH<sub>2</sub>) of the glycine (G) residue at the beginning of the GRGDY peptide sequence, which is the peptide's group involved in the reaction, is also shown in the illustration above. Thus, R<sub>1</sub> represents the alginate polymeric chain, whereas R<sub>2</sub> represents the peptide GRGDY sequence. EDC catalyses the formation of amide bonds between the alginate's carboxylic acids and the peptide's amino groups by activating carboxyl to form an urea derivative. Manufacturer-prepared EDC solution was tested as an alternative coupling agent, under the hypothesis that it would reduce the protonation of the peptide's amino group thus increasing the efficiency of the reaction. (Picture sourced from Instructions EDC Pierce, available at <http://www.piercenet.com>).

However, a manufacturer-prepared EDC solution was also tested as a possible better coupling agent for the incorporation of the GRGDY peptide on both SLG100 and SLG20 alginates. When EDC.HCl is used in standard coupling reactions, the hydrochloride salt may protonate the terminal amino groups of the peptidic chain, thus reducing the efficiency of the coupling reaction. Addition of a base would therefore be necessary to avoid this protonation. The use of the manufacturer-prepared EDC solution (i.e. without hydrochloride salt crystals) was tested in order to see whether it would increase the efficiency of the coupling reaction, by reducing the protonation of the terminal amino group of the GRGDY peptide. The EDC solution was used to the same concentration of 9X EDC as in the previous experiments with solid EDC. It was filtered with the same filters used for the reactant in the solid form, and added to the reaction at exactly the same time-point in the derivatisation procedure.

Amino acid analysis was performed on the alginate-GRGDY after completion of the coupling reaction involving the manufacturer-prepared EDC solution, and these results are also described in section 3.3.1. The results for the analysis of alginate/cells beads obtained by using alginate-GRGDY derivatised with liquid EDC are presented in chapter 5.

#### **3.2.2.4 Peptide source and concentration tested for the alginate derivatisation**

The peptide used in this work was provided by two different suppliers. The GRGDY peptide supplied by Neosystem Groupe SNPE was used in the first preliminary experiments; when this was no longer available peptide supplied by Albachem Limited was used. The amount of the GRGDY peptide that was added to the alginate was varied between 1X, 10X and 32X, where 1X was 1µg of peptide added per 1mg of alginate [Rowley *et al.*, 1999], and 10X and 32X were respectively ten and thirty-two times the peptide's concentration per 1mg of alginate. These investigations were performed to determine which was the lowest peptide concentration enabling incorporation of the GRGDY peptide on the alginate matrix prior to its use for the preparation of beads encapsulating cells.

The GRGDY peptide sequence of the product originally supplied by the manufacturer was analysed with nuclear magnetic resonance and mass spectrometry, in order to obtain information on the chemical structure of the peptide, and to confirm it was supplied as a complete pentapeptide sequence from the manufacturer (please see section 3.3.3). After completion of the derivatisation reaction, the alginates coupled with the different peptide concentrations were mixed with the cell suspension and used for the preparation of alginate/cells constructs. The results obtained from these analyses are presented in chapter 5.

### **3.2.3 Dialysis step as purification method of the alginate-GRGDY**

After completion of the 20-hour reaction it was necessary to remove from the reaction mixture the excess reagents and un-reacted peptide, which would otherwise bind to the cells and compete for binding sites with the alginate-GRGDY, since it is not bonded to any alginate. Removal of by-products toxic to the cells, such as urea, was also necessary. Gamma-irradiated Slide-A-Lyzer Dialysis Cassettes (Pierce, Rockford, Illinois) with a molecular weight cut-off (MWCO) of 3.5 kDaltons were used to ensure purification of the alginate-GRGDY by removal of the unwanted reactants. These devices effectively remove salts and small molecules less than 3,500 daltons from solutions and are normally used for a wide range of applications, including low molecular-weight contaminant removal, buffer exchange, desalting, equilibrium dialysis, and concentration. The cassette membrane is composed of low-binding regenerated cellulose and features a hermetically sealed sample chamber to retain the sample. The dialysis cassette was hydrated in autoclaved reverse osmosis (RO) purified water (MilliQ Synthesis A10, Millipore, Molsheim, France) filtered through a UV irradiated 0.22  $\mu\text{m}$  filter for 30 minutes prior addition of the alginate sample. The sample was then introduced into the cassette cavity by penetrating the self sealing port with a hypodermic needle attached to a syringe (please see schematic in figure 3.3). After removal of the needle, the gasket immediately resealed, ensuring that no sample was lost from the port of the cassette during dialysis.



**Figure 3.3:** Schematic of the dialysis step for the alginate-GRGDY purification using Slide-A-Lyzer Dialysis Cassettes with 3.5 kDa MWCO membranes. (Picture sourced from <http://www.piercenet.com>).

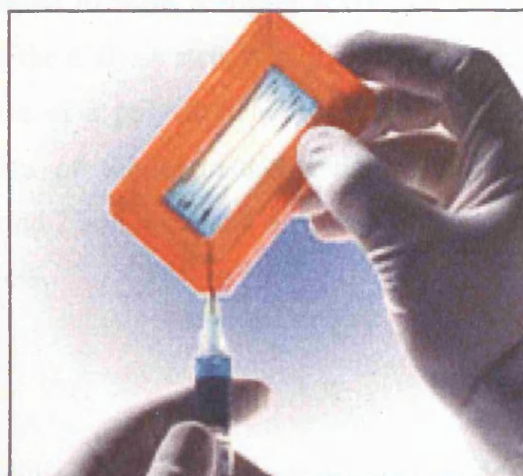
1. The cassette cavity was filled with the alginate-GRGDY solution sample through one of the self sealing ports in the corner of the cassette.



2. The dialysis was carried out for 5 days, within autoclaved filtered RO purified water. Water changes were performed every 12 hours throughout the 5-day dialysis cycle.



3. After completion of the dialysis, the dialysed alginate-GRGDY sample was withdrawn from the cassette with a sterile syringe and needle through the self sealing port.



The dialysis was carried on for a minimum of 5 days, since preliminary investigations conducted at the beginning of this research concluded that 5 days was a suitable time necessary for completion of dialysis, as opposed to a 2-day dialysis cycle. A shorter dialysis led to formation of alginate-GRGDY beads that were too weak and swelling within 24 hours after formation and addition of the medium of culture; the outer shell of the beads was still intact however the inner contents of the beads appeared to spill out due to the influx of water into the beads.

In order to maintain efficient dialysis all the way through the 5-day cycle, the dialysis water was changed every 12 hours, and was replaced with freshly autoclaved and filtered RO purified water. The whole procedure was performed within the laminar flow cabinet using previously autoclaved equipment, in order to ensure there was no build up of dialysed reactants in the water surrounding the reaction mixture. As a result, the whole dialysis step was performed in aseptic conditions, with the intention to remove the excess reactants and toxic by-products, while retaining the sterility of the alginate-GRGDY polymer, an essential prerequisite for its use in tissue engineering.

### **3.2.4 Concentration of derivatised alginate**

The dialysis cycle resulted in the alginate-GRGDY being diluted due to influx of water into the dialysis cassette, i.e. following the concentration gradient. Since the resulting alginate-GRGDY was too diluted to form a strong scaffold, the material needed to be re-concentrated. Following the dialysis step, two different concentration methods, either lyophilisation or the use of a polyethylene glycol (PEG) solution, were investigated for the concentration of the alginate-GRGDY matrix. These different procedures, (procedures no. 1 and 2 and no. 3 and 4 respectively in the flow diagram in Figure 3.1) are described below.

#### **3.2.4.1 Lyophilisation**

After completion of dialysis, a lyophilisation step was performed in order to re-concentrate the alginate-GRGDY, which had been diluted by the extensive dialysis. Particular care was taken during the lyophilisation procedure, in order to avoid phase



changes that could modify the pH and moisture content thus damaging the peptides. In early range-finding investigations performed at the beginning of this research a reduction of the alginate-GRGDY biological activity was observed when the lyophilisation was not performed properly, preventing cell elongation within the alginate-GRGDY/hMSCs three-dimensional constructs. These studies had shown that in order to maintain the stability of the peptide in the alginate hydrogels and the biological activity of the resulting derivatised alginate, it was necessary to perform a minimum 2-day lyophilisation cycle. In the subsequent experiments a 2-day lyophilisation step was performed on the derivatised alginate in aseptic conditions, in order to retain the sterility of the final alginate-GRGDY product. As opposed to concentration with polyethylene glycol (PEG) solution, lyophilisation proved to be a more appropriate re-concentration method, requiring the least handling, and thus further ensuring the sterility of the final product. After completion of the 2-day lyophilisation cycle, the alginate-GRGDY was either frozen and stored at  $-20^{\circ}\text{C}$  (procedure no.1), or it was immediately mixed with the cell suspension and directly used for the preparation of beads (procedure no.2).

#### **3.2.4.2 Polyethylene glycol (PEG) concentration step**

Concentration of the alginate with polyethylene glycol (PEG) was investigated as an alternative to the lyophilisation step in order to re-concentrate the alginate after dialysis. Preliminary investigations conducted at the beginning of this research had shown that freeze-drying the alginate-GRGDY may result in decreased biological activity, thus preventing cell binding to the matrix or compromising the cells capacity to elongate within the biomaterial. As a result, concentration of the alginate with the PEG solution was attempted as an alternative method to lyophilisation.

The use of solid PEG crystals was not considered because of cumbersome conditions. The use of the liquid Sterile Slide-A-Lyzer concentrating solution, which is supplied as a sterile product, was preferred. However, this procedure was problematic and required considerable handling of the sample, thus reducing the chances of maintaining sterility in the final alginate-GRGDY solution. The method involved suspending the dialysis cassette containing the dialysed sample solution in the sterile concentrating solution, and monitoring the weight over time. Frequent weighting of the alginate, while it was still within the dialysis cassette, was required.

A measurement of the alginate weight was in fact taken every 10 minutes, in order to monitor carefully the changing volume and concentration of the alginate and to avoid an excessive loss of the alginate solution weight, which would result in the undesirable over-concentration of the alginate. In addition, it was difficult to perform the weighting under aseptic conditions, and ultimately the weight measurement for the alginate samples was not accurate. The graph in figure 3.4 shows the weight values of the dialysis cassette monitored throughout the re-concentration of the alginate-GRGDY with the concentrating solution.

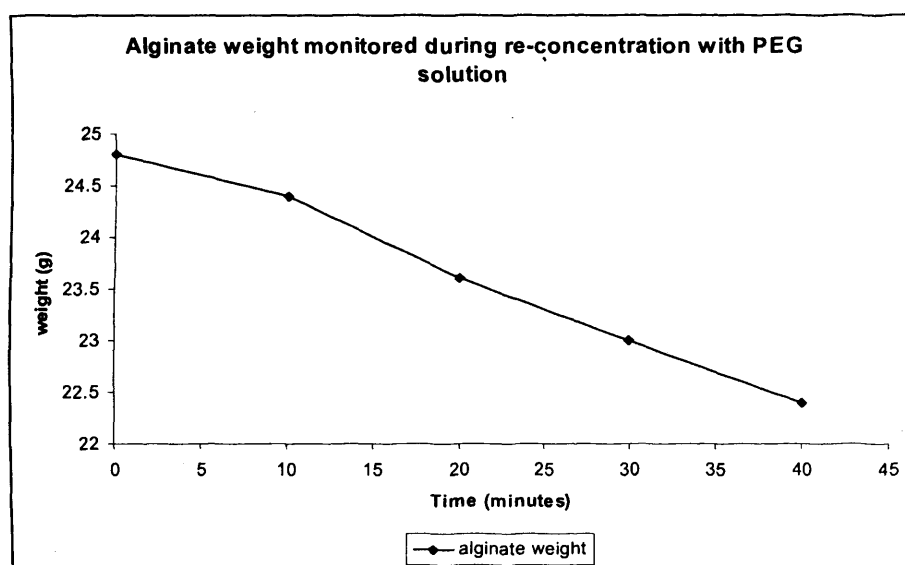


**Figure 3.4:** The weight of the dialysis cassette as monitored throughout the re-concentration of the alginate-GRGDY with the PEG concentrating solution.

The graph indicates that the weight of the cassette was rapidly decreasing. Since a working volume of 1mL was normally required for the preparation of the beads, and the volume of the alginate inside the cassette was visibly decreasing very quickly over time, the PEG re-concentration step was halted after 40 minutes. The volume of the resulting alginate solution was then measured with a sterile syringe and needle, mixed with the required volume of cell suspension and used for the preparation of the alginate/cells beads. The resulting alginate-GRGDY/cells constructs appeared to be considerably weaker than the constructs fabricated with lyophilised alginate, and started dissolving within few hours after formation and after addition of the growth medium (please see results in chapter 5).

Thus, it can be concluded that the PEG concentration step did not prove to be an ideal method for the re-concentration of the alginate-GRGDY after dialysis. Lyophilisation was therefore preferred and was used in most of the following experiments.

### **3.2.5 Freezing/no freezing step**

As shown in the diagram in figure 3.1, after completion of the whole derivatisation process, the lyophilised alginate-GRGDY was either frozen and stored at -20°C until use (procedure no.1 in the diagram), or immediately reconstituted and mixed with the cell suspension for the preparation of alginate/cells beads (procedure no.2). Similarly, long-term storage at -20°C or immediate use for the constructs preparation and further analysis were investigated for the derivatised alginate prepared with the alternative procedure involving PEG-concentration step (procedures no.3 and no.4 respectively). The analysis of the different samples allowed for the investigation of the effects of freezing, low temperature storage and thawing on the gel strength and on cell behaviour and performance (i.e. cell adhesion, elongation, viability and proliferation) after immobilisation within the alginate-GRGDY matrix. These results are presented in chapter 5.

### **3.2.6 Sterility of alginate-GRGDY**

For any biomaterial to be used as an implantable tissue engineered matrix in clinical applications, an essential requirement is for it to be non-toxic, biocompatible, non-immunogenic and pyrogen-free. For this reason Pharmacopea grade reactants (sulfo-NHS, EDC and GRGDY peptide) were used in the carbodiimide reaction and all these reagents were sterile filtered through 0.2µm 13mm syringe filters immediately prior to their use. This step ensured removal of microbes that would otherwise contaminate the alginate-GRGDY resulting from the derivatisation procedure.

### 3.2.7 Reconstitution of the alginate-GRGDY

After completion of the derivatisation procedure, the resulting alginate-GRGDY was reconstituted by dissolution in normal saline solution (0.9% NaCl in water for injections, pH=7-7.4) supplemented with the necessary amount of 1M sodium hydroxide (NaOH), as it is described in section 2.3.2.5. The alginate was typically reconstituted to the desired 1% w/v final concentration, so that the solution was isotonic for subsequent addition to the cell suspension. The addition of NaOH was deemed necessary to allow the complete dissolution of the sterile Pronova derivatised alginate following 5-day dialysis cycle. The extensive dialysis with water had most probably removed the majority of the sodium ions along the alginate polysaccharide chain, thus permitting protonation of the carboxylic groups of the biomaterial. As a result, precipitation of alginic acid crystals was observed in the reaction vessel [Doumeche *et al.*, 2004]. The addition of a base (i.e. NaOH) was necessary to solubilise the alginic acid precipitates [www.fao.org/docrep/W6355E/w6355e04.htm], permitting complete dissolution of the alginate-GRGDY. The alginate-GRGDY solution was then mixed with the cell suspension for the preparation of the alginate/cells constructs; these results are also described in chapter 5.

### 3.2.8 CaCl<sub>2</sub> solution as cross-linking agent

For the fabrication of alginate beads the alginate/cells mixture was syringed through a sterile 0.1mm diameter blunt needle and then dripped into a calcium chloride (CaCl<sub>2</sub>) solution, according to the method described in section 2.5.3. The resulting beads/droplets were left in the cross-linking solution for 15 minutes at room temperature and under agitation prior to being transferred into 24-well plates pre-loaded with the necessary amount of growth medium and to starting the culture.

The calcium chloride solution for the cross linking of the alginate was obtained by dissolving the calcium chloride (Pharmacopeia grade) in normal saline solution, as described in section 2.5.2. The dissolution in normal saline was preferred to the usage of water for cell culture applications or buffered phosphate saline solutions such as

PBS, for the same reasons described previously for the alginate dissolution (please see section 2.3.1).

Typically a 1% w/v  $\text{CaCl}_2$  solution, corresponding to a concentration of 90mM, was used for the cross-linking of the alginate. However, it is recognised that the physiological  $\text{CaCl}_2$  concentration for cells is 1.8mM, considerably lower. The high molarity (90mM) of the  $\text{CaCl}_2$  solution used in this research may therefore be toxic for the cells, but was found to be necessary to effectively cross-link the alginate molecules. In fact, previous studies proved that the 1%  $\text{CaCl}_2$  solution is the lowest concentration able to reproducibly and effectively work as cross-linking agent [Markusen, 2005].

### ***3.3 Characterisation of the alginate matrix***

#### **3.3.1 Characterisation of the alginate-GRGDY by amino acid analysis**

Amino acid analysis was employed in this project as a method of deducing the degree of derivatisation on the alginate, since it could be used to directly measure the amount of peptide present in the alginate sample.

Approximately 10 mg samples of the alginate-GRGDY resulting from the derivatisation procedure were sent for amino acid analysis (Alta Bioscience, University of Birmingham) in order to ascertain the degree of peptide attachment onto the alginate polymeric chain. The analysis was performed according to the procedure described in section 2.4.1. All the samples analysed were SLG100, whereas high M-unit (SLM100) or low viscosity (SLG20 and SLM20) alginates were derivatised and investigated mainly for the preparation of successful three-dimensional constructs with the cells (please see data presented in chapter 5).

The GRGDY sequence of the peptide used in the derivatisation of the alginate is shown in figure 3.5: a glycine (G) starts off the pentapeptide at the N-terminal side, and a tyrosine, Y (side chain =  $\text{CH}_2\text{-C}_6\text{H}_4\text{-OH}$ ) finishes the pentapeptide at the C-terminal side.

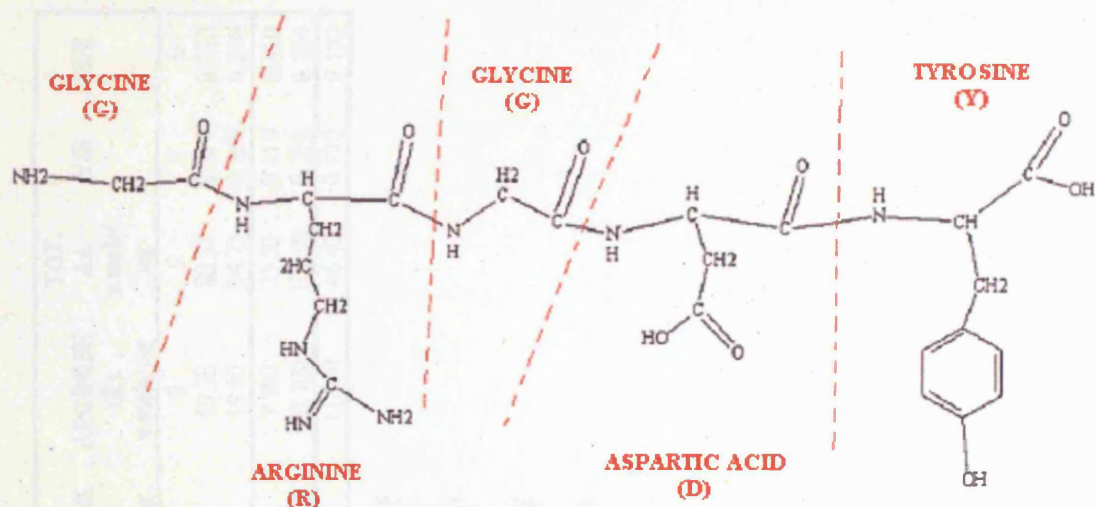


**Figure 3.5:** Chemical formula of the GRGDY peptide sequence.

The amino acid analysis permitted the quantitative assessment of the four constituent amino acids glycine (G x 2 glycine residues for each of the pentapeptide sequence), arginine (R x 1 arginine for each of the penptapeptide sequence), aspartic acid (D x 1 aspartic acid for each of the pentapeptide sequence) and tyrosine (Y x 1 tyrosine for each of the pentapeptide sequence) incorporated into the alginate after derivatisation. However, it was not possible to perform statistical analysis on the data obtained because only one measurement was taken from each sample. As a result, the comparison of the data can be characterised as indicative. Table 3.3 summarises all the amino acids data obtained from the analyses performed on approximately 10 mg samples of lyophilised SLG100 alginate-GRGDY.

Exp. no.	alginate-GRGDY number	ALGINATE	REACTANTS	PEPTIDE	ASPARTIC ACID (D) n.mole/mg	GLYCINE (G) n.mole/mg	TYROSINE (Y) n.mole/mg	ARGININE (R) n.mole/mg	TOT. AA n.mole/mg	Y/D	Y/R
1	- 1-Neosystem 2	SLG100	- 9X 12X	- 32X	0 17.40 18.30	0 38.40 41.40	0 5.47 5.45	0 19.30 19.60	0 80.57 84.75	0 0.314 0.298	0 0.283 0.278
2	6 1-Albachem	SLG100	9X	10X 32X	7.700 24.000	16.900 48.400	3.220 9.340	7.700 23.700	35.50 105.00	0.418 0.389	0.418 0.394
3	10	SLG100	9X (liq. EDC)	32X	12.000	21.800	1.470	11.100	46.40	0.122	0.132

**Table 3.3:** Amino acid analysis data: The amino acids resulting from hydrolysis of the samples were separated by ion exchange chromatography, visualised by reaction with ninhydrin and then quantified. The values of the four amino acids constituting the GRGDY peptide are expressed in n.mol/mg of alginate. The analysis was performed by Alta Bioscience, University of Birmingham.

A first amino acid analysis was performed on high G alginate derivatised with either 9X or 12X EDC and sulfo-NHS. The conditions employed for the derivatisation of these alginates are summarised in table 3.1, where these polymers are respectively designated as “*alginate-GRGDY no. 1*” and “*alginate-GRGDY no. 2*”. The GRGDY peptide, which was supplied by Neosystem in this first experiment, was added at 32X concentration for the coupling reaction. Plain (non-derivatised) alginate SLG 100 was tested as negative control. As it is shown in table 3.3, no detectable amino acids were found in the plain alginate. On the other hand, all four component amino acids (G, R, D and Y) of the GRGDY pentapeptide were present in the alginate after derivatisation with either 9X (designated “*alginate-GRGDY no. 1 – Neosystem*” in table 3.3) or 12X reactants (designated “*alginate-GRGDY no. 2*” in table 3.3), indicating that a successful coupling reaction was achieved in both cases. In addition, no significant difference was observed in the amino acid content for the alginate-GRGDY coupled with either 9X or 12X reactants (EDC, sulfo-NHS) concentrations. 9X reactants, 32X peptide were therefore deemed to be sufficient to achieve derivatisation of the Pronova SLG100 alginate. As a result, 9X was maintained as the reactants concentration throughout all the subsequent experiments.

However, the most anomalous result observed in both cases was that the tyrosine level measured from this analysis was considerably lower than expected, since from the chemical structure of the GRGDY peptide (figure 3.5) the theoretical value expected for tyrosine is to be similar to the aspartic acid and arginine residues values (and therefore the Y/D and Y/R molar ratios are expected to be 1).

A lower concentration for the peptide was tested in a following experiment (indicated as experiment no. 2 in table 3.3): amino acid analysis was performed on alginate SLG100 derivatised with 9X reactants (EDC and sulfo-NHS) and 10X GRGDY peptide concentrations, (designated “*alginate-GRGDY no. 6*” in both table 3.1 and table 3.3) in order to see whether 10X was a sufficient peptide concentration to achieve successful coupling reaction. In the same experiment, the alginate SLG100 was coupled also with 9X reactants and with a higher (32X) GRGDY peptide concentration, and the amino acids levels were measured in the resulting alginate-GRGDY (designated “*alginate-GRGDY no. 1*” in table 3.1 and “*alginate-GRGDY no. 1 – Albachem*” in table 3.3), so that it was possible to have a direct comparison of the



alginate derivatised with either 10X or with 32X of the GRGDY peptide. These data are also presented in table 3.3 (experiment no. 2).

The peptide used in this second experiment was supplied by a different manufacturer (Albachem), since the peptide from the previous supplier (Neosystem) was no longer available. Amino acid analysis data revealed that, regardless of the peptide concentration used, it was possible to achieve successful incorporation of the complete pentapeptidic GRGDY sequence onto the alginate. As it is shown in table 3.3, the four G, R, D and Y amino acids appeared to be present in all the alginate-GRGDY samples, indicating that peptide attachment was achieved also when the GRGDY peptide was used at a lower (10X) concentration. In addition, the amino acid levels measured for the alginate coupled with 10X peptide were 3 times lower than those measured for the same alginate derivatised with the higher (32X) peptide concentration, indicating direct proportionality between the amino acid levels and the amount of peptide used for the carbodiimide reaction.

Interestingly, the amino acid levels obtained in this experiment from the alginate coupled with the 32X peptide concentration were higher (average increase of 27.5% for the D, G and R amino acids) than those obtained for the previous experiment (experiment number 1 in table 3.3), where the same reactants (9X) and peptide (32X) concentrations were used. These differences could be attributed to the different peptide's manufacturer, since the Neosystem peptide employed for the first experiment was no longer available, and the peptide supplied by Albachem Limited was used instead.

It is interesting to note that tyrosine level was considerably lower than the levels of the other amino acids, indicating that loss of tyrosine, as seen in the previous experiment, occurred again during the coupling reaction.

Finally, amino acid levels were assessed on SLG100 alginate derivatised with the manufacturer-produced EDC in solution. The amino acid levels detected are also included in table 3.3 (experiment no. 3). 9X reactants and 32X GRGDY peptide (Albachem Limited) concentrations were used, since from all previous experiments these proved to be sufficient concentrations for the achievement of the peptide incorporation onto the alginate polymer. The resulting derivatised alginate is designated "*alginate-GRGDY no. 10*" in both table 3.1 and table 3.3.

The four constituent amino acids of the pentapeptide sequence were all present, indicating that the coupling of the peptide was possible also with the use of the manufacturer-produced EDC in solution. However, lower amino acids levels were measured in comparison to the amino acid levels detected in the previous derivatisation experiments, where solid EDC.HCl was used. A 2-fold decrease was observed for the amino acids aspartic acid (D), glycine (G) and arginine (R) in this experiment, indicating that the use of liquid EDC did not improve the efficiency of the coupling reaction. One reason that the EDC.HCl worked better could be that it is a hydrochloride salt, and therefore in this form the EDC is already protonated when placed into the reaction mixture. This therefore permits the EDC to couple straight away to an activated carboxylic acid group on the alginate and form the O-acylisourea intermediate (as shown in the reaction represented in figure 3.2). Of note is that, as in the previous experiments, tyrosine level was always lower than the levels of the other amino acids, indicating that the use of liquid EDC did not prevent tyrosine loss.

From the amino acid analysis data described above, it can be concluded that successful incorporation of the GRGDY pentapeptide onto the SLG100 alginate polysaccharide chain was achieved with 9X sulfo-NHS and solid EDC and with 32X peptide concentrations. However, in all cases a significant loss of tyrosine was observed, being 64 % the average tyrosine loss observed in all the derivatisation experiments performed. The coupling reaction was also achieved with 10X peptide concentration. Nevertheless, the amino acid levels measured for the 32X peptide reaction were higher, and it was assumed that a higher peptide concentration would have allowed better cell survival after immobilisation of the cells in the alginate/cells constructs. For this reason the 32X peptide reaction was overall preferred for the derivatisation of the alginate scaffold. Interestingly, the use of EDC.HCl was associated with higher amino acids levels, as opposed to the use of the manufacturer-prepared EDC in solution; thus, EDC.HCL proved to be a better option, and was preferred in all subsequent derivatisation experiments.

### 3.3.2 Characterisation of the alginate-GRGDY by nuclear magnetic resonance

Nuclear magnetic resonance (NMR) spectroscopy was performed on alginate-GRGDY samples in order to qualitatively assess the presence of the peptide incorporated in the derivatised alginate after completion of the coupling reaction. The amount of peptide attached during the derivatisation procedure can be deduced from integrating the signals of the alginate and the peptide detected in the final NMR spectra of an alginate-GRGDY sample solution.

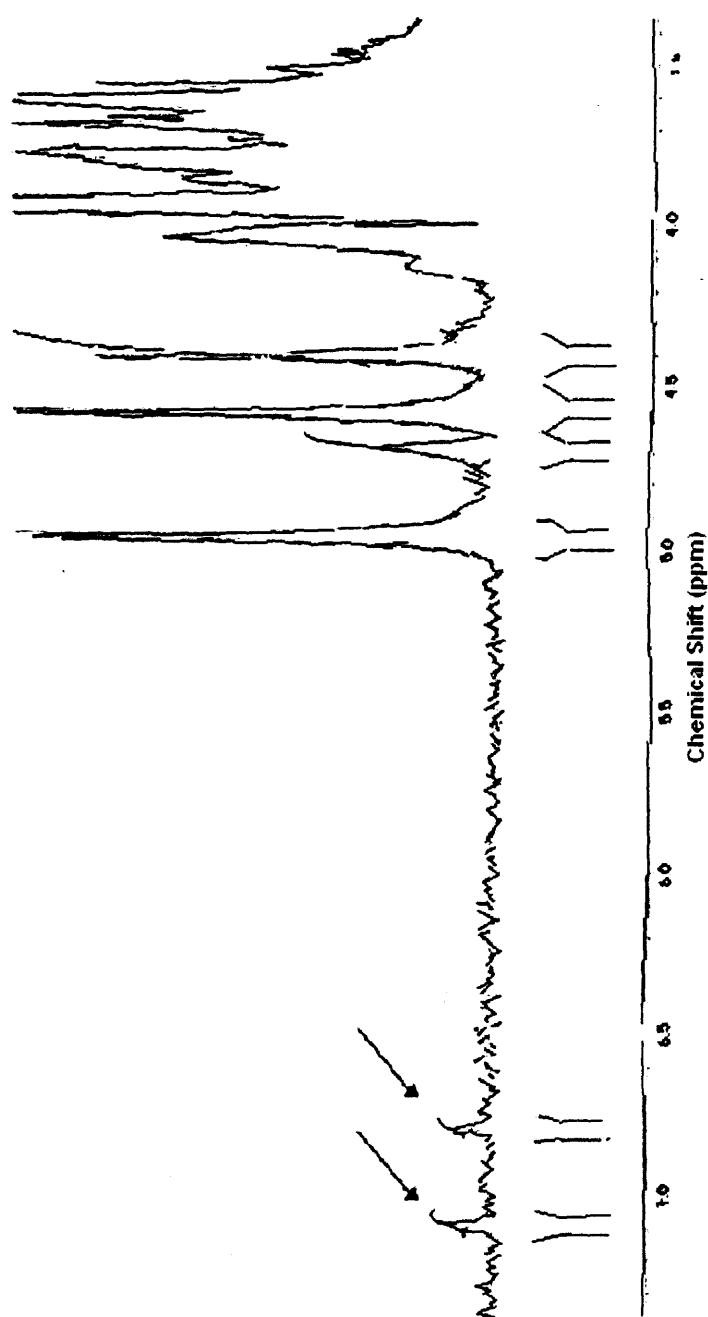
NMR spectroscopy, exploiting the magnetic properties of nuclei and measuring their radio frequency, allows identification of individual atoms in a pure molecule (please see section 2.4.2 for a more details description of this technique). Tyrosine has a very distinctive NMR spectrum, due to the aromatic ring present in its side chain. The most important signals for these investigations are the signals at  $\delta$  6.8 ppm from the H in the *meta* position on the aromatic ring on the side chain, and at  $\delta$  7.1 ppm from the H in the *ortho* position on the aromatic ring (slightly further downfield than the *meta*-H due to the proximity to the oxygen at the bottom of the aromatic ring). As a result, these two peaks at  $\delta$  6.8 ppm and  $\delta$  7.1 ppm should always be clearly readable in the typical NMR spectrum of the full H<sub>2</sub>N-GRGDY-COOH pentapeptide sequence.

In addition to these, in a NMR spectrum, the readable signal from the alginate manifests in 3 singlets at  $\delta$  4.4, 4.7 and 5.1 ppm. These are the signals from the anomeric protons present on both the M- and G-units repeating throughout alginate; in the alginate spectrum they tend to be shifted slightly downfield from the rest of the proton signals due to their proximity to oxygen atoms. Previous work by Penman and Sanderson (1972) identified the singlet at  $\delta$  5.1 ppm corresponding to the anomeric protons (H-1) on the guluronic acid residues throughout the alginate sample being analysed, and the singlet at  $\delta$  4.8 ppm corresponding to the anomeric protons on the mannuronic acid residues. Once both peaks are able to be distinguished, the integrals can be compared, and the G to M ratio in the alginate deduced. At concentrations that are convenient for <sup>1</sup>H NMR analysis, the alginate solution is too viscous and causes linear broadening in the spectrum [Johnson *et al.*, 1997]. For this reason, a partial acid hydrolysis was carried out on the alginate to reduce its viscosity and thus sharpen the peaks visible in the spectra. The hydrolysis also makes the peak from the anomeric

protons on the mannuronic acid residues clearly visible, thus allowing the G to M ratio to be deduced. The protocol followed for the alginate hydrolysis and the subsequent acquisition of the NMR signals is described in section 2.4.2.

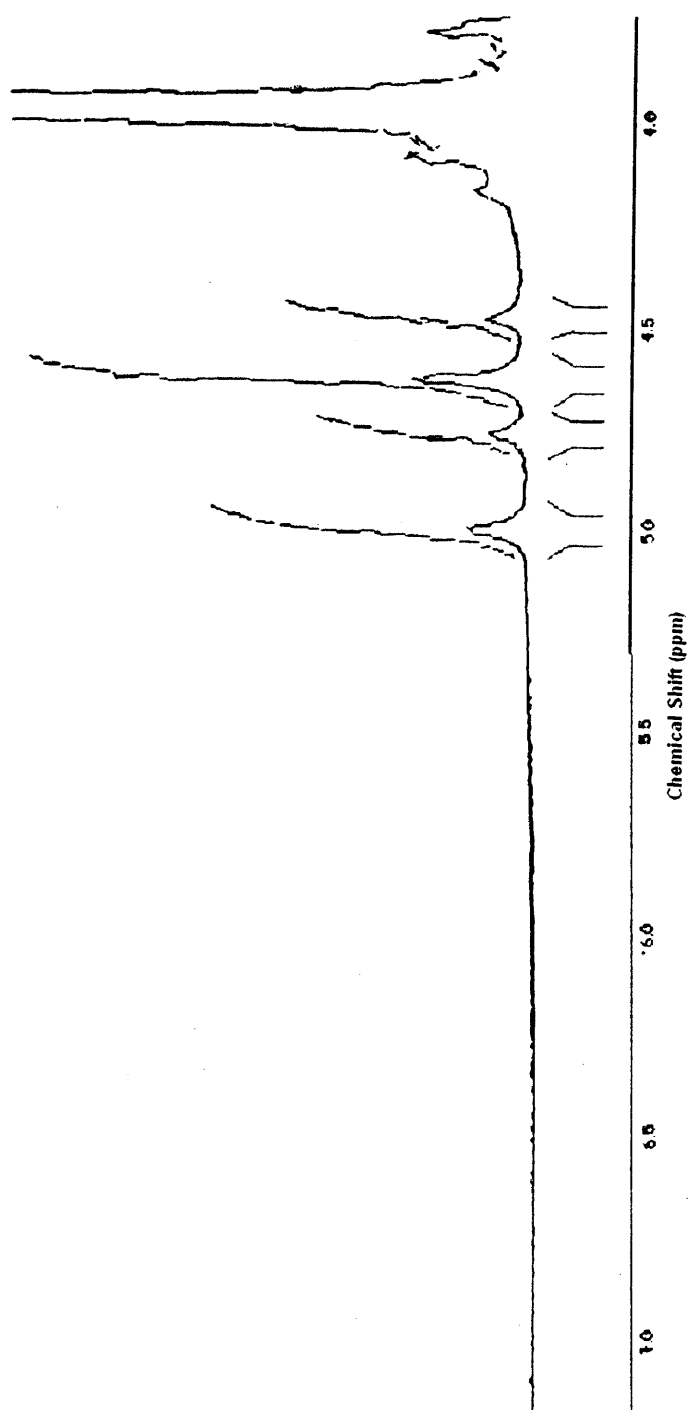
A whole series of preliminary NMR investigations was performed, firstly on different samples of plain (i.e. non-derivatised) high G Pronova sodium alginate, and secondly on mixtures of differing and known amounts of non-derivatised alginate and tyrosine. This series of experiments was performed in order to optimise the NMR protocol, so that it was possible to obtain spectra with clear signals, and ultimately to gain accurate integral values of the alginate and tyrosine peaks. The best signals were obtained on partially hydrolysed samples recorded with water suppression, at high temperature and using a 30° pulse sequence (as described in section 2.4.2). This method was therefore adopted also for the following NMR investigations on the alginate-GRGDY samples.

Figure 3.6 shows one of the spectra recorded on partially hydrolysed plain SLG100 alginate (8.3 mg) in deuterated water (D<sub>2</sub>O) after addition of 0.01 mg of tyrosine. The most important NMR signals of the tyrosine residue, at  $\delta$  6.8 ppm from the H in the *meta* position on the aromatic ring on the side chain, and at  $\delta$  7.1 ppm from the H in the *ortho* position on the aromatic ring, are evident in this spectrum.



**Fig.3.6:** 1-Dimensional nuclear  $^1\text{H}$  NMR spectrum for Pronova non-derivatised SLG100 alginate (8.3mg), after partial hydrolysis in  $\text{D}_2\text{O}$  (2mL) and subsequent addition of 0.01mg tyrosine. The peaks at 7.09 ppm and 6.9 ppm (highlighted by arrows), signalling the presence of the two unique proton chemical shifts on the tyrosine ring, are evident.

Nuclear magnetic resonance was also performed on alginate SLM100, derivatised with 9X reactants (EDC, sulfo-NHS) and 1X GRGDY peptide. The alginate-GRGDY resulting from the derivatisation procedure was dissolved in a normal saline solution made up with deuterated water (i.e. deuterated normal saline solution) prior the registration of the spectrum. The high M alginate-GRGDY dissolved completely in such a solution, and the three singlets at  $\delta$  4.4 ppm, 4.7 ppm and 5.1 ppm originating from the resulting alginate solution were clearly visible in the final spectrum (please see figure 3.7). However, no tyrosine peaks at  $\delta$  6.9 ppm and 7.1 ppm could be detected in the spectrum.



**Figure 3.7:** 1-Dimensional nuclear  $^1\text{H}$  NMR spectrum obtained for the derivatised (9X reactants, 1X peptide) SLM100 alginate after dissolution in deuterated normal-saline solution. The three singlets at  $\delta = 4.4$ , 4.7 and 5.1 ppm originating from the alginate solution were clearly visible whereas no tyrosine peaks at  $\delta = 6.9$  ppm and 7.1 ppm could be detected.

Finally, NMR was performed on SLG100 alginate-GRGDY samples, obtained from the coupling reaction with 9X reactants and 10X peptide. The high G alginate-GRGDY failed to dissolve well in either deuterated water ( $D_2O$ ) or in deuterated sodium hydroxide (NaOD), and the spectra recorded in these cases were both weak, with only very faint alginate signals visible. In addition, none of the tyrosine peaks at  $\delta$  6.9 ppm and 7.1 ppm were present in these spectra. Unlike the SLM100 alginate-GRGDY, the high G alginate derivatised with 10X peptide did not dissolve in deuterated normal-saline solution either, therefore indicating that it is not possible to employ the same NMR method for the analysis of high M and high G alginates. A possible reason for this is that the higher G-unit alginate is much harder to dissolve, due to the stronger conformation between many repeating G-units. NMR was therefore re-attempted on alginate SLG100, 9X reactants, 10X peptide after addition of 60  $\mu$ L of deuterated sodium hydroxide (NaOD) in a deuterated normal-saline solution. Complete alginate dissolution was achieved this time, however once again, no tyrosine peaks were detected (please see spectrum in figure 3.8).



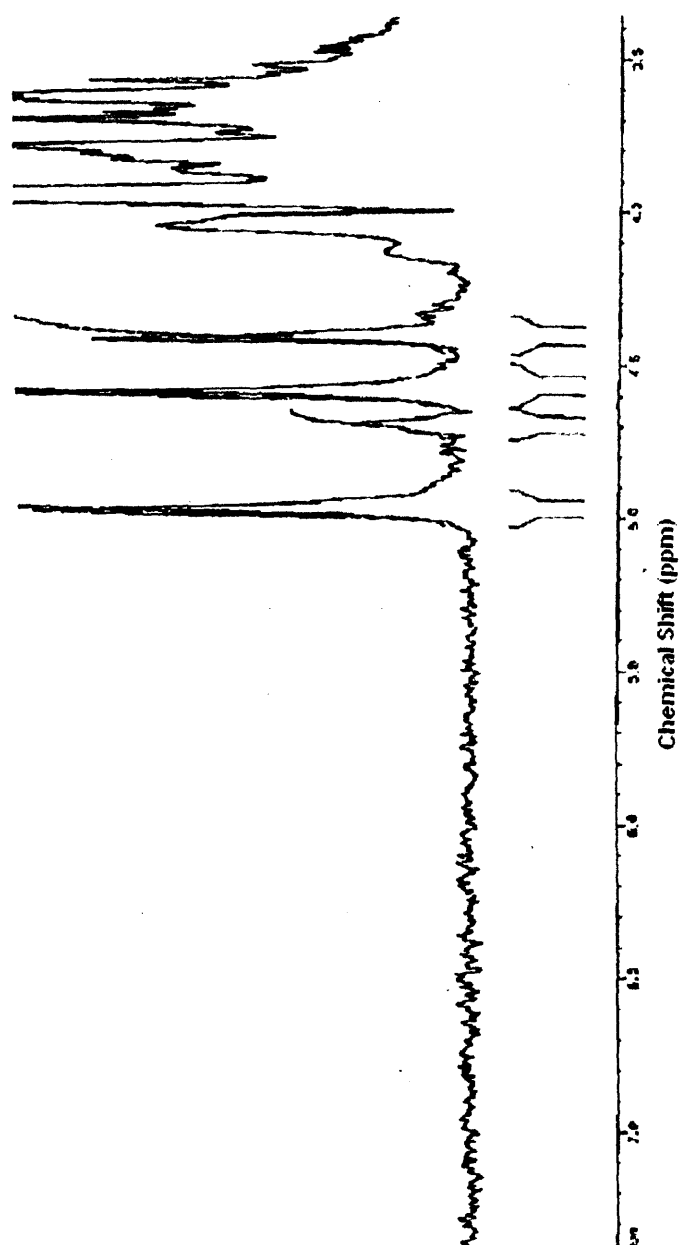


**Fig.3.8:** NMR spectrum recorded for Pronova SLG100 alginate coupled with 9X reactants (EDC and sulfo-NHS) and 10X GRGDY peptide, showing no detectable peaks for the tyrosine amino acid at 7.09 and 6.9 ppm. The spectrum was registered on the alginate-GRGDY after dissolution in deuterated normal-saline solution supplemented with deuterated sodium hydroxide.

In conclusion, no tyrosine peaks were detected when both derivatised SLG100 and SLM100 alginates were analysed with nuclear magnetic resonance (NMR) spectroscopy, either because the peptide concentrations (1X and 10X) used for the coupling reaction were too low, or because NMR was not sensitive enough to allow the detection of the tyrosine peaks in the alginate-GRGDY resulting from the derivatisation procedure. NMR can have a low sensitivity as millimolar concentrations of substrates can be detected via NMR, whereas it is rather difficult to detect less than 0.5  $\mu\text{M}$  of a substance using this technique [Syrota and Jehenson, 1991; Wishart, 2006]. Since the tyrosine value measured via amino acid analysis is considerably low, this implies that NMR might not be a sensitive enough method of detection for the tyrosine in the alginate-GRGDY samples. Increasing the magnet strength to 500 MHz was a possibility for enhanced detection, however all spectra had been previously recorded at 358°K, whereas it is undesirable to reach such high temperatures when using the Bruker 500. As a result, the amino acid analysis described above (section 3.3.1) proved to be a more suitable method for the characterisation of the coupling reaction. It can therefore be concluded that, for the purposes of this study (i.e. the evaluation of the peptide incorporation in the alginate matrix), the amino acid analysis is a much more useful and reliable technique, permitting the quantification of the GRGDY peptide attached to the alginate after completion of the coupling reaction.

### **3.3.3 Nuclear magnetic resonance (NMR) and mass spectroscopy (MS) for the analysis of the GRGDY peptide before use in the derivatisation of the alginate matrix**

As it is described in section 3.3.1, the amino acid analysis provided surprising results concerning the amount of tyrosine present in the alginate-GRGDY resulting from the derivatisation procedure. For this reason, in order to obtain information on the complete chemical structure of the Gly-Arg-Gly-Asp-Tyr (GRGDY) peptide supplied by the manufacturer, nuclear magnetic resonance (NMR) and mass spectrometry (MS) were performed on the peptide prior to its use in the alginate derivatisation procedure.

The signals at  $\delta$  6.8 ppm and 7.1 ppm, originating from the tyrosine residue, and therefore detectable in a typical NMR spectrum for the whole GRGDY pentapeptide sequence, have already been described in section 3.3.2.

As already described in section 2.4.3, mass spectrometry can be employed to obtain information on the peptidic composition of a given protein or peptide. A typical mass spectrum is an intensity versus  $m/z$  (mass-to-charge ratio) plot representing the chemical analysis of the sample. Hence, the mass spectrum of a sample is a pattern representing the distribution of components (atoms or molecules) by mass (more correctly mass-to-charge ratio) in a sample. The x-axis of a mass spectrum represents a relationship between the mass of a given ion and the number of elementary charges that it carries, and is written in  $m/z$ , denoting the quantity formed by dividing the mass of an ion by the unified atomic mass unit and by its charge number. The y-axis of a mass spectrum represents signal intensity of the ions.

The NMR spectrum performed on the GRGDY pentapeptide (Albachem) (figure 3.9) shows the two distinct peaks at  $\delta$  6.8 ppm and 7.1 ppm, generating from the four aromatic protons on the side chain of tyrosine. Additionally, the mass spectrum performed on the same Albachem peptide (figure 3.10) showed a peak at  $m/z$  567, corresponding to the correct molecular weight of the complete GRGDY pentapeptide.

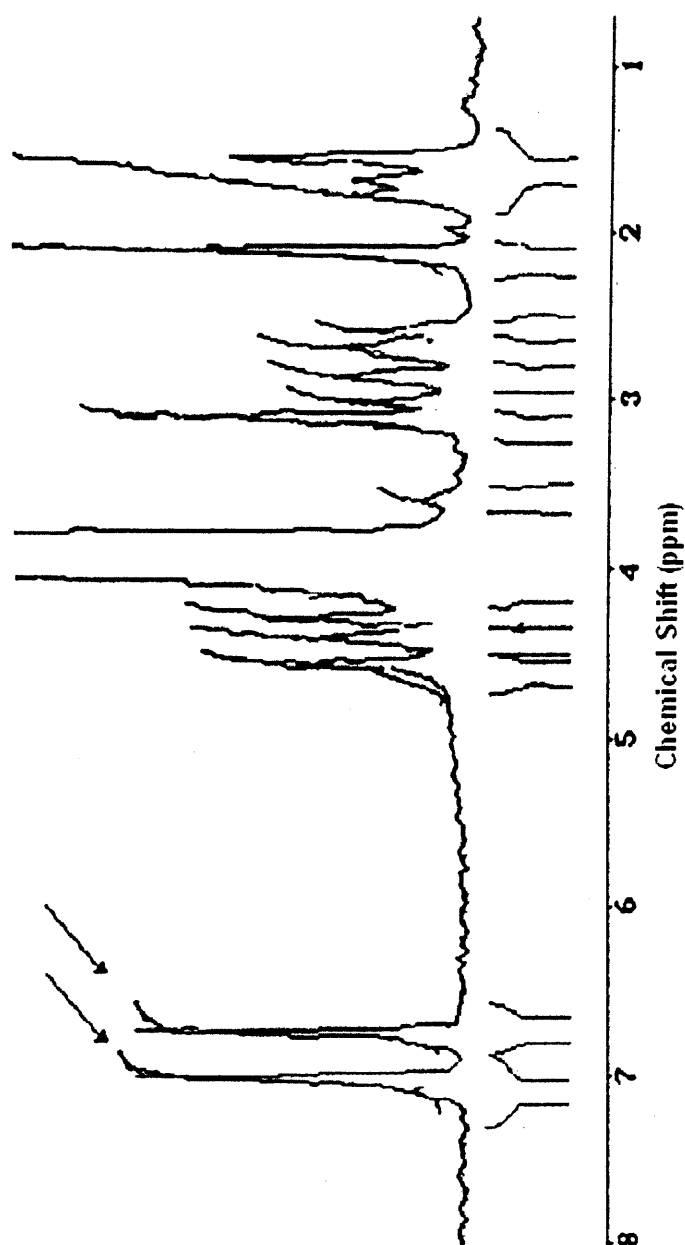


**Fig. 3.9:** 1-Dimensional nuclear  $^1\text{H}$  magnetic resonance spectrum of the GRGDY peptide (Albachem) before use in the carbodiimide reaction for the alginate derivatisation. The two peaks at  $\delta = 6.8$  ppm and  $7.1$  ppm (highlighted by arrows), originating from the four aromatic protons on the side chain of tyrosine, indicate that the peptide was a complete pentapeptide sequence.

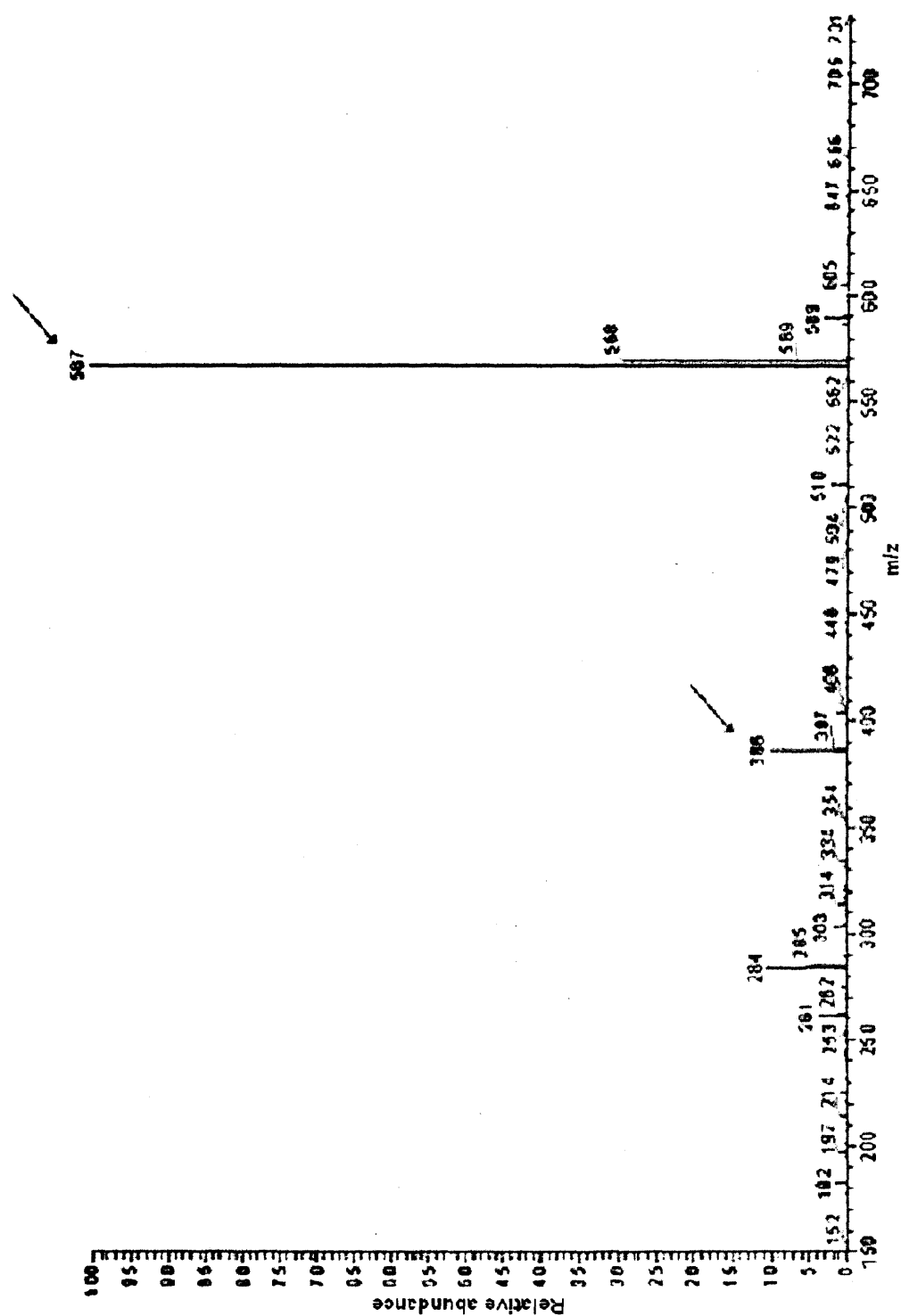


**Fig.3.10:** Mass spectrum of GRGDY peptide (Albachem) before use in the carbodiimide reaction for the alginate derivatisation. The peak at 567  $m/z$  (highlighted by the first arrow), signalling the presence of the complete peptide, is evident. In addition, a signal at 386  $m/z$  (highlighted by the second arrow), corresponding to the weight of the peptide minus the terminal tyrosine residue, is detectable.

These data confirmed that the peptide was intact before starting the derivatisation reaction, and that all the amino acids, including the terminal tyrosine residue, were present in the original peptide supplied by the manufacturer. However, on the mass spectrum shown in figure 3.10 a peak at  $m/z$  386, corresponding exactly to the weight of the peptide minus the end tyrosine, is also detectable. The amount of the shorter  $\text{NH}_2\text{-GRGD-COOH}$  peptide, as indicated by integration of the MS spectrum, was small but still notable. A possible reason for the presence of this signal, is that the terminal tyrosine residue on the end of the pentapeptide is unusually reactive and is lost easily at some stage during the MS process. Alternatively, the presence of the peak might indicate that some oligopeptide of the shorter sequence  $\text{NH}_2\text{-GRGD-COOH}$  was present in the original peptide sample supplied.

### **3.4 Conclusions and discussion**

The aim of the work described in this chapter was to investigate the carbodiimide coupling reaction between the alginate and the GRGDY peptide, and to test different protocols and working conditions with the intention of optimising the derivatisation chemistry.

Nuclear magnetic resonance and mass spectrometry methods were used to achieve a better characterisation of the GRGDY peptide supplied by the different manufacturer, prior to its use in the coupling reaction with the alginate. In addition, nuclear magnetic resonance spectroscopy and amino acid analysis were used for measuring the degree of peptide attachment onto the alginate-GRGDY resulting from the derivatisation procedure.

In each of the derivatisation experiments attempted ultra-pure Pronova sodium alginate was used; however different viscosities and guluronic (G)-unit to mannuronic (M)-unit ratio alginates were evaluated. Attention was focused mainly on experiments with high viscosity and high guluronic acid content (SLG100) alginate, since it was known from the literature that alginates with a higher guluronic acid monomer content formed more stable and rigid gels [Wang *et al.* 2003; Martinsen *et al.*, 1989; Constantidinis *et al.*, 1999]. Nevertheless, both high and low viscosity SLM alginates

were selected for investigation alongside high and low viscosity SLG alginates in some of the studies performed for the optimisation of the derivatisation procedure. This was done with the intention to see what effect these alginates had on the gel formed. No differences between the alginate types were visible during the derivatisation reaction and dialysis, only very slight variation after the alginate-GRGDY had been lyophilised, with the low viscosity alginates (SLG20 and SLM20) looking slightly less viscous and weaker than the high molecular weight (SLG100 and SLM10) alginates-GRGDY. However, differences were visible when making the three-dimensional alginate-GRGDY/cells constructs (please see data presented in chapter 5).

9X EDC and sulfo-NHS concentration, as defined by Rowley, proved to be sufficient for the incorporation of the GRGDY pentapeptide onto the alginate polysaccharide chain, as demonstrated by the amino acid analysis data.

Amino acid analysis was performed on SLG100 alginate-GRGDY derivatised with either solid EDC or with manufacturer-produced EDC in solution. The low levels of the four amino acids detected in the final SLG100 derivatised alginate with EDC in solution indicated that the use of such EDC solution did not improve the efficiency of the coupling reaction. The amino acids levels measured after derivatisation with the EDC in solution were in fact half as much as the amino acids levels obtained from the previous derivatisation experiment with solid EDC, and similar to the reaction with solid EDC, the tyrosine level was lower than the other three amino acids levels.

In addition, following the 20-hour reaction, a 5-day dialysis cycle in aseptic conditions was performed to remove the cell toxic reactants left over from the carbodiimide reaction (EDC and sulfo-NHS) and of the heavy metals and polyphenols from the commercial alginate.

Lyophilisation, as opposed to the use of a polyethylene glycol (PEG) concentrating solution, resulted as the most successful method for re-concentrating the alginate after completion of the dialysis cycle. In the derivatisation method investigated in this work a 3-day lyophilisation step, necessitating the least handling, was carried out in aseptic conditions thus potentially permitting the preparation of a final sterile product.

The amino acids analysis data presented in this chapter proved that the carbodiimide coupling reaction between the high G Pronova sodium alginate and the

GRGDY peptide was successful. As a result, the protocol adopted in the present research for the carbodiimide reaction and the whole alginate derivatisation procedure was successful.

Due to the surprisingly low tyrosine level that was detected through the amino acid analysis performed on the derivatised alginate, it was decided to conduct nuclear magnetic resonance and mass spectrometry on the GRGDY peptide prior to its addition to the reaction with the alginate, in order to verify the amino acidic composition of the original peptide. Both these techniques permitted to obtain sufficient information on the peptide sequence, showing that all the four amino acids of the GRGDY sequence were initially present and that the original product supplied by the manufacturer was indeed a complete pentapeptide sequence.

The nuclear magnetic resonance investigations into the alginate-GRGDY were not successful and NMR did not prove to be a suitable method to ascertain the attachment of the GRGDY peptide on the alginate. The main reason for this was that the tyrosine signals, which were being investigated in this technique, were too low in all the alginate-GRGDY samples prepared and tested to be detected in the NMR spectra.

As opposed to nuclear magnetic resonance, amino acid analysis permitted a more reliable quantification of the degree of the GRGDY peptide incorporation, showing that all four constituent amino acids were present in the derivatised alginate.

Even though the data from the amino acid analysis indicated that the GRGDY peptide had been successfully incorporated in the alginate after completion of the derivatisation procedure, in all the conditions investigated a significant loss of the terminal tyrosine residue (on average approximately 60%) from the alginate after derivatisation was observed. The low value of tyrosine present in all the alginate-GRGDY correlated with poor outcomes in later cell immobilisation experiments (please see data presented in chapter 5).



## **4. Characterisation of human mesenchymal stem cells (hMSCs) growth kinetics and metabolic activity in monolayer culture**

In order to understand and characterise the growth of cells encapsulated within alginate hydrogels, it was necessary to establish first their unencapsulated growth characteristics in tissue flasks. As a result, a whole series of experiments in tissue culture flasks were conducted with the purpose of investigating the cells growth kinetics during their *in vitro* expansion in such a culture environment. The aim of these studies was to identify the optimal condition of culture, allowing cell viability and promoting cell proliferation in monolayer. The intention was then to apply the optimal condition identified to the culture of the alginate/cells constructs obtained after immobilisation of the cells in the alginate matrix.

This chapter describes the investigations performed on cells cultured in a two-dimensional environment (tissue culture flasks and microwell plates), prior to the addition of the alginate matrix and the preparation of alginate/cells constructs. The studies performed on the constructs resulting after immobilisation of the cells in the alginate matrix are described in chapter 5.

### **4.1 Growth of human mesenchymal stem cells (hMSCs) in tissue culture plastic**

The cells used in the monolayer studies described in this chapter were multipotent fibroblast-like plastic-adherent cells isolated directly from frozen bone marrow samples of adult patients, according to the density gradient protocol described in section 2.1.1. It is recognized that these bone marrow-derived cells most likely consist of an heterogeneous population, including small and rapidly self-renewing cells that have the highest multipotentiality, together with slowly replicating, large and more mature progenitor cells at different stages of their differentiation pathway [Tavassoli and Friedenstien, 1983; Lichtman, 1981; Allen *et al.*, 1990]. However, as already mentioned (please see section 1.2.4.5), for simplicity they have been here

termed “mesenchymal stem cells” (MSCs), this being the designation in use at the beginning of this study.

Several investigators have previously observed that there is a large number of variables and parameters that must be considered in expanding hMSCs for experimental and clinical purposes [Sekiya *et al.*, 2002; Caplan, 2000; Phinney *et al.*, 1999]. Taken into consideration the lack of a uniform approach for MSCs isolation and expansion [Sotiropoulou *et al.*, 2005], in this research several of these variables and parameters were examined for the culture of these cells. The intention was to define an improved and optimal culture protocol for obtaining standardised preparations of hMSCs, while maintaining both their proliferative and multilineage capacities.

The cryo-preserved bone marrow samples used for the cells’ isolation were obtained from the Department of Haematology, University College London Hospital. The use of human clinical samples had been approved by the University College London Hospital Ethics of Human Research Committee (project reference number 03/0136). Frozen working cell banks were produced in order to supply experimental material for this research. In addition, only cells below passage 7 were used, due to gradual decrease in growth rate and loss of multipotentiality of the hMSCs following serial passage in culture [Bruder *et al.* 1997; DiGirolamo *et al.*, 1999].

The cells grown in tissue culture flasks and plates under the different culture parameters investigated were assessed according to their percent viability at each passage of culture, their growth kinetics, population doubling level (PDL), doubling time (Td, hours), specific cell growth rate ( $\mu$ , hours<sup>-1</sup>) and their specific glucose consumption rate (GCR, g/cell/hr). For the determination of these measurements, the cell concentration was obtained using a hemacytometer (please see section 2.6.2), whereas the exclusion assay with trypan blue dye (please see section 2.6.3) was performed to assess the cell viability. Finally, for the calculation of the specific glucose consumption rate, the glucose concentration in the medium of culture was determined using the Nova Biomedical BioProfile 400 analyzer (please see section 2.6.5).

## ***4.2 Single cell cloning by serial dilution***

Single cell cloning by serial dilution is widely used for the clonal isolation of hybridomas and other cell lines that are not attachment-dependent. However, it is also very useful for cloning attachment-dependent cells when the cell plating efficiency is very low, unknown or unpredictable. The technique is fast and easy; however, like for most clonal isolation methods, there is no guarantee that the colonies arise from single cells. As a result, re-cloning a second time is usually advised to increase the likelihood that the cells originated from a single cell. The working assumption is that a single cell gives rise to one visible colony of cells. Clones are normally detectable by microscopy after 4 to 5 days from plating and they should be ready to score after 7 to 10 days, depending on the growth rate of the cells. The plates are checked for wells that contain just a single colony. These colonies can then be sub-cultured from the original well into larger culture vessels.

In this research human MSCs cloning was attempted by limiting dilution. In order to obtain single cell-derived, clonally expanded human MSCs, seventh passage (p7) bone marrow-derived cells were suspended in growth medium at a density of  $3.78 \times 10^5$  cells/mL. Five microliters of the cell suspension were diluted with either 75.6mL or 37.8mL of growth medium. Two hundred microliters of the diluted cell suspensions were plated in each well of a 96-well, flat-bottomed culture plate, so that each well was plated with 5 cells/well in the first plate and with 10 cells/well in the second plate. The following day all wells from the plates seeded with either 5 cells/well or 10 cells/well were carefully evaluated microscopically over a 2-week period for the detection of single cells. The aim of this study was then to count the number of colonies that would form from a single cell after an incubation period. However, in both cases the cells failed to adhere to the plastic surface and to grow in monolayer. No discernible adherent spindle-shaped cells were observed and no cell colonies were detected. It was therefore not possible to achieve successful cell cloning by limiting dilution in expanded hMSCs derived from a frozen bone marrow sample.

As a result in all subsequent experiments, following the cell separation by discontinuous density gradient centrifugation with Ficoll, putative hMSCs were recovered from the mononuclear layer and were identified based on their ability and tendency to adhere in monolayer condition to the plastic surface of the culture

vessels. Adherent cells were then enriched over increasing passage level by removing the non-adherent cells through medium refreshments. The resulting attachment-dependent, fibroblast-like cells were grown in tissue culture flasks and plates and were characterised under different culture conditions according to the methods described in section 2.6.

Isolation of bone marrow MSCs using the plastic adherent method was first described by Friedenstein *et al.* (1968), who noticed that the precursor cells obtained were growing in plastic cultureware forming colonies capable of giving rise to chondrocytes and osteoblasts. Since at present no unique phenotype has been identified that permits the reproducible isolation of MSC precursors, the isolation and characterization of stromal cell function still relies primarily on their ability to adhere to plastic and their expansion potential [Fibbe, 2002]. The majority of research groups continue to use this traditional method for isolating bone marrow MSCs [Haynesworth *et al.*, 1992; Gronthos & Simmons, 1996; Pittenger *et al.* 1999; Prockop *et al.* 2001; Gronthos *et al.* 2003]. Thus, this was also the isolation method preferred in this research for obtaining MSCs preparations.

#### **4.3 Influence of basal growth medium and Mesenchymal Stem Cell Stimulatory Supplement on hMSCs monolayer culture: preliminary conclusions**

It is known that specific cell lines can be grown *in vitro* in optimally formulated culture or nutrient media [Hanss and Moore, 1964; Fahey *et al.*, 1966; Ham and McKeehan, 1979]. The growth of various mammalian cells *in vitro* has been achieved in several chemically defined media supplemented with various sera, preferably fetal calf or newborn calf serum and other incompletely defined growth factors. One distinct source of variability is therefore the choice of a culture medium with appropriate formulation. This is, among the others, an important *in vitro* condition, having direct influence on stem and progenitor cells expansion and maintenance in culture.

The study described in this section aimed to expand *in vitro* MSCs from human frozen bone marrow by using two different growth media that are commercially available and widely used for the culture of these cells. Culture media tested were low-glucose (1 g/L) DMEM medium (BioWhittaker, Walkersville, MD, USA) and MesenCult medium (StemCell Technologies Inc., Vancouver, BC, Canada). The influence of these media in the culture system of bone marrow-derived MSCs has already been investigated in a previous study [Jager *et al.* 2003], but rather than analysing cell growth characteristics, this study focused on the impact that these culture solutions have on the cells' osteoblastic differentiation.

In this research low-glucose DMEM and MesenCult medium formulations were used for the cell expansion in either their serum-free formulation, or after addition of either 2% or 10% (v/v) serum (full description of these media is given in section 2.1.5.1). The Mesenchymal Stem Cell Stimulatory Supplement from StemCell Technologies Inc., consisting of Fetal Bovine Serum supplemented with L-glutamine, was used for the serum-supplementation of both media. Thus, this study compared the effects of the two selected growth media and the Mesenchymal Stem Cell Stimulatory Supplement on the proliferative capacity and the growth rate of hMSCs expanded in tissue culture vessels.

Fourth passage (p4) bone marrow-derived hMSCs were plated in non-coated 12 well tissue culture plates (please see section 2.1.5.1). The culture was maintained for 12 days and the cells were assessed for cell count and cell viability at four different time-points, according to the protocols described in section 2.6.2 and 2.6.3 respectively. The growth rate ( $\mu$ ), the population doubling level (PDL) and the doubling time ( $T_d$ ) were calculated as described in section 2.6.4.

The results obtained from this study are presented in figure 4.1, which shows the growth kinetics curves for all the conditions investigated, and in table 4.1, which presents the values of the population doubling level, the doubling time and the cell growth rate for each of these conditions.

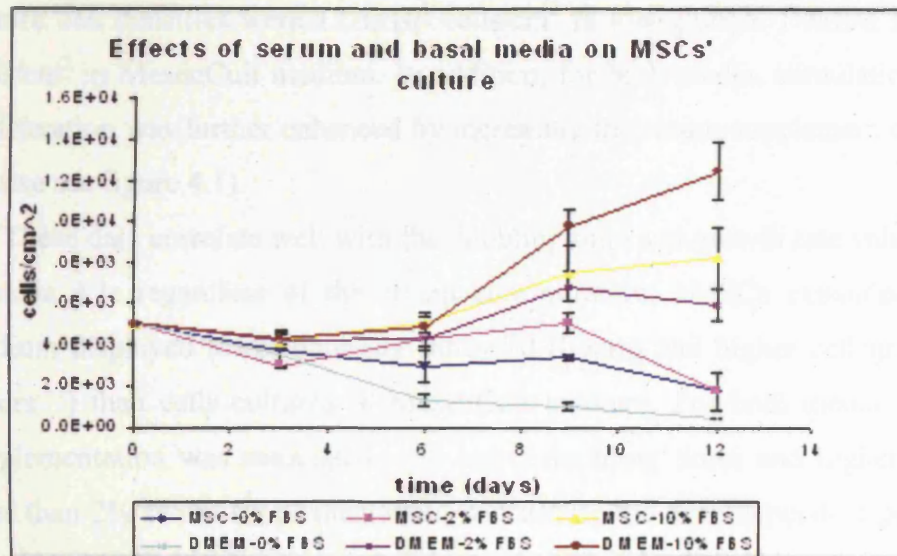


**Fig. 4.1:** Cell growth for p4 human MSCs cultured in either non-supplemented MesenCult or DMEM media, or in these same media after addition of either 2% or 10% (v/v) serum (Mesenchymal Stem Cell Stimulatory supplement) concentrations. Data are presented as means  $\pm$  s.e. of three independent measurements (please see section 2.6.9).

**Table 4.1:** Population Doubling Level (PDL), Doubling Time (Td) and cell growth rate ( $\mu$ ) values calculated for the hMSCs expanded in 3 different serum conditions for each of the two basal media under examination (MesenCult medium and low-glucose DMEM). The values are calculated from day 6 to day 9 of culture.

Growth conditions day6-day9	PDL	Td(hours)	$\mu(\text{hours}^{-1})$
0%FBS, MSCCM	0.147	490.3	0.0014
2%FBS, MSCCM	0.233	309.5	0.0022
10%FBS, MSCCM	0.554	130.0	0.0053
0%FBS, CDMEM	-0.415	-173.5	-0.0040
2%FBS, CDMEM	0.655	109.9	0.0063
10%FBS, CDMEM	1	72	0.0096

MesenCult medium seemed to have advantages in MSCs survival when cells were maintained in serum-free culture, resulting more effective than DMEM medium in impeding cell death. However, for both media, the serum-free culture was associated with significant cell death over time, and supplementation with the Mesenchymal Stem Cells Stimulatory Supplement appeared to be an essential requirement for cell survival and cell growth. Moreover, after addition of the serum-supplement, the DMEM medium clearly permitted better cell growth and higher cell density as compared to the MesenCult medium. After 12 days in 10% serum-supplemented

culture cell densities were  $12.5 \times 10^3$  cells/cm<sup>2</sup> in low-glucose DMEM and  $8.25 \times 10^3$  cells/cm<sup>2</sup> in MesenCult medium. In addition, for both media, stimulation of the cell proliferation was further enhanced by increasing the serum-supplement concentration (please see figure 4.1).

These data correlate well with the doubling time and growth rate values presented in table 4.1: regardless of the serum concentration, hMSCs expanded in DMEM medium displayed lower doubling times T<sub>d</sub> (hours) and higher cell growth rates  $\mu$  (hours<sup>-1</sup>) than cells cultured in MesenCult medium. For both media, 10% serum-supplementation was associated with lower doubling times and higher cell growth rates than 2% serum-supplementation, confirming the dose-dependent positive effect of serum-supplementation on hMSCs growth and proliferation rate.

Cell viability was calculated with the trypan blue dye exclusion assay over the 12-day period of culture examined for all the conditions investigated. At the end of the culture, human MSCs expanded in serum-free condition retained approximately 70% cell viability for both the MesenCult and DMEM media (72.4% and 71.8% respectively). However, as expected, cell viability was considerably higher for both media in the culture samples supplemented with Mesenchymal Stem Cell Stimulatory Supplement (respectively 92.4% and 92.7% for the 2%-serum MesenCult and DMEM media, and 96.2% and 98.5% for the 10%-serum media). These data once again confirmed the need for serum-supplementation in the protocol to be developed for the culture of hMSCs, indicating that serum remains a critical factor for guaranteeing cell survival and cell growth.

Finally, cell morphology by means of light microscopy was also evaluated for all the different medium and serum conditions described. A difference in the number and density of spindle-shaped, fibroblast-like cells was already noticed after 6 days in culture, with the low-glucose DMEM medium giving more visible colonies and greater densities than the MesenCult medium. At the end of the 12-day culture period colonies of adherent cells with a fibroblast-like morphology appeared significantly more densely packed on culture plates with the low-glucose DMEM. The plates where the MesenCult medium was used did not present the same cell growth and cell density.

It can be concluded from these results that the usage of MesenCult medium did not lead to any advantage for the proliferation of human mesenchymal stem cells. Low-glucose DMEM medium, which is less expensive, was therefore chosen and

adopted as the standard medium of culture for these cells in all the subsequent experiments. The formulation for the standard “complete DMEM” medium used in this research is given in section 2.1.5.1. These data correlate well also with other studies investigating the isolation and expansion of murine and human marrow-derived mesenchymal stem cells, where the first adherent fibroblast-like cell colonies were achieved only after 5 days in low-glucose DMEM culture [Meirelles and Nardi, 2003; Pittenger *et al.*, 1999; Lee *et al.*, 2003]. In addition, this study confirmed the well documented significant positive effect of serum-supplementation on hMSCs survival and expansion in tissue culture plates, which is further discussed in the section below (section 4.4).

In all the subsequent studies, supplementation with the less expensive Fetal Bovine Serum (FBS) was preferred to the usage of the Mesenchymal Stem Cell Stimulatory Supplement, which was found to consist only of Fetal Bovine Serum supplemented with L-glutamine.

The effects of FBS-supplementation in the low-glucose DMEM culture medium for the *in vitro* expansion of hMSCs were further investigated in the following experiments.

#### **4.4 Studies on Fetal Bovine Serum**

The data presented above demonstrated a significant positive effect of serum supplementation on hMSCs growth. The use of animal-derived serum for the large-scale expansion of cells to be used in cellular therapy is an interesting and well known subject. To this date, MSCs have been expanded in a culture medium supplemented with Fetal Calf Serum in most of the reported clinical trials [Sotiropoulou *et al.*, 2006; Meuleman *et al.*, 2006], and all current protocols for *in vitro* culture of hMSCs include Fetal Bovine Serum as nutritional supplement [Shahdadfar *et al.*, 2005]. However, due to its inherent characteristics, serum is an undesirable additive to cells that are expanded for therapeutic purposes in humans (please see section 1.4.2). Because of undefined composition, risk of contaminations, cost factor and also animal welfare considerations concerning the production of sera, the switch to serum-free alternatives is promoted by regulatory authorities, industry and the research community in general [Falkner E. *et al.*, 2004;



[http://www.aahr.asn.au/campaigns/fetal\\_calf\\_serum.html](http://www.aahr.asn.au/campaigns/fetal_calf_serum.html); “Australian Code of Practice for the care and use of animals for scientific purposes” 7<sup>th</sup> edition 2004 (1.8 page 6); Even *et al.*, 2006]. It follows that a serum-free medium, allowing the generation of an adequate number of pathogen-free MSCs, is urgently needed for clinical use. As already mentioned in section 1.4.2, the possibility of growing certain types of cells in serum-free formulations has been undertaken by several laboratories [Sato, 1975; Mattinger *et al.*, 2002; Bednarz *et al.*, 2001; Pei *et al.*, 2003; Amit *et al.*, 2003]. However, in these studies replacement of serum with supplements of better defined composition was found to be not very successful for the growth of normal cells in conventional culture media. As a result, a number of fundamental questions relating to the feasibility of employing serum-free culture systems for the successful expansion of hMSCs are still unanswered.

Following the preliminary results described in the previous section, other studies were performed, focusing on investigating further the effects of different Fetal Bovine Serum (FBS) concentrations on hMSCs proliferation. Both the impacts of serum alone (section 4.4.1) and in combination with other culture parameters (section 4.5, 4.6 and 4.8.2) on hMSCs behaviour in monolayer condition were investigated. Fetal Bovine Serum specifically selected by the manufacturer (Stem Cell Technologies Inc.) for optimal hMSCs growth was used for this purpose.

#### **4.4.1 Effects of Fetal Bovine Serum (FBS) on hMSCs growth and metabolism in monolayer culture**

To compare the effects of different serum concentrations on the proliferative capability of hMSCs, fourth passage (p4) bone marrow-derived hMSCs were established in parallel low-glucose DMEM cultures either with no serum or after supplementation with one of three different concentrations of FBS (2%, 10% and 15% (v/v)). The cells were plated in non-coated 24-well microplates and grown for 13 days. At day 3, 7, 10 and 13, the cells were harvested and enumerated with haemocytometer (as described in section 2.6.2) and the viable cells were identified and counted with trypan blue dye (as described in section 2.6.3). In addition, for each serum condition, the spent medium was recovered from the wells at each harvesting time-point. The recovered medium was then analysed with the Nova Biomedical

BioProfiler for the assessment of the glucose and lactate concentrations (as per protocol described in section 2.6.5). Cell morphology was evaluated over the 13-day period of culture by means of light microscopy (as described in section 2.6.1).

The results obtained from this study are presented in figures 4.2, 4.3 and 4.4, and in tables 4.2 and 4.3.

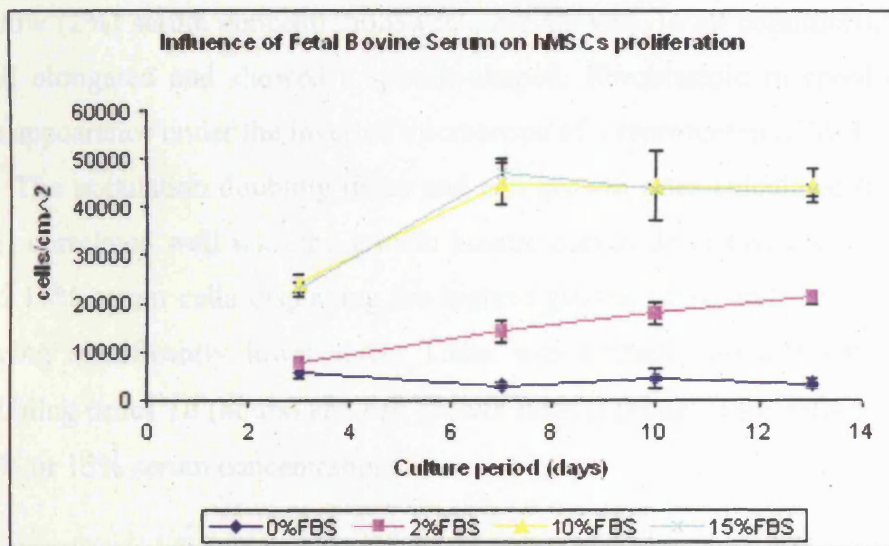


**Fig. 4.2:** Effects of Fetal Bovine Serum on cell proliferation. Human MSCs were cultured in non-coated plates, with low-glucose DMEM medium supplemented with 1ng/ml bFGF. The low-glucose DMEM was either used with no serum supplementation or after addition of increasing (2%, 10% and 15%) serum concentrations (v/v). The —●— line represents the cell growth curve for cells cultured in standard control conditions (“complete DMEM”, i.e. medium supplemented with 10% FBS and 1ng/mL bFGF). Data are presented as means  $\pm$  s.e. of three independent measurements (please see section 2.6.9).

As it is evident from figure 4.2, a significant difference in cell growth between media with high (10% and 15%), low (2%) serum concentrations and the serum-free medium condition was observed. 10% FBS- and 15% FBS-supplemented cells displayed very similar growth curves, the cell proliferation reaching a plateau at approximately  $45 \times 10^3$  cells/cm<sup>2</sup> after 7 days in culture in both cases. Also cells cultured in the presence of 2% serum displayed certain cell growth, and in this condition linear cell growth was maintained over the 13-day period examined.

However, the cells plated in low serum concentration expanded only approximately 4-fold (4.26) in 13 days, whereas the same number of cells plated in both the high serum concentrations expanded 9-fold (8.9 for 10%-serum cells and 8.72 for 15%-serum cells) over the same culture period. On the other hand, serum-free culture did not support cell proliferation, and resulted instead in a 1.5-fold decrease in cell growth over the 13-day period.

The analysis of the cultures at the inverted light microscope revealed no discernible morphological differences between cells expanded in high (10% or 15%) or low (2%) serum concentrations (data not shown). In all conditions, the cells were well elongated and showed a spindle-shaped, fibroblastoid morphology, indicating the appearance under the inverted microscope of a representative MSC culture.

The population doubling times and cell growth rates calculated (please see table 4.2) correlated well with the growth kinetic curves described above, with the 10%- and 15%-serum cells displaying the highest growth rates, and the lower serum cells having significantly lower rates. There was virtually no difference between the doubling times  $T_d$  (hours) and cell growth rates  $\mu$  (hours<sup>-1</sup>) for cells cultured in either 10% or 15% serum concentrations.

**Table 4.2:** Population Doubling Level (PDL), Doubling Time ( $T_d$ ) and cell growth rate ( $\mu$ ) values calculated for hMSCs expanded in all four different serum conditions tested during the first week of culture.

<b>Growth conditions day0-day7</b>	<b>PDL</b>	<b><math>T_d</math>(hours)</b>	<b><math>\mu</math> (hours<sup>-1</sup>)</b>
<b>0%FBS</b>	-0.763	-220.33	-0.003
<b>2%FBS</b>	1.511	111.22	0.006
<b>10%FBS</b>	3.165	53.08	0.013
<b>15%FBS</b>	3.235	51.93	0.013

High cell viability (please see table 4.3) was retained over the 13-day culture period under examination for both cells maintained in serum-free (>92.29%) and cells grown in serum-supplemented (>94.14%) conditions. However, even though not statistically significant ( $p = 0.049$ , Anova single factor test), a slight decrease in viability was observed over time for the serum-free cells. As expected, the 10%- and

15%-FBS cultures consistently yielded the highest cell viability values throughout the same period of culture (>96.58% and >95.29% respectively).

**Table 4.3:** Percent cell viability values obtained for hMSCs cultured in four different serum conditions (0 %, 2 %, 10 % and 15 % v/v). Cell viability was determined by means of the exclusion assay with trypan blue dye at four harvesting time-points during the 13-day period of culture under examination.

<b>Growth conditions</b>			
<b>0%FBS</b>	<b>day</b>	<b>viability average (%)</b>	<b>std. err. (±%)</b>
	3	94.95	4.51
	7	97.22	4.81
	10	96.49	6.08
	13	92.29	2.20
<b>2%FBS</b>	<b>day</b>	<b>viability average</b>	<b>std. err. (±%)</b>
	3	95.59	4.10
	7	96.50	2.48
	10	94.14	1.08
	13	96.16	1.14
<b>10%FBS</b>	<b>day</b>	<b>viability average</b>	<b>std. err. (±%)</b>
	3	97.44	0.96
	7	98.75	0.77
	10	96.58	0.78
	13	100.00	0.00
<b>15%FBS</b>	<b>day</b>	<b>viability average</b>	<b>std. err. (±%)</b>
	3	95.29	1.59
	7	99.28	0.90
	10	97.04	0.32
	13	98.42	0.70

As shown by the metabolites analyses performed with the Nova Biomedical BioProfiler (please see figure 4.3), cells cultured in either serum-free or 2%-serum conditions were not metabolising any glucose or producing any lactate, and were therefore metabolically inactive. On the other hand, hMSCs cultured in the presence of either 10%- or 15%-serum were characterised by a more intense metabolic activity. These data correlate well with the growth kinetics data presented in figure 4.2 and described above.

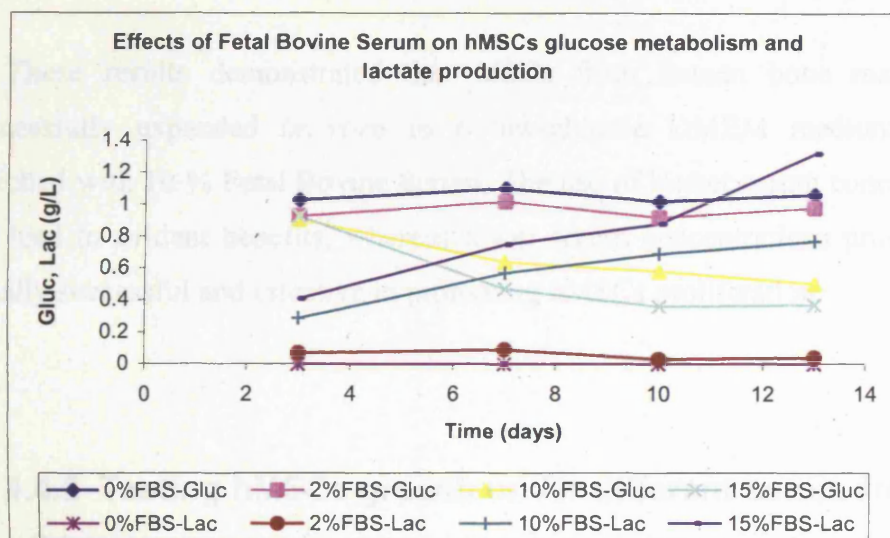


**Fig. 4.3:** Glucose consumption and lactate production measured over the 13-day culture period for *in vitro* expanded hMSCs maintained under different Fetal Bovine Serum culture conditions.

The specific glucose consumption rate (g/cell/hour) was calculated according to the equation described in section 2.6.5.2. Interestingly, no significant difference in specific glucose consumption rate was observed for the different serum conditions up to 10 days in culture. However, 10% FBS-supplemented cells appeared to metabolise glucose at an increasing rate during the last 3 days of culture (please see figure 4.4).

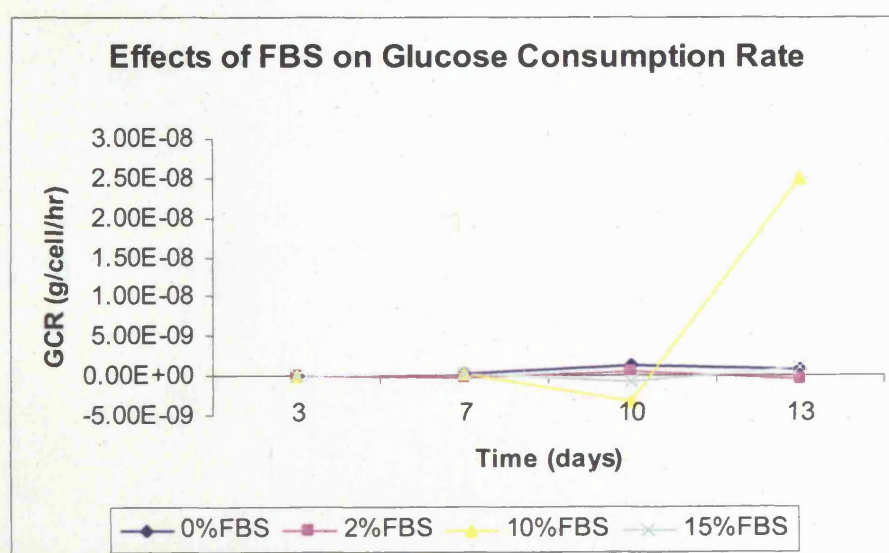


**Fig. 4.4:** Impact of different Fetal Bovine Serum concentrations on hMSCs specific glucose consumption rate during *in vitro* expansion in tissue culture plates.

These results demonstrated that MSCs from human bone marrow can be successfully expanded *in vitro* in a low-glucose DMEM medium formulation enriched with 10 % Fetal Bovine Serum. The use of higher serum concentrations did not lead to evident benefits, whereas lower serum concentrations proved to be not equally successful and effective in promoting hMSCs proliferation.

#### **4.4.2 Testing hMSCs growth under different serum-free media conditions**

Given the numerous disadvantages associated with the usage of Fetal Bovine Serum in cell preparations to be used for clinical purposes (please see section 4.4 and section 1.4.2), another approach to avoid additives of animal origin in our culture system was investigated. A study was performed to compare the effects of eleven different serum-free formulations on *in vitro* expanded hMSCs (please see section 2.1.5.2.2 for a detailed description of the study protocol). The commercially available serum-free media investigated in this experiment are listed in table 4.4. The composition of these media is not published, but it is understood that most of them do not contain animal derived components, some formulations containing only a very low amount of defined proteins.



**Table 4.4:** Serum-free media investigated for the expansion of hMSCs in tissue culture flasks. Following the manufacturer's suggestion, the Knockout D-MEM medium (medium number 7) was supplemented with 15% Knockout Serum Replacement (Gibco, Cat. No.=10828).

No.	Medium	Manufacturer	Protein free	Phenol red	Animal origin-free	Optimised for
1	CD Hybridoma Medium without L-glutamine	Gibco	X	no	X	Human, mouse, rat hybridomas, myelomas.
2	Stem Pro-34 SFM without L-glutamine without antibiotics	Gibco				Human hematopoietic progenitor cells
3	Protein free Hybridoma Medium PFHM II (1X)	Gibco	X	X	X	Human, mouse, rat hybridomas, myelomas
4	Hybridoma-SFM serum-free Hybridoma Medium	BioWhittaker	no	X	no	Human, mouse, rat hybridomas, myelomas
5	Ultraculture medium	BioWhittaker	3mg/mL		no	Most cell types
6	UltraDOMA Hybridoma serum-free growth Medium, defined 1X	BioWhittaker	30µg/mL		no	Murine, human and chimeric cell lines
7	Knockout D-MEM optimised D-MEM Medium for ES cells	Gibco				Murine and human embryonic stem (ES) cells
8	Ex-cell 325 PF CHO serum-free Medium, protein-free	SAFC Biosciences	X		X	Chinese Hamster Ovary (CHO) cells
9	Ex-cell 302 CHO serum-free Medium	SAFC Biosciences				Transformed CHO cells
10	Ex-cell 620-HSF hybridoma serum-free Medium	SAFC Biosciences	11mg/L			Hybridoma and CHO
11	Ex-cell CD CHO serum-free Medium, chemically defined	SAFC Biosciences			X	CHO cells

These media formulations were compared with the standard low-glucose complete DMEM medium (formulated as described in section 2.1.5.1) for their use in serum-free cultivation of hMSCs. Low-glucose DMEM is routinely used for culturing human mesenchymal progenitor cells [Gotherstrom *et al.* 2003; Jager *et al.*, 2003; Romanov *et al.*, 2003; Pittenger *et al.*, 1999; Lee *et al.*, 2003]. In addition, low glucose concentration in DMEM-based media has demonstrated to consistently support human bone marrow-derived MSCs growth [Sotiropoulou *et al.*, 2005]. A DMEM formulation, supplemented with FBS and appropriate additives, is generally the medium recommended also for expanding *in vitro* mouse embryonic stem cells

[Robertson, 1987; Hogan *et al.*, 1994]. On the other hand, the media investigated in this study have been designed for cultivation of several cell types in serum-free conditions (please see table 4.4). The Knockout-DMEM medium, used without serum supplementation, for example, is a special basal medium formulated specifically to improve the morphology and performance of Embryonic Stem Cells. Interestingly, this medium has already been found to be superior for murine MSCs preparation in comparison with other commercially available media [de Camargo Bittencourt *et al.*, 2006].

In this experiment hMSC cultures were simply assessed by means of inverted light microscopy, as this was intended to be exclusively a qualitative and preliminary exercise, designed to evaluate the survival and growth of MSCs in serum-free conditions. The objective was to perform an initial rough screening, and to select among the media formulations investigated those ones, if there were any, allowing cell survival and proliferation, as compared to the standard 10% serum-supplemented complete DMEM medium.

Persuading cells to grow in serum-free condition is a process that usually involves gradual weaning. In this study, for each of the media listed in table 4.4, hMSCs were sub-cultured using the sequential adaptation protocol described in section 2.1.5.2.2. The cultures were examined at the inverted light microscope every 2-3 days during culture for the qualitative evaluation of cell proliferation and cell morphology. The visual evaluation of the cultures was intended as a simple procedure, providing a rapid method of assessing and predicting the quality of the cultures. Photographs using an inverted light microscope and a digital camera were taken at the end of the culture (data not shown).

During incubation in the 50:50 (v/v) mixture of the traditional serum-supplemented DMEM - : serum-free medium, a marked reduction in cell proliferation was observed. Under this condition, for media number 5, number 6 and number 7 the desired 80% confluence was reached after 17 days of culture, whilst all of the other serum-free cultures did not permit a similar cell growth. However, the cells were harvested at the same time even if confluence was not reached in all media with the purpose to evaluate the more effective serum-free formulation for MSC expansion and for reduced culture period. Cell proliferation was further hampered during the following sub-culturing passage in the 10:90 (v/v) serum-supplemented - : serum-free



mixtures. This condition was unsuccessful for most of the serum-free media investigated, as in most cases cell proliferation was not observed. On the contrary, MSC cultures showed significant morphological abnormalities. The cells varied in size and shape, with noticeable granules in the cytoplasm, and debris was formed in the medium. After about 6-7 days in the majority of the cultures the granular cells began to be vacuolated, rounded and finally detached from the base of the flasks. However, cell survival and proliferation were noticed in three of the serum-free media under investigation. Medium number 5 [UltraCulture medium (BioWhittaker)], medium 6 [UltraDOMA Hybridoma serum-free medium, defined 1X (BioWhittaker)] and medium 7 [Knockout DMEM optimised D-MEM medium for EScells 1x, high glucose, with sodium -pyruvate, without L-glutamine (Gibco) supplemented with 15% Knockout Serum Replacement] were the only media that enabled prolonged cultivation without serum-supplementation. Even though cell growth was worse than what observed in control (10% serum-supplemented) cultures, these three serum-free media did allow cell proliferation, and 70-80% confluence was seen in these conditions approximately eleven days after plating. Cell morphology evaluation by inverted light microscopy revealed in these cultures the presence of expanding adherent spindle-shaped fibroblastoid cells compatible with undifferentiated MSCs. In these three medium formulations, cell morphology was also very similar to that observed for the cells maintained in the control flasks (please see figures 4.5 and 4.6 for representative examples of the different cell morphologies observed for hMSCs expanded in the Knockout D-MEM optimised medium from Gibco and the Ex-cell 302 CHO serum-free medium from SAFC).

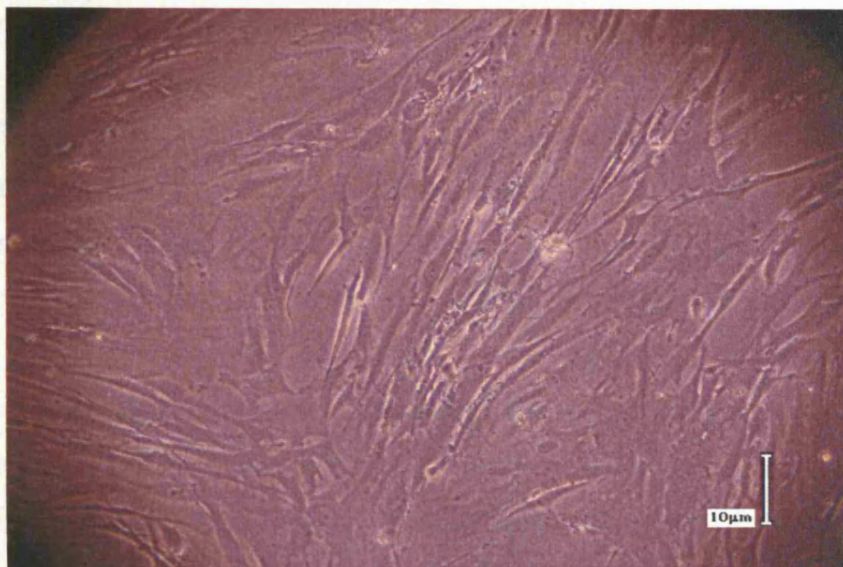


**Fig. 4.5:** Morphology of hMSCs expanded in 10:90 (v/v) complete DMEM - : Knockout optimised D-MEM medium (formulated with high glucose, with sodium pyruvate, without L-glutamine, supplemented with 15% Knockout Serum Replacement and supplied by Gibco).

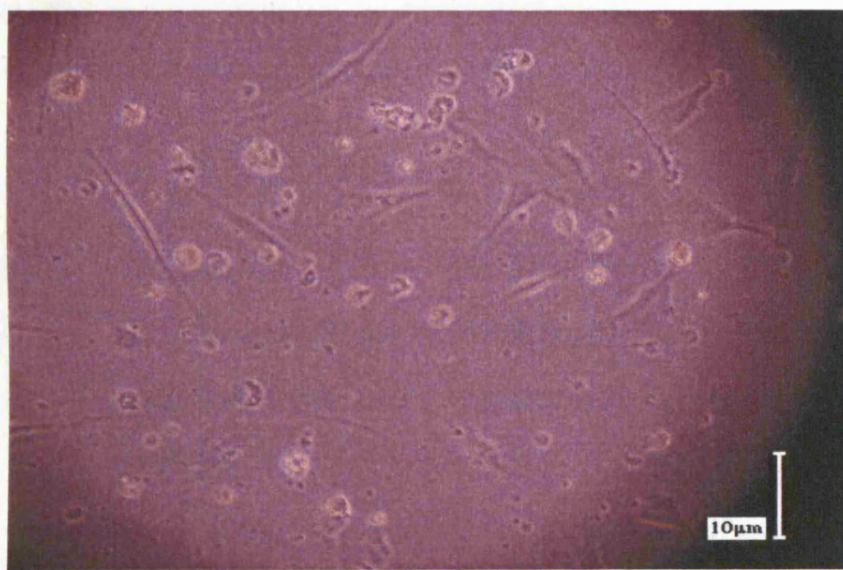


**Fig. 4.6:** Morphology of hMSCs expanded in 10: 90 (v/v) complete DMEM : Excell 302 CHO serum-free medium, protein free (SAFC Biosciences).

These preliminary results indicated that long-term culture of hMSCs without serum supplementation is possible in the UltraCulture, the UltraDOMA Hybridoma and the Knockout DMEM optimised media. This study therefore suggested that these media might represent a promising alternative for human MSCs culture in serum-free environment. However, due to time constraint it was not possible to characterise and

verify the purity and homogeneity of the resulting MSCs in this study. It would then be necessary to investigate further the effects of these three media conditions on the MSCs growth kinetics, multipotentiality and metabolic activity. In future experiments both the hMSCs isolation from frozen bone marrow samples and their expansion in tissue flasks could be performed in each one of these three formulations in totally serum-free conditions. If successful cell isolation and expansion were then achieved in a reproducible way under any of these conditions, the characterization of the resulting cell population would confirm whether or not the purity, homogeneity and “stemness” of the cells are preserved. Growth rate and population time analyses, differentiation potential assay, flow cytometric analysis of specific surface antigens (for the determination of MSC markers, osteogenic precursor markers, etc.) could be performed to ascertain whether these media are truly suitable for the preparation of pure MSC populations without serum supplementation. If this is the case, deployment of these media will permit avoidance of serum in the hMSCs culture system, thus excluding any variability in medium composition and also minimising the risk of infection resulting from the supplementation with serum.

#### **4.5 Influence of Fetal Bovine Serum (FBS) and basic Fibroblast Growth Factor (bFGF) on hMSCs proliferation and metabolic activity in monolayer culture**

In addition to serum requirements, the combination of cytokines delivered to the cell microenvironment is one more key feature for any stem cell culture system. Maintenance of the concentrations of these cytokines and their associated receptors over time is also extremely important [Bianchi *et al.*, 2001; Locklin *et al.*, 1999; Deasy. *et al.*, 2002]. Significant efforts have been made to define cytokine and growth factors supplementation strategies to control stem cell responses. The cytokine composition of the medium is particularly challenging to optimise in stem cell culture because multiple cell types compete for several cytokines that each influence stem cell fate directly or indirectly [Zandstra and Nagy, 2001].

The addition of supplementary factors for the successful isolation and expansion of MSCs, and in particular the use of bFGF for proliferation enhancement, are currently objects of thorough studies [van den Bos *et al.*, 1997; Hori *et al.*, 2004; Solchaga *et al.*, 2005; Bianchi *et al.*, 2003]. Basic Fibroblast Growth Factor (bFGF) is undoubtedly the most common growth supplement in MSC culture media. bFGF-supplementation in MSC culture has already demonstrated to increase cell proliferation and affect their multilineage differentiation capacity [Sotiropoulou *et al.*, 2005]. Several studies have previously reported that in various culture systems bFGF acts as a potent mitogen for MSCs, whilst maintaining their differentiation potential and increasing at the same time their telomere length [Kotobuki *et al.*, 2004; Bianchi *et al.*, 2003]. Other investigations suggest that bFGF addition in bone marrow stromal cells *in vitro* culture is associated with a higher osteogenic differentiation potential, as compared to cell samples maintained in the absence of the growth factor. This indicates that the growth factor might favour their osteogenic potential [Martin *et al.*, 1997; Reyes and Verfaillie, 1999; Nagai *et al.*, 1999].

Given the significant impact that growth factors addition has shown in stem cell culture systems, it was of interest to this research to better define the role of basic Fibroblast Growth Factor (bFGF) on MSCs proliferation potential and viability.

The aim of this experiment was to investigate the combined effects of Fetal Bovine Serum (FBS) and basic Fibroblast Growth Factor (bFGF) on hMSCs growth and metabolism in monolayer culture. For this purpose, fourth passage (p4) hMSCs were expanded in 24-well tissue culture plates in low-glucose DMEM medium formulated with increasing FBS and bFGF concentrations (see section 2.1.5.4 for a detailed protocol description). The cells were harvested and evaluated for cell density, viability and metabolism at different time-points over the 2-weeks period examined.

The growth kinetics data obtained for all FBS and bFGF conditions are shown in the graph in figure 4.7.



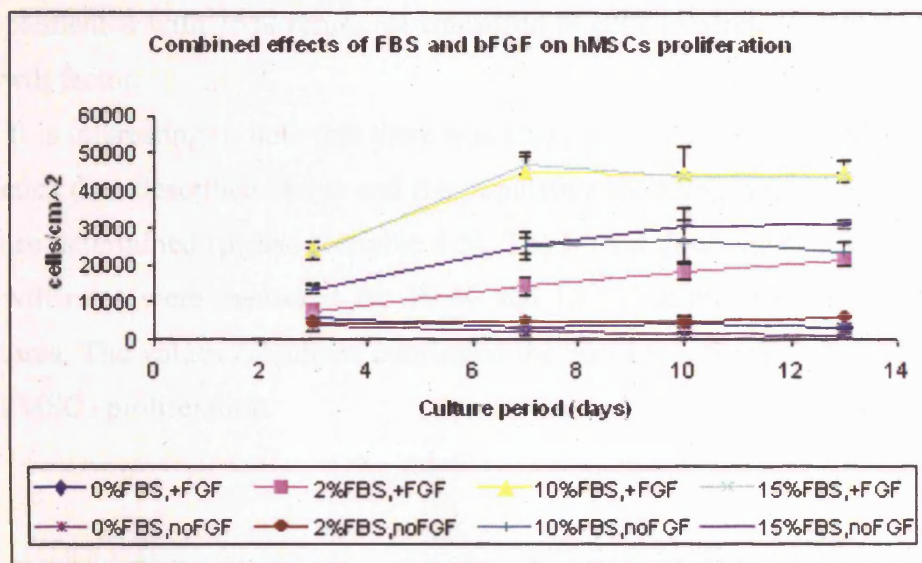


**Fig. 4.7:** Effects of Fetal Bovine Serum (FBS) and basic Fibroblast Growth Factor (bFGF) on hMSCs proliferative capacity. Fourth passage (p4) human MSCs were plated in 24-well plates and cultured with growth medium with increasing serum and bFGF concentrations for up to 13 days. Data are presented as means  $\pm$  s.e. of three independent measurements (please see section 2.6.9).

It is evident from these data that medium supplementation with bFGF resulted in a significant positive effect on cell expansion in all the serum concentration conditions examined. In particular, cell death was observed over time (13-day culture period) in any case when hMSCs were maintained in serum-free DMEM medium. However, the presence of bFGF in this serum-free microenvironment significantly hampered cell death; bFGF-supplemented cultures exhibited only 1.5-fold decrease in cell proliferation over 13 days, as opposed to a marked 4.7-fold decrease in cell growth observed over the same time period for serum-free/ bFGF-free cultures. Addition of bFGF resulted essential particularly in serum-deprivation (2% FBS) condition, where cell proliferation resulted heavily compromised in the absence of the growth factor. Over the same time period (13-day culture period) bFGF-withdrawal resulted in 1.2 fold increase in cell growth, as opposed to a 4.2 fold increase calculated for bFGF-supplemented cells. Finally, bFGF-supplementation led to higher cell proliferation also in standard (10% FBS) and 15% FBS culture conditions. The growth factor had similar positive effect in these two higher serum conditions. After 13 days in bFGF-supplemented medium culture, a 1.9-fold cell growth increase was measured for standard (i.e. 10%) serum cultures, and a 1.4-fold increase for cells

supplemented with 15% serum, as compared to cells expanded in the absence of the growth factor.

It is interesting to note that there was also a good correlation between the growth kinetics data described above and the population doubling time and cell growth rate values determined (please see table 4.5). The lowest doubling times and highest cell growth rates were measured for 10 % and 15 % serum- and bFGF-supplemented cultures. The values calculated confirmed the positive influence of the growth factor on hMSCs proliferation.

**Table 4.5:** Population Doubling Level (PDL), Doubling Time (Td) and cell growth rate ( $\mu$ ) values calculated for hMSCs expanded in all the different FBS and bFGF conditions under investigation during the first week of culture.

<b>Growth conditions day0-day7</b>	<b>PDL</b>	<b>Td(hours)</b>	<b><math>\mu</math> (hours<sup>-1</sup>)</b>
<b>0%FBS,+FGF</b>	-0.763	-220.33	-0.003
<b>2%FBS,+FGF</b>	1.511	111.22	0.006
<b>10%FBS,+FGF</b>	3.165	53.08	0.013
<b>15%FBS,+FGF</b>	3.235	51.93	0.013
<b>0%FBS,noFGF</b>	-1.248	-134.62	-0.005
<b>2%FBS,noFGF</b>	-0.046	-3629.01	0.000
<b>10%FBS,noFGF</b>	2.337	71.89	0.010
<b>15%FBS,noFGF</b>	2.337	71.89	0.010

The percent viability values for cells expanded in the absence of the growth factor are presented in table 4.6. The effects of bFGF on cell viability can be easily deduced by comparing these values with the viability data obtained for the same cells maintained in bFGF-supplemented DMEM medium (please see table 4.3). Supplementation with bFGF appears to have a significant positive effect on hMSCs viability particularly in serum-free culture. In the presence of serum, the positive effect of the growth factor on cell viability was much less evident, and was virtually void for 2 % serum cells.

**Table 4.6:** Percent cell viability values obtained for hMSCs expanded in the absence of bFGF under different serum conditions. Data are shown for each harvesting time-point during the 13-day period of culture evaluated.

<b>Growth conditions</b>			
<b>0%FBS,noFGF</b>	<b>day</b>	<b>viability average (%)</b>	<b>std. err. (±%)</b>
	3	100.00	0
	7	100.00	0
	10	83.62	1.96
	13	67.14	15.45
<b>2%FBS,noFGF</b>	<b>day</b>	<b>viability average</b>	<b>std. err. (±%)</b>
	3	100.00	0
	7	93.17	2.21
	10	84.39	9.54
	13	96.63	3.45
<b>10%FBS,noFGF</b>	<b>day</b>	<b>viability average</b>	<b>std. err. (±%)</b>
	3	100.00	0
	7	95.14	2.69
	10	95.29	1.79
	13	95.28	1.73
<b>15%FBS,noFGF</b>	<b>day</b>	<b>viability average</b>	<b>std. err. (±%)</b>
	3	99.09	1.58
	7	97.69	1.27
	10	96.13	1.58
	13	95.26	0.75

The graph in figure 4.8 indicates the glucose depletion and lactate production measured in the spent medium recovered from the cultures over the 13-day period under examination. These data are given for hMSCs cultured in 10 % FBS-supplemented DMEM medium, either with or without 1ng/mL bFGF. It is evident from the graph that in standard (10% v/v) serum condition cell metabolism results favoured after addition of bFGF in the medium of culture.

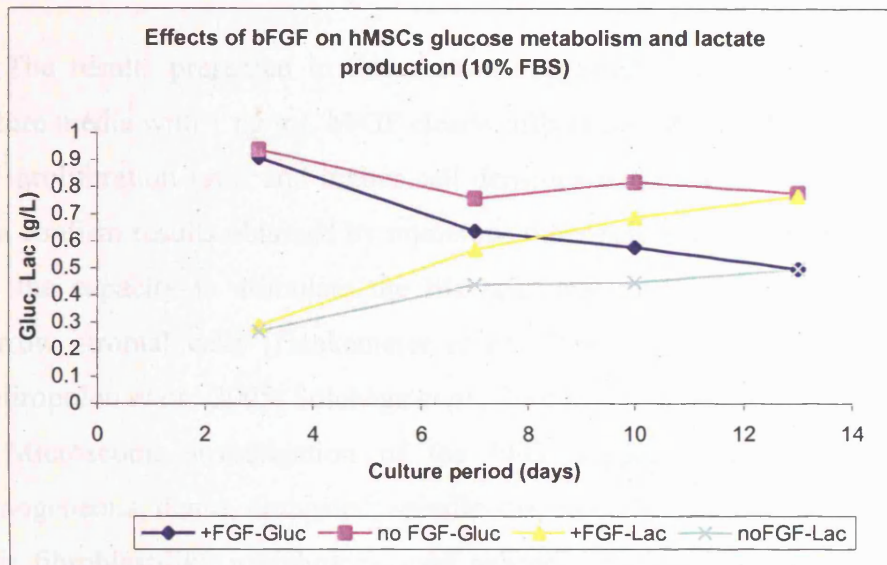


**Fig. 4.8:** Influence of bFGF-supplementation on hMSCs metabolic activity. The graph indicates changing in glucose and lactate concentrations measured in the spent medium over time in culture.

As it is shown in figure 4.9, hMSCs maintained in bFGF-supplemented culture displayed a significant increase in glucose metabolism rate during the last 3 days of culture, but there was almost no difference in specific glucose consumption rate up to 10 days in culture.

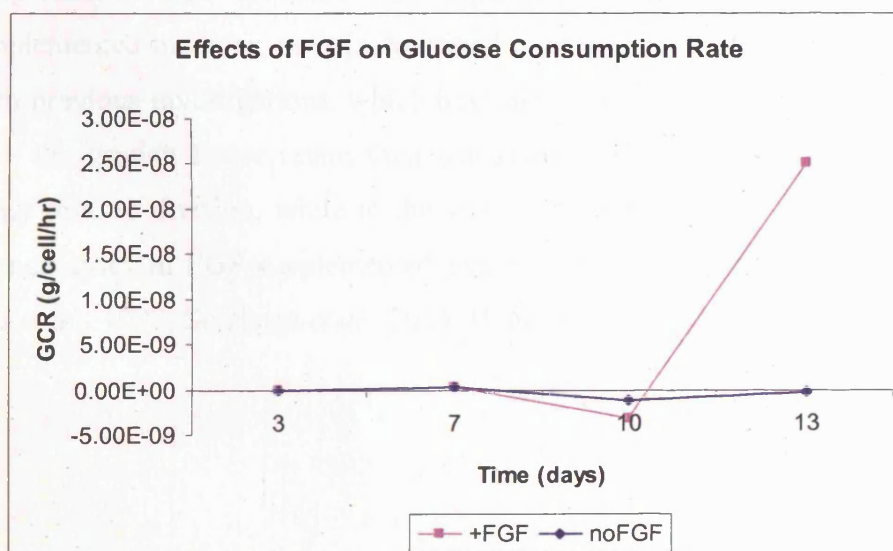


**Fig. 4.9:** Impact of bFGF-supplementation on hMSCs specific glucose consumption rate.



The results presented in this section suggested that supplementation of MSCs culture media with 1 ng/mL bFGF clearly affects cell proliferation, resulting in higher cell proliferation rates and higher cell densities within two weeks of culture. These data confirm results obtained by numerous other research groups indicating that FGF has the capacity to stimulate the life span and proliferation rate of human bone marrow stromal cells [Hankemeier *et al.*, 2005; Martin *et al.*, 1997] and MSCs [Sotiropolou *et al.*, 2005; Solchaga *et al.*, 2005].

Microscopic investigation of the bFGF-supplemented cell cultures showed homogeneous, dense, elongated, spindle-shaped cells which were retaining unaltered their fibroblast-like morphology over subsequent expansion passages. This was in line with other studies showing that the characteristic fibroblast-like phenotype was retained for over 4 weeks when bFGF was added in bone marrow stromal cells' culture systems [Hankemeier *et al.*, 2005; Martin *et al.*, 1997]. However, it must be noticed that other groups [Sotiropolou *et al.*, 2005; Solchaga *et al.*, 2005] have observed that bFGF-addition critically alters MSCs morphology and phenotype, resulting in cells that tend to shorten and lose their spindled shape over time, a phenomenon which was not seen in this research.

Finally, supplementation of bFGF in the DMEM culture medium did not limit the differentiation capacity of MSCs. Osteogenic, adipogenic and chondrogenic potential were retained after the cells were expanded over consecutive passages in bFGF-supplemented medium, as it is described in section 4.7. These results are consistent with previous investigations, which have also indicated that MSCs expanded *in vitro* with the growth factor retain their osteogenic and adipogenic potential throughout many mitotic division, while at the same time appear to be able to differentiate to chondrocytes in FGF-supplemented pellet cultures [Tsutsumi *et al.*, 2001; van den Bos *et al.*, 1997; Solchaga *et al.*, 2005; Bianchi *et al.*, 2003].

#### **4.6 Growth kinetics and metabolic activity of hMSCs maintained in different culture vessel coatings under different serum conditions**

The surface of the culture plates and their impact on cell expansion is an additional parameter investigated in this research. It is known that extracellular matrix (ECM) components interact with specific cell surface adhesion receptors and control various cellular functions, including differentiation, proliferation, migration and apoptosis [Magnusson and Mosher, 1998]. By regulating cell differentiation and function, cell-ECM interactions are thought to orchestrate tissue organization both during fetal development and throughout normal adult life [Darribere *et al.*, 2000; Damsky, 1999]. The use of an ECM as a coating for tissue culture surfaces permits the development of culture systems mimicking closely *in vivo* conditions. Such *in vitro* models, which incorporate components of the *in vivo* environment, usually succeed in supporting normal cell culture and function. It follows from these considerations that the choice of ECM is an important component to consider when optimising *in vitro* systems for cell culture.

Previous studies have indicated that culture surface properties have significant impact on the behaviours of MSCs. For instance, enhanced cell attachment and spreading, together with a significant increase in the number of adherent cells, were observed when hMSCs were cultured on fibronectin-coated dishes [Ogura *et al.*, 2004]. In other studies hMSCs growth rate and proliferative life span resulted markedly increased in tissue culture dishes coated with a basement membrane-like extracellular matrix with similar composition to that of Matrigel [Matsubara *et al.*, 2004]. Results presented by other groups have suggested that Matrigel coating itself, used at an appropriate density, provides a favourable substrate that improves the efficiency of MSC expansion and their neuronal differentiation [Qian and Saltzman, 2004]. A short description of fibronectin's properties and matrigel composition are given in section 1.4.4.

Since MSCs are known to be strongly affected by the properties of culture substrates [Fried *et al.*, 1996; Gronthos *et al.*, 2001], the possibility of improving the yield of bone marrow-derived MSCs through culture surface modification was investigated.

To compare the growth potential of hMSCs expanded in monolayer culture in different culture surfaces, fourth passage (p4) cells were incubated and maintained in either standard non-coated tissue plates or in plates coated by the supplier with either fibronectin or matrigel. For each of these coating conditions, DMEM medium with increasing serum concentrations (0%, 2 % or 10% v/v) was used (please see section 2.1.5.2.3 for a detailed protocol description). The cultures were maintained for 13 days. Cell proliferation, cell viability and cell growth rates were evaluated at day 3, 7, 10 and 13 as previously described (please see sections 2.6.2, 2.6.3 and 2.6.4 respectively). In addition, morphology of hMSCs was observed by phase-contrast microscopy, following the protocol presented in section 2.6.1. Finally, for each condition a sample of spent medium was recovered from the wells at all four time-points and was then analysed with the Nova Biomedical Bioprofiler for the measurement of glucose and lactate concentrations (please see section 2.6.5 for a description of this technique).

The growth curves obtained for all coatings conditions are represented respectively in figures 4.10 (10 % serum), 4.11 (2 % serum) and 4.12 (serum-free).

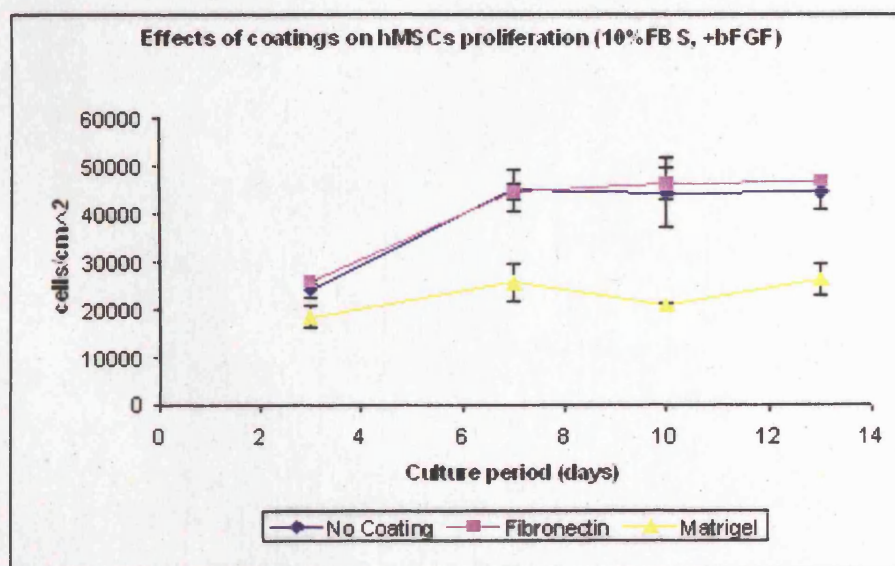


**Fig. 4.10:** 10% serum-supplemented hMSCs expanded in non-coated plates (control, —●— line), fibronectin-coated plates (—■— line) or matrigel-coated plates (—★— line). Data are presented as means  $\pm$  s.e. of three independent measurements (please see section 2.6.9).

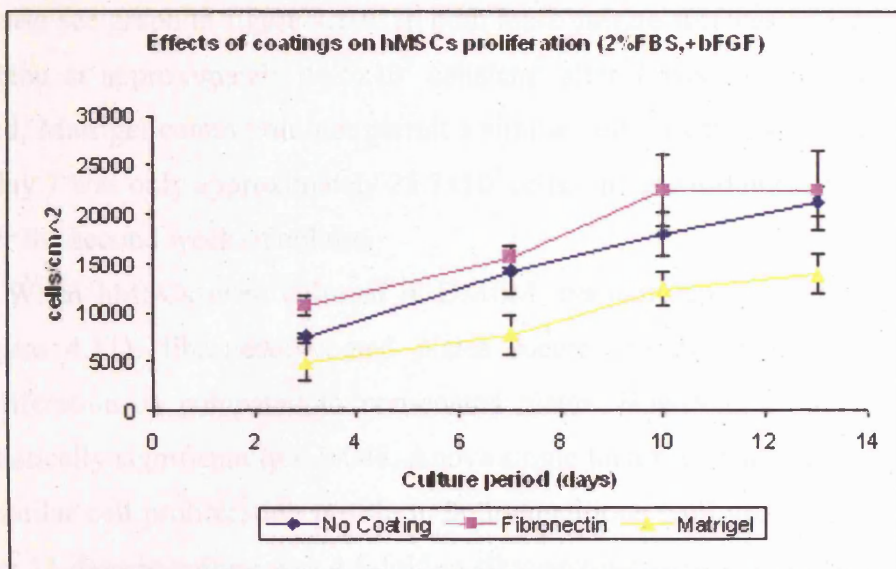


**Fig. 4.11:** 2% serum-supplemented hMSCs cultured in non-coated plates (control, —◆— line), fibronectin-coated plates (—■— line) or matrigel-coated plates (—▲— line). Data are presented as means  $\pm$  s.e. of three independent measurements (please see section 2.6.9).

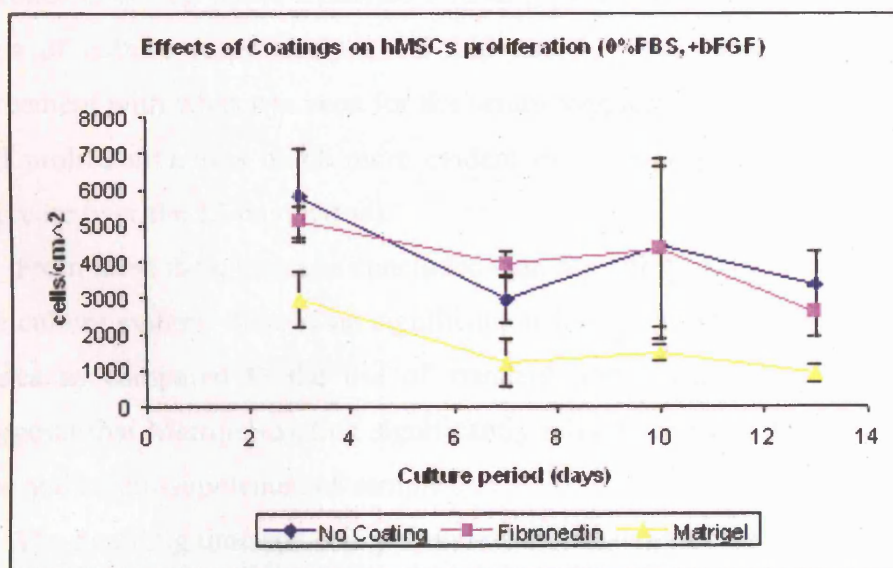


**Fig. 4.12:** Serum-free hMSCs cultured in non-coated plates (control, —◆— line), fibronectin-coated plates (—■— line) or matrigel-coated plates (—▲— line). Data are presented as means  $\pm$  s.e. of three independent measurements (please see section 2.6.9).

In standard (10 % FBS) serum condition the growth kinetics curves exhibited a similar pattern for cells expanded in either non-coated or fibronectin-coated plates

(please see graph in figure 4.10). In both these culture surfaces cell growth reached a plateau at approximately  $44.5 \times 10^3$  cells/cm<sup>2</sup> after 1 week in culture. On the other hand, Matrigel coating did not permit a similar cell growth, as cell density measured at day 7 was only approximately  $25.7 \times 10^3$  cells/cm<sup>2</sup> and did not increase significantly over the second week of culture.

When hMSCs were cultured in DMEM medium supplemented with 2% serum (figure 4.11), fibronectin-coated plates seemed to permit a slightly better cell proliferation as compared to non-coated plates. However, the difference was not statistically significant ( $p = 0.048$ , Anova single factor test), and the cells experienced a similar cell proliferation profile in both conditions (cell growth increase measured over 13 days in culture was 4.5-fold in fibronectin-coated plates and 4.3-fold in non-coated vessels). On the other hand, as opposed to fibronectin and non-coated plates, Matrigel-coated plates significantly limited cell expansion, as in this case only a 2.8-fold increase in cell growth was measured over the same time period.

Also in serum-free culture (figure 4.12) hMSCs expanded in either non-coated or fibronectin-coated plates exhibited similar growth kinetics, experiencing over the 13 days of culture respectively a 1.5-fold and 1.9-fold decrease in cell growth. In agreement with what was seen for the serum-supplemented cultures, the reduction in cell proliferation was much more evident in the Matrigel-coated samples (5.5-fold decrease over the 13-day period).

From these data, it can be concluded that, regardless of the serum concentration in the culture system, there is no significant advantage in the use of fibronectin-coated plates as compared to the use of standard non-coated plates. Besides, evidence suggests that Matrigel-coating significantly inhibits cell proliferation in both serum-free and serum-supplemented samples.

The doubling time and cell growth rate values determined for hMSCs expanded in the different coating plates are shown in table 4.7. These values are in accordance with the growth kinetic data described above. Cells expanded in either non-coated or fibronectin-coated plates were characterised by the lowest doubling times and the highest cell growth rates, and these values were similar for these two coating conditions. Higher doubling time and lower cell growth rate values were observed for the Matrigel-coated samples, confirming the negative impact of Matrigel on hMSCs proliferation capacity. Well in accordance with the results presented in the previous



sections, doubling time values decreased and cell growth rate values increased by increasing FBS concentration in the DMEM medium formulation.

**Table 4.7:** Population Doubling Level (PDL), Doubling Time (Td) and cell growth rate ( $\mu$ ) values calculated for hMSCs expanded in all the different conditions under investigation from day 0 to day 7 of culture.

<b>Growth conditions day0-day7</b>	<b>PDL</b>	<b>Td(hours)</b>	<b><math>\mu</math> (hours<sup>-1</sup>)</b>
<b>10%FBS,NC</b>	3.165	53.08	0.0131
<b>10%FBS,FN</b>	3.154	53.27	0.0130
<b>10%FBS,Matrigel</b>	2.361	71.16	0.0097
<b>2%FBS, NC</b>	1.511	111.22	0.0062
<b>2%FBS, FN</b>	1.646	102.06	0.0068
<b>2%FBS, Matrigel</b>	0.640	262.67	0.0026
<b>0%FBS,NC</b>	-0.763	-220.33	-0.0031
<b>0%FBS,FN</b>	-0.347	-483.50	-0.0014
<b>0%FBS,Matrigel</b>	-2.067	-81.26	-0.0085

Microscopic observation of the cultures revealed that in both the non-coating and fibronectin-coating conditions most of the cells attached to the vessel surface and exhibited a fibroblast-like spindle shape. Under these conditions the cells proliferated to form a uniform confluent cell monolayer every 3 to 4 days. hMSC attachment and spreading over the culture vessels' surface were not observed in Matrigel-coated plates. Lower cell numbers were noticed in the samples expanded in Matrigel-coating as compared to non-coating and fibronectin-coating samples (please see figures 4.13, 4.14 and 4.15).

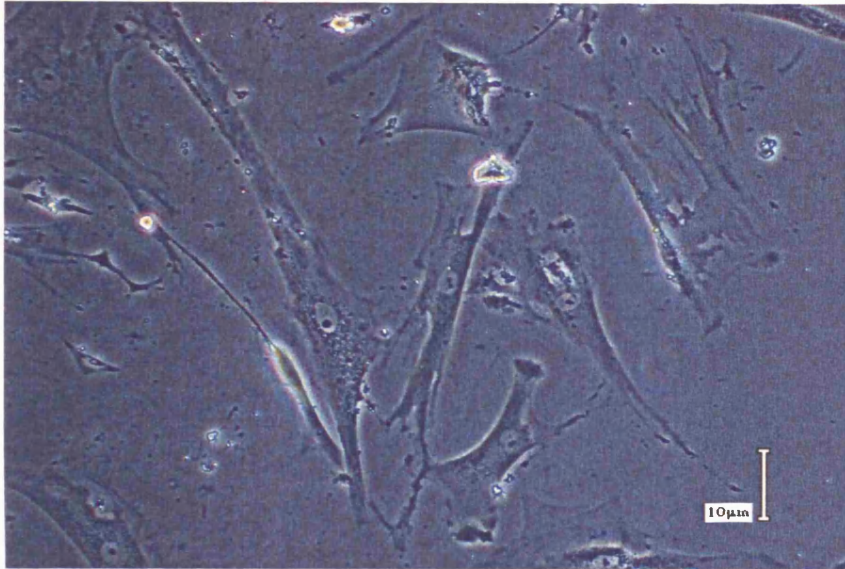


**Fig. 4.13:** Morphology of hMSCs expanded in non-coated plates in medium supplemented with 10% FBS.

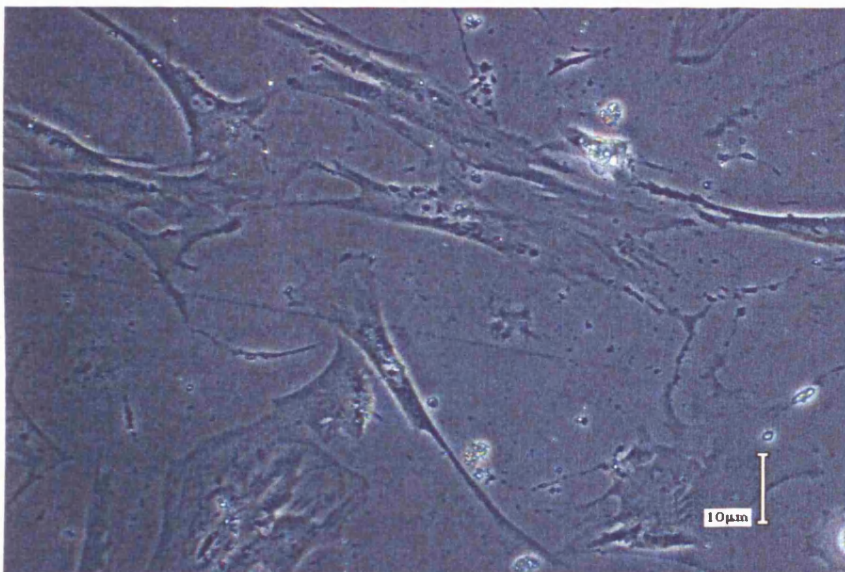


**Fig.4.14:** Morphology of hMSCs expanded in fibronectin-coated plates in medium supplemented with 10% FBS.

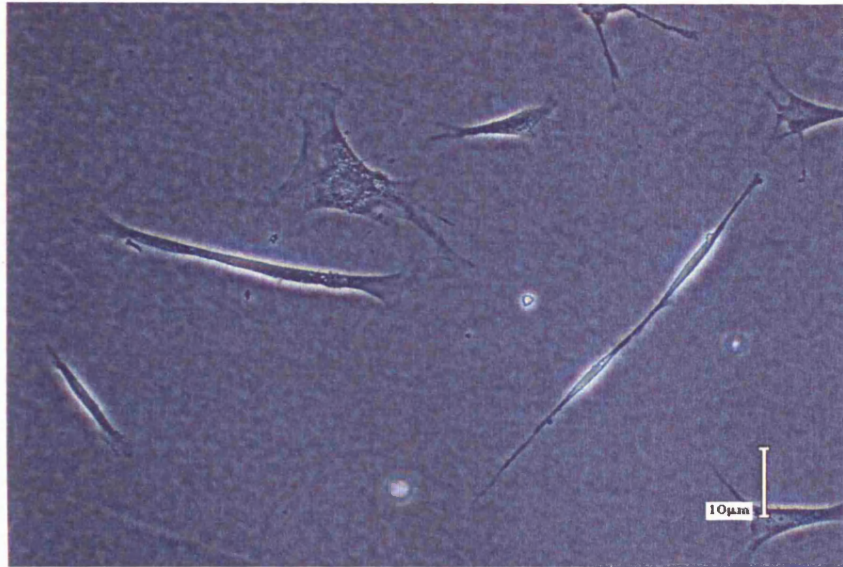


**Fig. 4.15:** Morphology of hMSCs expanded in Matrigel-coated plates in 10% FBS-supplemented medium.

Cell viability was assessed at each time-point for all serum and coating conditions. These data are presented in table 4.8. Regardless of the coating condition, 10 % serum-supplementation permitted the highest cell viability, whilst serum deprivation significantly affected cell viability, particularly for cells cultured in fibronectin-coated or matrigel-coated plates. Overall, the culture within Matrigel-coated plates was associated with the lowest cell viability values. There was no significant difference between cell viability for non-coating and fibronectin-coating conditions, both in 10 % FBS- or 2 % FBS- supplemented media. On the other hand, the viability measured in serum-free culture was higher for cells expanded in non-coated plates than for cells grown in fibronectin-coated plates.



**Table 4.8:** Percent cell viability values obtained for hMSCs expanded in all the different conditions tested at each harvesting time-point during the 13-day period of culture.

<b>Growth conditions</b>			
<b>10%FBS,NC</b>	<b>day</b>	<b>viability average</b>	<b>std. err. (±%)</b>
	3	97.44	0.96
	7	98.75	0.77
	10	96.58	0.78
	13	100	2.20
<b>10%FBS,FN</b>	<b>day</b>	<b>viability average</b>	<b>std. err. (±%)</b>
	3	97.38	1.97
	7	99.06	0.04
	10	98.67	0.37
	13	99.26	0.50
<b>10%FBS,Matrigel</b>	<b>day</b>	<b>viability average</b>	<b>std. err. (±%)</b>
	3	97.68	1.40
	7	98.57	1.15
	10	96.42	0.51
	13	95.70	1.15
<b>2%FBS, NC</b>	<b>day</b>	<b>viability average</b>	<b>std. err. (±%)</b>
	3	95.59	4.10
	7	96.50	2.48
	10	94.14	1.08
	13	96.16	1.14
<b>2%FBS, FN</b>	<b>day</b>	<b>viability average</b>	<b>std. err. (±%)</b>
	3	99.32	1.18
	7	97.77	1.63
	10	97.14	1.46
	13	95.28	2.44
<b>2%FBS, Matrigel</b>	<b>day</b>	<b>viability average</b>	<b>std. err. (±%)</b>
	3	100	0.00
	7	100	0.00
	10	94.35	2.37
	13	87.80	3.26
<b>0%FBS,NC</b>	<b>day</b>	<b>viability average</b>	<b>std. err. (±%)</b>
	3	94.95	4.51
	7	97.22	4.81
	10	96.49	6.08
	13	92.29	2.20
<b>0%FBS,FN</b>	<b>day</b>	<b>viability average</b>	<b>std. err. (±%)</b>
	3	98.72	2.22
	7	94.89	0.41
	10	95.37	4.24
	13	85.61	2.91
<b>0%FBS,Matrigel</b>	<b>day</b>	<b>viability average</b>	<b>std. err. (±%)</b>
	3	98.25	3.04
	7	100	0.00
	10	84.85	26.24
	13	51.98	16.85

The metabolic activity data obtained confirmed the overall effects of the different culture plates surfaces on MSCs behaviour. These data are presented in figure 4.16 (10 % serum), figure 4.17 (2 % serum) and figure 4.18 (serum-free). In standard (10 %) serum condition, hMSCs expanded in traditional non coated-coated plates exhibited higher metabolic activity than cells maintained in fibronectin-coated or matrigel-coated plates. On the other hand, cells grown in serum-free cultures resulted metabolically inactive, and regardless of the surface conditions examined they resulted unable to consume any glucose or produce any lactate.

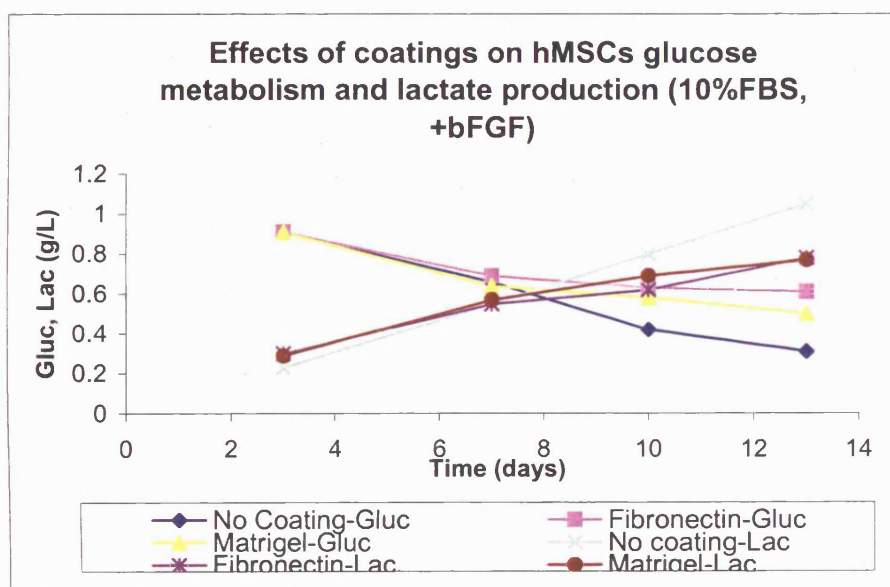


**Fig. 4.16:** Effects of coatings on hMSCs metabolic activity. Cells were cultured in low-glucose DMEM medium supplemented with 10% (v/v) Fetal Bovine Serum (FBS) and 1 ng/mL basic Fibroblast Growth Factor (bFGF).

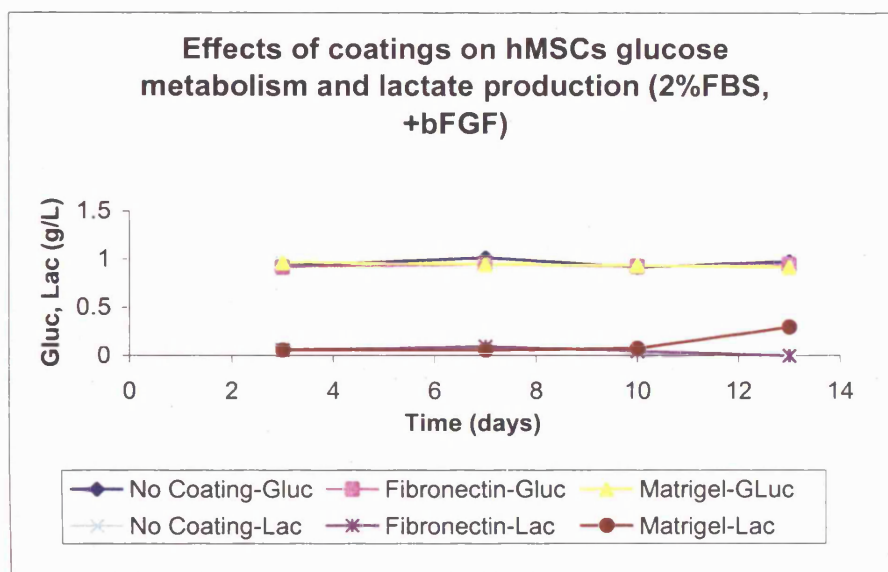


**Fig. 4.17:** Effects of coatings on hMSCs metabolism. The cultures were maintained in low-glucose DMEM medium supplemented with 2% FBS and 1ng/mL bFGF.

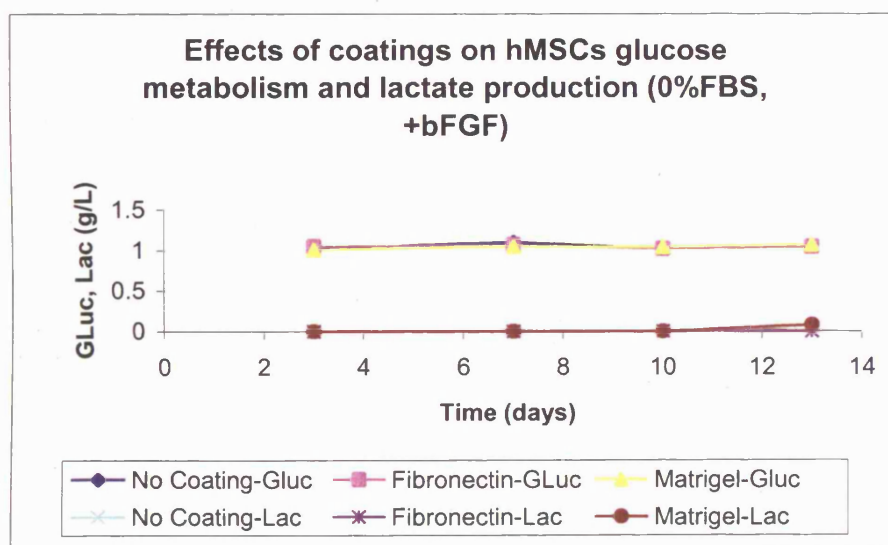


**Fig. 4.18:** Effects of coatings on hMSCs metabolic activity. Cells were expanded in serum-free low-glucose DMEM medium supplemented with 1 ng/mL bFGF.

The specific glucose consumption rates (g/cell/hour) were calculated for each serum and coating conditions as it is described in section 2.6.4. The values obtained are presented in figure 4.19, 4.20 and 4.21. In the 10 % serum-supplemented culture

samples a significant increase in GCR was observed during the last 3 days of culture only for hMSCs expanded in non-coated plates, whereas no significant increase in GCR was detected for cells expanded in fibronectin- or Matrigel-coated plates. Results for 2% serum or serum-free cells are more difficult to interpret (figure 4.19 and figure 4.21).

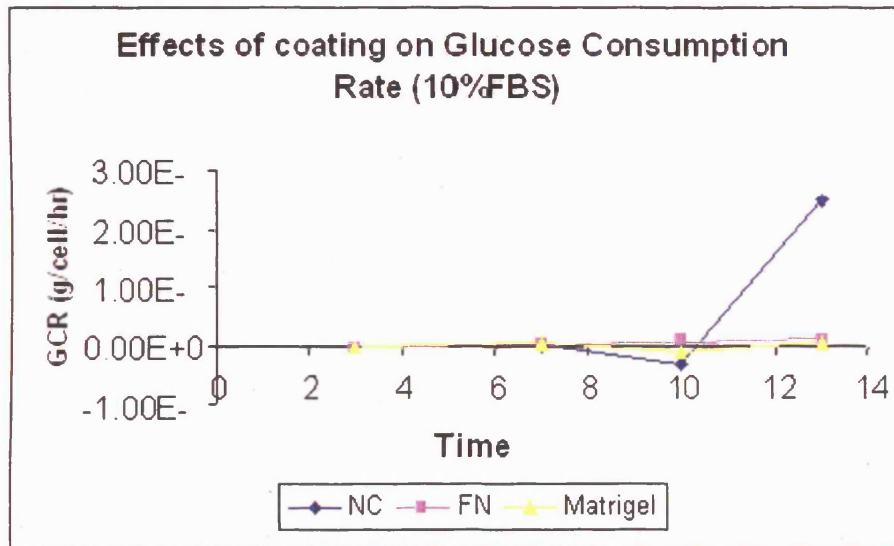


**Fig. 4.19:** Impact of coatings on 10% serum-supplemented hMSCs specific glucose consumption rate.

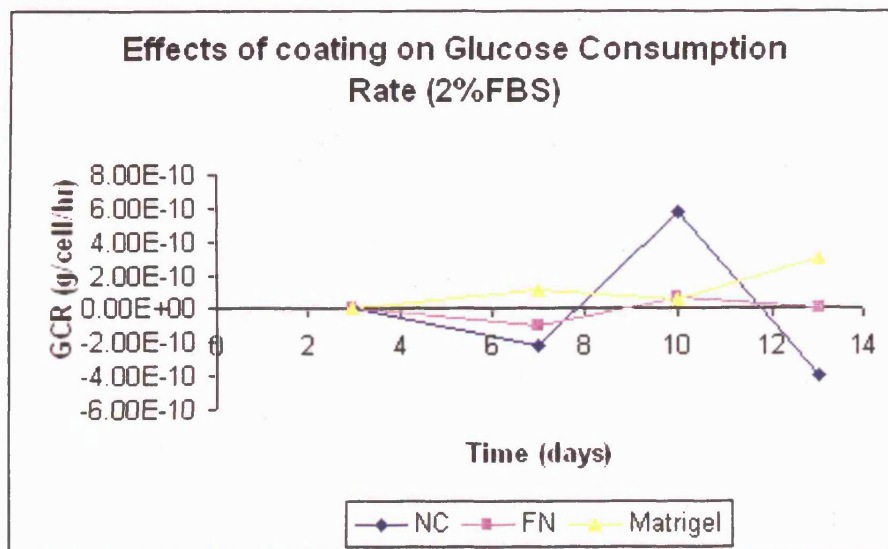


**Fig. 4.20:** Effects of coatings on 2% serum-supplemented hMSCs specific glucose consumption rate.

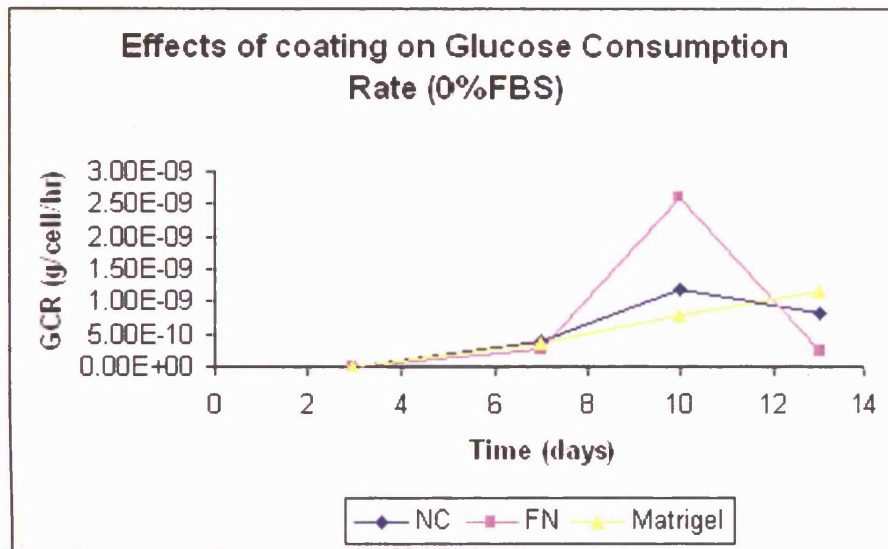


**Fig. 4.21:** Effects of coatings on serum-free hMSCs specific glucose consumption rate.

In conclusions, evaluation of different culture surfaces (i.e. standard non-coated, fibronectin-coated and Matrigel-coated plates) for hMSCs, revealed that, regardless of the serum concentration in the culture system, those based on Matrigel impeded cell growth, viability and metabolic activity. On the contrary, both standard non-coated and fibronectin-coated plates consistently supported hMSCs growth and metabolism.

#### **4.7 Multipotentiality of human adult mesenchymal stem cells expanded in monolayer culture**

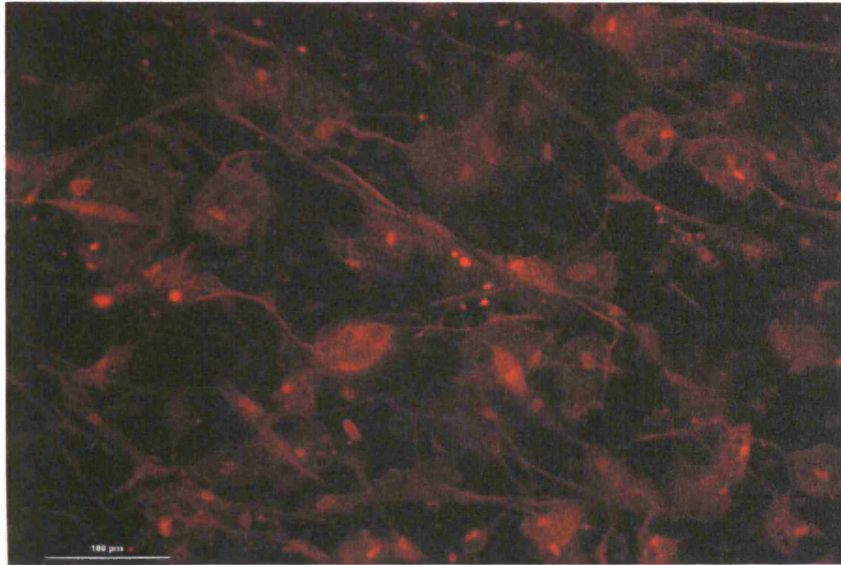
For regeneration of human cartilage, bone and even osteochondral defects, different cell sources are being investigated. In general, stem and progenitor cells are preferable to final differentiated cells due to their proliferation and differentiation capacity [Caplan and Goldberg, 1999; Lemare *et al.*, 1998]. *In vitro*, culture-expanded bone marrow-derived mesenchymal stem cells have indeed shown the capacity to differentiate into a number of mesenchymal lineages, including osteogenic, chondrogenic and adipogenic [Pittenger *et al.*, 1999; Muraglia *et al.*, 2000; Jiang *et al.*, 2002]. MSCs' ability to retain their multilineage differentiation

potential for over a significant number of cell doublings in culture is what makes them so attractive for a broad range of tissue engineering applications [Reyes *et al.*, 2001]. *In vivo*, several studies in a variety of animal models have shown that hMSCs may be useful in the repair or regeneration of cartilage [Wakitani *et al.*, 2002], damaged bone [Livingston *et al.*, 2001; De Kok *et al.*, 2003], tendon [Award, *et al.*, 2003] and meniscus [Murphy *et al.*, 2003]. Other investigations have indicated that MSCs may result useful also for repair of skeletal muscle [Wakitani *et al.*, 1995], while there has been also some evidence that hMSCs can also be induced to differentiate into neurons *in vitro* [Woodbury *et al.*, 2000].

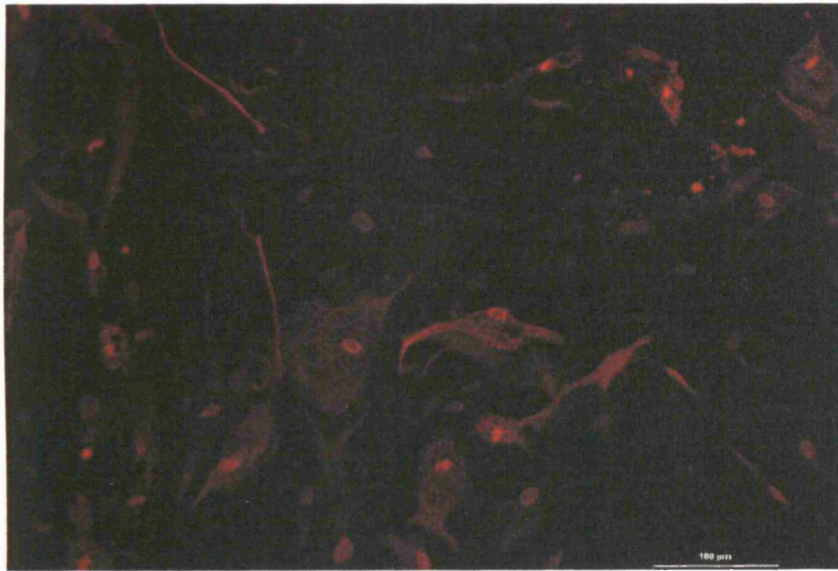
The differentiation potential of MSCs into multiple mesenchymal lineages – that is, bone, cartilage and adipose tissue – is most commonly used as a functional criterium defining MSC precursor cells [Fibbe, 2002]. In order to assess their multipotency, fourth passage (p4) bone marrow-derived plastic adherent MSCs isolated from a sample of adult frozen bone marrow were tested with the “Human Mesenchymal Stem Cell Functional Identification Kit” (R&D Systems), which permits the identification of human bone marrow-derived stem cells (BMSCs)/mesenchymal stem cells (MSCs) based on their ability to differentiate into mature phenotypes of adipocytes, osteocytes and chondrocytes. Prior to the start of this study, the cells were expanded *in vitro* in “complete DMEM” medium, formulated as described in section 2.1.5.1, until the necessary numbers of cells was achieved. The typical morphology of the hMSCs expanded for this experiment and seen prior the switch to the differentiation media is shown in figure 4.28 a).

In order to assess their adipogenic potential, hMSCs were plated at a density of  $2.1 \times 10^4$  cells/cm<sup>2</sup> and were cultured with adipogenic medium, as it is described in section 2.6.7.1. Morphologic changes in the cells, as well as the formation of neutral lipid vacuoles, were noticeable 3 weeks after induction and were visualised by goat anti-mouse FABP-4 immuno-staining (figure 4.22 A, B). Adipogenic differentiation was not observed 21 days after induction in the negative control samples (not been treated with the same FABP-4 antibody (figure 4.22 C)).





*A*



*B*

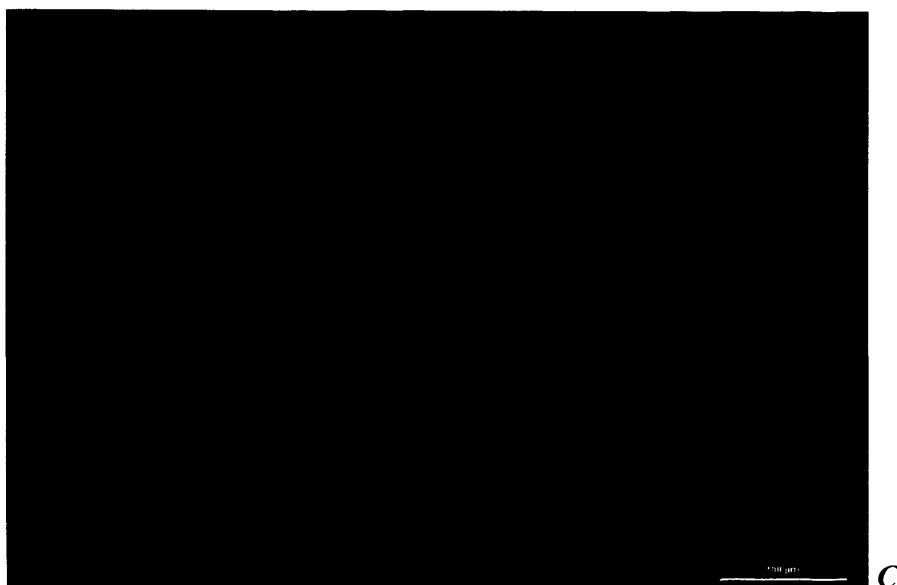


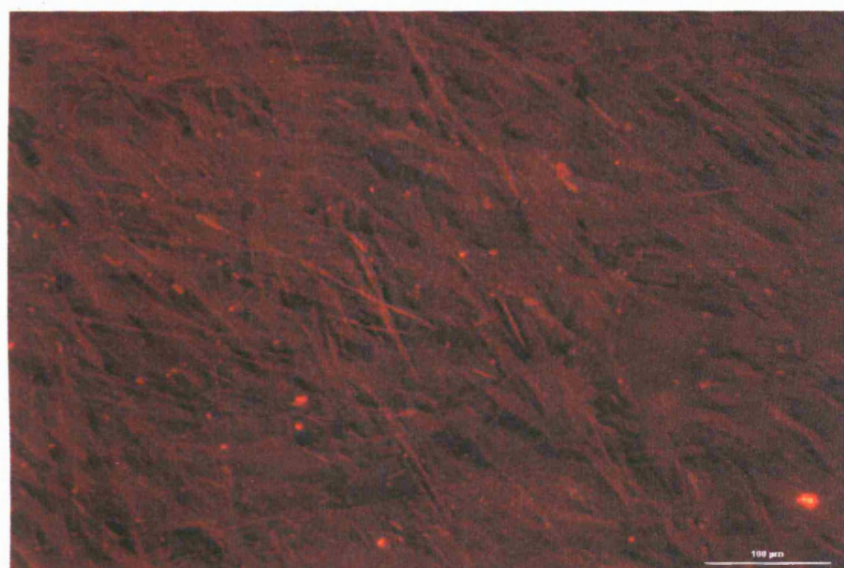
**Fig. 4.22:** Adipogenic differentiation of bone marrow-derived hMSCs. Monolayer MSCs were treated with adipogenic medium. After 21 days, the cells were fixed and immuno-stained for goat anti-mouse FABP-4. *A*, *B* (positive staining) and *C* (negative control).

To investigate the osteogenic potential of the bone marrow-derived MSCs, the same cells were plated at a density of  $4.2 \times 10^3$  cells/cm<sup>2</sup> and were incubated under conditions appropriate for inducing differentiation for osteogenic lineage (please see section 2.6.7.1). When induced to differentiate under osteogenic conditions, the spindle shape of the bone marrow-derived cells flattened with increasing time of induction and formed mineralized matrix, as evidenced by microscopic evaluation. The osteocytes phenotype was shown after 21 days of induction by immunofluorescence staining for mouse anti-human osteocalcin antibody (figure 4.23 A, B). Osteogenic differentiation, as determined by positive immunostaining for osteocalcin antibody, was achieved in all the osteogenic medium-treated samples tested with the osteocalcin antibody. The immunofluorescence assay performed on induced cells not treated with human osteocalcin (negative controls) stained negative for the antibody (figure 4.23 C).





*A*



*B*

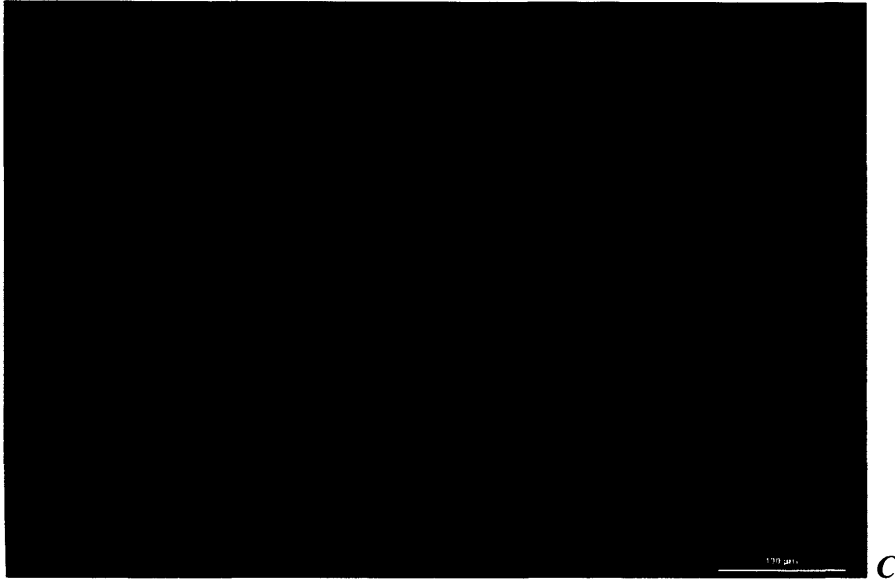
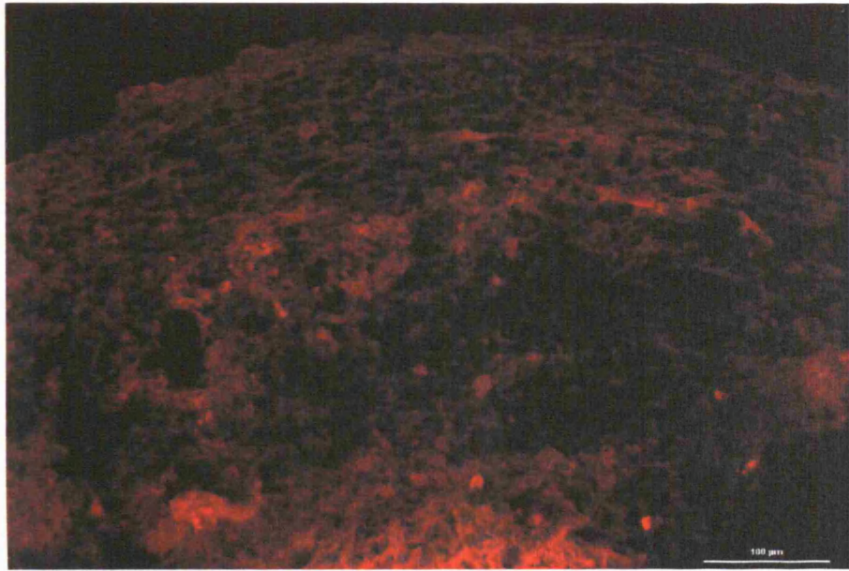
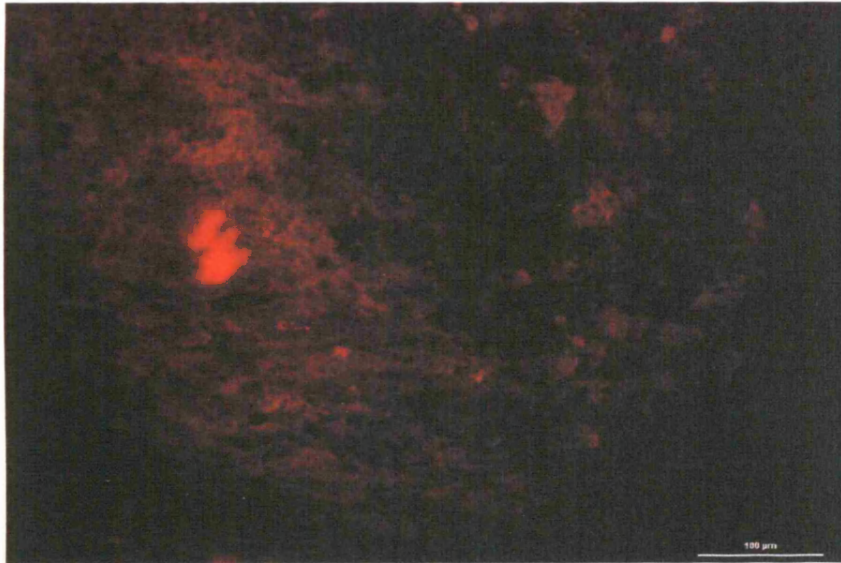


**Fig. 4.23:** *A, B* (positive staining) and *C* (negative control): mouse anti-human Osteocalcin staining for hMSCs induced for 21 days with osteogenic medium.

Finally, the chondrogenic potential of the expanded bone marrow-derived cells was evaluated by culturing  $2.5 \times 10^5$  cells under the pelleted micromass system in chondrogenic medium, as it is described in section 2.6.7.1. After 3 weeks of induction in the chondrogenic growth medium, the TGF $\beta$ -treated micromasses displayed positive immuno-staining for the goat anti-human aggrecan antibody (figure 4.24 A, B). The positive immunohistochemical analysis performed 21 days after induction confirmed the cartilage phenotype of the tissue generated *in vitro*. On the contrary, differentiated micromasses untreated with the primary antibody (negative control cells) did not display positive immuno-staining (figure 4.24 C).



*A*



*B*



**Fig. 4.24:** *A, B* (positive staining) and *C* (negative control): goat anti-human Aggrecan staining for hMSCs induced for 21 days with chondrogenic supplement.

This study confirmed that human bone marrow-derived MSCs, expanded under appropriate culture conditions, can be induced to differentiate *in vitro* toward the adipogenesis, osteogenesis and chondrogenesis pathways. Under these conditions, the cells showed the ability to successfully differentiate toward the three different lineages, as demonstrated by the positive staining for the specific antibodies provided with the “Human Mesenchymal Stem Cell Functional Identification kit”, defining the mature phenotypes of adipocytes, osteocytes and chondrocytes. As a result, it can be concluded that hMSCs originally isolated from a human frozen bone marrow sample retain their multipotentiality after 4 expansion passages in culture.

#### **4.8 Dissolved oxygen tension (DOT) as an important parameter for hMSCs *in vitro* expansion**

It is recognised that the dissolved oxygen tension (i.e. the exact oxygen level at the cells/medium interface) is lower than the oxygen level in the humidified gas mixture within the incubator. This is due to oxygen consumption by living cells. However, since to our knowledge there is no practical methodology that can be employed to measure the actual dissolved oxygen tension (DOT), we here make no

formal distinction between the two values, and refer to both simply as to “DOT” or “oxygen level”.

This parameter has been demonstrated to play an important role on the growth kinetics and functionality of a broad range of cell types grown *in vitro*, including rat marrow-derived MSCs [Lennon *et al.*, 2001], human articular chondrocytes [Martin *et al.*, 2004; Domm *et al.*, 2004], human embryonic stem cells [Ezashi *et al.*, 2005] and human MSCs [Moussavi-Harami *et al.*, 2004; Rochefort *et al.*, 2006]. The importance of the oxygen levels in *in vitro* settings has already been elucidated in section 1.5.5. Due to the established significance of this parameter on cell behaviour, dissolved oxygen tension was thoroughly investigated in this research. Firstly, the effects of the oxygen level alone on hMSCs proliferation rate and metabolism were investigated (section 4.8.1). These studies were followed by experiments focusing on the combined effects of the DOT and FBS-supplementation (section 4.8.2), and the combined effects of the oxygen level and supplementation with bFGF (section 4.8.3). To ensure maintenance of the desired gas mixture and DOT, incubators with two air sensors, one for CO<sub>2</sub> and the other O<sub>2</sub>, were used for all these studies.

#### **4.8.1 Studies investigating hMSCs’ proliferation and metabolic activity under different dissolved oxygen tensions**

This section describes the studies performed on hMSCs cultures maintained in standard serum (10 %-supplementation), bFGF (1 ng/mL-supplementation) and coating (traditional non-coated tissue culture plates) conditions, where focus was kept on varying the DOT value alone. A first experiment was conducted by growing hMSCs for a 13-day period in one or the other of the following dissolved oxygen tensions: 21 % (the typical ambient O<sub>2</sub> level employed in most culture settings), 10 % or 2 % (please see table 4.9 for clarification on the terminology adopted in this research for defining the “ambient” and “hypoxic” conditions).

**Table 4.9:** Terminology adopted in this research to define the different oxygen levels investigated during *in vitro* expansion of hMSCs in monolayer culture.



Oxygen level	21 oxygen	6-10% oxygen	1-2% oxygen
Terminology adopted in this research	Ambient (hyperoxic)	Normoxic	Hypoxic

To understand the effect of relatively long-term, low DOT on hMSCs expansion, in a second study ambient oxygen (21 %) culture was compared with 6 % and 1 % DOT samples over a longer (21 days) time period. In order to characterize the growth kinetics and metabolic activity of hMSCs under the various oxygen regimes, sixth passage (p6) hMSCs were expanded in 24-well tissue culture plates that were maintained in culture at 37°C, 5% CO<sub>2</sub> in air in three different humidified (>95%) incubators, each one set at one of the three selected DOTs for each experiment. All the cultures were performed in traditional complete DMEM medium, formulated as described in section 2.1.5.1. The cells were harvested and evaluated for cell density, viability and metabolism at different time-points over the culture period under examination.

In both studies, hMSCs grown at the 21 % standard DOT were characterised by the highest proliferation potential, as it is evident from the graphs in figure 4.25 and figure 4.26. On the other hand, cells maintained at lower oxygen regimes (10 %, and 2 % in figure 4.25, 6 % and 1 % in figure 4.26) did not show a similar growth capacity.

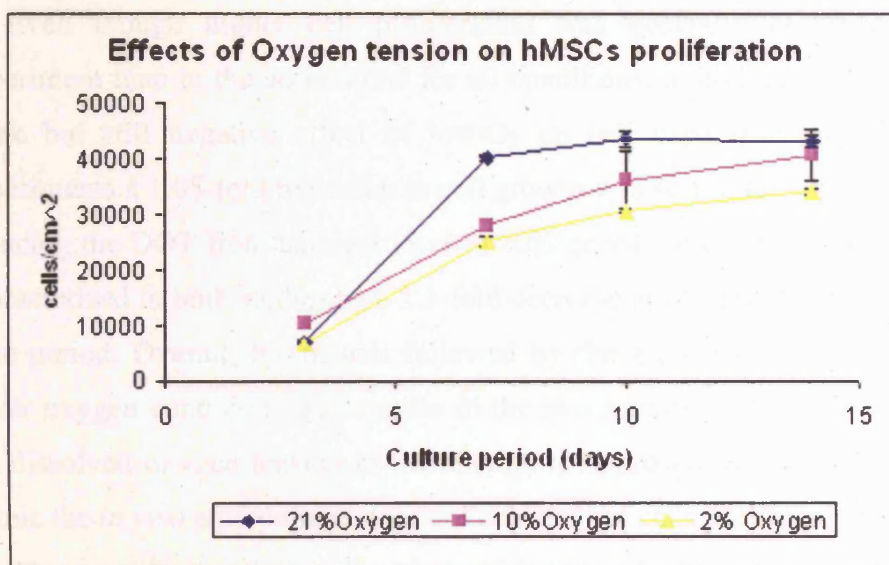


**Fig. 4.25:** Effects of dissolved oxygen tension (DOT) on hMSCs proliferation. hMSCs were expanded in non-coated plates, in low-glucose DMEM medium supplemented with 10% FBS and 1ng/ml bFGF. The cells were incubated at 5%CO<sub>2</sub>, 37°C and either 21% DOT (standard culture condition, —●— line), or 10% DOT (—■— line), or 2% DOT (—▲— line). Data are presented as means  $\pm$  s.e. of three independent measurements (please see section 2.6.9).

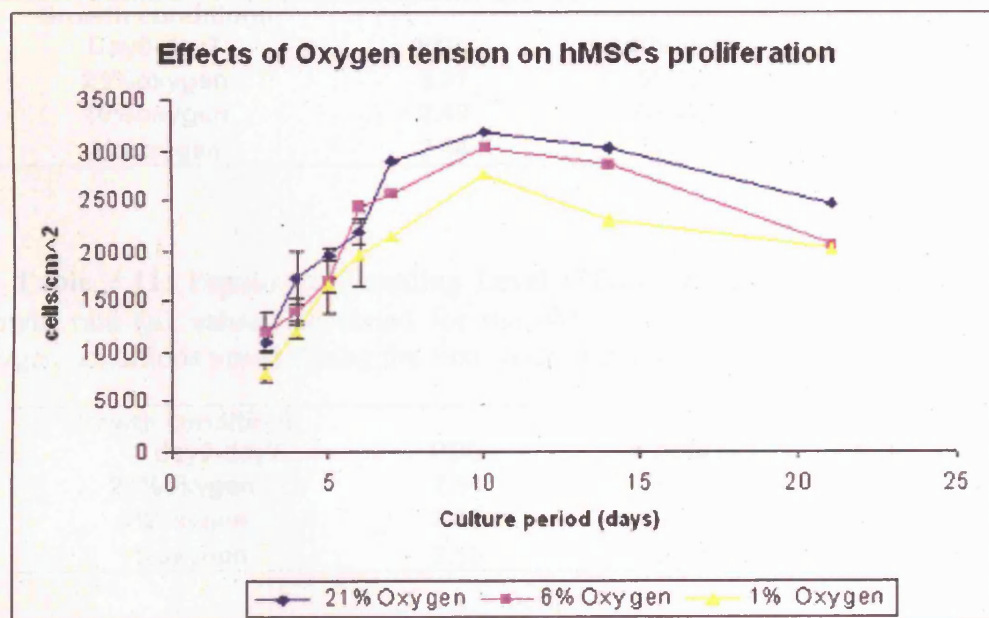


**Fig. 4.26:** Impact of dissolved oxygen tension (DOT) on hMSCs proliferation. hMSCs were cultured in non-coated plates, in low-glucose DMEM medium supplemented with 10% v/v FBS and 1ng/ml bFGF. The cells were incubated at 5%CO<sub>2</sub>, 37°C and either 21 % DOT (standard culture condition, —●— line), or 6 % DOT (—■— line) or 1 % DOT (—▲— line). Data are presented as means  $\pm$  s.e. of three independent measurements (please see section 2.6.9).

Even though higher cell proliferation was generally observed in the first experiment than in the second one for all conditions, in both studies the same rather weak but still negative effect of low-O<sub>2</sub> on cell expansion was noted. In both experiments a 1.05-fold reduction in cell growth was seen after 2 weeks in culture by reducing the DOT from ambient level to 10% or 6%, whereas hypoxic cultures were characterized in both studies by a 1.3-fold decrease in cell proliferation over the same time period. Overall, the pattern followed by the growth kinetics curves under the lower oxygen conditions was similar in the two studies, and indicated that reducing the dissolved oxygen tension in the attempt to approach the physiologic values and mimic the *in vivo* environment does not enhance the cells proliferative capacity.

These results correlate well with the population doubling time and the cell growth rate values obtained for both studies, and shown in table 4.10 and table 4.11.

**Table 4.10:** Population Doubling Level (PDL), Doubling Time (Td) and cell growth rate ( $\mu$ ) values obtained for hMSCs expanded in the three dissolved oxygen tension conditions tested during the first week of culture.

Growth conditions Day0-day7	PDL	Td(hours)	$\mu$ (hours <sup>-1</sup> )
21%oxygen	3.01	55.79	0.012
10%oxygen	2.49	67.42	0.010
2%oxygen	2.34	71.89	0.009

**Table 4.11:** Population Doubling Level (PDL), Doubling Time (Td) and cell growth rate ( $\mu$ ) values calculated for the hMSCs expanded in the three different oxygen conditions tested during the first week of culture.

Growth conditions day0-day7	PDL	Td(hours)	$\mu$ (hours <sup>-1</sup> )
21%oxygen	2.54	66.21	0.010
6%oxygen	2.36	71.30	0.010
1%oxygen	2.10	80.12	0.009

hMSCs expanded in the 21 % standard *in vitro* oxygen concentration were characterized by the lowest doubling time and the highest cell growth rate calculated during the first week of culture. On the other hand, the same cells expanded at the lower DOTs required longer times to double and proliferate. Even though this



dissimilarity was small, particularly for the second experiment where the difference was not statistically significant (p value = 0.048, Anova single factor test; table 4.11), a trend was observed for which by reducing oxygen levels in the culture settings the doubling times increased and concordantly the cell growth rates decreased.

As it is evident from the data shown in both table 4.12 and table 4.13, cell viability was not significantly affected by decreasing the oxygen level in the culture environment. For all three the oxygen levels investigated, high cell viability ( $\geq 98.47$ ) was retained after 13 days of *in vitro* expansion in the first experiment (please see table 4.12). In addition, only a slight decrease in cell viability was observed over time for cells maintained in culture for a longer time period in the second experiment (please see table 4.13), indicating no O<sub>2</sub> effect on cell viability.

**Table 4.12:** Percent cell viability values calculated for the cells cultured in the three different dissolved oxygen tension conditions under investigation at each harvesting time-point during the 13-day period of culture examined.

<b>Growth conditions</b>			
<b>21%Oxygen</b>	<b>day</b>	<b>average viability</b>	<b>std. err. (±%)</b>
	3	96.93	1.28
	7	98.22	0.86
	10	99.49	0.20
	13	98.47	0.63
<b>10%Oxygen</b>	<b>day</b>	<b>average viability</b>	<b>std. err. (±%)</b>
	3	96.37	0.92
	7	98.06	0.61
	10	99.03	0.86
	13	99.06	0.55
<b>2%Oxygen</b>	<b>day</b>	<b>average viability</b>	<b>std. err. (±%)</b>
	3	98.41	2.75
	7	97.84	0.96
	10	99.27	0.32
	13	99.02	0.50

**Table 4.13:** Percent cell viability values calculated for hMSCs cultured in the three different dissolved oxygen tension conditions tested at the beginning (day 3) and at the end (day 21) of the culture period.

Growth conditions			
21%oxygen	day	average viability	std. err. (±%)
	3	96.15	2.03
	21	90.97	2.94
6%oxygen	day	average viability	std. . (±%)
	3	96.83	0.25
	21	92.01	1.51
1%oxygen	day	average viability	std. err. (±%)
	3	96.63	2.94
	21	90.67	2.71

hMSCs maintained in either ambient or low (1-10%) oxygen were essentially identical as viewed by phase contrast microscopy. Individual subcultured cells appearing as adherent, fibroblast-like healthy cells were similar to one another in morphology and size regardless of the oxygen condition (please see figures 4.27 and 4.28).

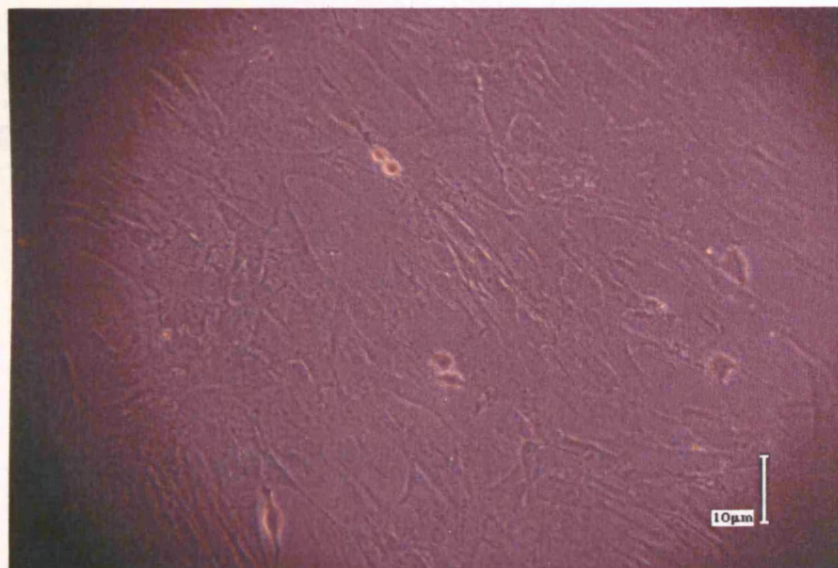


**Fig. 4.27:** Morphology of hMSCs expanded in the traditional 21% Dissolved Oxygen Tension.

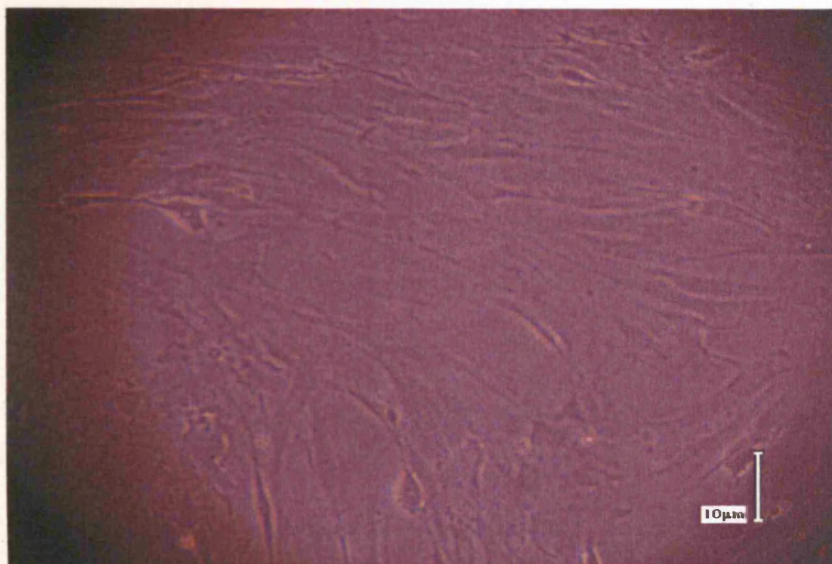


**Fig. 4.28:** Morphology of hMSCs expanded in 2% Dissolved Oxygen Tension condition.

As it is shown in figure 4.29 and figure 4.30, in line with the positive effect of high DOT on cell proliferation rate and cell density, hMSCs expanded in the traditional 21 % oxygen condition were characterised by a more intense metabolic activity, as compared to cells maintained in lower oxygen conditions. Interestingly, in both studies the positive effect of DOT on cell metabolism appeared to be concentration-dependent, the metabolic activity was the lowest for cells maintained in hypoxic (2 % or 1% oxygen) conditions.

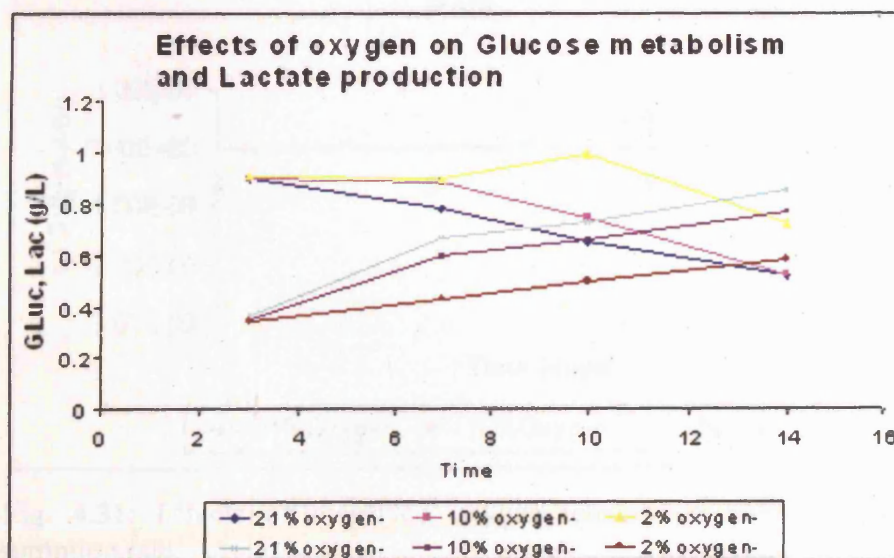


**Fig. 4.29:** Impact of dissolved oxygen tension on hMSCs metabolic activity.



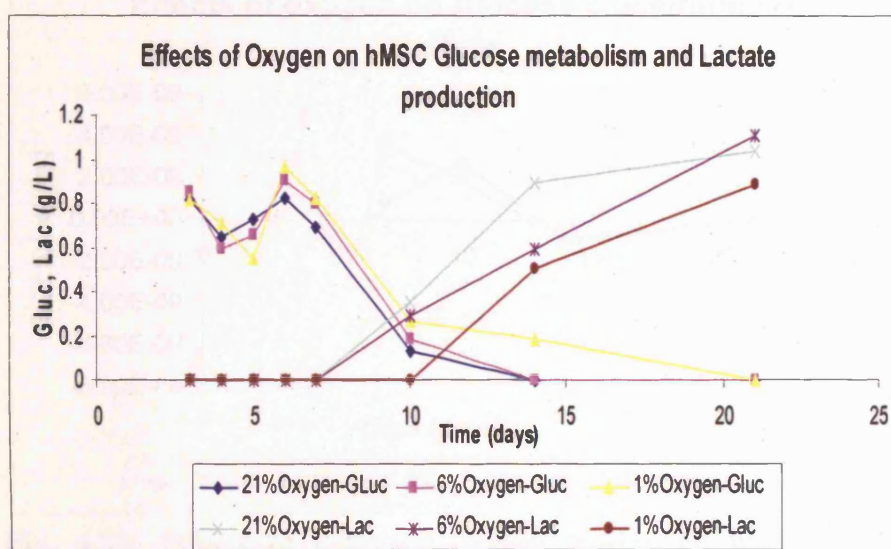


**Fig. 4.30:** Effects of dissolved oxygen tension on hMSCs metabolic activity. The cells were cultured in either 21 % or 6 % or 1 % dissolved oxygen tensions for 21 days.

Specific glucose consumption rate data are presented in figure 4.31 and figure 4.32. Interestingly, cells expanded in the ambient (21%) oxygen condition seemed to be characterised by a significant increase in GCR (g/cell/hour) during the last 4 days in culture.

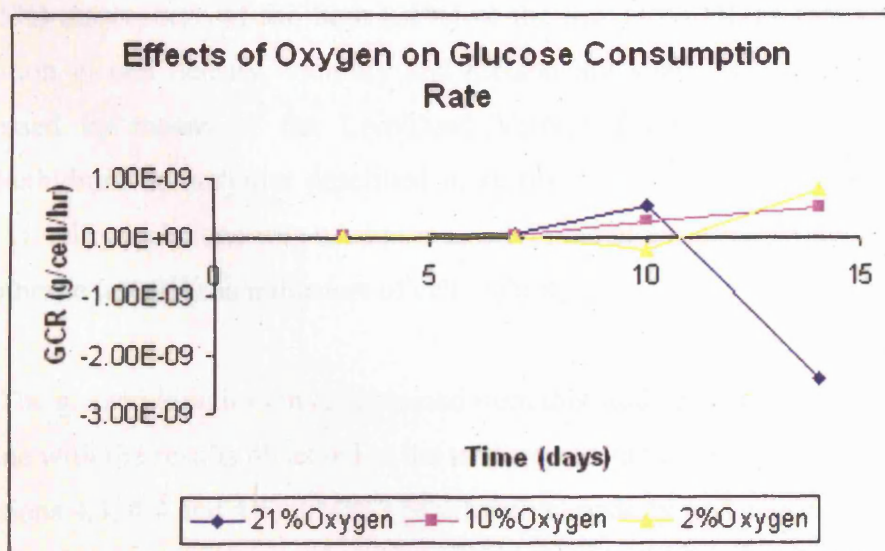


**Fig. 4.31:** Effects of dissolved oxygen tension on hMSCs specific glucose consumption rate.

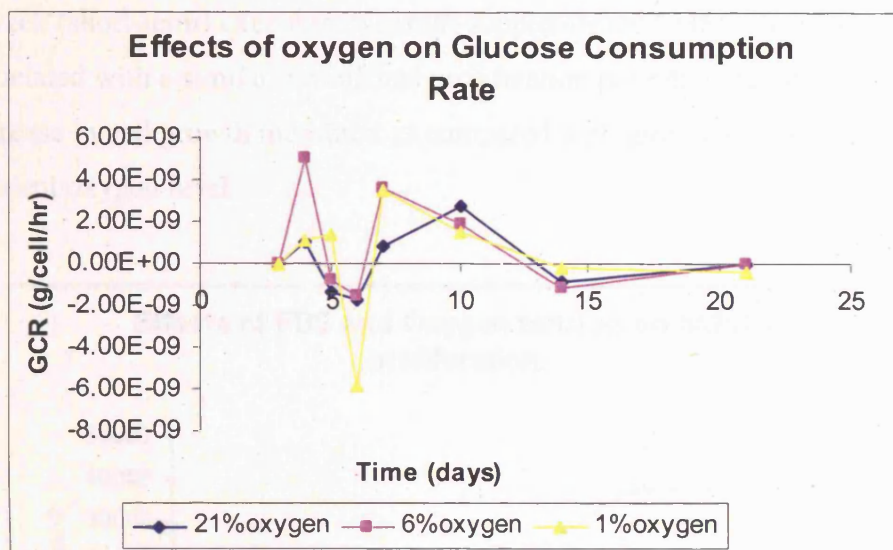


**Fig. 4.32:** Effects of dissolved oxygen tension on hMSCs specific glucose consumption rate. The cells were cultured in either 21% or 6% or 1% dissolved oxygen tensions for 21 days.

#### 4.8.2 Combined effects of dissolved oxygen tension (DOT) and Fetal Bovine Serum (FBS) on hMSCs proliferation and metabolism

In order to evaluate the combined effects of high and low dissolved oxygen tension and FBS-supplementation during *in vitro* expansion, hMSCs were cultured in either complete DMEM or serum-free DMEM for two weeks under a humidified (>95%) atmosphere of the high (21%) or the low (1%) DOTs (5% CO<sub>2</sub> in air). In addition to cell density, viability and metabolism analyses, the cell samples were assessed by means of the Live/Dead Viability/Cytotoxicity assay with calcein AM/ethidium homodimer described in section 2.6.6. This two-colour fluorescence cell viability technique was used to measure intracellular esterase activity and plasma membrane integrity as indicators of cell viability.

The growth kinetics curves obtained from this study are presented in figure 4.33. In line with the results observed in the studies presented in the previous sections (sections 4.3, 4.4 and 4.6), hMSCs proliferative capacity was significantly enhanced by culture in FBS-supplemented medium. Regardless of the dissolved O<sub>2</sub> tension maintained over the 14-day period of culture, serum-free culture did not allow cell growth. In addition, and in accordance with the results shown above (section 4.8.1),



2-week (short-term) exposure of serum-supplemented hMSCs to 1 % oxygen was associated with a similar diminished proliferation potential, being 1.2-fold the decrease in cell growth measured as compared with growth of cells expanded in ambient oxygen level.

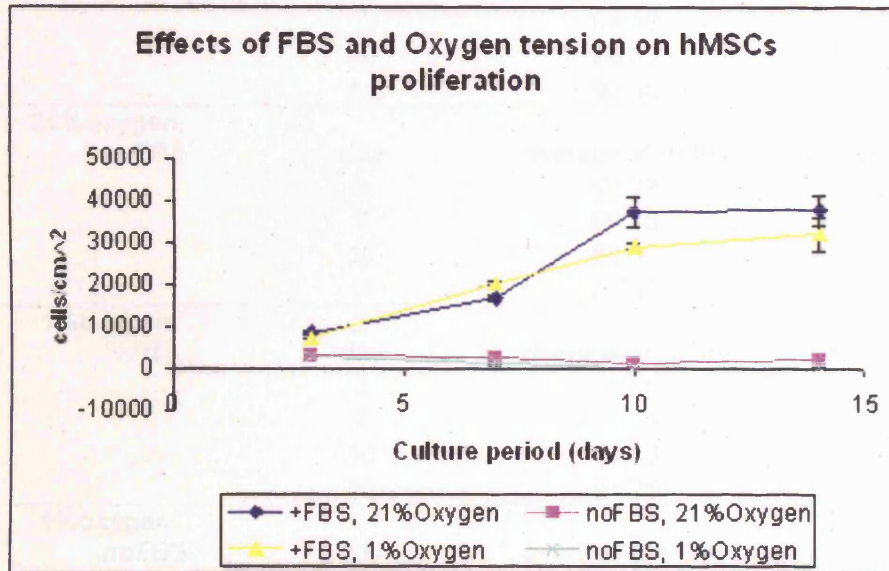


**Fig. 4.33:** Effects of dissolved oxygen tension (DOT) on hMSCs proliferation in serum-free and 10% serum culture conditions. hMSCs were cultured in non-coated plates, in low-glucose DMEM medium supplemented with 1ng/ml bFGF. The cells were incubated in 5%CO<sub>2</sub>, 37°C incubators with 21%O<sub>2</sub> level (10%serum standard culture condition = —◆— line; serum-free condition = —■— line) or 1%O<sub>2</sub> level (10%serum or serum-free = —▲— and —×— lines respectively). Data are presented as means +/- s.e. of three independent measurements (please see section 2.6.9).

These data were confirmed by the cell viability measurements obtained with the trypan blue dye exclusion assay and presented in table 4.14. High cell viability (>91%) was maintained over the 2-week period in serum-supplemented cultures, whereas serum-deprivation resulted in important cell death over time. Interestingly, this phenomenon was particularly evident and significant for serum-free cells expanded in hypoxic (1% O<sub>2</sub>) condition, for which cell viability measured 14 days after plating was reduced to 55%.

**Table 4.14:** Cell viability values calculated for hMSCs cultured in all the different conditions tested at each harvesting time-point during the 13-day period of culture examined.

<b>Growth conditions</b>			
<b>21%oxygen, +FBS</b>	<b>day</b>	<b>average viability</b>	<b>std. err. (±%)</b>
	3	92.74	1.68
	7	94.10	3.10
	10	98.05	20.32
	14	92.30	5.69
<b>21%oxygen, noFBS</b>	<b>day</b>	<b>average viability</b>	<b>std. err. (±%)</b>
	3	90.37	4.20
	7	90.48	16.50
	10	66.35	19.20
	14	82.93	1.84
<b>1%oxygen, +FBS</b>	<b>day</b>	<b>average viability</b>	<b>std. err. (±%)</b>
	3	88.00	5.43
	7	94.11	3.43
	10	99.23	57.24
	14	91.75	20.39
<b>1%oxygen, noFBS</b>	<b>day</b>	<b>average viability</b>	<b>std. err. (±%)</b>
	3	77.07	1.98
	7	73.82	16.14
	10	25.00	33.06
	14	55.56	18.86

Cell proliferation was determined for this study also by means of the MTT Cell Proliferation assay described in section 2.7, which confirmed the cell count/viability data obtained with hemacytometer and trypan blue dye exclusion assay described above. These data are shown in figure 4.34. The highest formazan absorbance values (index of mitochondria activity observable only for living and functional cells) were measured for serum-supplemented cells. FBS permitted significant cell growth over time, particularly in ambient oxygen level: the increase in absorbance readings measured from the first (day 2) and the last measurements (day 13) was 2.9-fold for cells expanded in traditional (21 %) oxygen settings, and 2.6-fold for cell expansion performed in hypoxic (1 %) condition.

Also the ambient (21 %) dissolved O<sub>2</sub> tension seemed to have a positive influence on cell proliferation, and this effect was particularly noticeable and significant during the second week of culture. Absorbance readings taken from high oxygen cultures at

day 9 and day 13 were in fact approximately 1.3-fold higher than the measurements detected for 1 % oxygen cells.

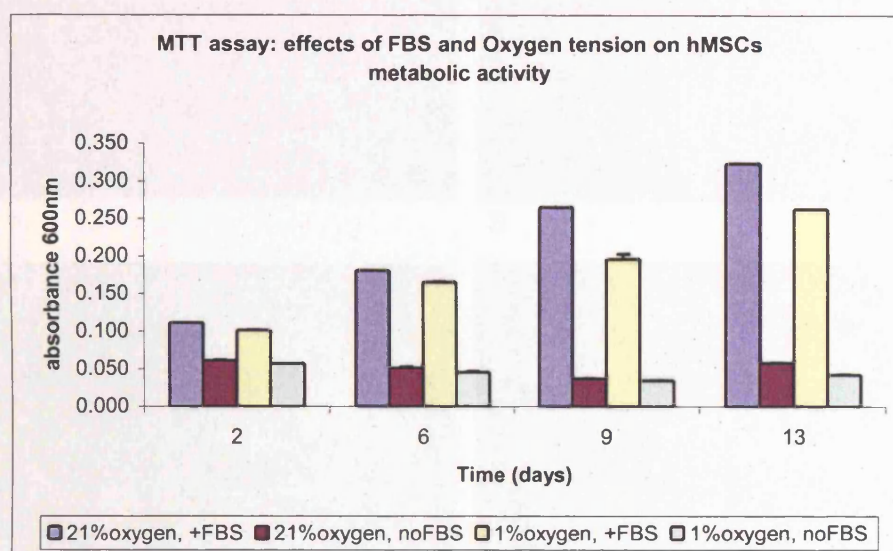


**Fig. 4.34:** Cell metabolic activity measured by means of the MTT Cell Proliferation assay. Data are presented as means  $\pm$  s.e. of three independent measurements.

Cell proliferation data were also confirmed in this study by the evaluation of the hMSCs culture with both phase contrast microscope and Live/Dead cytotoxicity assay. Photographs at the phase contrast and the confocal microscopes were taken at day 6 of culture. Cells expanded in 10% serum-supplemented growth medium at 21%  $O_2$  level appeared as healthy adherent, spindle-shaped cells at phase contrast microscopy analysis (please see figure 4.35 a). After treatment with the calcein AM/ethidium homodimer dyes provided with the Live/Dead Viability/Cytotoxicity assay, these same cell samples revealed at the confocal microscope the presence of intact, elongated cells displaying intense green fluorescence along their entire length (figure 4.35 c). No red fluorescence from ethidium homodimer could be detected in any serum-supplemented ambient oxygen cells, indicating that under these conditions hMSCs retain their membrane integrity.



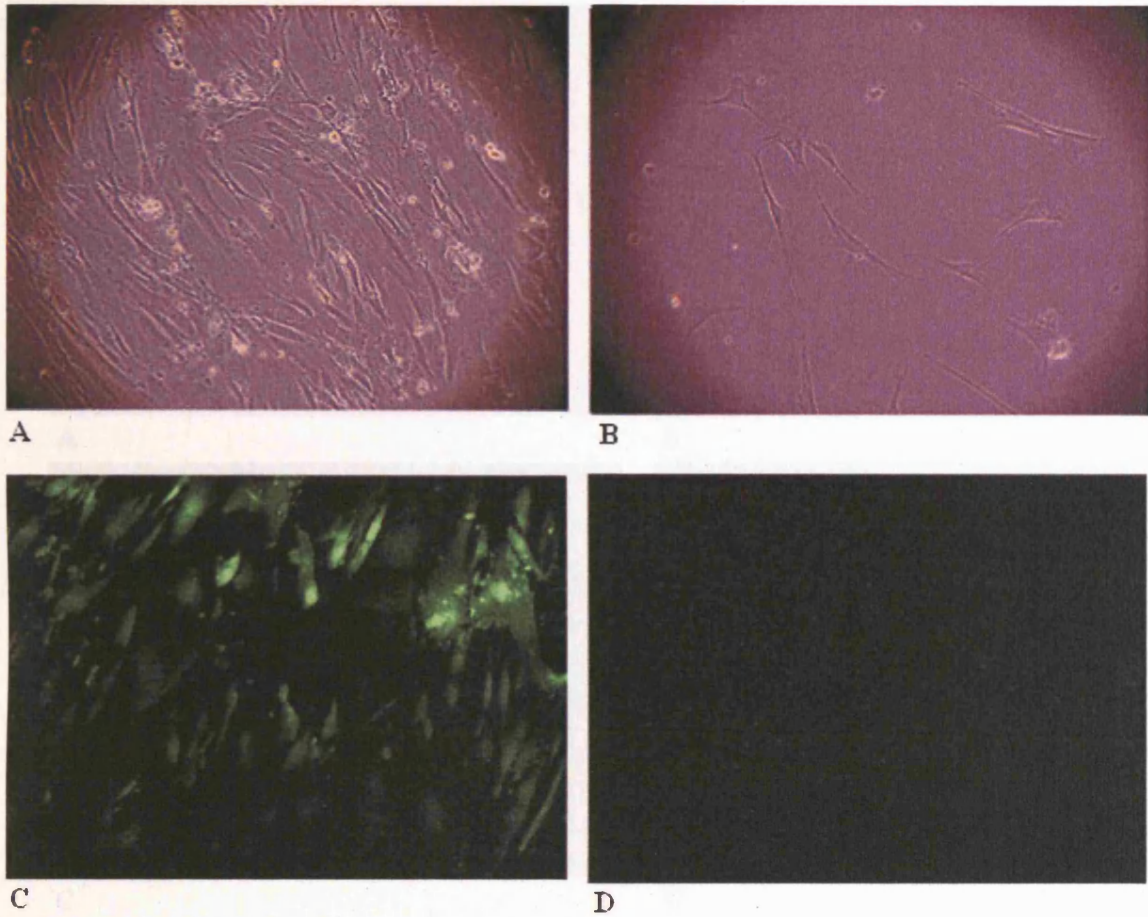


**Figure 4.35:** Photographs taken for cells maintained at 21% DOT, with or without serum. The photographs were taken at day 6 of culture with the phase contrast microscope (**A** and **B**) and with the confocal microscopes (**C** and **D**) after treatment with the calcein AM/ethyidium homodimer dyes.

**A)** 21% oxygen, +FBS, day 6, phase contrast microscope; **B)** 21% oxygen, no FBS, day 6, phase contrast microscope; **C)** 21% oxygen, +FBS, day 6, confocal microscope; **D)** 21% oxygen, no FBS, day 6, confocal microscope.

Similar healthy morphology and intense green fluorescence were observed for serum-supplemented cells grown in hypoxic (1% oxygen) condition. However, in this case viable cells were visible in lower numbers, while a weak red fluorescence was noticeable at the confocal microscopy analysis (please see figure 4.36 c). These results indicate that hypoxia might be associated with cytotoxicity, a phenomenon that has already been observed for hepatocytes [Khan and O'Brien, 1995].

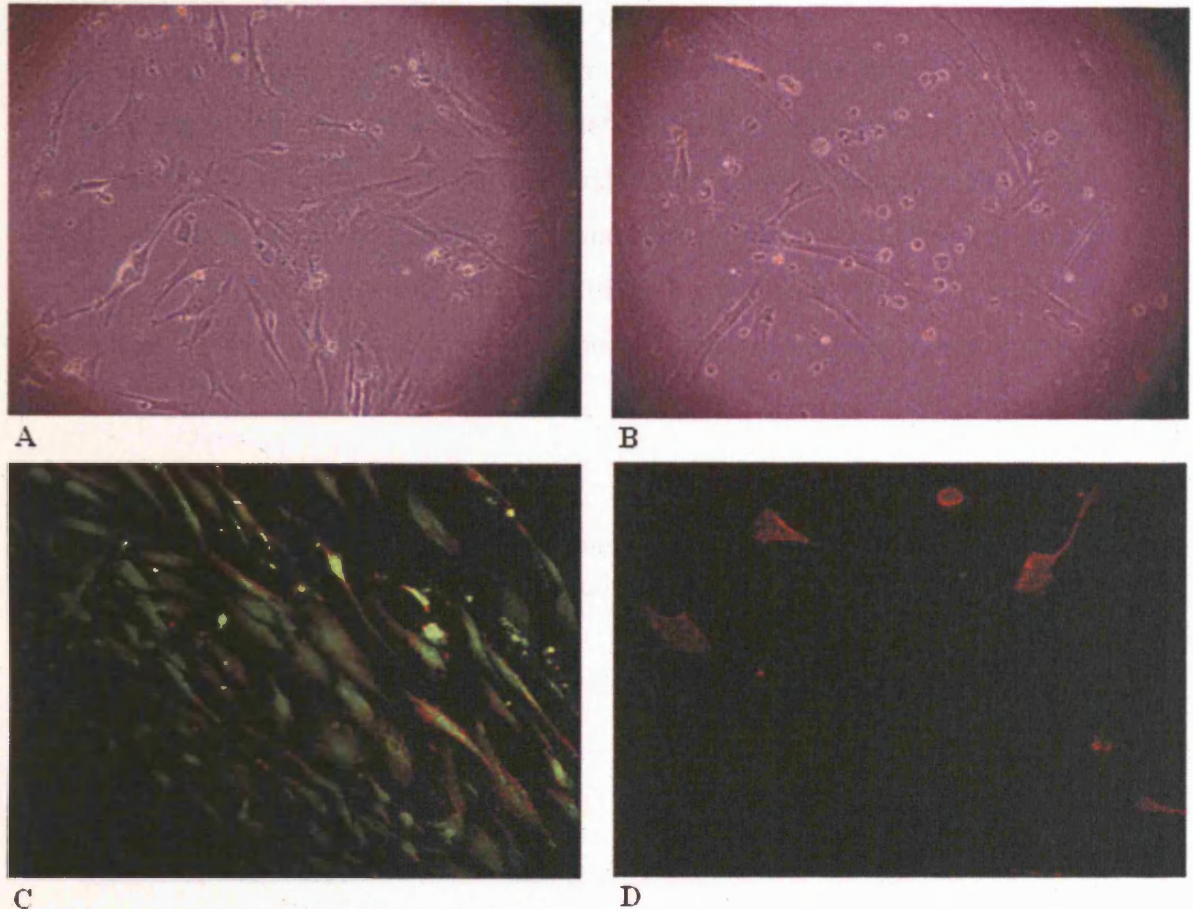


**Figure 4.36:** Photographs taken for cells maintained at 1% DOT, with or without serum. The photographs were taken at day 6 of culture with the phase contrast microscope (**A** and **B**) and with the confocal microscopes (**C** and **D**) after treatment with the calcein AM/ethidium homodimer dyes.

**A)** 1% oxygen, +FBS, day 6, phase contrast microscope; **B)** 1% oxygen, no FBS, day 6, phase contrast microscope; **C)** 1% oxygen, +FBS, day 6, confocal microscope; **D)** 1% oxygen, no FBS, day 6, confocal microscope.

In marked contrast, in all serum-free samples examined only very few adherent and elongated cells were visible at inverted light microscope (figure 4.35 b and figure 4.36 b), most of the cells having been removed with medium refreshments after detachment from the culture surface. Green calcein fluorescence was absent from all serum-free samples, confirming very low cell viability in this culture condition (please see figure 4.35 d and figure 4.36 d). Diffuse red fluorescence of low intensity was noticed in the cultures maintained in serum-free and hypoxic condition (figure 4.36 d), revealing damaged plasma membranes in these cell samples.



The doubling time and cell growth rate values determined for hMSCs expanded in high and low oxygen with or without serum are shown in table 4.15. These values are in accordance with the growth kinetic data described above and with the results described in the previous sections. In standard serum-supplemented cultures, 21 % DOT cells displayed lower doubling time and higher cell growth rate values than cells cultured in hypoxic condition. The lack of cell growth in serum-free culture was confirmed by the (negative) doubling time and cell growth rate values (please see table 4.15).

**Table 4.15:** Population Doubling Level (PDL), Doubling Time (Td) and cell growth rate ( $\mu$ ) values calculated for the cells expanded in all the different conditions tested during the first 10 days of culture.

Growth conditions			
Day0-day10	PDL	Td(hours)	$\mu$ hours <sup>-1</sup>
21%oxygen,+FBS	2.898	82.81	0.0084
21%oxygen,-FBS	-2.017	-118.97	-0.0058
1%oxygen,+FBS	2.537	94.59	0.0073
1%oxygen,-FBS	-3.892	-61.67	-0.0112

In 10% serum-supplemented samples, high DOT seemed to permit a slightly more intense metabolic activity as compared to low DOT (figure 4.37). However, in serum-free condition hMSCs appeared to be metabolically inactive, regardless of the oxygen level employed during *in vitro* cell expansion (figure 4.38).

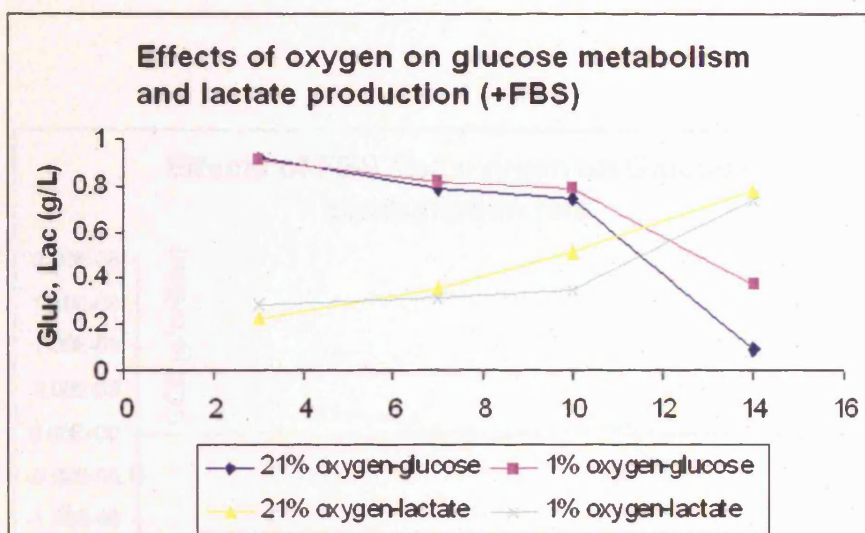


**Fig. 4.37:** Effects of dissolved oxygen tension on hMSCs metabolic activity. Cells were cultured in either 21 % or 1 % dissolved oxygen tension in FBS-supplemented low-glucose DMEM medium.

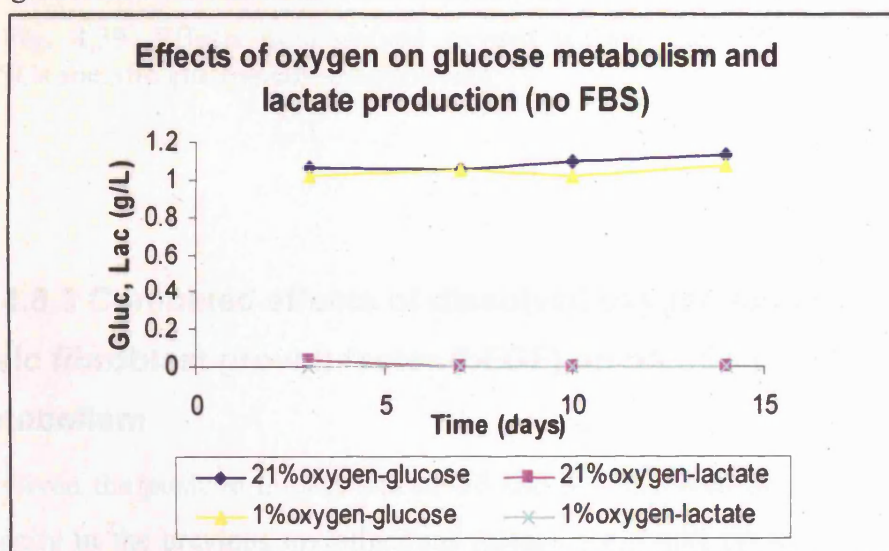


**Fig. 4.38:** Effects of dissolved oxygen tension on hMSCs metabolic activity. Cells were cultured in either 21% or 1% dissolved oxygen tensions in serum-free low-glucose DMEM medium.

According to the data presented in figure 4.39, there appeared to be no significant difference in specific glucose consumption rate (g/cell/hour) for hMSCs cultured for up to 10 days in the different FBS and oxygen conditions. However, cells expanded in serum-supplemented medium at the ambient (21%) oxygen experienced a significant increase in GCR over the last 4 days in culture, whereas cells maintained in hypoxic conditions in serum-free DMEM medium appeared to be characterised by a significant decrease in GCR over the same culture period (day10-day14).

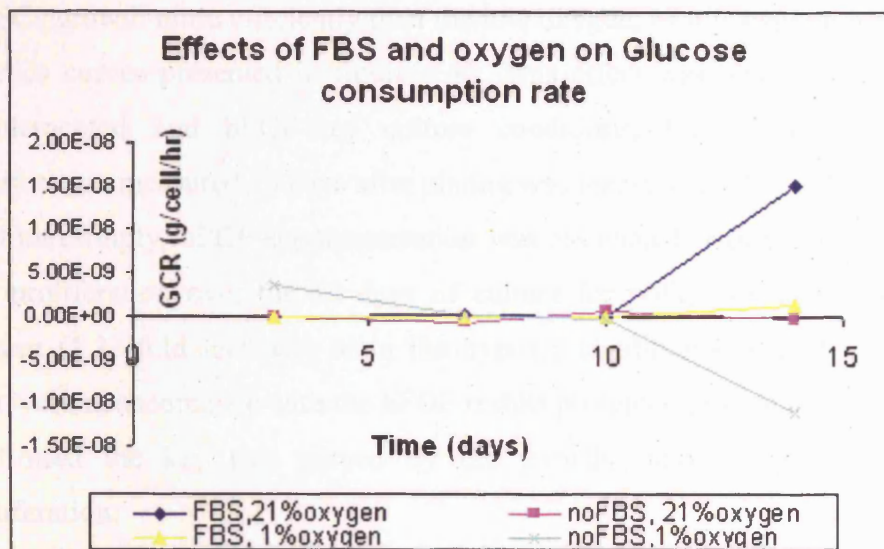


**Fig. 4.39:** Effects of dissolved oxygen tension and FBS-supplementation on hMSCs specific glucose consumption rate.

#### 4.8.3 Combined effects of dissolved oxygen tension (DOT) and basic fibroblast growth factor (bFGF) on hMSCs proliferation and metabolism

Given the positive impact that bFGF had demonstrated on hMSCs proliferative capacity in the previous investigations (please see results presented in section 4.5), the combined effects of dissolved oxygen tension and bFGF-supplementation were also evaluated.

For this purpose, hMSCs were cultured in either complete (bFGF-supplemented) DMEM or in the same DMEM medium formulated without bFGF. The cultures were maintained for two weeks in two separate incubators (>95% humidity, 5% CO<sub>2</sub> in air), one equipped with ambient (21%) and the other with low (1%) DOT. Growth kinetics, cell doubling time and viability were assessed as for the previous experiments. In addition, in this study mitochondrial activity and cell apoptosis were determined with the Guava Nexin assay, following the protocol described in section 2.6.8. This technique was performed in order to identify and distinguish in our samples apoptotic cells from dead cells and debris.



Once again, the high DOT maintained during *in vitro* expansion supported hMSCs growth more efficiently than the low oxygen, as it is evident from the growth kinetics curves presented in figure 4.40. This effect was observed for both bFGF-supplemented and bFGF-free culture conditions, for which increase in cell proliferation measured 13 days after plating was respectively 1.3 and 1.4-fold.

Interestingly, bFGF-supplementation was associated with significantly increased cell proliferation over the 13 days of culture for both cells expanded in ambient oxygen (1.33-fold increase) or in the hypoxic condition (1.4-fold increase). These data were in accordance with the bFGF results presented previously (section 4.5), and confirmed the key role played by the growth factor in the hMSCs *in vitro* proliferation.

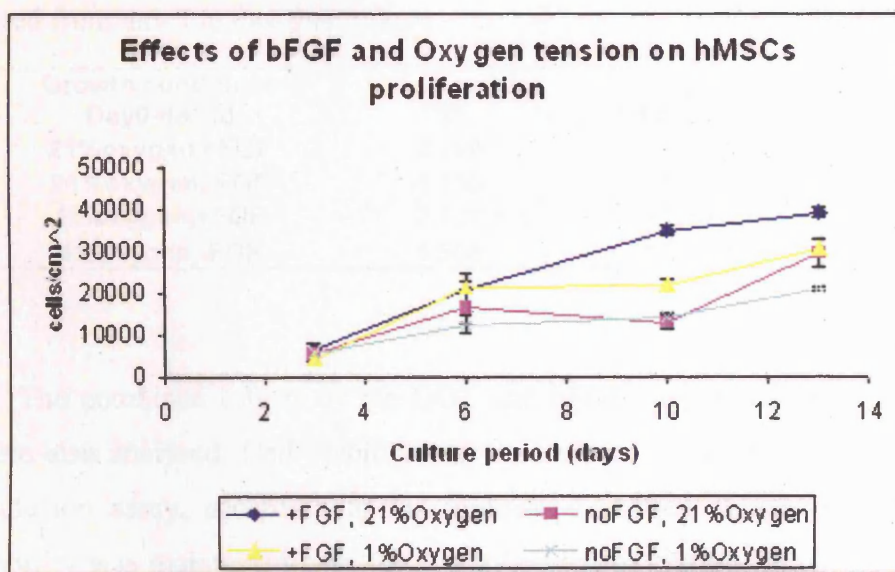


**Fig. 4.40:** Growth kinetics curves obtained for hMSCs maintained for a 13-day period under different dissolved oxygen tension (DOT) conditions, with either bFGF-supplemented or bFGF-free growth medium. hMSCs were cultured in non-coated plates, in low-glucose DMEM medium supplemented with 10 % Fetal Bovine Serum. The cells were maintained in 5% CO<sub>2</sub>, 37°C incubators with either 21 % O<sub>2</sub> level (with bFGF, standard culture condition, represented by the —◆— line; bFGF-free condition, represented by the —■— line) or 1% O<sub>2</sub> level (with or without bFGF, —▲— line and —×— line respectively). Data are presented as means +/- s.e. of three independent measurements (please see section 2.6.9).

The population doubling and growth rate values obtained from this investigation confirmed the positive effect of the basic Fibroblast Growth Factor. bFGF-supplementation allowed the cells to double faster both in high and low oxygen regimes, as demonstrated by the Td values shown in table 4.16. The effect of the growth factor was particularly important in ambient oxygen condition. In accordance with the data described in the previous sections (4.8.1 and 4.8.2), the lowest doubling time and highest cell growth rate values were measured for cells grown at the standard 21 % DOT in complete DMEM medium after bFGF-supplementation. Interestingly, even though doubling times were lower for cells in ambient oxygen, there appeared not to be a significant difference in cell growth rates for bFGF-deprived cells grown in either ambient or hypoxic conditions.

**Table 4.16:** Population Doubling Level (PDL), Doubling Time (Td) and cell growth rate ( $\mu$ ) values calculated for hMSCs expanded in all the different conditions tested from day 3 to day 6 of culture.

<b>Growth conditions Day0-day10</b>	<b>PDL</b>	<b>Td(hours)</b>	<b><math>\mu</math> (hours<sup>-1</sup>)</b>
<b>21%oxygen,+FGF</b>	2.799	85.7	0.008
<b>21%oxygen,-FGF</b>	1.350	177.8	0.004
<b>1%oxygen,+FGF</b>	2.127	112.8	0.006
<b>1%oxygen,-FGF</b>	1.506	159.3	0.004

The combined effects of the DOT and bFGF-supplementation on cell viability were also analysed. Cell viability was assessed as usual using the trypan blue dye exclusion assay, according to the protocol described in section 2.6.3. High cell viability was maintained over the 13-day period of culture for all the three different oxygen conditions tested (please see table 4.17). As in all the studies described above (section 4.8.1 and 4.8.2), regardless of DOT, the cells did not experience any dramatic loss in cell viability over time. In addition, cell viability was not affected by supplementation of the growth medium with bFGF, as the percentage of viable hMSCs was over 90.05 % for all culture conditions, regardless of bFGF-supplementation. These results confirmed that even though bFGF may promote considerably hMSCs viability in serum-free cultures (please see results described in tables 4.3 and 4.6), this effect is not so relevant for cells expanded in serum-supplemented DMEM.

**Table 4.17:** Percent cell viability values calculated for hMSCs cultured in all the different conditions tested at the beginning (day 3) and at the end (day 13) of the culture period.

<b>Growth conditions</b>			
<b>21%oxygen, +FGF</b>	<b>day</b>	<b>average viability</b>	<b>std. err. (±%)</b>
	3	89.67	3.45
	13	92.42	2.49
<b>21%oxygen, noFGF</b>	<b>day</b>	<b>average viability</b>	<b>std. err. (±%)</b>
	3	91.43	3.09
	13	94.22	1.01
<b>1%oxygen, +FGF</b>	<b>day</b>	<b>average viability</b>	<b>std. err. (±%)</b>
	3	82.92	3.45
	13	90.05	2.39
<b>1%oxygen, noFGF</b>	<b>day</b>	<b>average viability</b>	<b>std. err. (±%)</b>
	3	92.09	8.60
	13	92.33	2.71

At the end of the 13-day culture period under examination the Nexin assay, which is based upon the Guava EasyCyte system, was performed in order to investigate the effects of both DOT and bFGF-supplementation on hMSCs' apoptosis. The protocol for the Guava Nexin assay is described in detail in section 2.6.8, and the results from this analysis are presented in table 4.18. It must be noted that no significant difference was detected with this technique in percentages of viable cells for all oxygen and bFGF conditions, and high cell viability (>97%) was observed in all conditions over the 13-day period of culture examined (please see table 4.18). In the same way, similar percentages of early apoptotic (0.2-0.4%) and late apoptotic (1.1-1.4%) cells were measured for all cell samples, regardless of the dissolved oxygen tension in culture settings or the bFGF presence in the growth medium. These data demonstrated that, even though hMSCs incubated under hypoxia had decreased rates of proliferation, there was no increase in apoptosis for these samples. The results were consistent with previous reports [Salim *et al.*, 2004, Hung *et al.*, 2007] but not with other published studies [e.g. Fink *et al.*, 2004; Lennon *et al.* 2001]. The conflicting results may in part be explained by the variation in the DOT, the duration of hypoxic culture and the system used in each study to control the oxygen level [Hung *et al.*, 2007].



**Table 4.18:** Influence of dissolved oxygen tension and bFGF-supplementation on hMSCs viable, early apoptotic and late apoptotic cell populations, as obtained with the Nexin cell apoptosis assay performed on the Guava EasyCyte system. Data are presented for measurements taken at the end of the 13-day culture period.

Growth conditions	Average viable cells	Standard error	Average early apoptotic cells	Standard error	Average late apoptotic cells	Standard error
21%oxygen, +FGF	97.00	0.523	0.35	0.159	1.36	0.184
21%oxygen, noFGF	97.11	0.137	0.37	0.053	1.10	0.094
1%oxygen, +FGF	97.98	0.554	0.22	0.106	1.19	0.486
1%oxygen, +FGF	97.78	0.205	0.28	0.059	1.17	0.225

As it is shown in figure 4.42, cells expanded in the absence of bFGF appeared to be unable to metabolise any glucose or produce any lactate, and this metabolic inactivity was observed for both cell samples expanded in high or low DOTs. On the other hand, bFGF-supplementation seemed to permit a slightly higher metabolic activity, and in this case cells maintained in high DOT seemed to be more metabolically active than cells expanded in hypoxic conditions (figure 4.41).

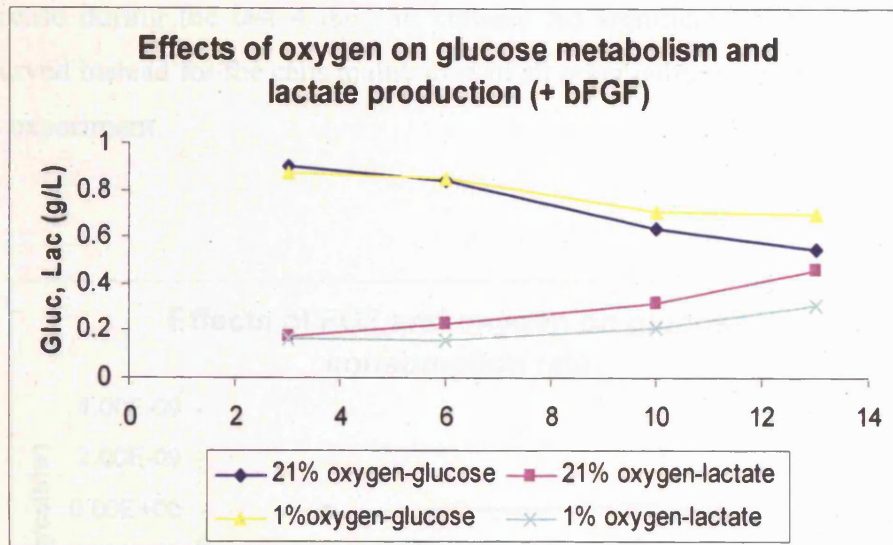


**Fig. 4.41:** Effects of dissolved oxygen tension on hMSCs metabolic activity. The cells were cultured in either 21 % or 1 % dissolved oxygen tensions in bFGF-supplemented low-glucose DMEM medium.

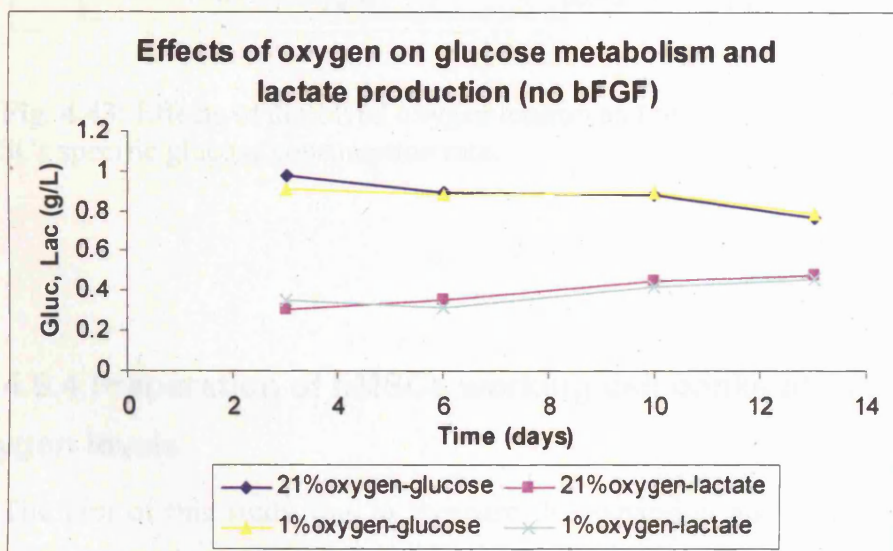


**Fig. 4.42:** Effects of dissolved oxygen tension on hMSCs metabolic activity. Cells were cultured in either 21 % or 1 % dissolved oxygen tensions in bFGF-free low-glucose DMEM medium.

The specific glucose consumption rate data are presented in figure 4.43. These data are quite difficult to interpret. However, it can be noted that cells expanded in hypoxic condition, in bFGF-free medium appeared to be characterised by an increase in GCR from day6 to day10 in culture, whereas GCR for these cells seemed to

decrease during the last 4 days in culture. No significant difference in GCR was observed instead for the cells maintained in all other culture conditions investigated in this experiment.

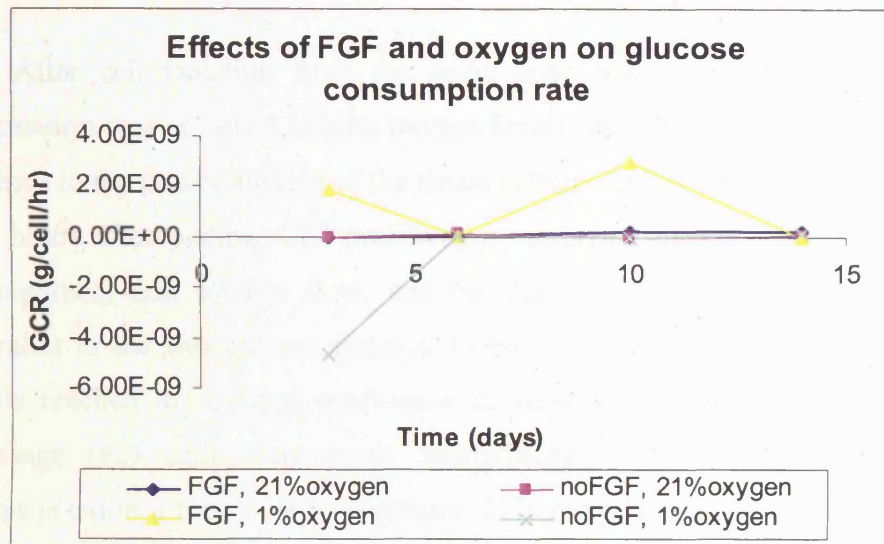


**Fig. 4.43:** Effects of dissolved oxygen tension and bFGF-supplementation on hMSCs specific glucose consumption rate.

#### 4.8.4 Preparation of hMSCs working cell banks at 21% and 1% oxygen levels

The aim of this study was to compare the expansion and behaviour of human mesenchymal stem cells maintained in monolayer culture under two different dissolved oxygen tensions (i.e. 21 % and 1 %). In order to do so, after cell isolation from the same bone marrow sample by discontinuous density gradient centrifugation, two hMSC cultures were performed in parallel in T75 flasks that were maintained throughout the whole experiment in the two different DOTs selected. The standard low-glucose “complete DMEM” formulation was used for the cell expansion for both the oxygen cultures. Once a sufficient number of cells was reached within the T75 flasks, two separate working cell banks were prepared for each of the two different DOT conditions under investigation. The resulting cells were transferred and

maintained in liquid nitrogen (-196°C) for long-term storage, in order to supply material for future studies investigating further the effects of DOT on MSCs proliferation and function in culture. The protocols followed for the cell isolation and the creation of the working cell banks are described in sections 2.1.1 and 2.1.4 respectively.

After cell isolation from the same bone marrow source, successful hMSCs expansion was achieved in both oxygen levels. In both conditions the cells started to adhere to the plastic surface of the tissue culture vessels and began to elongate within 48 hours after plating. Cell proliferation occurring in both oxygen conditions was comparable and equally slow, and the desired 80 % confluence was reached in parallel in the two culture systems. In both oxygen conditions the primary culture cells reached the desired confluence 22 days after plating. In both cases, second passage (p2) cells were again approximately 80 % confluent and ready for trypsinisation after 11 days in culture. 21% oxygen and 1% oxygen-cells displayed similar cell growth rates ( $\mu$ ) values (0.0022 and 0.0021 hours<sup>-1</sup> respectively) and doubling time (Td) values (318.3 and 329.9 hours respectively). Both oxygen cell types displayed also similar morphology, as assessed by the microscopic evaluation of the culture samples. In both cases, the cells appeared to have a spindle-shape fibroblast-like morphology, characteristic of healthy bone marrow-derived MSCs (data not shown).

Despite the extremely high doubling time values measured, the microscopic evaluation of the samples, performed every other day during the whole culture period, revealed over time the presence of healthy, elongated spindle-like cells adhering to the plastic surface of the tissue flasks. In addition, successful cell expansion leading to cell numbers sufficient for the preparation of a working cell bank was achieved in both oxygen conditions. In conclusion, no discernable differences were noticed in the cell behaviour during this expansion procedure, indicating that oxygen level does not affect hMSCs proliferation capability and cell morphology in primary culture.

## **4.9 Conclusions on MSCs monolayer culture studies**

The increasing number of clinical protocols using hMSCs underscores the need for serum supplements other than Fetal Bovine Serum [Shahdadfar *et al.*, 2005]. As a result, supplementation of the cell culture medium with FBS was one of the principal parameters investigated in this study. In conclusions, this research substantiated the significant positive influence of FBS in promoting cell proliferation rate for MSCs derived from human bone marrow samples. Serum, which delivers important nutrients, proteins and growth factors to the culture system (please see section 1.5.2), resulted essential for cell survival and long-term cell expansion in *in vitro* monolayer conditions. Importantly, the 10 % v/v serum concentration traditionally employed in standard culture protocols, resulted the most appropriate for yielding highest cell densities and allowing hMSCs metabolic activity.

Preliminary studies were also conducted to define the optimal basal growth medium for hMSCs expansion, and low-glucose DMEM was chosen against the more expensive MesenCult medium because of its advantages in terms of number of cells generated after 12 days in serum-supplemented culture ( $12.5 \times 10^3$  cells/cm<sup>2</sup> versus  $8.25 \times 10^3$  cells/cm<sup>2</sup> counted in 10% serum-supplemented cultures).

Several serum-free media have also been investigated in a preliminary qualitative study whereby media effects were observed purely by means of inverted light microscopy. Interestingly, among all the formulations examined, UltraCulture (BioWhittaker), UltraDOMA Hybridoma (BioWhittaker) and Knockout D-MEM (Gibco) optimised media permitted survival and proliferation of attachment-dependent fibroblast-like cells resembling pure MSCs. Future studies could be performed to characterise the cell samples grown in these medium formulations and to prove whether these cultures retain all the unique and desirable features characteristic of unadulterated authentic stem cells.

The cytokines released in the MSCs' microenvironment appears to be an additional essential factor for proper development. Among all growth factors, Fibroblast Growth Factor, which is known to be an effective mitogen for a variety of cells of mesenchymal or neuroectodermal origin *in vitro* [Basilico and Moscatelli, 1992; Scherping *et al.*, 1997], demonstrated to play a key role in promoting hMSCs proliferation and activity. bFGF appeared to be able to significantly obstruct cell death in serum-free cell samples. In addition, in the standard 10% serum-

supplemented cultures, after 13 days, bFGF-addition resulted in a 1.9-fold increase in cell growth as compared to cells expanded in bFGF absence. Interestingly, the most remarkable positive influence of bFGF was observed in low (2%) serum concentration samples, for which the growth factor permitted a 4.2-fold cell growth increase over 13 days, as opposed to the 1.2-fold increase measured over the same time period for bFGF-free cells.

Also the culture surface properties investigated in this research were demonstrated to have a significant influence on hMSCs behaviour. Matrigel proved not to be a favourable coating surface for cell growth, leading to both significant cell death over time and metabolic inactivity. Its negative effect was noticed regardless of the serum concentration used for the medium supplementation. Moreover, the use of fibronectin-coated plates did not reveal any particular advantage as compared to the traditional non-coated plates frequently employed for tissue culture. Similar growth kinetics were observed for cells grown in fibronectin-coated or non-coated vessels in all serum conditions, and a similar increase in cell density (approximately 9-fold increase for 10% serum condition and 4.5-fold increase for 2% serum samples) was observed over 13 days in culture for both culture surfaces. Cell morphology and cell viability were also similar under these two coating conditions.

Finally, in this research several investigations were performed in order to elucidate the impact of oxygen levels on hMSCs expansion potential and metabolic activity. It has already been envisaged that among all tissue environmental factors affecting MSCs functionality and differentiation, perhaps the most important is oxygen level [Salim, 2004]. However, to date, studies focusing on mesenchymal stem cells responses to hypoxia have been inconclusive [Lennon *et al.*, 2001; Ma *et al.*, 2001]. Since in the bone marrow environment oxygen level is low, and normally ranging from 5.7 % to 7.1 % (40-50 mmHg) [Ishikawa and Ito, 1988; Grant and Smith, 1963; Harrison *et al.*, 2002], it was decided to test whether hypoxia can enhance proliferation and growth potential of MSCs isolated from human bone marrow samples. In conclusion, the results of these studies clearly demonstrated that the exposure of hMSCs to high (21%) dissolved oxygen tension (maintained by exposure to 5 %CO<sub>2</sub> in air) during *in vitro* expansion is beneficial for cell growth. On the other hand, exposure to low DOT during culture did not significantly improve the cells proliferation capacity. However, no significant treatment effect by DOT was found in the percentages of viable cells.

Overall, the best results, yielding highest cell growth kinetics (average  $38.9 \times 10^4$  cells/cm<sup>2</sup> counted after 13-14 days in culture), highest cell viabilities (average 96.08% +/-3.01% over 2-week culture), and lowest doubling times (average 58.36 hours calculated from day 0 to day 7) were derived from the combined use of the high DOT and serum-/bFGF-supplemented low-glucose DMEM medium and non-coated culture vessels. It was also demonstrated that hMSCs expanded for four subsequent passages in monolayer culture under these conditions appeared to retain their undifferentiated state and their ability to differentiate toward the phenotypes of fully mature adipocytes, osteocytes and chondrocytes.



## **5. Characterisation of alginate/cells constructs**

Following the studies establishing the growth kinetics of unencapsulated cells expanded in tissue flasks and microwell plates (described in chapter 4), interest was focused on investigating the growth of cells within alginate hydrogels. The optimal conditions of culture identified in monolayer, allowing cell viability and promoting cell proliferation, were employed for the growth of the alginate/cells constructs resulting after immobilisation of the cells in the alginate matrix. This chapter describes the results obtained from the characterisation of these constructs.

### **5.1 Alginate-GRGDY as scaffold for cell growth**

The ultimate research goal was the fabrication of alginate/hMSCs constructs suitable for use in the clinic. In order to do so, a cell adhesion site was first incorporated onto the alginate molecules to create a scaffold able to encourage cell adhesion and proliferation (please see results presented in chapter 3).

Sodium alginate is often used as a material for the encapsulation and immobilisation of a variety of cells for different applications, since, subject to diffusion limitations, cells can maintain viability within cross-linked alginate gels [Trivedi *et al.*, 2001; Park and Chang, 2000]. However, mammalian cells cannot interact with unmodified alginate gels [Smentana, 1993]; thus, the alginate surface chemistry is often modified to improve cellular functions (i.e. cell adhesion, spreading, migration and differentiation functions) [Saltzman, 2000]. Following incorporation of the RGD ligand sequence, alginate scaffolds encapsulating calvarial osteoblasts [Alsberg *et al.*, 2001], pre-adypocytes [Halberstadt *et al.*, 2002] and fibroblasts [Marler *et al.*, 2000] have shown encouraging results in *in vivo* studies. In addition, *in vitro* studies have shown that alginate covalently modified with the GRGDY pentapeptide has the potential to promote mouse skeletal myoblasts attachment and proliferation [Rowley *et al.*, 1999]. More recently it has also been demonstrated that human MSCs have the ability to adhere, elongate and retain high viability within alginate-GRGDY beads [Markusen *et al.*, 2006]. However, in these studies no hMSCs proliferation has been observed within these matrices.



Thus, studies were conducted in this research to investigate further the effects of non-derivatised alginate and alginate-GRGDY on cell behaviour and performance following the fabrication of constructs incorporating cells.

## **5.2 Culture and characterisation of cells in alginate constructs**

Several experiments were performed in order to evaluate cell behaviour and performance after immobilisation within either plain alginate or alginate-GRGDY 2-2.5 mm diameter beads. In addition to the bone marrow-derived hMSCs employed in the monolayer studies, human foreskin fibroblasts were also used for the fabrication of alginate/cells constructs. The fibroblasts (Karocell, Stockholm) were kindly provided by Dr. Stephen Minger, Wolfson Centre for Age-Related Diseases, King's College London. Following mixing of the alginate matrix with the cell suspension, gel beads were produced by extrusion of alginate/cells droplets into the  $\text{CaCl}_2$  cross-linking solution. The beads were cultured in 24-well non-coated plates in "complete low-glucose DMEM" (as defined in section 2.1.5.1) in a humidified 37°C incubator at 21% DOT, 5%  $\text{CO}_2$  (i.e. the optimal culture conditions identified in the monolayer studies). Following digestion with a trisodium citrate solution (please see section 2.5.5), the cell suspension was analysed at selected time-points with haemocytometer (please see section 2.6.2) and trypan blue exclusion dye assay (please see section 2.6.3) for the determination of cell count and cell viability. In some cases cell viability was confirmed by means of the calcein AM/ethidium homodimer assay (please see section 2.6.6 for full description of the methodology). hMSCs behaviour and functionality were also examined after seeding the cells on the surface of alginate disks (layers), which were maintained under the same culture conditions and were characterised using the same techniques employed for the beads.

Scaffold-cells interactions were also analysed in order to assess the biological activity of the alginate matrices. In particular, eventual changes in the cell morphology, evaluated by way of light microscopy were observed. Cells remaining rounded and spherical indicated that no interaction with the biomaterial was occurring, whereas elongated cells would have indicated association with the matrix.

Cell studies were performed also to simultaneously establish the alginate derivatisation procedure, since different Pronova ultra-pure alginates (i.e. high and low G-subunits contents and high and low viscosity) were used for the preparation of the constructs. Alginates resulting from the coupling reaction with 9X reactants (EDC, sulfo-NHS) and different GRGDY peptide concentrations (1-32X) according to alternative derivatisation procedures were investigated.

Finally, the MTT assay (described in section 2.7) was employed in few preliminary studies as an additional method for the evaluation of cell proliferation within alginate/hMSCs beads.

### **5.3 High and low G-content and high and low viscosity alginates for the fabrication of hMSCs-containing beads**

During beads fabrication, the gelation of the alginate takes place due to interchain chelation of the  $\text{Ca}^{2+}$  ions of the cross-linking solution with blocks of guluronic acid (G) residues between two different polysaccharide chains [Grant *et al.*, 1973; Smidsrod and Skjak-Braek, 1990; Rowley *et al.*, 1999]. The divalent  $\text{Ca}^{2+}$  cations cooperatively bind between the G-blocks of adjacent alginate chains, creating ionic interchain bridges which cause gelling of aqueous solutions. Mannuronic acid (M) blocks and alternating MG blocks do not participate in gel cross-linking [Smidsrod and Skjak-Braek, 1990; Draget *et al.*, 1994; Wang *et al.*, 1993]. As a result, the cross-linking density and thus mechanical strength of the network depend on the ratio of guluronic/mannuronic acid residues, the length of the guluronic acid residues, the molecular weight (MW) of the polymer, and the  $\text{Ca}^{2+}$  ion concentration at the time of gelation [Martinsen *et al.*, 1989; Drury and Mooney, 2003; Kong *et al.*, 2004a; Kong *et al.*, 2004b; Wong M., *et al.*, 2001]. High guluronic alginates have long been advocated for use in encapsulated cell systems [Colton, 1996], due to their strength and stability. In addition, rat bone marrow cells have shown to be able to adhere and proliferate on high G-content unmodified alginate hydrogel discs [Wang *et al.*, 2003]. However, other groups have shown that unmodified high G alginates have also the ability to inhibit normal cell growth and overall metabolic activity [Stabler *et al.*, 2002]. On the other hand, high-G alginates chemically modified with RGD-

containing peptides demonstrated to permit mouse skeletal myoblasts adhesion and to promote higher proliferation rates than lower G-content substrates [Rowley and Mooney, 2002].

Moreover, recent studies have indicated that high MW alginates are associated with low cell viability, due to the high shear forces required to mix cells with these (high viscosity) solutions [Kong *et al.*, 2003]. However, these polymers are normally preferred for use in encapsulated cell systems because of their gel-forming ability, while low MW alginates tend to form brittle hydrogels [Colton, 1996; Weber *et al.*, 2002]. Interestingly, alginates that maintain the required mechanical rigidity and allow at the same time higher cell viability have been recently created by combining low MW alginate molecules with a small fraction of high MW alginate [Kong *et al.*, 2003].

Given these interesting and sometimes contradictory findings, it was of interest to see whether the alginate composition and viscosity, together with the GRGDY peptide incorporation procedure, had any different effect in terms of both alginate-cell interactions (i.e. alginate biological activity) and bead strength and stability.

As a result, initial studies with hMSCs were performed using high G-subunits high viscosity (SLG100) alginate and high M-subunits high and low viscosities (SLM100 and SLM20) alginates. Each of these biomaterials was used either in its plain (i.e. non derivatised) form or after completion of the standard derivatisation method described in section 2.3. In particular, for the derivatisation procedure these alginates were coupled with 9X EDC and sulfo-NHS and 1X GRGDY peptide (i.e. alginate 3, 4 and 5 in table 3.1). Alginate beads were made with 25% v/v fourth passage (p4) hMSCs resuspended in “complete DMEM” medium to a final concentration of  $1 \times 10^7$  cells/mL in each of the alginate solutions under investigation.

Interestingly, the high mannuronic acid content (M) alginates did not prove to be ideal biomaterials for cell immobilisation, as both the SLM100 and SLM20 beads completely dissolved within 24 hours from cross-linking. This is in line with the well-documented structural integrity of high guluronic acid (G) content alginates, which develop stiffer, more porous gels that maintain their integrity for longer periods of time, as opposed to alginates rich in mannuronic acid (M) [Stabler *et al.*, 2002]. Thus, following complete dissolution, the SLM100 and SLM20 beads were discarded, while the culture of the SLG100 alginate beads was carried on over a 2-week period. The scaffold was evaluated immediately after cross-linking (day 0) and at two additional

time-points during culture (i.e. day 4 and day 7) for cell density and viability, using a haemocytometer and trypan blue. In addition, the culture of the beads was monitored and evaluated by means of light microscopy, and photographs were taken four days after beads preparation (please see figure 5.1 *A* and *B*). No cell adhesion was observed on both control alginate or alginate-GRGDY beads. In both alginate types the cells remained rounded and failed to elongate and acquire their typical spindle-shaped morphology.

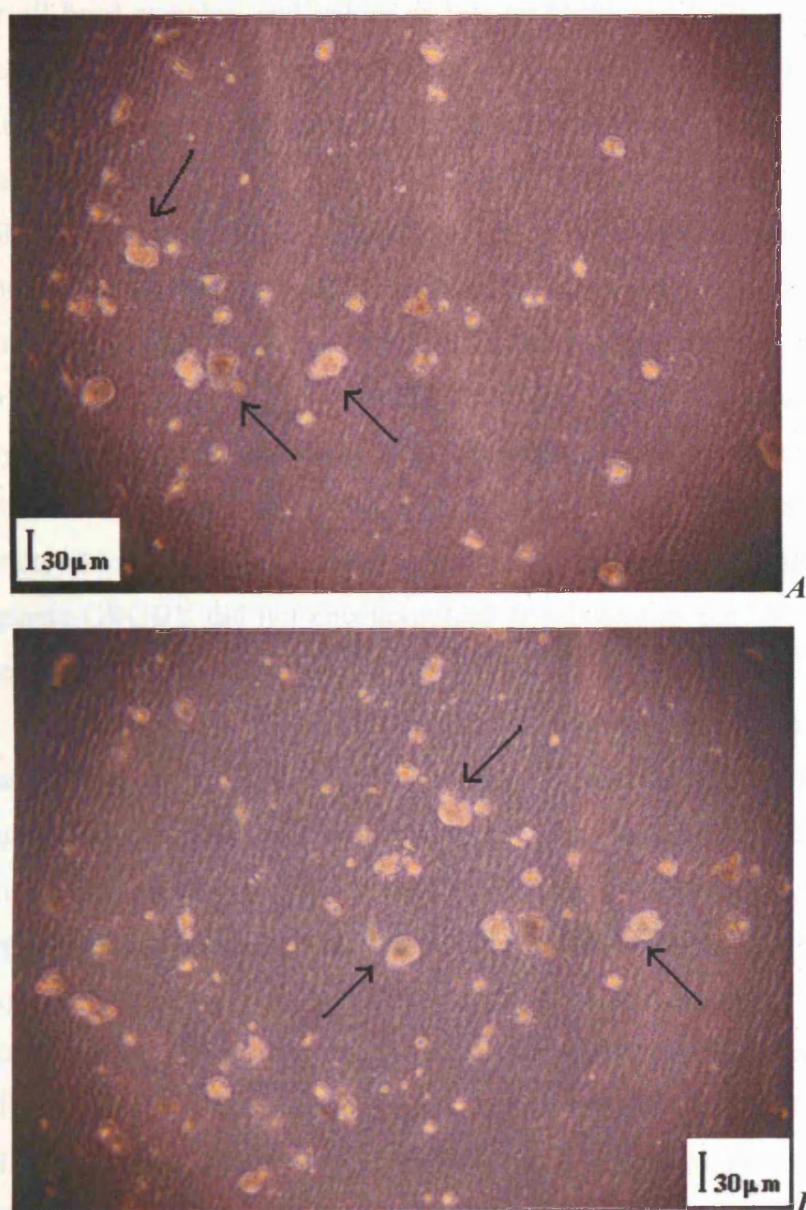


**Fig. 5.1 *A* and *B*:** hMSCs immobilised within SLG100 alginate-GRGDY beads. The alginate was derivatised with 9X reactants and 1X peptide, and after lyophilisation it was frozen at  $-20^{\circ}\text{C}$ . The alginate-GRGDY was then thawed and mixed with the cell suspension for beads preparation (i.e. standard derivatisation

protocol). The photographs were taken at the inverted light microscope 4 days after beads fabrication. The arrows indicate some of the cells failing to adhere to the alginate-GRGDY matrix.

High cell viability was measured immediately after cross-linking for both the control (average  $90.37 \pm 1.6\%$ ) and the derivatised SLG100 (average  $92.18 \pm 3.1\%$ ) alginates. However, a significantly decrease in cell viability was observed over time for all bead samples, and values as low as  $8 \pm 1\%$  and  $9 \pm 2\%$  were measured after 1 week of culture for the non derivatised matrix and the alginate-GRGDY respectively. Viability measurements were not taken after this time-point, as the data suggested that, regardless of the alginate condition (i.e. uncoupled alginate or alginate-GRGDY), neither cell elongation nor cell growth were occurring within the beads. The cell density of the hMSCs immobilised in the alginate-GRGDY beads decreased from  $2.12\text{--}2.5 \times 10^4$  to  $1.3\text{--}1.4 \times 10^4$  cells /bead during the first 4 days in culture, and further down to  $0.5\text{--}0.7 \times 10^4$  cells /bead during the subsequent three days (day4-day7). Similar cell densities were measured for the beads created with the non-derivatised alginate (data not shown). These results indicate that, despite the positive results shown by other groups [Rowley *et al.*, 1999; Markusen, 2005], SLG100 alginate-GRGDY did not encourage cell attachment in the hMSCs-containing beads created in this research.

However, it must be noted that, due to time constraints, no amino acid analysis was performed on this SLG100 alginate, which was made with a lower (i.e. 1X) peptide concentration as compared to the alginate-GRGDY that was analysed for amino acid levels (i.e. 10-32X peptide). Therefore it could be excluded that the 1X peptide concentration was too low to allow successful incorporation of the GRGDY sequence onto the alginate biomaterial. In addition, the hMSCs used for the fabrication of the constructs in this experiment were not characterised by the expected cell growth rates and kinetics in the control monolayer condition either. Thus, the cells themselves might have been associated with low cell proliferation capacity independently of the alginate matrix. Therefore the cell source employed in this particular experiment could not be excluded as possible additional cause to the poor cellular functions observed within the beads. As a result, the biological activity of the SLG100 alginate and its appropriateness as a scaffold material for cell immobilisation

was investigated further in additional studies, which are described in the following sections.

Nevertheless, in accordance with other groups findings [Stabler *et al.*, 2002], this study confirmed that the chemical composition of the alginate has a significant effect on its physical properties and suggested that high-G content alginates should be preferred over the high-M content polymers for their gelling properties and their strength and stability. As a result, SLG100, which permitted the fabrication of stronger and more stable beads, was chosen and adopted as the preferred alginate biomaterial for all subsequent matrix/cells constructs studies.

#### ***5.4 Fabrication of alginate-GRGDY/hMSCs beads using alginate modified according to different derivatisation procedures***

The aim of this study was to test the effects of SLG100 alginates prepared according to different derivatisation procedures (alginates 6, 7, 8, 9 in table 3.1) on both the cell behaviour after immobilisation and the mechanical properties of the resulting constructs. The coupling reaction for all of these alginates was performed using exactly the same reactants concentrations (i.e. 9X reactants and 10X peptide) under the same working conditions (20-hour reaction at  $T=20-22^{\circ}\text{C}$ , under constant mixing on a platform roller, in the dark). However, after completion of the carbodiimide reaction and the 5-day dialysis cycle, alternative methods (i.e. lyophilisation with or without freezing step, PEG concentration with or without freezing step) were used for the purification and the concentration steps, as described in section 3.2 (please see figure 3.1).

Fourth passage (p4) hMSCs (25% v/v) were mixed with each of the four alginate solutions to a final concentration of  $1 \times 10^7$  cells/mL, and the resulting alginate/cell mixtures were treated with  $\text{CaCl}_2$  for gel cross-linking and beads fabrication.

Particular care was taken on the cell choice, with respect of their proliferation potential in the control monolayer culture, and only hMSCs associated with high growth rate ( $0.012 \text{ hours}^{-1}$ ) and low doubling time (55.79 hours) were used for the fabrication of the beads. This permitted a more accurate comparison of the cell

performance in monolayer condition (tissue flasks) and within alginate-GRGDY beads.

No significant differences were noted among all bead samples in terms of gel stiffness and mechanical behaviour. Stable and rigid constructs were obtained for all alginate conditions, and all beads held regular structure and shape over the 10-day period examined. However, despite the structural integrity and stability, no cell attachment and elongation within the alginate polymers were observed (please see photograph in figure 5.2). Regardless of the derivatisation procedure employed for the fabrication of the alginate matrix, hMSCs demonstrated to be unable to adhere to and elongate within the alginate-GRGDY biomaterial.

In addition, a significant drop in cell viability, comparable to that observed for the control constructs (i.e. beads prepared with non derivatised-alginate) was measured over time (please see table 5.1 and photograph in figure 5.3). The cell density values measured for hMSCs immobilised in the alginate-GRGDY beads also decreased consistently over time, similarly to what was seen for cells immobilised in the control (i.e. non derivatised) alginate (please see table 5.1).

Thus, no discernable differences were observed between the non derivatised alginate and all the alginate-GRGDY types investigated.

Beads conditions			
	day	Viability average	Cells/beads
<b>Control (non derivatised) alginate</b>	0	91.4±0.9%	2.70-2.91x10 <sup>4</sup>
	4	55.9±2.6%	1.67-1.69x10 <sup>4</sup>
	7	8.5±1.2%	0.82-0.91x10 <sup>4</sup>
<b>Standard protocol (no.1)</b>	0	92.18±2.9%	2.95-3.09x10 <sup>4</sup>
	4	62.3±1.3%	1.70-1.2x10 <sup>4</sup>
	7	7.2±0%	0.90-0.97x10 <sup>4</sup>
<b>Protocol no.2</b>	0	89.7±1.6%	2.7-2.93x10 <sup>4</sup>
	4	57.1±2.8%	41.50-1.9x10 <sup>4</sup>
	7	7.9±1.3%	0.60-0.75x10 <sup>4</sup>
<b>Protocol no.3</b>	0	90.2±0%	3.0-1.3x10 <sup>4</sup>
	4	52.8±5.7%	1.6-0.9x10 <sup>4</sup>
	7	9.1±3.1%	0.8-0.95x10 <sup>4</sup>
<b>Protocol no.4</b>	0	93.2±0.3%	2.80-2.93x10 <sup>4</sup>
	4	64.2±3.2%	1.57-1.81x10 <sup>4</sup>
	7	6.9±3.4%	0.63-0.71x10 <sup>4</sup>

**Table 5.1:** Percent cell viability and cell concentration values obtained for hMSCs immobilised in non-derivatised alginate (control beads) and alginates modified with the GRGDY peptide according to different derivatisation protocols. All alginates were coupled with 9X sulfo-NHS and EDC and with 10X peptide concentrations (the resulting derivatised alginates are designated as “alginate-GRGDY number 6”, “number 7”, “number 8” and “number 9” respectively in table 3.1) Data are shown for each harvesting time-point during the first week of culture.

Interestingly, amino acid analysis data revealed that the GRGDY peptide was successfully incorporated onto the alginate after completion of the derivatisation procedure according to the standard protocol (procedure no. 1 in figure 3.1). This alginate (final alginate-GRGDY number 6 in table 3.1) contained all the four constituent amino acids of the GRGDY sequence, as it appears from the results shown in table 3.3 (final alginate-GRGDY number 6). However, as already mentioned in section 3.3.1, a significant tyrosine loss was also detected in these samples. Ultimately, it can be hypothesised that this phenomenon was responsible for the low biological activity of the alginate-GRGDY, resulting in lack of matrix-cells



interactions and cell death over time. Amino acid analysis was not performed on the other alginate-GRGDY types resulting from the alternative derivatisation procedures (i.e. alginates numbers 7, 8, 9 in table 3.1) due to time constraints. Hence, such analyses will need to be performed in future in order to investigate further the effects of the different derivatisation protocols on the peptide attachment. This measure will permit to determine whether the alternative steps involved in the derivatisation process (e.g. freezing for long-term storage, lyophilisation and PEG concentration) ultimately affect the efficiency of the coupling reaction and, subsequently the cellularity of the final alginate-GRGDY/hMSCs constructs.

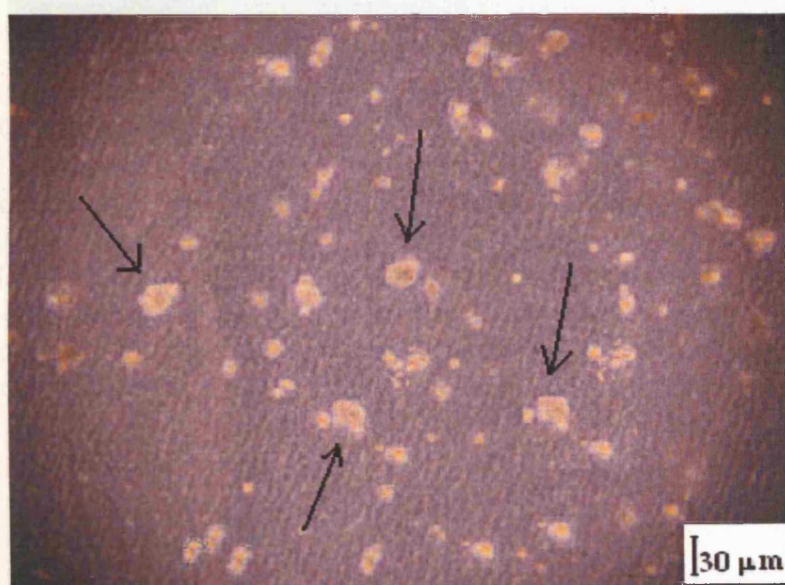


**Fig. 5.2:** hMSCs immobilised within SLG100 alginate-GRGDY beads. The alginate was derivatised with 9X reactants and 10X peptide, according to the standard derivatisation protocol described in section 2.3.2. The photographs were taken at the inverted light microscope after 5 days in culture. The arrows indicate some of the cells failing to adhere to the alginate-GRGDY matrix.

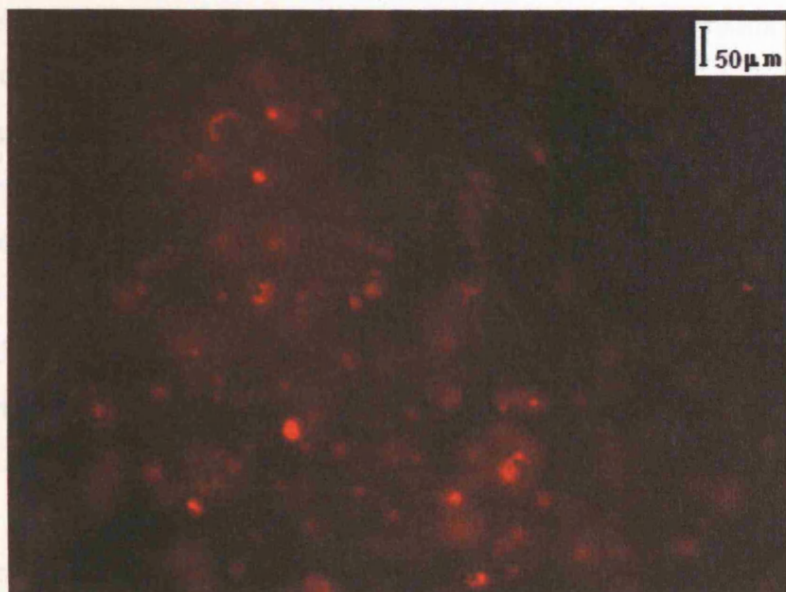


**Fig. 5.3:** Fluorescence photograph obtained for hMSCs immobilised within SLG100 alginate-GRGDY beads stained with calcein AM/ethidium homodimer for the qualitative evaluation of cell viability. The alginate was derivatised with 9X reactants and 10X peptide prior to the beads preparation. The resulting alginate-GRGDY was mixed with the cell suspension and used for beads preparation following the lyophilisation and freezing steps (i.e. standard derivatisation procedure). The photograph was taken at the confocal microscope 5 days after beads fabrication. The intense red fluorescence originates from the Ethidium homodimer-1 bound to the cellular DNA after permeation of the damaged cell membranes.

### **5.5 Alginate-GRGDY/fibroblasts beads**

In place of hMSCs, human foreskin fibroblasts were used in this study for the preparation of alginate beads, in order to see whether different cell types exhibit different adhesion properties, and whether the GRGDY ligand may favour fibroblast attachment and functionality as opposed to what was observed in this research for hMSCs.

Several *in vitro* studies have already indicated that fibroblasts can be successfully encapsulated in alginate beads to be employed in different therapeutic applications [Peirone *et al.*, 1998; Schwinger *et al.*, 2002; Keshaw *et al.*, 2004; Ueng *et al.*, 2000].

In this study SLG100 alginate coupled with 9X reactants and 10X peptide according to the standard derivatisation protocol (alginate-GRGDY no. 6 in table 3.1) was mixed with the cell suspension ( $1 \times 10^7$  cells/mL) and the resulting matrix-cells mixture (25% v/v of cells) was gelled into 2-2.5 mm diameter beads following the

previously described (please see section 2.5.3) cross-linking treatment in 90 mM  $\text{CaCl}_2$ . Sixth passage (p6) fibroblasts were used in this study, and a culture in T25 tissue flasks was run in parallel in order to have a direct comparison with cell performance in the monolayer condition. Control beads were simultaneously fabricated with non-derivatised SLG100 alginate and were assessed in parallel with the alginate-GRGDY constructs. As in the previous experiments, cell morphology and alginate biological activity were evaluated by means of light microscopy, and cell densities and viabilities were assessed with haemocytometer and trypan blue dye exclusion assay respectively following cell release with trisodium citrate solution.

Both control (i.e. non derivatised) alginate and alginate coupled with the GRGDY peptide formed stable gel beads, which retained a defined regular shape over the 10-day period tested. However, similarly to what was observed in the previous experiment for the hMSCs, the fibroblasts failed to interact with both the unmodified polymer and the alginate-GRGDY, and could not elongate and acquire their characteristic spindle-shaped morphology (please see photographs in figure 5.4 A and B). Moreover, while the cells were proliferating extensively in tissue flasks (growth rate =  $0.014 \text{ hours}^{-1}$ , doubling time = 49.8 hours), no cell proliferation was observed within the beads. Cell viability data indicated significant cell death over time, both for the control beads and the alginate-GRGDY constructs (please see table 5.2). The cells, having failed to adhere to the alginate scaffold, completely dissociated from the matrix as small spherical entities floating in the growth medium within 48 hours from cross-linking.

Light microscopy also revealed that in these constructs the cells tended to position in close proximity to the outer surface of the matrix/cells beads. This inhomogeneous cell distribution may have been caused by the particular method employed for the beads fabrication in this research. It has already been reported that the diffusion-setting method for the gelation of the alginate with  $\text{CaCl}_2$  results in an inhomogeneous alginate distribution within the gels [Skjak-Braek *et al.*, 1989]. In general, it is well documented that a very rapid and irreversible binding reaction of multivalent cations is typical for alginates; a direct mixing of these two components therefore rarely produces homogeneous gels [Draget *et al.*, 2005] (please see section 6.4 for a more detailed description of this phenomenon).

Ultimately, a similar poor cellular behaviour within the alginate-GRGDY beads was therefore observed for the hMSCs and the fibroblasts, as both cell types appeared



to be unable to interact with the biomaterial and to spread out as spindle-shaped elongated healthy cells within the alginate beads.

As mentioned in the previous section, amino acid analysis was performed on the alginate used here for the preparation of the beads (alginate number 6 in table 3.1), revealing the presence of a complete GRGDY sequence attached to the polymer, yet with a very low tyrosine level (please see alginate-GRGDY number 6 in table 3.3 for the amino acid content data). Thus, the most probable cause for the lack of alginate-cells interactions observed in these studies was the significant loss of the final tyrosine residue of the GRGDY sequence, which, according to the amino acid analysis data, was being cleaved off (at some stage) during the derivatisation procedure. This event probably determined the poor results in terms of cellularity described in this research for the studies performed on the alginate/cells beads. However, despite the lack of cell adhesion and proliferation, it must be noted that constructs fabricated with SLG100 alginate retained good mechanical properties (i.e. considerable stiffness, structural integrity and stability) over the 10-day week period of culture under examination.

Beads conditions			
	Day	Viability average	Cells/bead
<b>Control (non derivatised) alginate</b>	0	94.4±1.3 %	2.46-2.78x10 <sup>4</sup>
	4	65.7±1.6 %	1.52-1.61x10 <sup>4</sup>
	7	9±2.1%	0.92-0.98x10 <sup>4</sup>
<b>SLG100 alginate-GRGDY</b>	0	92.67±3.4%	2.65-2.91x10 <sup>4</sup>
	4	67.0±0.3 %	1.59-1.64x10 <sup>4</sup>
	7	11.3±1%	0.92-0.99x10 <sup>4</sup>

**Table 5.2:** Percent cell viability and cell concentration values obtained for human foreskin fibroblasts immobilised in non-derivatised alginate (control beads) and in alginate modified with the GRGDY peptide according to the standard derivatisation procedure. 9X sulfo-NHS and EDC and 10X peptide were used for the coupling reaction (the resulting derivatised alginate is designated as “alginate-GRGDY no. 6” in table 3.1). Data are shown for each harvesting time-point during the first week of culture.

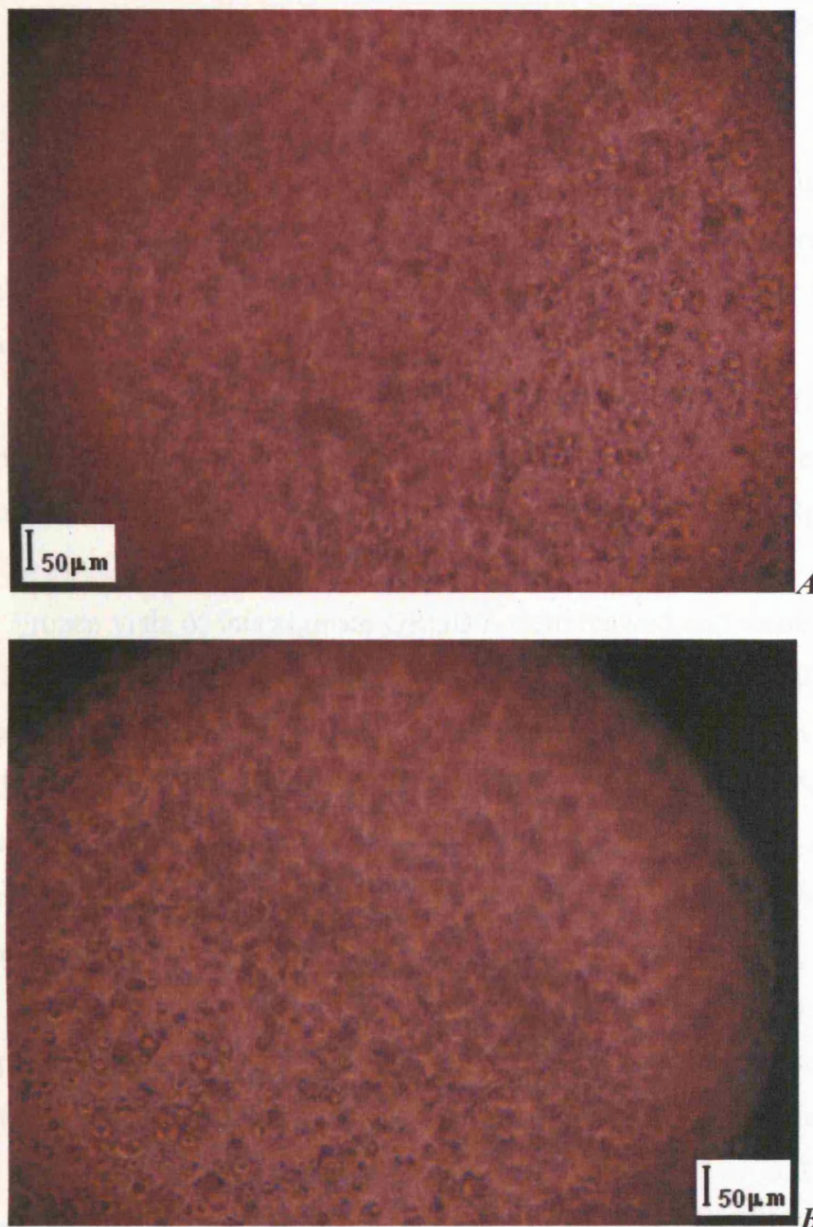


**Fig. 5.4 A and B:** Human foreskin fibroblasts immobilised within SLG100 alginate-GRGDY beads. The alginate was derivatised with 9X reactants and 10X GRGDY peptide according to the standard derivatisation procedure described in section 2.3.2. The photograph was taken at the inverted light microscope 6 days after beads fabrication. The small spherical morphology indicates that the cells were unable to adhere to the alginate-GRGDY matrix within the beads.

## **5.6 Additional studies on alginate-GRGDY for the immobilisation of fibroblasts**

Additional studies were performed in order to investigate further the possibility for the alginate-GRGDY (fabricated according to the standard derivatisation procedure described in this research) to act as a suitable substrate for cell viability and growth.

Thus, SLG100 alginate coupled with the same (i.e. 9X) EDC and sulfo-NHS concentrations as in the previous experiments, but with a higher (i.e. 32X) peptide concentration, was used for the fabrication of the constructs (alginate no. 1 in table 3.1).

Frozen vials of this alginate-GRGDY were thawed and reconstituted with normal saline solution as described in section 2.3.2.5. The resulting alginate solution was mixed with fifth passage (p5) human foreskin fibroblasts in suspension ( $1 \times 10^7$  cells/mL) and the alginate-GRGDY/fibroblast mixture (25% v/v of cells) was then used for the fabrication of the constructs. Fibroblasts were also simultaneously expanded in monolayer culture, and were also grown within non-derivatised alginate beads acting as control.

The expectation was that the higher peptide concentration (32X) used in this experiment, which had already led to the incorporation of higher amino acid levels onto the alginate chain (please see data for alginate designated as “alginate-GRGDY no. 1-Albachem” in table 3.3), would have resulted in cell adhesion and cell proliferation within the constructs. However, once again neither cell attachment nor cell elongation were observed in the alginate-GRGDY beads (please see photograph in figure 5.5). As for all the experiments described above (sections 5.3, 5.4 and 5.5), significant loss of cell viability was observed over time (please see photograph in figure 5.6). The percentage of detectable viable cells at day 7 of culture was in fact only  $10.4 \pm 0.9\%$  and  $9.07 \pm 3.4\%$  for the control beads and the derivatised alginate constructs respectively. Concurrently, cell numbers calculated after dissolution of both bead types with trisodium citrate decreased considerably over time, dropping from initial values in the  $2.15\text{--}2.79 \times 10^4$  cells/bead range (day 0) to merely  $0.49\text{--}0.76 \times 10^4$  cells/bead at day 7.

Thus, the use of alginate coupled with higher peptide concentrations did not improve the biological activity of the resulting polymer hydrogels. According to the

amino acid analysis data (please see section 3.3.1), also in this case a significant loss of tyrosine was occurring during the derivatisation process. Hence, the negative results in terms of cell performance consistently observed after cell immobilisation corroborate the hypothesis of the correlation between tyrosine loss and lack of cell adhesion, and ultimately lack of cell survival, within the alginate-GRGDY beads.

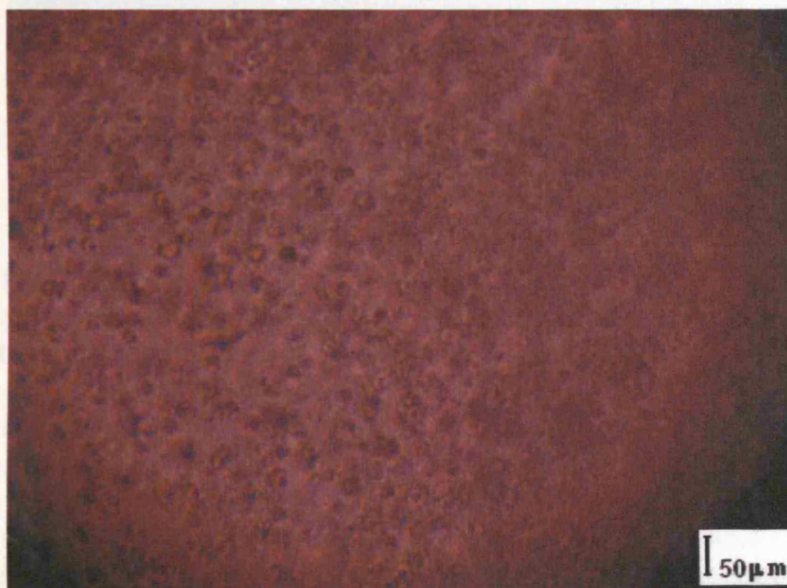


**Fig. 5.5:** Human foreskin fibroblasts immobilised in SLG100, 9X reactants, 32X GRGDY peptide alginate-GRGDY. The photograph was taken at the inverted light microscope 5 days after beads fabrication. Small, spherical cells failing to adhere to the scaffold and to elongate are clearly visible within the bead.



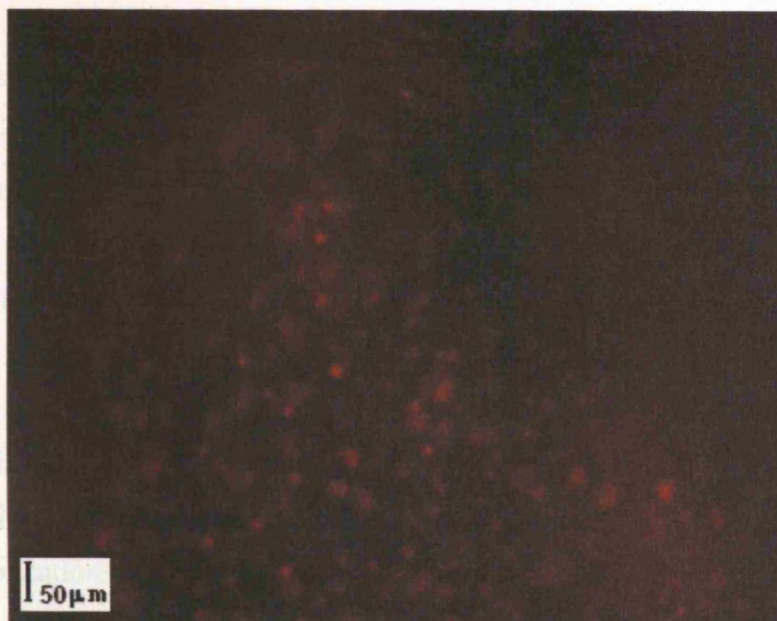


**Fig. 5.6:** Fluorescence photograph obtained for human foreskin fibroblasts immobilised within SLG100 alginate-GRGDY beads stained with calcein AM/ethidium homodimer for the qualitative evaluation of cell viability. The alginate was derivatised with 9X reactants and 32X peptide prior to the beads preparation. The resulting alginate-GRGDY was mixed with the cell suspension and used for beads preparation following the lyophilisation and freezing steps (i.e. standard derivatisation procedure). The photograph was taken at the confocal microscope 5 days after beads fabrication. The intense red fluorescence originates from the Ethidium homodimer-1 bound to the cellular DNA after permeation of the damaged cell membranes.

### ***5.7 hMSCs immobilised in alginate-GRGDY disks***

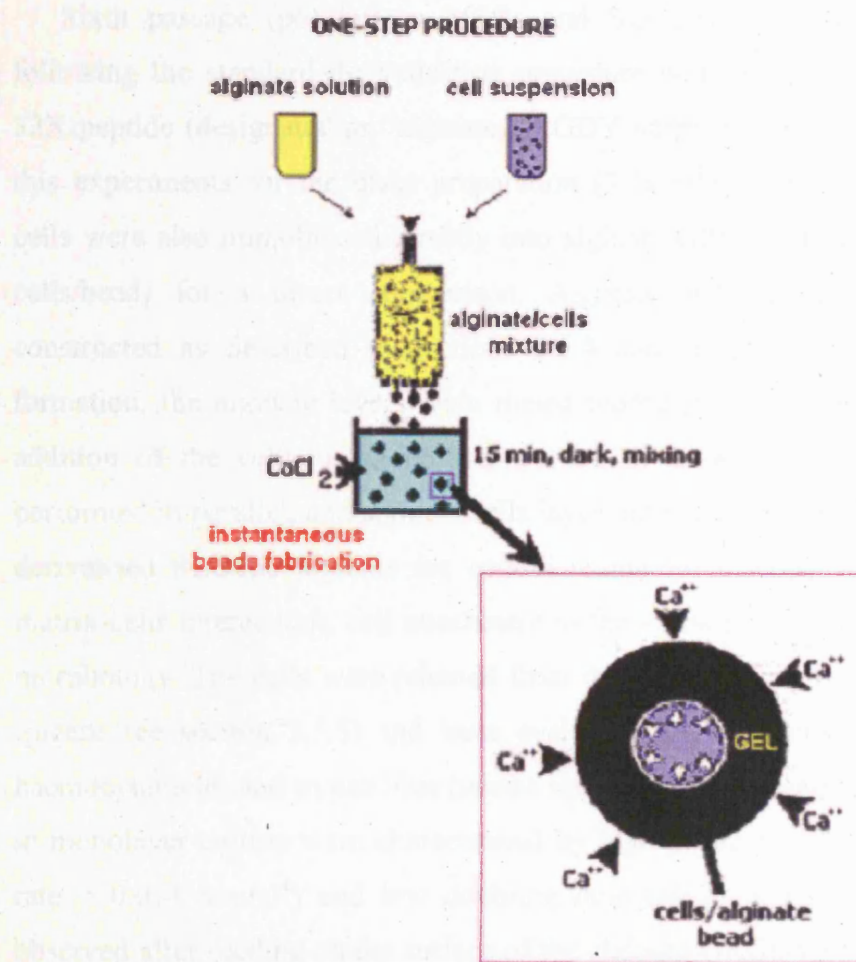
Given the lack of cell attachment observed for both hMSCs and human foreskin fibroblasts after immobilisation within alginate-GRGDY beads, it was decided to investigate hMSCs performance and functions after seeding the cells on top of alginate-GRGDY disks (or layers).

Despite the project's aim to immobilise the cells within the alginate hydrogels in a one-step process, alginate disks were fabricated to de-couple the cell seeding step from the alginate scaffold formation, in order to investigate the possible detrimental effects of high molar concentration of the cross-linking solution. During the beads preparation procedure the cells were immediately mixed with the alginate and the resulting suspension was then syringed into the  $\text{CaCl}_2$  cross-linking solution (please

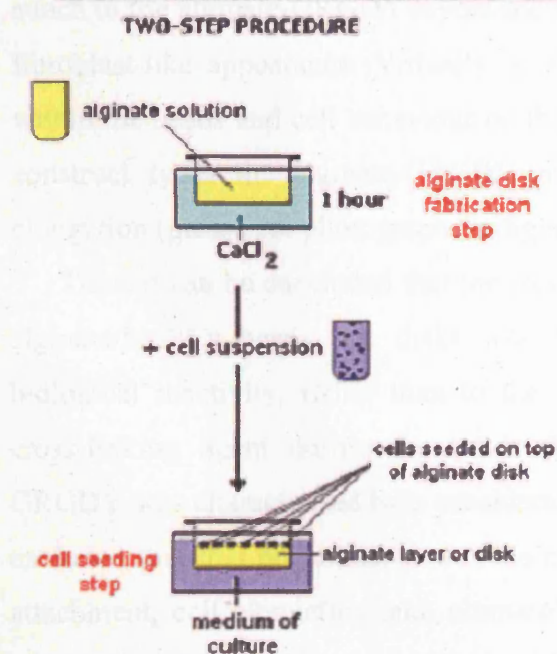
see schematic representation in figure 5.7). Thus, the final alginate/cells beads were instantaneously formed within the cross-linking solution.

However, the 1%  $\text{CaCl}_2$  solution used (corresponding to 90mM) was hypertonic, being 1.8mM the physiological  $\text{CaCl}_2$  concentration for cell maintenance and growth, i.e. level in DMEM medium (BioWhittaker Product Catalog, 2001). During cell immobilisation in alginate beads the cells are exposed to the calcium chloride solution for prolonged time periods. This procedure can, in principle, cause unwanted and uncontrolled physiological effects. In addition, only recently attachment-dependent cells have been reported to be successfully immobilised within alginate beads, whilst alginate encapsulation systems are in most cases employed only for cell therapy applications involving the use of suspension adapted cells. Even Rowley's and Mooney's studies had been performed by constructing alginate layers and then seeding on the surface with cells [Rowley, 1999].

Given the potential harmful effect of the cross-linking solution on the overall cell performance, and given that no cell adhesion was observed from the cell immobilisation studies with alginate-GRGDY beads (described in the sections 5.3 and 5.6 above), experiments were conducted by pre-forming the alginate-GRGDY matrices as layers in the bottom of a microwell, and then seeding the cells separately onto the surface of the alginate (please see section 2.5.4 for a full description of the method employed for disks preparation). This procedure made it possible to decouple the alginate preparation and the cell seeding steps, and therefore to test the detrimental effects of the cross-linking solution on cell behaviour. A schematic representing the different procedures for beads and disks fabrication is given in figure 5.7.



**A**



**B**

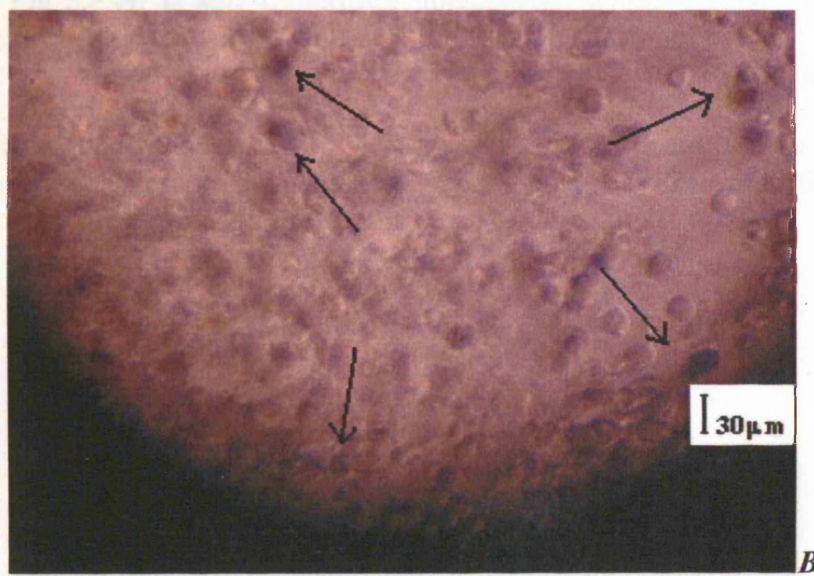
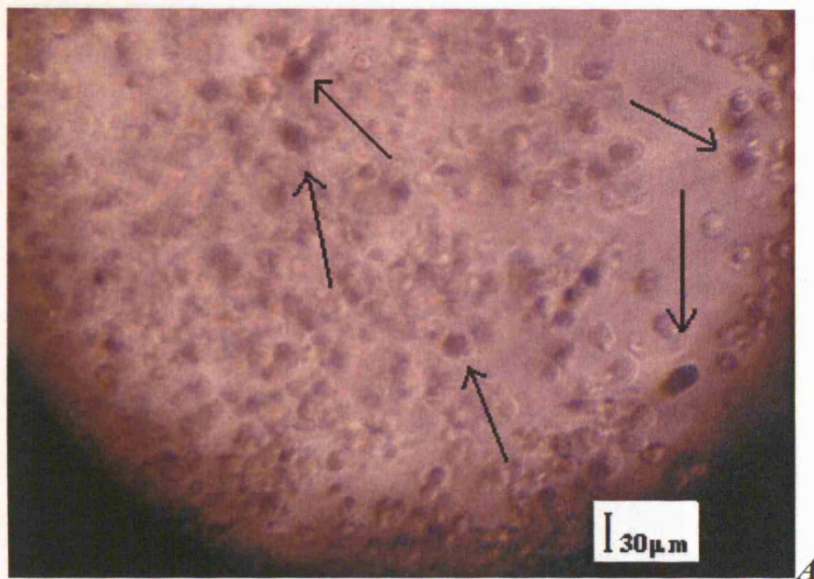
**Fig. 5.7:** Schematic of the cross-linking procedures for the preparation of alginate/cells beads (A) and layers (B). Figure A adapted from Draget *et al.* 2005.

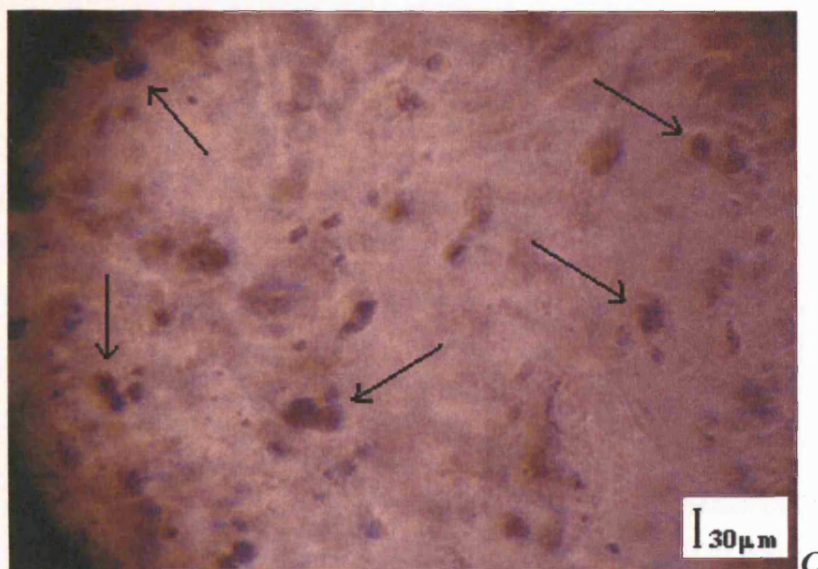
Sixth passage (p6) human MSCs and SLG100 Pronova alginate derivatised following the standard derivatisation procedure with 9X EDC and sulfo-NHS and 32X peptide (designated as “alginate-GRGDY number 1” in table 3.1) were used in this experiments for the disks preparation ( $3.3 \times 10^4 \text{ cells/cm}^2$  -  $5 \times 10^4 \text{ cells/cm}^2$ ). The cells were also immobilised directly into alginate-GRGDY beads (average  $2.52 \times 10^4$  cells/bead) for a direct comparison. Alginate-GRGDY disks and beads were constructed as described in sections 2.5.4 and section 2.5.3 respectively. After formation, the alginate layers were rinsed thoroughly of excess  $\text{CaCl}_2$  prior to the addition of the cells. A monolayer culture in 24-well tissue culture plates was performed in parallel, and alginate/cells layers and beads were created also with non-derivatised SLG100 alginate for control. Light microscopy was used to evaluate matrix-cells interactions, cell attachment to the surface of the alginate disks and cell morphology. The cells were released from the matrix with trisodium citrate solution (please see section 2.5.5) and were evaluated for cell density and viability with haemocytometer and trypan blue (please see sections 2.6.2 and 2.6.3). While the cells in monolayer culture were characterised by high proliferation potential (cell growth rate =  $0.014 \text{ hours}^{-1}$ ) and low doubling time (50.86 hours), cell growth was not observed after seeding on the surface of the alginate-GRGDY disks. The cells did not attach to the alginate-GRGDY layers and could not spread out to acquire their typical fibroblast-like appearance. Virtually no difference was observed among cellularity within the beads and cell behaviour on the surface of the hydrogel disks, and in both construct types the alginate-GRGDY matrix did not support cell adhesion and elongation (please see photographs in figures 5.8 and 5.9).

Thus, it can be concluded that the lack of cell response that was seen for both the alginate/hMSCs beads and disks was most likely due to the alginate-GRGDY biological inactivity, rather than to the harmful treatment with the high molarity cross-linking agent during the beads fabrication procedure. Since the alginate-GRGDY was characterised by a considerable loss of the tyrosine residue, it cannot be excluded that this phenomenon was the major cause responsible for the lack of cell attachment, cell elongation and, ultimately, cell proliferation observed for both the alginate beads and disks. According to this hypothesis, tyrosine loss probably altered the chemical conformation of the GRGDY sequence, ultimately preventing cell attachment. Thus, the hMSCs, which are strongly anchorage dependent, could not attach to the alginate matrix of both beads and disks simply because the polymer,

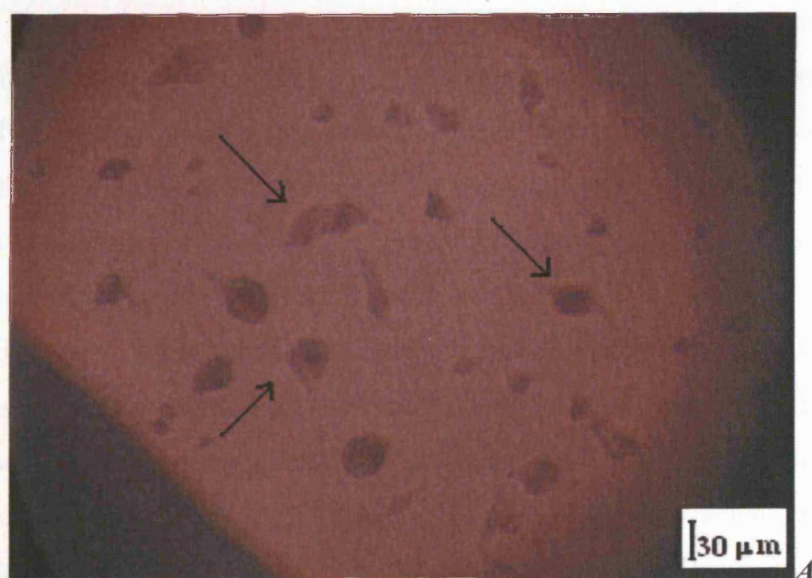
having lost the tyrosine residue, could not provide cell adhesion sites. However, other possibilities cannot be excluded, since there are several other parameters that may affect the beads fabrication procedure, and thus the cell adhesion properties of the resulting scaffold. It is known that the gelation process, which occurs when divalent cations take part in the interchain binding between G-blocks, depends on both the alginate and gelling ion concentrations [Martinsen *et al.*, 1989]. Thus, future studies could be performed investigating cell immobilisation within alginate beads made with different  $\text{Ca}^{2+}$  concentrations, or by using different length exposures to the cross-linking solution. Furthermore, it is true that for the immobilisation of living cells calcium has become the primary choice as a gel-inducing agent. However, alginate forms gels with most di- and multivalent cations. While monovalent cations and  $\text{Mg}^{2+}$  ions do not induce gelation [Sutherland, 1991], ions like  $\text{Ba}^{2+}$  and  $\text{Sr}^{2+}$  produce stronger alginate gels than  $\text{Ca}^{2+}$  [Clark and Ross-Murphy, 1987]. Like  $\text{Ca}^{2+}$ , these ions are considered to be sufficiently biocompatible for applications involving immobilisation of living cells [Smidsrod and Skjak-Braek, 1990]. Moreover, as compared to  $\text{Ca}^{2+}$ , they have a higher affinity for alginate [Smidsrod, 1974], and consequently are associated with higher gel stability [Clark and Ross-Murphy, 1987]. As a result, the use of alternative gelling cations, such as  $\text{Ba}^{2+}$  or  $\text{Sr}^{2+}$ , could be investigated. Ultimately, further studies are needed to elucidate whether the lack of cell adhesion to the alginate beads and disks was caused in both matrices by the tyrosine loss and subsequent biological inactivity of the alginate-GRGDY matrix, or by other mechanisms.







**Fig 5.8 A, B and C:** hMSCs immobilised within alginate-GRGDY beads. The alginate polymer was coupled with 9X EDC and sulfo-NHS and 32X GRGDY peptide, and was derivatised according to the standard protocol described in section 2.3.2. The photographs were taken at the inverted light microscope 4 days after the fabrication of the constructs. It is evident from the photographs that the cells were unable to adhere to the alginate-GRGDY and to elongate within the beads. The arrows indicate some of these cells.





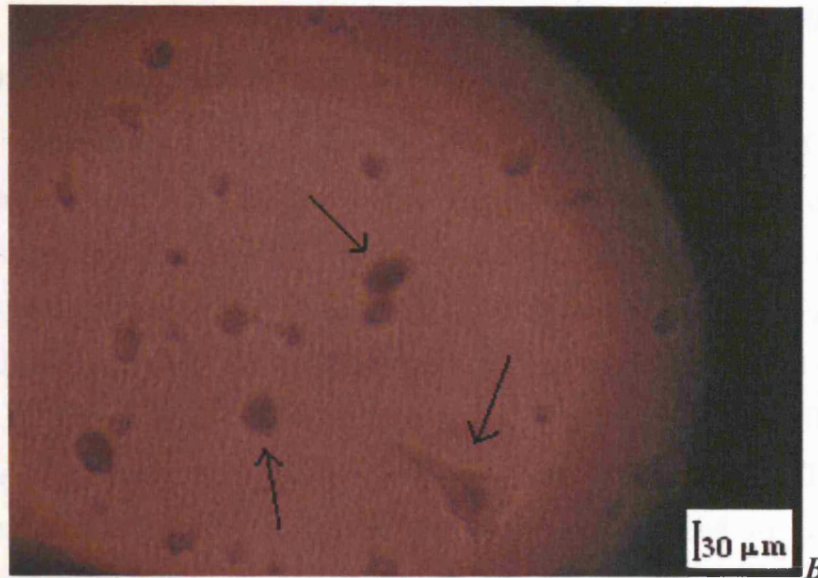


**Fig 5.9 A and B:** hMSCs seeded on top of alginate-GRGDY disks. The alginate polymer was coupled with 9X EDC and sulfo-NHS and 32X GRGDY peptide, and was derivatised according to the standard protocol described in section 2.3.2. The photographs were taken at the inverted light microscope 4 days after the fabrication of the constructs. The arrows indicate big cells failing to attach to the alginate-GRGDY layers.

### **5.8 MTT assay: analysis of cell proliferation within alginate matrices**

Experiments were performed using the MTT (3-(4,5-dimethylthiazol-2-yl)-2,5-diphenyltetrazolium bromide) assay for the determination of viable cell numbers within the alginate matrix. The MTT Cell Proliferation assay is a rapid colorimetric method, which is commonly used for the quantitative assessment of cellular survival and proliferation, based on the metabolic activity of viable cells (please see section 2.7 for a more detailed description of the MTT technique). Only active mitochondria of live cells can cleave the tetrazolium ring of the MTT compound. The absorbance subsequently measured for the blue formazan product generated from the MTT dye is linearly related to the quantity of viable cells added per well. Thus, the assay can be used to detect the cell proliferation rate and conversely, when metabolic events lead to apoptosis or necrosis, the reduction in cell viability [Mosmann, 1983; Ferrera *et al.*, 1993; Ciapetti *et al.*, 1992].



### **5.8.1 Comparison of cell numbers derived from MTT absorbance readings and from haemocytometer**

In order to confirm the linearity of the MTT assay, a series of cell standard curves were created from individual cell suspensions using T150 (150 cm<sup>2</sup>) flasks. Seventh passage (p7) human MSCs were harvested from tissue flasks and brought in cell suspension in Dulbecco's phosphate buffered saline with 1g/L D-glucose and 36mg/L sodium pyruvate (DPBSG, BioWhittaker), following the method described in section 2.1.3. The resulting cell suspension was serially diluted with DPBSG and seeded in a 96-well tissue culture plate as it is described in section 2.7.1. The MTT assay was then performed on the resulting samples as described in section 2.7, and the absorbance was measured at 600nm on a spectrophotometer (please see section 2.7.4.3).

The cell standard curves obtained for the T150 flasks were plotted according to the cell density (cell number/mL) measured simultaneously by haemocytometer count. Figure 5.10 shows one of the typical standard curves obtained from this analysis. The curve indicates that the MTT absorbance readings detected with the spectrophotometer correlated very closely to the cell concentration measured with the haemocytometer. This study confirmed that by following the MTT assay protocol described in section 2.7 it was possible to establish a linear relationship between the formazan absorbance readings and the cell concentration within the samples. This relationship was established for a cell suspension of hMSCs from tissue flask cultures harvested at day 4 of culture.

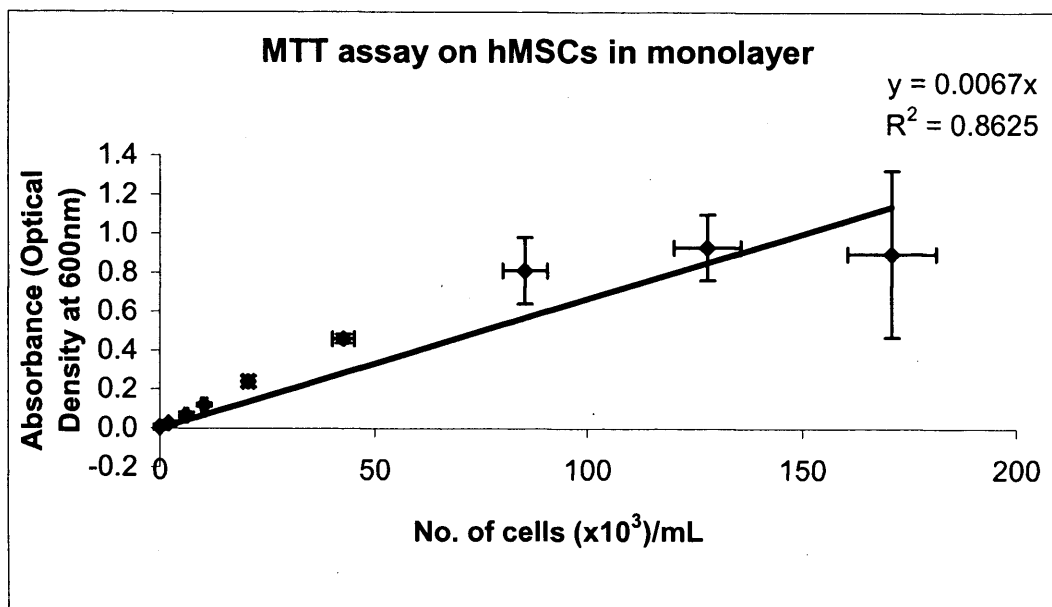


**Fig.5.10:** MTT absorbance values at 600 nm detected from human MSCs (p7) cultured in monolayer.

In this research the MTT assay was used to confirm the decrease of cell viability observed for cells encapsulated within the alginate beads.

Indeed, the MTT assay has already been used in previous studies for the determination of the status of several cell types in different alginate matrices [Barralet *et al.*, 2005; Lawson *et al.*, 2004; Markusen *et al.*, 2006; Rokstad *et al.*, 2005; Mahler *et al.*, 2003; Khattak *et al.*, 2006; Khattak *et al.*, 2006; Zhang *et al.*, 2005]. In this research, the technique was used at a preliminary stage, hence, prior to perform the assay on the matrix/cells beads, experiments were performed to confirm that the alginate biomaterial does not interfere with the absorbance readings measured and does not affect the validity of the results. In addition, only beads fabricated with non-derivatised alginate were tested for cell viability in the MTT experiments.

### **5.8.2 MTT cell proliferation assay on hMSCs expanded in monolayer condition in the presence of increasing concentrations of alginate in solution**

The aim of this study was to test any potential interference of the alginate biomaterial on the MTT absorbance readings measured during determination of cell viability for hMSCs expanded as a monolayer.

ProNova non-derivatised SLG100 alginate was used for this purpose. Sixth passage (p6) hMSCs cells were resuspended in complete DMEM, and seeded onto 24-well microplates in monolayer condition ( $6 \times 10^3$  cells/cm<sup>2</sup>) according to the usual plating protocol (please see section 2.1.2). 24 hours after plating, the medium of culture was removed from the wells and replaced with alginate in solution (1% w/v), which was serially diluted in complete DMEM medium. The cells were maintained in culture in the resulting alginate/DMEM solutions (alginate final concentration ranging from 0 to 100% v/v) for 10 days, with alginate/DMEM refreshments performed every 2-3 days. The MTT assay was performed on the resulting cell samples at the end of the culture period (day 10), following the protocol described in section 2.7.8.

The absorbance readings obtained for the microwell samples were plotted according to the alginate solution concentration in the DMEM medium. The data obtained from this analysis are shown in figure 5.11.

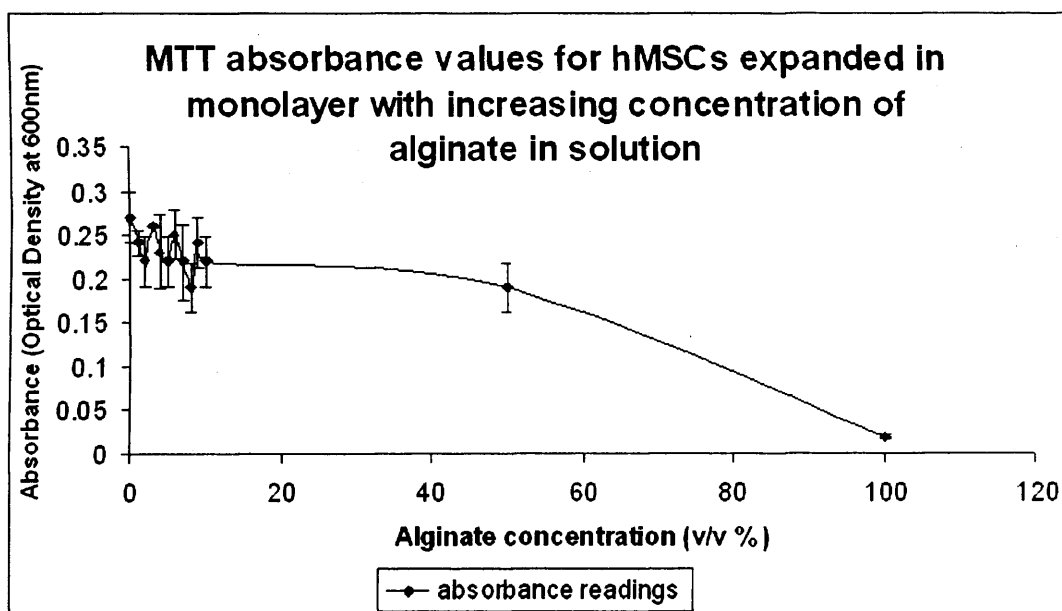


**Fig. 5.11:** MTT absorbance values obtained for hMSCs in microwell ( $6 \times 10^3$  cells/cm<sup>2</sup>) after 10 days in culture in the presence of an increasing concentration of alginate in solution (0, 1, 2, 3, 4, 5, 6, 7, 8, 9, 10, 50 and 100 v/v %).

As it is evident in the graph, the alginate solution did not affect the MTT absorbance readings detected with the spectrophotometer up to a 50% v/v concentration. Whilst no significant difference was observed between the absorbance readings measured for cells expanded in the alginate solutions with concentration ranging from 0% to 50% v/v, a significant decrease in the absorbance value was observed for hMSCs expanded in the complete (100% v/v) alginate solution. These results indicate that the cells experienced a dramatic drop in cell viability following a 10-day culture in the alginate solution. As it is shown in the graph, cells that had been completely deprived of the DMEM medium of culture over the 10-day period, and had been grown instead in the complete alginate solution, retained no cell viability. The absorbance readings measured for these DMEM-deprived cells were in fact comparable to those measured for the blank (i.e. complete DMEM medium only) microwells.

According to these data, hMSCs can be cultured in monolayer condition in the presence of alginate solution with a concentration up to 50% v/v, without experiencing cell death due to the presence of the alginate polymer.

### **5.8.3 MTT cell proliferation assay on hMSCs expanded in monolayer culture in the presence of an increasing number of cell-free alginate beads**

Experiments were also performed using cell-free alginate beads to test whether the presence of the alginate polymer, after cross-linking treatment and gelling into hydrogel beads, had any effect on the absorbance values measured for samples of hMSCs expanded in monolayer culture.

Pronova non-derivatised SLG100 alginate and sixth passage (p6) hMSCs were used in these studies. The cells were harvested from T150 flasks and resuspended in Dulbecco's phosphate buffered saline with 1 g/L D-glucose and 36 mg/L sodium pyruvate (DPBSG, BioWhittaker). The cell suspension was seeded into two 96-well plates ( $2.05 \times 10^4$  cells/well) as it is described in section 2.7.6 and an increasing number of cell-free alginate beads (0, 1, 2, 3 and 4) were added to the microwells in culture. The culture was performed under the optimal conditions identified in the monolayer studies (please see results from chapter 4) and was maintained for a 10-day period. The MTT cell proliferation assay was performed at the end of the culture

period (day 10), following the protocol described in section 2.7. The MTT solution was left in incubation at 37°C for one 1 hour and the absorbance values were read on the spectrophotometer at 600nm within 1 hour from isopropanol/HCl addition, following the standard MTT assay protocol, as described in section 2.7.4.3.

The results are presented in figure 5.12.

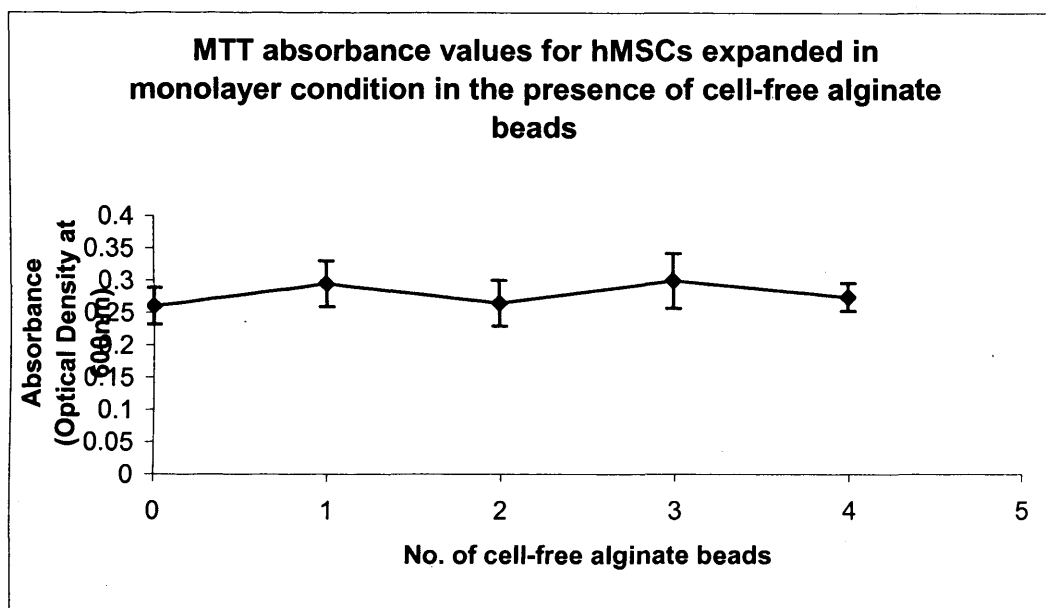


**Fig. 5.12:** MTT absorbance values measured at 600 nm for hMSCs expanded in monolayer condition ( $2.05 \times 10^4$  cells/well) in the presence of an increasing number of non-derivatised alginate beads. The assay was performed 10 days after plating.

It is apparent from this graph that there was no significant difference in the absorbance values detected for hMSCs expanded in monolayer in the presence of an increasing number of cell-free alginate beads. Thus, the presence of the alginate biomaterial in the assay does not interfere with the absorbance readings for the period examined. As a result, it can be concluded that short-term culture of hMSCs microwell samples in the presence of alginate gel beads is possible without experiencing a subsequent change in absorbance readings and in the cell proliferation potential.

### 5.8.3.1 MTT cell proliferation assay on hMSCs immobilised in alginate beads

The MTT assay was then used to measure cell proliferation potential for hMSCs immobilised in Pronova SLG100 alginate beads (average  $4.47 \times 10^3$  cells/bead). The constructs were fabricated according to the usual protocol (please see section 2.5.3) and were maintained in culture over a 14-day period. The microwells were seeded with an increasing number of beads (0, 2, 4 and 6) and were cultured under the optimal culture conditions identified from the monolayer studies described in chapter 4. At selected time-points (day 1, day 4, day 7 and day 14) cell proliferation within the beads was assessed by means of the MTT assay. These data are presented in figure 5.13.

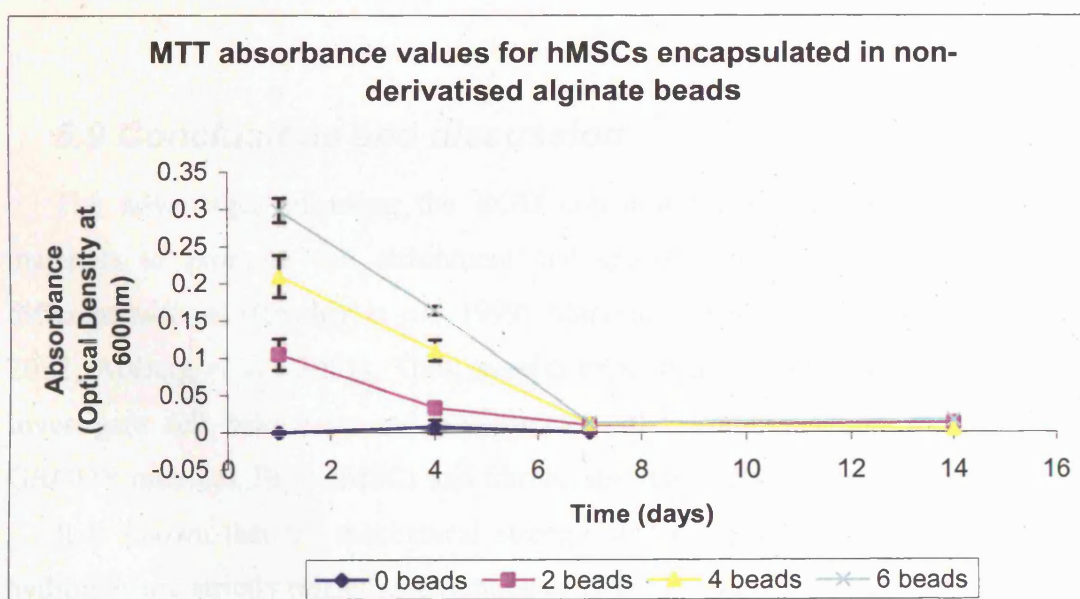


**Fig. 5.13:** MTT absorbance readings measured at 4 different time-points (day 1, day 4, day 8, day 14) for an increasing number of alginate/hMSCs beads (average  $4 \times 10^3$  cells/bead). The constructs were maintained in the culture conditions that in the extensive monolayer studies presented in chapter 4 were associated with the highest growth kinetics and cell viability data.

The graph in figure 5.13 indicates that there was a good linear relationship between the number of beads evaluated and the formazan absorbance readings measured with the spectrophotometer. This relationship was established for constructs cultured over a 4-day period. The absorbance measurements taken at the additional time-points (day 8 and day 14) indicate that the cells were characterised by a significant decrease in cell viability after immobilisation within the alginate bead matrices. In conclusions, the MTT assay data confirmed the lack of cell proliferation experienced by hMSCs immobilised within non-derivatised alginate beads. Ultimately, the absorbance readings measured with the MTT assay appeared to be consistent with the cell density and cell viability measurements obtained with the haemocytometer and the trypan blue exclusion dye assay. In principle, this proves that the MTT cell proliferation assay can be used in future studies as a reliable method for the quantitative assessment of the proliferation and mitochondrial metabolic activity of viable cells encapsulated in alginate-GRGDY constructs.

## **5.9 Conclusions and discussion**

The advantages of using the RGD containing alginate matrices as scaffold materials to promote cell attachment and growth have already been shown by different authors [Rowley *et al.*, 1999; Markusen *et al.*, 2006; Halberstadt *et al.*, 2002; Alsberg *et al.*, 2001]. Thus, several experiments were performed in order to investigate cell behaviour and performance after immobilisation within alginate-GRGDY matrices. Both hMSCs and fibroblasts were analysed for this purpose.

It is known that the mechanical strength and compression modulus of alginate hydrogels are strictly related to the ratios of G to M subunits, as well as to the lengths of G blocks [Smidsor and Skjak-Braek, 1990]. In addition, recent evidence suggests that the alginate viscosity may have significant impact on the viability of encapsulated cells [Kong *et al.*, 2003]. As a result, it was interest of this research to evaluate the effects of alginates with different chemical compositions and viscosities on cell behaviour and mechanical integrity during the fabrication of alginate-cells beads. High mannuronic acid (M) content alginates (i.e. alginate SLM100 and SLM20) proved not to be ideal biomaterials for cell immobilisation and beads preparation. The constructs created with these alginates appeared to be weak and

fragile, and quickly dissolved after treatment with the cross-linking solution. On the other hand, the use of high guluronic acid (G) content alginates permitted the fabrication of stronger beads, which retained their structural integrity over time. These results are well in accordance with previous studies indicating that alginate containing the highest percent of guluronic acid is the most mechanically stable [Wong *et al.*, 2001] and that the strength of the network depends on the overall fraction of G units [Smidsor and Skjak-Braek, 1990; Martinsen *et al.*, 1989; Stabler *et al.*, 2002].

Moreover, regardless of the peptide concentration used for the coupling reaction (i.e. 10X or 32X), both hMSCs and fibroblasts in SLG100 alginate beads did not interact with the biomaterial and did not elongate to acquire their characteristic spindle-shaped morphology. The initial cell viability within the constructs was high ( $>92.18\% \pm 2.9\%$ ) but no cell proliferation was observed over time. A similar lack of cell adhesion and cell growth was also seen after seeding the cells on the surface of alginate-GRGDY disks. Ultimately, additional studies are needed to clarify the mechanisms responsible for the lack of cell attachment in the modified alginate matrices.

Finally, preliminary studies proved that the MTT assay can be used as a reliable method for the quantification of metabolically active cells within the alginate matrix. The assay proved not to be adversely affected by the presence of the alginate polymer itself within the samples, and MTT data revealed lack of cell proliferation after immobilisation within non-derivatised alginate constructs. These results are in accordance with the cell proliferation data obtained with the haemocytometer measurements presented in sections 5.3-5.6. However, further studies including the assessment of positive control samples (i.e. alginate/cells beads characterised by good proliferation kinetics from haemocytometer data) will need to be conducted to confirm the consistency and thus the validity of the MTT data presented in this research.

In conclusions, in this research it was not possible to obtain immobilised cells, which were associating with the matrix once the GRGDY peptide motif was incorporated into the alginate polymer. These findings are inconsistent with previous studies indicating that, after incorporation of RGD-containing sequences, alginate matrices are able to promote adhesion, proliferation and differentiation of different cell types, including mouse skeletal myoblasts [Rowley *et al.*, 1999; Rowley *et al.*,



2002]. In particular, previous studies have shown that also adult hMSCs can be encapsulated in alginate beads with a substantially retained viability (>80%), and that the GRGDY peptide encourages hMSCs attachment and elongation within the three-dimensional matrix [Markusen *et al.* 2006].

The lack of cell adhesion and functions within alginate-GRGDY matrices observed in this research may have been caused by the loss of the final tyrosine residue from the GRGDY peptide sequence bound to the alginate polymeric chain (please see amino acid analysis data presented in chapter 3). The detachment of the tyrosine residue may have caused a significant stereochemical change in the overall three-dimensional configuration of the resulting alginate-GRGDY. This may have caused a rearrangement of the charge distribution along the polymeric chain of the modified matrix. Since the polyelectrolyte nature of the alginate molecule is also an important parameter for its function [Draget *et al.*, 2005], the altered stereochemistry and conformational properties of the resulting scaffold may ultimately have been responsible for obstructing and preventing cell adhesion to the biomaterial. Thus, the chemistry and structural configuration of the adhesion ligand chosen for the covalent coupling to alginate hydrogels seems to play a critical role in the specific adhesion properties of the resulting matrix.

Overall, further optimisation of the alginate derivatisation process is required to achieve the appropriate adhesion properties for optimal cell binding, and more work is required to design a practical and reproducible system for hMSCs immobilisation.

## **6. Conclusions**

### **6.1 *The goal of this thesis***

The final goal of this research was the fabrication of functional tissue-engineered constructs suitable for clinical use. For this purpose, selected cell types were mixed with a natural water-soluble polymer and, following gelling of the polymer by addition of a cross-linking agent, the resulting polymer/cells mixture was processed into homogeneous gel beads.

This approach may for example be applicable for the fabrication of blood vessel substitutes that can potentially be employed for the treatment of blood vessels diseases (e.g. coronary artery disease and atherosclerosis), thus addressing a noteworthy clinical need (please see section 1.1.6).

Essential requirements for the fabrication of any functional tissue-engineered substitute are structural uniformity and homogeneous cell distribution. In the specific case of living blood vessels, in order to resemble the cell elements that compose the *media* and *adventitia* layers (i.e. smooth muscle cells and fibroblasts respectively), the cells must be able to elongate and spread out within the scaffold, thus giving rise to flattened cell layers lining the surface of the graft, so that it can ultimately acquire a normal vessel-like appearance.

In particular, this research project was focused on investigating both alginate hydrogels and hMSCs respectively as the matrix and the cell source to be used for the fabrication of functional matrix/cells constructs.

### **6.2 *The alginate biopolymer***

In first instance, it was intended to devise a process for producing a scaffold suitable for addition to the cell suspension and, ultimately, for the fabrication of

functional scaffold/cells constructs where cell adhesion was encouraged and cell viability maintained over time.

Sodium alginate, which has a major use in tissue engineering applications [Atala *et al.*, 1994; Hauselmann *et al.*, 1996], was the natural polymer selected among all other biomaterials for the fabrication of the constructs. Alginate is relatively biocompatible and approved by the Food and Drug Administration (FDA) for human use as wound dressing material [Atala, 2004]. Because of their gentle gelling properties, low toxicity, abundance in source and low price alginates are widely used for cell encapsulation *in vitro* and *in vivo* and for several tissue engineering applications [Drury and Mooney, 2003; Rowley and Mooney, 2002; Kuo and Ma, 2001]. However, it must be noted that the hydrophilic nature of the alginate normally discourages protein adhesion and cell attachment [Smentana, 1993; West *et al.*, 1997]. As a result, in applications that require some anchorage-dependent cell cultures (the majority of mammalian cell types, e.g. mesenchymal stem cells and smooth muscle cells), alginate hydrogels have been chemically modified to covalently attach cell adhesion molecules [Rowley *et al.*, 1999; Alsberg *et al.*, 2001; Markusen *et al.*, 2006]. In this research, studies were performed on the biomaterial itself, whereby the alginate was chemically modified using aqueous carbodiimide chemistry with a protein containing the Arg-Gly-Asp (RGD) attachment site, a sequence known to promote cell attachment [Ruoslahti, 1996]. The alginate biomaterial modified by addition of RGD-containing peptides has already demonstrated to permit and support adhesion and proliferation for several cell types, including endothelial cells, preadipocytes, fibroblasts and skeletal myoblasts [Rowley *et al.*, 1999; Greene *et al.*, 2000; Loeb sack *et al.*, 2001]. In this research the alginate was covalently modified to attach the RGD adhesion ligand according to the method described by Rowley and colleagues (1999), which was modified with respect to the reactants (i.e. EDC and sulfo-NHS) concentrations. The GRGDY pentapeptide was chosen as the RGD-containing sequence to mimic cell adhesion proteins and promote cell adhesion on the alginate scaffold.

## 6.2.1 Derivatisation of the alginate polymer

Several conditions were investigated in order to optimise the derivatisation of the alginate, and the degree of peptide attachment in the resulting biomaterial was examined and assessed by means of nuclear magnetic resonance (NMR) and amino acid analysis. The material employed in this research was supplied in sterile form with negligible endotoxin level ( $\leq 100$  EU/gram) [www.novamatrix.biz]. Thus, the alginate did not require autoclaving or filtration, which in previous studies [Markusen, 2005] proved to be ineffective techniques for the sterilisation of the alginate biomaterial. Autoclaving would have been particularly undesirable because it would reduce the alginate viscosity and molecular weight [Leo, 1990; Vandenbossche and Remon, 1993] and would denature the GRGDY peptide.

High ( $> 100$  mPa·s) and low (20-100 mPa·s) viscosities alginates, with different guluronic and mannuronic acid compositions (i.e. either high G alginates with  $\geq 60$  % guluronic acid content, or high M alginates with  $\geq 50$  % mannuronic acid content) were investigated. No major dissimilarities were identified among these biomaterials during the derivatisation reaction and the subsequent dialysis step. However, after reconstitution and derivatisation with the GRGDY peptide, low viscosity (SLG20 and SLM20) alginates appeared to be slightly more heterogeneous and less viscous than the high molecular weight (SLG100 and SLM100) products.

Based on the results from previous range-findings studies [Markusen, 2005], it was decided to perform investigations focusing on the use of 9X-12X reactants (EDC and sulfo-NHS) and 1X-32X GRGDY peptide concentrations. These concentrations were multiples of the 1X reactants concentrations described by Rowley (1999), where 1X reactants correspond to 1mg of alginate containing 38  $\mu$ g of sulfo-NHS, 67  $\mu$ g of EDC and 1  $\mu$ g of peptide. 9X, 12X and 32X were respectively 9, 12 and 32 times the reactants concentration, as defined by Rowley. 9X EDC and sulfo-NHS and 32X peptide proved to be sufficient concentrations for the incorporation of the pentapeptide onto the alginate polysaccharide chain. Amino acid analysis data revealed that alginate-GRGDY samples prepared in this condition did contain all the constituent amino acid residues of the pentapeptide sequence (i.e. G, R, D and Y). It follows that higher level of reactants were required in this research for the polymer-GRGDY covalent binding, as compared to what was

observed by Rowley in his work. This discrepancy may be explained by the variation in the reactants that have been used in each study. Rowley tested alginates supplied by different manufacturers in his investigations, but he also used the same ProNova Biopolymers high G content sodium alginate that was used in this research. It must be noted that ProNova polymers are manufactured in compliance with US FDA (Food and Drug Administration) guidelines for current GMP (Good Manufacturing Practice) practice (Code of Federal Regulations, Title 21, Part 210 and 211), and adhere to the most stringent standards [www.novamatrix.biz]. These products are developed through use of validated analytical methods and automated manufacturing processes. Under these circumstances variability of results should be an exception. However, the GRGDY peptide and the other reactants used in this research have been provided by different manufacturers, as compared to the products used by Rowley and colleagues, and also by Markusen in most of her studies. These variations, together with batch to batch variability, cannot be excluded as possible cause to the different reactants concentrations required to achieve successful polymer-GRGDY binding through the carbodiimide chemistry reaction described.

Following the dialysis cycle, it was necessary to re-concentrate the alginate-GRGDY, which had been extensively diluted due to the influx of water into the dialysis cassette. The results presented in this research revealed that lyophilisation, as opposed to the use of a polyethylene glycol (PEG) solution, is more appropriate for re-concentrating the alginate after the dialysis cycle. Previous studies [Markusen, 2005] had shown that a 2-day lyophilisation cycle was sufficient for re-concentrating the alginate, whilst retaining the stability of the peptide in the alginate hydrogels and the biological activity of the resulting alginate-GRGDY. These results were confirmed by the amino acid analysis data presented in this thesis, which showed successful incorporation of the peptide sequence onto the alginate following a 2-day lyophilisation cycle.

### **6.2.2 Alginate-GRGDY characterisation**

Nuclear magnetic resonance (NMR) was performed on the alginate-GRGDY samples as a qualitative measure to assess the incorporation of the GRGDY peptide

in the alginate biomaterial. However, this technique did not prove to be a suitable method to ascertain the attachment of the peptide onto the alginate. The signals at  $\delta$  6.8 ppm and 7.1 ppm, typically originating from a tyrosine residue, were not detected when both derivatised SLG100 (coupled with 10X peptide) and SLM100 (coupled with 1X peptide) alginates were analysed with NMR spectroscopy. It can therefore be concluded that this technique is probably not sensitive enough to allow the detection of the tyrosine peaks in the alginate-GRGDY samples. NMR has in fact very low sensitivity and only millimolar concentrations of substrates (lower limit of detection = 1-5  $\mu$ M) can be detected with this methodology [Syrota and Jehenson, 1991; Wishart, 2006], while amino acid analysis data revealed that the level of tyrosine was indeed very low (i.e. < 9.3n.mole/mg) in the alginate samples resulting from the derivatisation procedure. This might explain why NMR failed to detect the tyrosine residue and, ultimately, to measure the degree of peptide attached to the alginate polymer.

As opposed to NMR, amino acid analysis allowed for a more reliable quantification of the degree of peptide incorporated in the polysaccharide chain of the SLG100 alginate. Amino acid analysis data demonstrated that all four component amino acids (G, R, D and Y) of the GRGDY pentapeptide were present in the alginate coupled with either 9X or 12X EDC and sulfo-NHS and either 32X or 10X peptide. These data indicated that a successful polymer-GRGDY coupling reaction was achieved under these conditions. No significant difference was observed in the amino acid content for the alginate-GRGDY coupled with either 9X or 12X EDC and sulfo-NHS concentrations. As a result, 9X was the concentration maintained for these reactants throughout all the subsequent experiments. It is also interesting to note that there seemed to be a direct proportionality between the peptide concentration used in the carbodiimide chemistry reaction and the amino acid levels measured following the derivatisation procedure. However, even though successful incorporation of the GRGDY peptide was achieved, the amino acid analysis also revealed that a significant (approximately 60 %) loss of the final tyrosine residue was occurring during derivatisation in all the SLG100 alginate samples. This phenomenon will require future investigations.

Markusen [Markusen, 2005 and 2006] did not measure the amino acid levels in her final alginate-GRGDY, thus one can only assume that her alginate-GRGDY contained an intact sequence (complete of tyrosine) from the positive results she obtained from her cell adhesion studies. On the other hand Rowley did quantify the GRGDY ligand incorporated onto the alginate by labelling it with a radioactive tag ( $^{125}\text{I}$ ), and saw no tyrosine loss. It was rather unexpected to observe in this research a consistent tyrosine loss from the alginate-GRGDY samples. This was indeed surprising, especially considering that the same derivatisation procedure described by both Rowley and Markusen was followed, but neither Rowley nor Markusen did observe a similar phenomenon in their studies. Possible causes for these discrepancies are difficult to speculate. As already mentioned, the divergent results may perhaps be attributed to different manufacturers and batch to batch variabilities. In particular, the amount of EDC present in the reaction is known to have a dramatic effect on peptide incorporation efficiency [Rowley *et al.*, 1999]; thus, even a small difference in the concentration of EDC appearing in the reaction vessel may have been responsible for such different outcomes. In addition, EDC-mediated cross-linking of the alginate with diamines is known to be affected by both the pH and the NaCl concentration of the reaction medium [Rowley *et al.*, 1999], therefore the divergent results may also be attributed to possible changes of these parameters, which in this research have not been monitored throughout the whole derivatisation procedure.

### **6.3 Characterisation of human mesenchymal stem cells expanded in monolayer culture**

Primarily studies using multipotent fibroblast-like plastic-adherent cells isolated from frozen bone marrow samples of adult patients were performed. These cells were recovered from the bone marrow according to a well-established density gradient protocol [Friedenstein *et al.*, 1968]. It is acknowledged that these cells represent a heterogeneous population, which includes a variety of progenitor cells at different stages of their differentiation pathways [Tavassoli *et al.* 1983; Lichtman, 1981; Allen *et al.*, 1990; Bianco *et al.*, 2001]. As a result, Horwitz *et al.* (2005) have



recently proposed to term this cell population as “mesenchymal stromal cells”, which is a more general and, thus, more appropriate definition. However, these cells are here defined as “mesenchymal stem cells” (MSCs), as this was the accepted and popularised term at the beginning of this research, when stem cells were more generally defined as cells having the ability to self-renew and, under proper culture conditions, the potential to differentiate into a variety of cell and tissue types (i.e. including tissues other than those originating in the mesodermal germ layer) [Quarto *et al.*, 1998; Pereira *et al.*, 1995; Caplan, 1991; Lalan *et al.*, 2001; Stock and Vacanti, 2001].

Prior to the cell immobilisation in the alginate matrix, studies were performed to identify the optimal conditions for cell expansion in monolayer culture.

Despite the need for vast number of hMSCs as therapeutic means, there is only limited information on the optimisation of culture conditions required for their large-scale production for clinical applications [Bianco *et al.*, 2001; Tuan *et al.*, 2002; Sotiropoulou *et al.*, 2005]. Nevertheless, Athersys has recently licensed a noteworthy invention for providing a substantially homogeneous stem cell population of non-embryonic origin that can be maintained in culture in the undifferentiated state or can be differentiated to form cells of multiple tissue types. In their patent, the methods of isolation and culture, as well as therapeutic uses for the isolated cells are described [Furcht *et al.*, 2005]. However, one must remember that the scale-up of a MSCs reservoir that can be available for “off-the-shelf” use implies the utilisation of allogeneic cells. In this case, significant issues of host rejection, disease transmission and ethical disquiet need to be overcome.

Although the long-term goal remains the production of a sufficient number of safe cells that can be ready in advance of need, a more realistic short-term goal is to develop an optimised protocol for the MSCs *in vitro* expansion. As a result, several variables were investigated in this research to improve the hMSCs expansion protocol in monolayer condition. In particular, attention was focused on changing medium composition in respect of serum concentration and FGF-supplementation, on modifying the plastic surface of the culture vessels through coating with different biomolecules, and on testing different oxygen tensions. Following measurements taken with a haemocytometer and the Nova Biomedical BioProfile 400 analyser, the monolayer cell samples were assessed according to their growth kinetics, their

doubling time, cell growth rate and their specific glucose consumption rate. In addition, cell percent viability was assessed at each expansion passage by means of the trypan blue dye exclusion assay.

### **6.3.1 Basal growth medium formulation**

The choice of an appropriate medium formulation is an important *in vitro* condition, having direct influence on stem and progenitor cells expansion and maintenance in culture [Sotiropoulou *et al.*, 2005; Robertson, 1987; Hogan *et al.*, 1994]. Preliminary studies were conducted in order to evaluate two different commercially available basal medium formulations toward their proliferation promoting capacity on hMSCs *in vitro*. Following direct comparison with the more expensive MesenCult medium (StemCell Technologies Inc.), low-glucose DMEM medium (BioWhittaker) demonstrated to permit better cell growth and higher cell densities, and was therefore preferred in all subsequent experiments for hMSCs expansion.

Most basal cell media cannot support the growth of mammalian cells by themselves. As a result, it is a common practice to supplement cell culture media with animal sera [Shah, 1995]. Serum additives are typically provided by fetal bovine serum (FBS), which is capable of supporting the growth of a variety of cell types. The availability and ease of storage of FBS [Barnes and Sato, 1980], together with its rich content of growth factors and nutrients for proliferation and differentiation [Lambert and Birch, 1985; Palsson and Bhatia, 2004], have led to its adoption as the standard medium supplement. However, the use of animal-derived sera in tissue culture systems is a practice that raises ethical, scientific and safety concerns [Even *et al.*, 2006]. Serum is an ill-defined mixture, containing by-products like bacterial endotoxins and contaminants such as viruses, prions and mycoplasma [Merten, 1999; Falkner, 2004], which ultimately impair the use of culture-derived products. Given its undefined composition, batch to batch variability, which may seriously affect experimental data, is also normally associated to serum use [Morris and Warburton, 1975]. In addition, FBS is harvested from bovine fetuses taken from pregnant cows, and it is estimated that between 44 and 144 heads of cattle must be slaughtered to obtain only one litre of FBS [Hodgson, 1991]. This consideration

has obviously captured the attention of several animal welfare associations, which believe that researchers have a moral and legal obligation to replace animals with alternatives when they are available [AAIIR [http://www.aahr.asn.au/campaigns/fetal\\_calf\\_serum.html](http://www.aahr.asn.au/campaigns/fetal_calf_serum.html); “Australian Code of Practice for the care and use of animals for scientific purposes” 2004]. Given the recognized controversy that is currently surrounding the use of animal-derived serum for proliferation enhancement during *in vitro* cell culture [Falkner *et al.*, 2004; Even *et al.*, 2006; [www.focusonalternatives.org.uk](http://www.focusonalternatives.org.uk)], interest of this work was to investigate the possibility for hMSCs expansion in serum-free culture settings. Extensive studies were performed to investigate the effects of fetal bovine serum on hMSCs proliferative capacity and metabolic activity. The data obtained from these investigations revealed that 10 % serum-supplementation resulted necessary to achieve good cell growth, high cell viability and to retain cellular metabolic activity. However, three commercially available serum-free formulations (i.e. UltraCulture and UltraDOMA Hybridoma optimised media, both from BioWhittaker, and the Knockout DMEM medium from Gibco) also showed interesting and encouraging preliminary data, resulting capable of permitting long-term culture of hMSCs in serum-free environment.

In addition to serum requirements, bFGF has also demonstrated to have a significant impact in stem cell culture [Kotobuki *et al.*, 2004; Bianchi *et al.*, 2003; Martin *et al.*, 1997; Reyes and Verfaillie, 1999; Nagai *et al.*, 1999]. As a result, the effects of bFGF-supplementation on hMSCs proliferation potential and viability were also investigated. In line with previous data [Sotiropoulou *et al.*, 2005; Kotobuki *et al.*, 2004; Bianchi *et al.*, 2003] the data presented in this research revealed that bFGF-supplementation significantly improves and favours cell expansion and proliferation. Addition of 1 ng/mL bFGF was associated with higher cell proliferation rates, higher cell densities and lower doubling times, as compared to the values observed for cells maintained in bFGF-free growth medium. What is particularly interesting is that the growth factor seemed to favour considerably hMSCs expansion also in serum-deprivation (2% FBS) condition, where cell proliferation resulted heavily compromised in the absence of the growth factor. Moreover, the presence of bFGF in serum-free microenvironment also significantly hampered cell death. These findings suggest that bFGF-supplementation may well

represent an essential additive for those culture systems that are being developed to avoid FBS use for cell *in vitro* expansion.

### 6.3.2 Different coating conditions for the culture vessels

Previous studies have shown that the behaviour of mesenchymal stem cells is also significantly affected by the culture surface properties employed in their *in vitro* settings [Ogura *et al.*, 2004; Matsubara *et al.*, 2004; Qian and Saltzman, 2004]. In line with these considerations, the culture surface of the vessels employed in this study demonstrated to have a considerable impact on hMSCs expansion. Among the different coatings tested, Matrigel seemed to significantly hamper cell growth, cell viability and metabolic activity. On the other hand, the use of fibronectin-coated plates did not have such a negative effect, but did not lead to any advantage as opposed to the use of the traditional non-coated vessels either. Both non-coated and fibronectin-coated plates consistently supported hMSCs proliferation and metabolic activity, and these coatings effects were observed regardless of the serum concentration used for the medium supplementation.

These findings are rather unexpected, given that fibronectin contains the RGD cell adhesive site [Ruoslahti and Pierschbacher, 1986; Magnusson and Mosher, 1998], a peptide sequence with well-documented cell adhesion properties. Indeed fibronectin has been shown to support attachment of different cell types both *in vitro* [Prajapati *et al.*, 1996; Ejim *et al.*, 1993] and *in vivo* [Whitworth *et al.*, 1995; Sethi *et al.*, 2002]. In addition, enhanced cell adhesion and spreading have been previously observed for hMSCs expanded in fibronectin-coated dishes [Ogura *et al.*, 2004]. However, other investigators have also seen no difference in MSCs growth on surfaces coated with either fibronectin or the polystyrene control [Qian and Saltzman, 2004]. Similarly to what Qian observed in his studies, this research also revealed that the typical morphology of undifferentiated MSCs was retained on both fibronectin-coated and non-coated surfaces. The inconsistency of the data presented by different groups is not easy to explain. Indeed the expectation would have been that the RGD sequence contained in the fibronectin coating would have favoured cell attachment, whereas this research (and Qian's group) shows that hMSCs adhesion occurred at the same extent in the fibronectin-coated and the traditional non-coated plates. However, given their complexity, cell-cell and cell-matrix

interactions are still unclear, and virtually nothing is known of the interactions between stromal precursor cells and the extracellular matrix *in vivo* [Gronthos *et al.*, 2001]. That stromal precursors possess a high binding affinity to the extracellular matrix components commonly found in the reticular marrow (e.g. fibronectin, collagen I, collagen III) is a reality. However, it is also true that the attachment of cells to various glycoproteins may depend on their original location and their stage of cellular differentiation [Gronthos *et al.*, 2001]. Because the cell population investigated in this research most likely comprised mesenchymal stromal cells at different stages of their differentiation pathway, and because the exact location of these cells in the marrow spaces is still a matter of conjecture [Gronthos *et al.*, 2001], this may perhaps justify more easily the differential binding affinity to fibronectin that is observed by different investigators.

### **6.3.3 Dissolved oxygen tension (DOT)**

Dissolved oxygen tension (DOT), which is known to have a profound influence on the growth potential and functionality of different cell lines [Lennon *et al.*, 2001; Martin *et al.*, 2004; Domm *et al.*, 2004; Ezashi *et al.*, 2005; Moussavi-Harami *et al.*, 2004; Rochefort *et al.*, 2006], was an additional parameter investigated in this research for hMSCs *in vitro* expansion. The ambient 21 % O<sub>2</sub> traditionally employed in most culture environments was compared with lower oxygen levels, ranging from 1 % to 10 % O<sub>2</sub>. The results presented in this thesis revealed a positive effect of the high (21 %) DOT on cell proliferation rate and cell density. hMSCs grown at the 21 % standard oxygen DOT were characterised by the highest proliferation potential and the lowest doubling time; on the other hand, cells maintained at lower oxygen regimes (10 %, 6 %, 2 % and 1 %) did not demonstrate a similar growth capacity. However, it must be noted that no oxygen effect on cell viability was observed in this research. In addition, no evident changes in cell morphology were seen among cells expanded in all the different oxygen regimes investigated (i.e. 1%, 2%, 6%, 10% and 21%). One hypothesis that can be drawn as to why no oxygen effect on cell viability was seen is that the cells might have been able to quickly adapt to the change of environment and the different oxygen levels applied to the incubators settings. The cells were in fact transferred to the lower oxygen levels after incubation in the ambient (i.e. 21%) O<sub>2</sub> condition, and were maintained under the

different low oxygen regimes selected only for the limited culture period under investigation (i.e. 2 weeks). This might explain why a significant oxygen effect was seen mostly on cell proliferation capacity and growth rate, while no significant changes in cell viability and morphology were observed as a result of the short-term hypoxic treatments. To date, studies focusing on the MSC responses to hypoxia have been inconclusive [Lennon *et al.*, 2001; Mackay *et al.*, 1998; Wang *et al.*, 2005], and the mixed results reported for MSCs proliferation and differentiation under hypoxia highlight the need for further studies elucidating the pathways involved in hypoxic processes for these cells [Ma *et al.*, 2001; Malladi *et al.*, 2006].

#### **6.3.4 Optimal culture conditions identified for hMSCs growth in monolayer**

The extensive monolayer studies performed in this research permitted to identify the optimal culture conditions for hMSCs, allowing cell viability and promoting cell proliferation during *in vitro* expansion in tissue culture microwell plates. Overall, the combined use of 10 % (v/v) serum- / 1 ng/mL bFGF-supplemented low-glucose DMEM medium and non-coated culture vessels in high (21 %) oxygen tension was associated with the highest cell growth kinetics (average  $38.9 \times 10^4$  cells/cm<sup>2</sup> counted after 13-14 days in culture), highest cell viabilities (average 96.08% +/-3.01% over 2-week culture), and lowest doubling times (average 58.36 hours calculated from day 0 to day 7). In addition, hMSCs expanded for four subsequent passages in monolayer culture under these conditions proved to retain their undifferentiated state and their differentiation potential. Fourth passage (p4) hMSCs induced for 21 days with adipogenic, osteogenic and chondrogenic differentiation media demonstrated the ability to respectively differentiate to the phenotypes of adipocytes, osteocytes and chondrocytes.

### **6.4 Matrix/cells constructs**

The overall objective of this research was the fabrication of functional tissue-engineered constructs with the potential to be employed in therapeutic applications. Following studies focusing first on the alginate matrix itself and then on the cell

expansion in monolayer culture, investigations were therefore performed on the fabrication of alginate/cells beads and disks. By utilising the capability of the alginate to form a gel-like structure, alginate/cells constructs were prepared, and the optimal parameters identified in monolayer condition were applied to the culture of these constructs.

In order to ensure the functionality of a tissue engineered construct whereby attachment-dependent cells are employed, the cell elements must in the first place effectively interact with the polymer scaffold, which must therefore possess good cell adhesion properties. Cell elongation and alignment are also essential requirements in the specific case of smooth muscle cells and fibroblasts immobilised within constructs intended as human blood vessel replacements. Thus, the preparation of a natural matrix covalently modified with the GRGDY peptide (containing the well-known RGD adhesive site) has been investigated in this research ultimately to create a guidance scaffold, one that would have encouraged cell attachment and elongation after processing of the matrix/cells suspension into gel beads. However, the studies performed on the constructs demonstrated that, after immobilisation within the alginate matrix, both hMSCs and human foreskin fibroblasts failed to adhere to the alginate-GRGDY polymer. Light microscopy revealed that the cells appeared to be small and rounded, and cell attachment was not observed even several days after plating. Histological staining confirmed that the cells resulted unable to spread and elongate within the biomaterial and could not acquire their characteristic spindle-shaped morphology. Lack of cell proliferation and significant cell death were also observed over time for all cell types within constructs prepared with either the unmodified or the derivatised alginates.

In several cases light microscopy also revealed that the cells tended to position in close proximity to the outer surface of the matrix/cells beads. This inhomogeneous cell distribution may have been caused by the intrinsic structural inhomogeneity of the alginate beads, which is a result of the rapid and virtually irreversible gelling mechanism taking place during the process of beads fabrication. It has in fact been reported that gels made by the diffusion-setting method utilised also in this research (please see section 2.5.3 for the full description of the method) often exhibit a polymer concentration gradient within the gel bead, due to the fast gelation rate with  $\text{CaCl}_2$  [Skjak-Braek *et al.*, 1989; Draget *et al.*, 2005; Thu *et al.*, 2000; Melvik and Dornish, 2004]. The rapid gelling kinetics of this methodology cause an



inhomogeneous distribution of the alginate, the highest concentration being at the surface and gradually decreasing towards the centre of the gel [Draget *et al.*, 2005]. This result has been explained by the fact that the diffusion of gelling ions create a sharp gelling zone that moves from the surface toward the centre of the gel. The activity of the alginate (and of the gelling ion) equals zero in this zone, and alginate molecules diffuse from the internal, non-gelled part of the gelling body toward the zero-activity region [Skjak-Braek *et al.*, 1989]. It is important to note that structural uniformity in scaffolds to be used for tissue engineering applications is necessary to ensure uniform porosity in all areas of the gel, thus permitting homogeneous cell distribution and, ultimately, uniform tissue formation [Kuo and Ma, 2001]. Thus, the particular gelling mechanism described above may explain why heterogeneous cell distribution was observed in the alginate beads fabricated in this research. Importantly, for tissue engineered scaffolds a homogeneous structure is desirable not only for uniform cell distribution, but also for well-controlled material properties. This is because the mechanical properties of the matrix result more consistent throughout the gel and between samples if the structure is homogeneous [Kuo and Ma, 2001].

Despite the lack of cell adhesion and cell proliferation within the alginate-GRGDY constructs, these studies also demonstrated that, among all the alginate types evaluated, high G high viscosity (SLG100) alginate was the most appropriate for the fabrication of rigid and stable gel beads. Alginate polymers with many repeating G-units are in fact normally more rigid and inflexible, and tend to form gels at rather specific concentrations of cations, as compared to alginate chains of repeating M-units, which form a softer gel over a wider range of conditions [<http://www.cybercolloids.net/library/alginate/structure.php>]. It has in fact been shown that a polymer of repeating G-units forms stiffer intra-molecular H-bonding [<http://www.lsbu.ac.uk/water/hyalg.html>]. Thus, the difference in strength of bonding between two subsequent uronic units results in the desirability of higher G-unit-containing alginates for use when culturing with cells. High purity and high G-unit alginate has in fact shown to retain 27% of its initial strength after 12 days in culture, compared to the high M-unit alginate, which loses its strength quicker [Wang *et al.*, 2003].

Ultimately, in this research alginate hydrogels covalently modified with the GRGDY peptide did not encourage cell attachment and elongation. This data are not

in line with previous studies where cell attachment was observed in constructs prepared with alginates chemically modified with RGD-containing sequences [Rowley *et al.*, 1999; Alsberg *et al.*, 2001; Halberstadt *et al.*, 2002; Marler *et al.*, 2000; Alsberg *et al.*, 2002; Markusen *et al.*, 2006]. In addition, importantly, the method described by Rowley and Mooney for the preparation of alginates modified through the covalent bonding of synthetic peptides containing the well-known RGD attachment ligand is now also protected by a US patent [Mooney *et al.*, 2003].

It can be hypothesised that the tyrosine loss consistently observed in this work was responsible for the lack of cell adhesion and ultimately cell survival and proliferation within the alginate scaffold. The missing tyrosine may have changed the structural conformation of the remaining peptide, thus affecting cell adhesion and resulting in the cells not binding to the normally well-recognised RGD attachment site. According to this hypothesis, the low value of tyrosine present in all the alginate-GRGDY samples analysed does account for as to why none of the cells successfully attached, after immobilisation within the derivatised alginate. If this is true, it will be particularly interesting to understand why tyrosine is lost during the derivatisation procedure, and at which stage of the process this loss occurs.

Different hypothesis can be drawn as to why this phenomenon was observed in all the alginate samples. Firstly, it must be noted that the significant tyrosine loss observed cannot be accounted for by the acid hydrolysis reaction during the amino acid analysis since, unlike other amino acids, tyrosine is not affected by the acid hydrolysis [[www.altabioscience.bham.ac.uk/services/amacid/](http://www.altabioscience.bham.ac.uk/services/amacid/)].

A second possibility could have been that an endopeptidase was present in the alginate, which could be cleaving the tyrosine off during the 20-hour reaction. If this were the case, the tyrosine would then be lost during the dialysis and therefore would not be present in the final alginate-GRGDY sample, thus confirming the results seen in the amino acid analysis. However, the ProNova alginate used in this research was supplied by the manufacturer as a sterile product, and the level of endotoxins in each vial of the original product is stated to be less than 100 EU/gram [[www.novamatrix.biz](http://www.novamatrix.biz)], corresponding to a quality for the purified polymer that exceeds FDA specifications for implantable polymers [Prokop and Wang, 1997]. Thus, one can conclude that also this second possibility is quite unlikely.

A reaction occurring between the tyrosine side chain and the coupling reactants could have been another possibility. The activation of tyrosine on the phenol ring ( $\text{HO-C}_6\text{H}_5$ ) for example could cause subsequent cleavage from the rest of the peptide. However, due to the high stability of the amide bond, this possibility is also considered to be unlikely.

In conclusion, neither of the above causes is very likely, and further work is needed to understand the mechanisms leading to tyrosine loss. This will probably permit in future to reproduce a derivatisation procedure that allows incorporation of normal tyrosine levels onto the alginate, thus ultimately permitting the fabrication of functional alginate-GRGDY scaffolds able to encourage cell attachment.

Interestingly, NovaMatrix has recently developed a new high quality, ultrapure peptide-coupled alginate, which is protected by a US patent licensed from the University of Michigan. The Novatach GRGDSP-coupled alginate is a trial product that could result particularly useful in cell therapy and tissue engineering applications where cell-to-matrix interaction is beneficial [[www.novamatrix.biz](http://www.novamatrix.biz)]. Thus, to use this product for the development of an alginate scaffold with optimal cell adhesion properties is an interesting alternative that can be investigated in future studies.

## 6.5 Conclusions

The investigations carried out in this research revealed some interesting findings in relation to the *in vitro* expansion of adult mesenchymal stem cells and their association with an alginate scaffold for tissue engineering applications.

- A procedure already described and employed for the derivatisation of the alginate matrix with the GRGDY cell adhesion sequence has been here reproduced, and some of the parameters involved have been further investigated in the attempt to optimise the process. Successful incorporation of the peptide onto the alginate polyaccharide chain was achieved under the conditions employed. However, some additional complexities, mainly the loss of the final tyrosine residue from the GRGDY sequence bound to the alginate, have been identified as critical in this process, and will need to be explored in future studies.
- Amino acid analysis has proven to be a useful and appropriate technique to ascertain the amount of peptide incorporated in the alginate biomaterial, and may be employed in future to elucidate the mechanisms underlying the tyrosine loss phenomenon.
- The effects of changes in several culture parameters on the *in vitro* hMSCs expansion as a monolayer have been used to establish their optimal growth conditions, associated with the highest cell growth rates and viabilities, the lowest doubling times, and maintenance of undifferentiated state and multipotentiality over time. These conditions can be applied to the culture of alginate/hMSCs constructs to promote cell proliferation once cell adhesion to the matrix will be achieved.
- Despite not promoting cell attachment after derivatisation with the GRGDY cell adhesion sequence, high G high viscosity alginate proved to be an appropriate biomaterial for the fabrication of rigid and stable gel constructs.

In conclusions, there are many questions that remain to be answered and that will require more work in future. Nevertheless, the findings observed in this research are of interest to the field of tissue engineering, as they highlight some of the fundamental complexities encountered when attempting the long-term *in vitro* expansion of hMSCs and the design of a practical cell immobilisation system to be implanted *in vivo*.

## **7 Recommendations for future work**

### **7.1 Additional parameters to be considered for optimisation of the alginate derivatisation procedure**

The work conducted in this research allowed for the optimisation of the procedure developed to introduce the cell attachment GRGDY peptide sequence onto the alginate polysaccharide chain. However, in order to further improve the derivatisation protocol, other conditions affecting the outcome of the coupling reaction will need to be investigated in future studies. These include the pH and osmolality of the alginate-GRGDY, which should be measured at every stage of the reaction to ensure that they are maintained at a physiological level relative to the extracellular matrix. In particular, it is well known that degradation of the alginate is a function of pH [Draget *et al.*, 2005]. In addition, the pH of the reaction medium has also been reported to affect cross-linking of alginate mediated by the EDC with diamines [Rowley *et al.*, 1999], and it has been proved that for optimal peptide incorporation in this system a neutral pH is indeed necessary [Rowley, 1999]. Thus, this parameter should be monitored carefully during the coupling reaction.

The light exposure of the reactants is an additional parameter that can potentially affect the efficiency of the derivatisation procedure. As a result, light exposure could also be carefully controlled and reduced to a minimum throughout the whole derivatisation process, in order to ensure maintenance of the stability of all the reactants and to avoid the peptide denaturation.

Future studies could also be performed to verify and adjust the viscosity of the reconstituted alginate-GRGDY, which is directly related to the molecular weight of the alginate [Smidsrod and Haug, 1972; Mackie *et al.*, 1980], and ultimately reflects the polymer chain stiffness and its gelling properties [Draget *et al.*, 2005].

It is also necessary to consider that any biomaterial to be implanted as a scaffold in tissue engineering applications should be biocompatible, non-toxic, and pyrogen-free. The derivatisation procedure employed in this research for the preparation of the alginate-GRGDY matrix was conducted in aseptic conditions. Sterile reagents and autoclaved equipment were used for both the initial coupling

reaction and the subsequent dialysis and lyophilisation cycles. However, this process needs to be further improved with respect to the sterility conditions, and a method involving the least handling of both the reagents and materials used should be developed. The alginate and all of the reactants could be tested for sterility at each stage of the process so that every component and every process step could be tested to see if contamination is introduced. Endotoxins tests, together with polymerase chain reaction (PCR) for mycoplasma screening and detection could be performed for this purpose. This would ensure the preparation of a final alginate-GRGDY product that is sterile and therefore suitable for *in vivo* applications in the clinic.

One of the main drawbacks observed for all alginate-GRGDY samples after completion of the coupling reaction was a significant loss of the tyrosine residue at the end the GRGDY sequence. Furthermore, results obtained from the studies performed on the alginate/cells constructs revealed that both hMSCs and human foreskin fibroblasts failed to adhere to the alginate-GRGDY matrix.

As already mentioned, tyrosine loss might have been responsible for the lack of alginate-cells interactions. In particular, the missing tyrosine may have caused a conformational change in the structure of the remaining peptide associated to the alginate, and this may have ultimately impaired cell attachment. Thus, the loss of tyrosine may be associated with biological inactivity of the alginate-GRGDY matrix.

In order to better elucidate the causes of tyrosine loss more amino acid analysis will need to be performed on alginate samples harvested at different time points during the coupling reaction. This will make it possible to understand why, and at what stage of the reaction the tyrosine loss occurs. Alternatively, two-dimensional or three-dimensional liquid chromatography techniques, using ion exchange and size exclusion chromatography as initial separation techniques and coupled to electrospray ionisation mass spectrometry, could be used. These methods have been previously used to analyse complex peptide mixtures [Langrock *et al.*, 2006]. These techniques would also allow the effective direct measurement of the amino acid levels eliminating the need for the spectrophotometric detection.

Another strategy that could be considered in the future is the utilisation of a different adhesion peptide sequence for the covalent modification of the alginate

polymer, one with a chemical conformation that perhaps could permit better recognition of the RGD ligand and would therefore facilitate the matrix-cells interactions. For instance, for improved cell functionality and viability, NovaMatrix has recently introduced a new peptide-coupled alginate, the Novatach GRGDSP-coupled alginate. This product is particularly indicated to facilitate and promote the scaffold/cells interaction and has therefore major utility in formulations where cell-to-matrix interaction is beneficial [www.novamatrix.biz].

Ultimately, understanding the reason why tyrosine loss was observed during the derivatisation procedure described in this research will probably permit to avoid the occurrence of this phenomenon in future.

## **7.2 human Mesenchymal Stem Cells (hMSCs) characterisation**

One of the great challenges facing mesenchymal stem biology is the development of a simple and reproducible method to identify and recover from bone marrow samples a pure hMSC population [Horwitz, 2002; Sotiropoulou *et al.*, 2005]. Given the heterogeneous composition of the bone marrow stromal microenvironment, it is necessary to remove from the unfractionated bone marrow cell population those accessory cells that do not meet clearly defined “stem criteria” (i.e. long-term self-renewal capacity and the ability to differentiate *in vivo* into specific, multiple cell types) [Wang *et al.*, 1990; McIntyre and Bjornson, 1986]. However, since there is no universal antigenic definition of MSCs and there is no universal assay, the approach to isolation and purification still varies widely from different research groups and investigators [Horwitz, 2002].

The progenitor cells described and investigated in this research have been recovered from bone marrow samples by isolation of the mononuclear fraction of marrow cells through density gradient centrifugation, followed by their tendency to adhere to the plastic surface of the culture vessels, according to the protocol described by Friedenstein and colleagues [Friedenstein *et al.*, 1968]. The resulting heterogeneous cell population comprises several progenitors at different stages of their differentiation pathways. In line with these considerations, it is acknowledged



that future studies are needed to verify and confirm the purity and “stemness” (i.e. self-renewal capacity and multilineage differentiation) of these cells. To this end, several approaches can be followed.

The colony-forming-unit-fibroblast (CFU-F) assay has been used by several groups as indicative of the numbers of marrow-derived stromal cells in test populations [Owen *et al.*, 1987; Perkins and Fleischman, 1990]. However, it is clear that this assay does not, on its own, directly detect self-renewal potential or multilineage capacity [Zandstra and Nagy, 2001].

Although there are no universally accepted antigenic determinants for mesenchymal stem cells [Horwitz *et al.*, 2002] and opinions seem still to differ [De Bari *et al.*, 2006], a series of markers defining the phenotype of mesenchymal stem and progenitor cells have been recently agreed upon [Tyndall *et al.*, 2007]. Mesenchymal stem cells are known to express the antigens CD105 and CD73 reactive respectively with the monoclonal antibodies SH2 and SH3-SH4. These CD antigens have been explored as important antigenic determinants in the identification of these cells [Haynesworth, 1992; Barry *et al.*, 2001]. Pittenger has reported that CD29, CD44 and CD90 are also important determinant [Pittenger *et al.*, 1999], while Gronthos and Simmons described STRO-1 antibody that also seems to identify an immature population of mesenchymal cells [Gronthos *et al.*, 1998; Simmons *et al.*, 1991]. Thus, flow cytometry could be performed for the characterisation of hMSCs by immunophenotyping. As the panel of antibody markers for monitoring the hMSCs profile of antigen expression grows and develops, this technique will result more and more useful for the identification of these cells.

In addition, karyotype analysis, performed to monitor the genetic stability of a cell culture [Rutzky *et al.*, 1980], can be employed to analyse the physical structure of hMSCs genome and visualise their chromosomes. The resulting chromosome mapping would permit to understand whether the cells show significant chromosome abnormalities or, on the contrary, retain a normal karyotype.

Furthermore, differentiation potential assays similar to the one employed in this research should be performed to demonstrate that the cells retain the multilineage potential that is a key attribute of mesenchymal stem cells functionality.

Ultimately, what is probably required is to combine these (and possibly others) assays to better determine the biological properties of hMSCs and to confirm their identity. This measure may facilitate all current efforts to optimise the production of authentic marrow-derived progenitor stem cells that possess the “stem criteria” defined above, and that may therefore demonstrate a real potential for a variety of clinical applications.

### ***7.3 Strategies to be considered for the fabrication of functional alginate/cells constructs***

The results presented in this research showed that both hMSCs and human foreskin fibroblasts were not able to adhere to and elongate within the alginate matrix. The expectation would have been that the cells would have elongated along the pores of the alginate hydrogel containing the GRGDY peptide. It is possible that the pore size of the alginate-GRGDY matrix may have been too small or restrictive. It has in fact been previously suggested that alginate used in the physical form of a hydrogel contains small pore size that does not allow cell movement [Eiselt, 2000].

Zmora and colleagues found that the morphology of rat hepatocytes seeded in macroporous high G alginate scaffolds (pore diameter ranging from  $110\pm30\mu\text{m}$  to  $210\pm80\mu\text{m}$ ) was either elongated or spherical based upon the pore microstructure [Zmora, 2002]. The different pore microstructures were created by freezing the alginate matrix and examining the structure using a scanning electron microscope. The freezing regimen can in fact have a critical effect on the polymer pore microstructure [Lin and Yeh, 2004; Zmora *et al.*, 2002], and the effects of freezing rate on the morphology of scaffolds for tissue engineering applications have been reported in many works [Mohan and Nair, 2005; Kang *et al.*, 1999]. Hydrogels that are used for tissue engineering should have pores within the inter-molecular network large enough to provide sufficient space for cell growth and extracellular matrix production [Kang *et al.*, 1999]. Uniform pore size and distribution are necessary also to permit diffusion of growth factors and nutrients to the surrounding cells and to ensure removal of metabolic wastes from the system [Kuo

and Ma, 2001; Kang *et al.*, 1999]. Thus, the porosity, pore structure and pore size distribution, which are directly related to the scaffold diffusion properties, are particularly important for cell growth and nutrient supply of cells [Melvik and Dornish, 2004; Mohan and Nair, 2005]. Since this issue has not been addressed in this research, the alginate pore size and microstructure could be examined in future studies. Numerous methods and materials have been continuously developed for preparing porous materials for cell scaffolding [Laurencin *et al.*, 1996; Liu and Kodama, 1992; Whang and Healy, 2001]. Interconnecting macroporous scaffolds with >90% porosity can typically be processed from alginate gels under mild conditions using lyophilisation (freeze-drying) [Klock *et al.*, 1997] or carbon-dioxide foaming [Eiselt *et al.*, 2000] techniques [Velema and Kaplan, 2006]. Macroporous alginate beads have for instance been fabricated by incorporating gas pockets within the alginate beads, stabilising the gas bubbles with surfactants such as BSA or Pluronic (F68 or F108), and subsequently removing the gas [Eiselt *et al.*, 2000].

This work also revealed that, after immobilisation within the alginate biopolymer, in several samples the majority of the cells tended to locate on or near the outer surface of the matrix/cells beads. This inhomogeneity was probably caused by the particular gelation process taking place during beads formation. It has in fact been reported that alginate gels formed by diffusion of cross-linking ions into the alginate solution result in a polymer concentration gradient within the gel beads [Melvik and Dornish, 2004; Skjak-Braek *et al.*, 1989; Thu *et al.*, 2000]. However, the gel formation process may be carefully controlled. In particular, bead homogeneity results to be dependent upon the way in which the gelling ions are added in the system. For instance, it has been shown that slower gelation systems generate more uniform and mechanically stronger gels than faster gelation systems [Martinsen *et al.*, 1989; Skjak-Braek *et al.*, 1989] and that slowing the gelation rate can lead to more uniform and mechanically stronger hydrogels [Kuo and Ma, 2001]. Thus, the use of slow-gelling ions systems can be investigated in future studies in order to produce more homogenous alginate/cells beads. A similar approach has already been followed for example by Kuo and colleagues, who reported the fabrication of structurally uniform gels for tissue engineering

applications with the use of calcium carbonate-GDL (D-glucono- $\delta$ -lactone) and calcium carbonate-GDL-calcium sulfate systems [Kuo and Ma, 2001].

Finally, the beads size is an additional parameter that can be taken into consideration when preparing alginate beads in future investigations. The fabrication of smaller diameter constructs offers several advantages, including better transportation of nutrient and oxygen [Chicheportiche and Reach, 1988], and higher mechanical strength [Sugiura S., *et al.*, 2005]. This approach has already been successfully followed in several microencapsulating alginate systems, for which the use of 185  $\mu$ m diameter microcapsules has also given much less severe pericapsular reactions than those induced by standard size microcapsules [Halle' *et al.*, 1994; Robitaille *et al.*, 1999]. A critical diameter of approximately 400-500  $\mu$ m is indeed the preferred device geometry for cell immobilisation from a biocompatibility, functional and technological point of view [Hunkeler, 2001; Orive *et al.*, 2003]. Thus, to ensure both a better nutrient and oxygen supply to encapsulated cells and the fabrication of biocompatible constructs, future studies could investigate novel approaches for the preparation of smaller diameter beads. Alginate constructs as small as 300 $\mu$ m diameter beads for example could be fabricated by use of an electrostatic potential droplet generator. In such a system the beads size can be regulated by the following parameters: the droplet generator needle diameter, the electrostatic potential, the flow-rate of the cell-gel suspension and the distance between the needle and the gelling bath [Orive *et al.*, 2003; Klok and Melvik, 2002]. Thus, by adjusting these parameters in a droplet generator system alginate/cells beads with appropriate size can be fabricated.

## 8. References

- AAIIR –Australian Association for human Research Inc. “Use of fetal calf serum”; [http://www.aahr.asn.au/campaigns/fetal\\_calf\\_serum.html](http://www.aahr.asn.au/campaigns/fetal_calf_serum.html).
- Aebischer P., Goddard M., Tresco P.A. (1993) “Cell encapsulation for the nervous system”, in: “Fundamentals of Animal Cell Encapsulation and Immobilization” (Goosen M.F.A., Ed.), Boca Raton, FL: CRC Press, 197-224.
- Alberts B *et al.*, Molecular Biology of the Cell (Third Edition), Garland Publishing, NY, 1994.
- Allen T.D., Dexter T.M., Simmons P.J. “Marrow biology and stem cells” *Immunol Ser* 1990, 49: 1-38.
- Al-Rubeai M. and Spier R. “Quantitative cytochemical analysis of immobilised hybridoma cells” *Applied Microbiology and Biotechnology*, 1989, 31(4): 430-433.
- Alsberg E., Anderson K.W., Albeiruti A. Franceschi R.T., Mooney D.J. “Cell-interactive alginate hydrogels for bone tissue engineering” *J. Dent. Res.* 2001; 80: 2025-9.
- Alsberg E., Anderson K.W., Albeiruti A., Rowley J.A., Mooney D.J. “Engineering growing tissues” *Proc. Nat. Acad. Sci USA* 2002; 99(19): 12025-12030.
- Amit M, Shariki C, Margulets V, Itskovitz-Eldor “Feeder layer- and serum-free culture of human embryonic stem cells” *Biol. Reprod.*, 2003, 70 (3): 837-845.
- Atala A., Kim W., Paige K.T., Vacanti C.A., Retik A.B. “Endoscopic treatment of vescicoureteral reflux with a chondrocyte-alginate suspension” *J Urol*, 1994, 152: 641-643.
- Atala A. “Tissue engineering and regenerative medicine: concepts for clinical application” *Rejuvenation Research*, 2004, 7 (1): 15-31.
- “Australian Code of Practice for the care and use of animals for scientific purposes” 7<sup>th</sup> edition 2004 (1.8 page 6).
- Award H.A., Boivin G.P., Dressler M.R. *et al.*, “Repair of patellar tendon injuries using a cell-collagen composite” *J Orthop Res* 2003; 21: 420-431.
- Basilico C. and Moscatelli D. “The FGF family of growth factors and oncogenese” *Adv Cancer Res* 59, 115, 1992.
- Barnes D. and Sato G. “Serum-free cell culture: a unifying approach” *Cell*, 1980, 22: 649-655.

Barralet J.E., Wang L., Lawson M., Triffitt J.T., Cooper P.R., Shelton R.M. "Comparison of bone marrow cell growth on 2D and 3D alginate hydrogels" *Journal of Materials Science: Materials in Medicine*, 2005, 16: 515-519.

Barry F., Boynton R., Murphy M., Haynesworth S., Zaia J. "The SH-3 and SH-4 antibodies recognize distinct epitopes on CD73 from human mesenchymal stem cells" *Biochem Biophys Res Commun*, 2001, 289: 519-524.

Bednarz J., Doubilei V., Wollnik P.C.M., Engelmann K. "Effect of three different media on serum free culture of donor corneas and isolated human corneal endothelial cells" *Br. J. Ophthalmol.* 2001, 85: 1416-1420.

Bell E, Ehrlich HP, Buttle DJ, *et al.* "Living tissue formed in vitro and accepted as skin-equivalent tissue of full thickness" *Science*, 1981; 211: 1052-4.

Berthiaume F. "Laboratory in molecular and cellular sciences" Boston: Center for Engineering in Medicine, 1998.

Bianchi G., Muraglia A., Daga A., Corte G., Cancedda R., Quarto R. "Microenvironment and stem properties of bone marrow-derived mesenchymal stem cells" *Wound repair regen* 9, 460, 2001.

Bianchi G., Banfi A., Mastrogiacomo G. *et al.*, "Ex vivo enrichment of mesenchymal cell progenitors by fibroblast growth factor 2" *Exp Cell Res*, 2003; 28: 98-105.

Bianchi G., Banfi A., Mastrogiacomo G. *et al.*, "Ex vivo enrichment of mesenchymal cell progenitors by fibroblast growth factor 2" *Exp Cell Res*, 2003; 28: 98-105.

Bianco P., Riminucci M., Gronthos S., Robey P.G. "Bone marrow stromal stem cells: nature, biology, and potential applications" *Stem Cells*, 2001, 19: 180-192.

Bierman EL, "The effect of donor age on the *in vitro* life span of cultured human arterial smooth-muscle cells" *In vitro*, 1978; 14: 951-955.

Bisceglie V. "Über die antineoplastische Immunität; heterologe Einpflanzung von Tumoren in Hühner-Embryonen" *Ztschr Krebsforsch*, 1933; 40: 122-40.

Bos GW, Poot AA, Geugeling T, van Aken WG, Feijen J "Small-diameter vascular graft prostheses: current status" *Arch. Physiol. Biochem.* 1998; 106: 100-115.

Brittberg M, Lindahl A, Nilsson A, Ohlsson C, Isaksson O and Peterson L "Treatment of deep cartilage defects in the knee with autologous chondrocyte transplantation" *N. Engl. J. Med.* 1994, 331: 889-95.

Bruder S.P., Jaiswal N. and Haynesworth S.E. "Growth kinetics, self-renewal, and the osteogenic potential of purified human mesenchymal stem cells during extensive

subcultivation and following cryopreservation" *Journal of Cellular Biochemistry* 64: 278-294 (1997).

Bujan J., Garcia-Honduvilla N., Manuel Bellon J.M. "Engineering conduits to resemble natural vascular tissue" *Biotechnol. Appl. Biochem.*, 2004; 39: 17-27.

Butler M., "Animal Cell Culture & Technology" Abingdon, UK: Garland Science/BIOS Scientific Publishers, 2004.

Caplan A.I. and Goldberg V.M. "Principles of tissue engineered regeneration of skeletal tissues" *Clin. Orthop.*, 1999, 367(Suppl.): 12-6.

Caplan A.I. "Mesenchymal stem cells and gene therapy" *Clin Orthop* 2000; (379 suppl) S67-S70.

Caplan A.I. "Mesenchymal stem cells" *J Orthop Res.*, 1991, 9: 641-450.

Carrier R.L., Papadaki M., Rupick M., Schoen M., Bursac F.J., Langer R, Freed L.E., Vunjak-Novakovic G. "Cardiac tissue engineering: cell seeding, cultivation parameters and tissue construct characterization" *Biotechnology and Bioengineering*, 1999; 64: 580-589.

Chang S.C.N., Rowley J.A., Tobias G., Genes N.G., Roy A.K., Mooney D.J., Vacanti C.A., Bonassar L.J. "Injection molding of chondrocytes/alginate constructs in the shape of facial implants" *J Biomed Mater Res*, 2001, 55: 503-511.

Chen G., Ushida T., Tateishi T. "Scaffold Design for Tissue Engineering" *Macromolecular Bioscience* 2002; 2 (2): 67-77.

Chicheportiche D. and Reach G. "In vitro kinetics of insulin release by microencapsulated rat islets effect of the size of the microcapsules" *Diabetologia*, 1988, 31: 54-57.

Chick WL, Like AA, Lauris V "Beta cell culture on synthetic capillaries: an artificial endocrine pancreas" *Science*, 1975; 187: 847-9.

Chung T.W., Lu Y.F., Wang S.S., Lin Y.S., Chu S.H. "Growth of human endothelial cells on photochemically grafted Gly-Arg-Gly-Asp (GRGD) chitosans" *Biomaterials*, 2002, 23: 4803-4809.

Ciapetti G., Cenni E., Pratelli L. and Pizzoferrato A. "In vitro evaluation of cell/biomaterial interaction by MTT assay" *Biomaterials* 1993; 14(5): 359-364.

Clark A.H. and Ross-Murphy S.B. "Structural and mechanical properties of biopolymer gels" *Adv. Polymer Sci.*, 1987, 83: 57-192.

Colton C.K. "Engineering challenges in cell-encapsulation technology" *Trends Biotechnol.*, 1996, 14: 158-162.

Constantidinis I., Rask I., Long R.C., Sambanis A. "Effects of alginate composition on the metabolic, secretory and growth characteristics of entrapped  $\beta$ TC3 mouse insulinoma cells" *Biomaterials* 20 (1999) 2019-2027.

Damsky C.H., "Extracellular matrix-integrin interactions in osteoblast function and tissue remodelling" *Bone*, 1999; 25: 95-96.

Dar A., Shachar M., Leor J. Cohen S., "Optimization of cardiac cell seeding and distribution in 3D porous alginate scaffolds" *Biotech. Bioeng.* 80(3) (2002)305-312.

Darling R.C., Linton RR "Durability of femoropopliteal reconstructions. Endarterectomy versus vein bypass grafts" *Am. J. Surg.*, 1972; 123: 472-479.

Darribere T., Skalski M., Cousin H.L., Gaultier A., Montmory C. and Alfandari D. "Integrins: regulators of embryogenesis" *Biol Cell*, 2000; 92: 5-25.

Deasy B.M., Qu-Peterson Z., Greenberger J.S., Huard J. "Mechansims of muscle stem cell expansion with cytokines" *Stem Cells* 20, 50, 2002.

De Bari C., Dell'Accio F., Vanlauwe J., Eyckmans J., Khan I.M., Archer C.W., Jones E.A., McGonagle D., Mitsiadis T.A., Pitzalis C. et al., "Mesenchymal multipotency of adult human periosteal cells demonstrated by single-cell lineage analysis" *Arthritis Rheum*, 2006, 54(1): 1209-1221.

de Camargo Bittencourt R.A., Pereira H.R., Felisbino S.L., Murador P., de Oliveira A.P.E. and Deffune E. "Isolation of bone marrow mesenchymal stem cells" *Acta Ortop. Bras.* 2006; 14 (1): 22-24.

De Kok I., Peter S.J., Archambault M. *et al.*, "Investigation of allogeneic mesenchymal stem cell-based alveolar bone formation: preliminary findings" *Clin Oral Implants Res* 2003; 14: 481-489.

Department of Health and Human Services. Available: <http://www.nih.gov/news/stemcell/scireport.htm>, June 2001.

DiGirolamo C.M., Stokes D., Colter D. *et al.*, "Propagation and senescence of human marrow stromal cells in culture: a simple colony-forming assay identifies samples with the greatest potential to propagate and differentiate" *Br J Haematol*, 1999; 107: 275-281.

Domm C., Schunke M., Steinhagen J., Freitag S. and Kurz B. "Influence of various alginate brands on the redifferentiation of dedifferentiated bovine articular chondrocytes in alginate bead culture under high and low oxygen tension" *Tissue Engineering*, 2004, 10(11/12): 1796-1805.

Doran P.M., "Bioprocess Engineering Principles, Academic Press Ltd. (1995) 262-265, 277-279.

Doumeche, B., Kupperts M., Stapf S., Blumich B., Hartmeier W., Ansorge-Schumacher M.B. "New approaches to the visualization, quantification and



explanation of acid-induced water loss from Ca-alginate hydrogel beads" *Journal of microencapsulation* 21: 5 (2004) 565-73.

Draget K.I., Brae G.S., Smidsrod O. "Alginic acid gels – the effects of alginate chemical-composition and molecular weight" *Carbohydr Polym*, 1994, 25: 31-38.

Draget K.I., Skjak-Braek G., Smidsor O. *Int. J. Biol. Macromol.*, 1997, 21, 47.

Draget K.I., Smidsor O. and Skjak-Braek G. "Alginates from algae" *Polysaccharides and Polyamides in the Food Industry. Properties, Production and Patents*. Edited by A. Steinbuchel and S.K. Rhee, 2005, Wiley VCH Verlag GmbH & Co. KGaA, Weinheim, ISBN: 3-527-31345-1.

Drury J.L. and Mooney D.J. "Hydrogels for tissue engineering: scaffold desing variables and applications" *Biomaterials*, 2003, 24: 4337-3451.

Edelman E.R. "Vascular tissue engineering: designer arteries". *Circ. Res.* 1999; 85: 1115-7.

Eiselt P., Yeh J., Latvala R.K., Shea L.D., Mooney D.J. "Porous carriers for biomedical applications based on alginate hydrogels" *Biomaterials*, 2000, 21: 1921-1927.

Ejim O.S., Blunn G.W., Brown R.A. "Production of artificial-orientated mats and strands from plasma fibronectin: a morphological study" *Biomaterials*, 1993, 14(10): 743-748.

"European Commission focuses on human tissue engineering potential", Brussels, 22 January 2004, IP/04/85.

Even M.S., Sandusky C.B., Barnard N.D. "Serum-free hybridoma culture: ethical, scientific and safety considerations" *Trends in Biotechnology*, 2006, 24(3):105-108.

Ezashi T., Das P. and Roberts M. "Low oxygen tensions and the prevention of differentiation of human Embryonic Stem cells" *Developmental Biology*, 2005; 102(13): 4783-4788.

Fadok V.A. *et al.*, "Exposure of phosphatidylserine on the surface of apoptotic lymphocytes triggers specific recognition and removal by macrophages" *J. Immunol.*, 1992; 148: 2207-2216.

Fahey J.L., Finegold I., Rabson A.S., Manaker R.A. "Immunoglobulin Synthesis in vitro by Established Human Cell Lines" 1966; *Science* 152: 1259-1261.

Falanga V., D. Margolis, O. Alvarez, M. Auletta, F. Maggiasco, M. Altman, J. Jensen, M. Sabolinsky, and J. Hardin-Young 1998, "Rapid healing of venous ulcers and lack of clinical rejection with an allogeneic cultured human skin equivalent" Human Skin Equivalent Investigators Group. *Arch. Dermatol.* 134 (3): 293-300.

Falkner E., Appl H., Eder C., Macfelda K., Losert U., Schoffl H., Pfaller W. "Serum free cell culture media. Updated Product Guide 1/2004", Medical University of Vienna.

Federal Register, November 24, 2004, CFR Parts 16, 1270 and 1271 "Current Good Tissue Practice for Human Cell, Tissue and Cellular and Tissue-Based Product Establishment; Inspection and Enforcement; Final Rule".

Ferrera R., Larese A., Berthod F., Guidollet J., Rodriguez C., Dureau G. and Dittmar A. "Quantitative reduction of MTT by hearts biopsies in vitro is an index of viability" *Journal of Molecular and Cellular Cardiology* 25: 9 (1993), 1091-1099.

Fibbe W.E. "Mesenchymal stem cells. A potential source for skeletal repair" *Ann. Rheum. Dis.* 61, (Suppl.II) ii29-ii31, 2002.

Fink T., Abildtrup L., Fogd K., Abdallah B.M., Kassem M. *et al.*, "Induction of adipocyte-like phenotype in human mesenchymal stem cells in hypoxia" *Stem Cells* 2004, 22: 1346-1355.

Fremont B., Malandain C., Guyomard C., Chesne C., Guillouzo A., Campion J.-P. "Correction of bilirubin conjugation in the gunn rat using hepatocytes immobilized in alginate gel beads as an extracorporeal bioartificial liver" *Cell Transplant*, 1993, 2: 453-460.

Fried A., Shamay A., Wientroub S., Benayahu D. "Phenotypic expression of marrow cells when grown on various substrata" *J Cell Biochem*, 1996; 61 (2): 246-54.

Friedenstein A.J.P.S. and Petrakova K.V.. "Osteogenesis in transplants of bone marrow cells" *J. Embryol. Explor. Morph.* 1966, 16: 381-390.

Friedenstein A.J., Chailakhyan R.K., Gerasimov U.V., *Cell Tissue Kinet.*, 1987, 20: 263.

Friedenstein A.J., Petrakova K.V., Kurolesova A.I. & Frolova G.P. "Heterotopic of bone marrow. Analysis of precursor cells for osteogenic and hematopoietic tissues" *Transplantation*, 1968; 6: 230-247.

Furcht L.T., Verfaillie C.M. and Reyes M. "Multipotent adult stem cells and methods for isolation" United States Patent, August 2005. United States Athersys, Inc. 20050181502. Available at:  
<http://www.freepatentsonline.com/20060030041.html>.

Gallico G.G., O'Connor N.E., Compton C.C., Kehinde O., Green H. "Permanent coverage of large burn wounds with autologous cultured human epithelium" *N. Engl. J. Med.* 311: 7 (1984) 448-451.

Glicklis R., Shapiro L., Agbaria R., Merchuk J.C., Cohen S. "Hepatocyte behavior within three-dimensional porous alginate scaffolds" *Biotech. Bioeng.* 2000; 67: 344-53.

Gooch KJ, Blunk T, Vunjak-Novakovic G, Langer R, Freed LE "Mechanical forces and growth factors utilized in tissue engineering" *Frontiers in tissue engineering*, Edited by Patrick CW, Mikos AG, and McIntire LV, 1998; 68-75.

Gotherstrom C., Ringden O., Westgren M., Tammik C. and Le Blanc K "Immunomodulatory effects of human foetal liver-derived mesenchymal stem cells" *Bone Marrow Transplantation* 2003; 32: 265-272.

Grant J.L. and Smith B., "Bone marrow gas tensions, bone marrow blood flow, and erythropoiesis in man" *Ann Intern Med* 1963; 58: 801-9.

Grant G.T. *et al.*, "Biological interactions between polysaccharides and divalent cations: the egg-box model" *FEBS Lett.*, 1973, 32: 195-198.

Grasdalen H. B., Larsen B., O. Smidsrod « A p.m.r. study of the composition and sequence of uronate residues in alginates » *Carbohydr. Res.* 1979 ; 68 : 23-31.

Greene K.G., Burg K.J.L., Austin C.E., Culberson C.R., Halberstadt C.R., Holder W.D., Morton D.S., Loesback A.B. "The development of a seeding method for a porous hydrogel construct" Proceedings of the Sixth World Biomaterials Congress, 2000.

Greenwald SE, Berry CL "Improving vascular grafts: the importance of mechanical and haemodynamic properties" *J. Pathol.*, 2000; 190: 292-299.

Grigoryan R., Keshelava N., Anderson C., Reynolds P. "In vitro testing of chemosensitivity in physiological hypoxia" from Methods in Molecular Medicine, 2005, Vol. 110, Chemosensitivity, Vol. 1: *In vitro* assays, edited by R.D. Blumenthal Humana Press Inc, Totowa, NJ.

Gronthos S. and Simmons P.J. "The growth factor requirements of STRO-1-positive human bone marrow stromal precursors under serum-deprived conditions *in vitro*" *Blood*, 1995, vol.85, no.4, pp.929-940.

Gronthos S. and Simmons P.J. "The biology and application of human bone marrow stromal cell precursors" *J. Hematother.* 1996; 5: 15-23.

Gronthos S., Simmons P.J., Graves S.E., Robey P.G. "Integrin-mediated interactions between human bone marrow stromal precursor cells and the extracellular matrix" *Bone*, 2001; 28 (2): 14-81.

Gronthos S., Zannettino A.C., Hay S.J. *et al.* "Molecular and cellular characterization of highly purified stromal stem cells derived from human bone marrow" *J. Cell Sci.* 2003; 116: 1827-1835.

Gronthos S., Graves S.E., Simmons P.J. "Isolation, purification and in vitro manipulation of human bone marrow stromal precursor cells" In: Beresford, J N. and Owen M.E., Eds. Marrow stromal cell culture. UK: Cambridge University Press, 1998, 26-42.

- Guettier C. "Which stem cells for adult liver?" *Ann. Pathol.* 2005; 25: 33-34.
- Halberstadt C., Austin C., Rowley J., Culberson C., Loeb sack A., Wyatt S., Coleman S., Blacksten L., Burg K., Mooney D., Holder W. "A hydrogel material for plastic and reconstructive applications injected into the subcutaneous space of a sheep" *Tissue Eng.*, 2002, 8(2): 309-319.
- Halle' J.P., Leblond F.A., Pariseau J.F., Jutras P., Brabant M.J., Lepage Y. "Studies on small (<300 microns) microcapsules: II parameters governing the production of alginate beads by high voltage electrostatic pulses" *Cell Transplant*, 1994, 3: 365-372.
- Ham R.G. and McKeehan W.L. "Media and growth requirements" *Methods in Enzymol.* 1979; 58: 44-93.
- Hankemeier S., Keus M., Zeichen J., Jagodzinski M., Barkhausen T., Bosch U., Krettek C. and Van Griensven M. "Modulation of proliferation and differentiation of human bone marrow stromal cells by fibroblast growth factor 2: potential implications for tissue engineering of tendons and ligaments" *Tissue Engineering* 2005, 11(1/2): 41.
- Hansen J.T. 'Netter's Atlas of Human Physiology' and Jain R.K. 'Molecular regulation of vessel maturation' (Nature Medicine, 2003).
- Hanss J. and Moore G.E. "Studies of culture media for the growth of human tumour cells" *Exp. Cell Res.* 1964, 24: 243-256.
- Harrison J.S., Rameshwar P., Chang V., Bandari P., 2002 "Oxygen saturation in the bone marrow of healthy volunteers" *Blood* 99:394.
- Haug A., Larsen B., Smidsrod O. « A study of the constitution of alginic acid by partial acid hydrolysis » *Acta. Chem. Scand.*, 1966 ; 20 : 183-190.
- Hauselmann H.J., Fernandes R.J., Mok S.S., Schmid T.M., Block J.A., Aydelotte M.B., Kuettner K.E., Thonar E.J.M.A. "Phenotypic stability of bovine articular chondrocytes after long-term culture in alginate beads" *Journal of Cell Science* 107 (1994) 17-27.
- Hauselmann H.J., Masumd K., Hunziker E.B., Neidhart M., Mok S.S., Michel B.A., Thonar E.J.-M.A. "Adult human chondrocytes cultured in alginate form a matrix similar to native human articular cartilage" *Am J Physiol*, 1996, 271: C742-C752.
- Haynesworth S.E., Baber, M.A., Caplan A.I. "Cell surface antigens on human marrow-derived mesenchymal stem cells are detected by monoclonal antibodies" *Bone*, 1992, 13: 69-80.
- Haynesworth S.E., Goshima J., Goldberg V.M., & Caplan A.I. "Characterization of cells with osteogenic potential from human marrow" 1992; *Bone*, 13: 81-88.

Heissig B., Ohki Y., Sato Y. et al "A role for niches in hematopoietic cell development" *Hematology*, 2005; 10: 247-253.

Hodgson J. *Bio/Technology* 1991, 9: 1320-1324.

Hogan, B., Beddington R., Costantini F., Lacy E. "Manipulating the mouse embryo: A laboratory manual" (second edition). 1994: Cold Spring Harbor Laboratory Press.

Hori Y., Inoue S., Hirani Y. *et al.*, "Effect of culture substrates and fibroblast growth factor addition on the proliferation and differentiation of rat bone marrow stromal cells" *Tissue Eng.*, 2004; 10: 995-1005.

Hortelano G., Stockley T. "Implantable microcapsules for gene therapy for hemophilia" In: Kuhtreiber W.M., Lanza R.P., Chick W.L. editors. "Cell encapsulation technology and therapeutics" Boston, MA: Birkhauser, 1999, p. 321-9.

Horwitz EM, Keating A "Nonhematopoietic mesenchymal stem cells: what are they?" *Cytotherapy* 2000; 2: 387-8.

Horwitz et al "Clarification of the nomenclature for MSC: the international society for cellular therapy position statement" *Cytotherapy* (2005) Vol.7, No.5, 393-395.

Horwitz E.M. "Mesenchymal Cells Information Summary; Mesenchymal Cells: A Basic Review" ISCT Nonhematopoietic and Mesenchymal Stem Cell Committee, May 2002.

Hung S.-C., Pochampally R.R., Hsu S.-C., Sanchez X., Chen S.-C., Spees J. and Prockop D.J. "Short-term exposure of multipotent stromal cells to low oxygen increases their expression of CX3CR1 and CXCR4 and their engraftment in vivo" 2007, doi:10.1371/journal.pone.0000416.g002.

Hunkeler D. "Allo transplant xeno: as bioartificial organs move to the clinic" In: Bioartificial organs III: Tissue sourcing, immunoisolation and clinical trials" *Annals of New York Academy of Sciences*, 2001, p.1-6.

Huveneers-Oorsprong M.B.M., Hoogenboom L.A.P., Kuiper H.A., "The use of the MTT test for determining the cytotoxicity of veterinary drugs in pig hepatocytes" *Toxicology in Vitro* 1997; 11: 385-392.

Hynes RO, *Ann. Rev. Cell. Biol.* 1, 67, 1985.

<http://ustransplant.org>, 2002.

[http://www.aahr.asn.au/campaigns/fetal\\_calf\\_serum.html](http://www.aahr.asn.au/campaigns/fetal_calf_serum.html)

<http://www.cellgro.com> Mediatech, Inc. Cell Culture Reference Guide.

Jager M. *et al.* "Influence of different culture solutions on osteoblastic differentiation in cord blood and bone marrow derived progenitor cells" *Biomed Tech (Berl)* 2003; 48 (9): 241-244.

Jiang Y., Jahagirdar B.N., Reinhardt R.L. *et al.*, "Pluripotency of mesenchymal stem cells" *Science* 1999; 284: 143-147.

Jiang Y., Jahagirdar B.N., Reinhardt R.L., Schwartz R.E., Keene C.D., Ortiz-Gonzalez X.R., Reyes M., Lenvik T., Lund T., Blackstad M., Du J., Aldrich S., Lisberg A., Low W.C., Largaespada D.A. and Verfaillie CM "Pluripotency of mesenchymal stem cells derived from adult marrow" *Nature*, 2002; 418: 41-49.

Johnson F.A., Craig D.Q.M., Mercer A.D. "Characterisation of the block structure and molecular weight of sodium alginates" *J. Pharm. Pharmacol.* 1997; 49: 639-643.

JRCE - Joint Research Centre European Commission "Human tissue-engineered products –Today's markets and future prospects", October 2003.

Kadner A, Hoerstrup S, Zund G, Eit K, Maurus C, Melnitchouk S, Grunenfelder J, Turina M "A new source for cardiovascular tissue engineering: human bone marrow stromal cells" *Eur. J. Cardio-thorac. Surg.* 21(6): 1055-1060, 2002.

Kang H.-W., Tabata Y. and Ikada Y. "Fabrication of porous gelatin scaffolds for tissue engineering" *Biomaterials*, 1999, 20: 1339-1344.

Kerr J.F.R. *et al.* "Apoptosis: a basic biological phenomenon with wide-ranging implications in tissue kinetics" *Br. J. Cancer*, 1972; 26: 139-157.

Keshaw H., Forbes A., Day R.M. "Release of angiogenic growth factors from cells encapsulated in alginate beads with bioactive glass" *Biomaterials*, 2004, 26(19): 4171-4179.

Khan S., O'Brien P.J. "Modulating hypoxia-induced hepatocyte injury by affecting intracellular redox state" *Biochim Biophys Acta*, 1995, 1269(2):153-61.

Khattak S., Chin K.-S., Bhatia S., Roberts S.C. "Enhancing oxygen tension and cellular function in alginate cell encapsulation devices through the use of perfluorocarbons" *Biotechnology and Bioengineering*, 2006, 96(1): 156-166.

Khattak S., Spataro M., Roberts L., Roberts S. "Application of colorimetric assays to assess viability, growth and metabolism of hydrogel-encapsulated cells" *Biotechnology Letters*, 2006, 28(17): 1361-1370(10).

Klock G., Pfeffermann A., Ryser C., Grohn P., Kuttler B., Hahn H.-J., Zimmermann U. "Biocompatibility of mannuronic acid-rich alginate" *Biomaterials*, 1997, 18: 707-713.

Klokk T.I. and Melvik J.E. "Controlling the size of alginate gel beads by use of a high electrostatic potential" *Journal of Microencapsulation*, 2002, 19(4): 415-424.

Kong H.J., Smith M., Mooney D.J. "Designing alginate hydrogels to maintain viability of immobilized cells" *Biomaterials*, 2003, 24(22): 4023-9.

Kong H.J., Alsberg E., Kaigler D., Lee K.Y. and Mooney D.J. "Controlling degradation of hydrogels via the size of cross-linked junctions" *Advanced Materials*, 2004a, 16(21): 1917-1921.

Kong H.J., Kaigler D., Kim K., Mooney D.J. "Controlling rigidity and degradation of alginate hydrogels via molecular weight distribution" *Biomacromolecules*, 2004b, 5: 1720-1727.

Kotobuki N., Hirose M., Takakura Y *et al.*, "Cultured anutologous human cells for hard tissue regeneration: preparation and characterization of mesenchymal stem cells from bone marrow" *Artif Organs*, 2004; 28: 33-39.

Kozik A, Bradbury EM, Zalensky A, "Increased telomere size in sperm cells of mammals with long terminal (TTAGGG) in arrays". *Mol. Reprod. Dev.* 1998; 51, 98-104.

Kuo C.K. and Ma P.X. "Ionically cross-linked alginate hydrogels as scaffolds for tissue engineering: Part 1. Structure, gelation rate and mechanical properties" *Biomaterials*, 2001, 22: 511-521.

Kuo C. and Tuan R.S. "Tissue engineering with mesenchymal stem cells" *Engineering in medicine and biology magazine IEEE*, 2003; 22 (5): 51-56.

Kuznetsov SA *et al.* *J. Bone Miner. Res.* 12, 1335 (1997).

Kuznestov SA, Mahesh H, Robey PG "Effect of serum on human bone marrow stromal cells: *ex vivo* expansion and in vivo bone formation" *Transplantation* 2000, vol.70, no.12: 1780-1787.

Ishiwaka Y. and Ito T., "Kinetics of hemopoietic stem cells in a hypoxic culture" *Eur. J. Haematol.* 1998; 40(2): 126-9.

Lalan S., Pomerantseva I., Vanati J.P. "Tissue engineering and its potential impact on surgery" *World J. Surg.*, 2001, 25: 1458-1466.

Lambert K.J. and Birch J.R. "Animal Cell Biotechnology" 1: 85, 1985.

Langer R, Vacanti JP "Tissue engineering" *Science*, 1993; 260: 920-26

Langrock T., Czihal P., Hoffmann R. "Amino acid analysis by hydrophilic interaction chromatography coupled on-line to electrospray ionisation mass spectrometry", *Amino Acids*, 2006, 30: 291-297.

Laning J.C., J.E. De Luca and J. Hardin-Young, 1999. "Effects of immunoregulatory cytokines on the immunogenic potential of the cellular components of a bilayered living skin equivalent" *Tissue Engineering* 5 (2): 171-181.

Laurencin C.T., El Amin S.F., Ibim S.E., Willoughby D.A., Attawia M., Allcock H.R., Amrbois A.A. "A highly porous three-dimensional polyphosphazene polymer matrix for skeletal tissue regeneration" *J Biomed Mater Res*, 1996, 30(2): 133-8.

Lawson M.A., Barralet J.E., Wang L., Shelton R.M., Triffitt J.T. "Adhesion and growth of bone marrow stromal cells on modified alginate hydrogels" *Tissue Engineering*, 2004, 10(9-10): 1480-91.

Lee G.M., Han B.K., Kim J.H., Palsson B.O. "Effect of calcium chloride treatment on hybridoma cell viability and growth" *Biotechnology Letters*, 1992, 14(10): 891-896.

Lee G.M., Kim S.G. and Palsson B.O., "Enhanced specific antibody productivity of calcium alginate-entrapped hybridoma cell line-specific" *Cytotechnology*, 1994, 16(1): 1-15.

Lee H.S., Huang G.T., Chiang H., Chiou L.L., Chen M.H., Hsieh C.H., Jiang C.C. "Multipotential mesenchymal stem cells from femoral bone marrow near the site of osteonecrosis" *Stem Cells* 2003; 21: 190-9.

Lee K.Y. and Mooney D.J. "Hydrogels for tissue engineering" *Chem. Rev.* 2001; 101: 1860-77.

Lemare F., Steinberg N., LeGriel C., Demignot S., Adolphe M. "Dedifferentiated chondrocytes cultured in alginate beads: restoration of the differentiated phenotype and of the metabolic responses to interleukin-1 $\beta$ " *J. Cell. Physiol.*, 1998, 176: 303-13.

Lennon D.P., Edmison J. M. and Caplan A. I. "Cultivation of rat marrow-derived mesenchymal stem cells in reduced oxygen tension: effects on in vitro and in vivo chondrogenesis" *Journal of Cellular Physiology* 187: 345-355 (2001).

Leo W.J., McLoughlin A.J., Malone D.M. "Effects of sterilization treatments on some properties of alginate solutions and gels" *Biotechnology Progress*, 1990, 6(1): 51-53.

L'Heureux N, Paquet S, Labbe R, Germain L, Auger FA "A completely biological tissue-engineered human blood vessel" *FASEB J* 1998; 12: 47-56.

L'Heureux N. *et al.*, "Human tissue-engineered blood vessels for adult arterial revascularization" *Nat Med*, 2006, 12: 361-365.

L'Heureux N., Dusserre N., Marini A., Garrido S., de la Fuente L. and McAllister T. "Technology insight: the evolution of tissue-engineered vascular grafts – from research to clinical practice" *Nature Clinical Practice, Cardiovascular Medicine*, 2007, 4 (7): 389-395.

Lichtman M.A. "The ultrastructure of the hematopoietic environment of the marrow: a review" *Exp Hematol* 1981, 9: 391-410.



Lin H.-R. and Yeh Y.-J. "Porous alginate/hydroxyapatite composite scaffolds for bone tissue engineering: Preparation, characterization, and *in vitro* studies" *Journal of Biomedical Materials Research Part B: Applied Biomaterials*, 2004, 71B (1): 52-65.

Lindvall O., Kokaia Z., Martinez-Serrano A. "Stem cell therapy for human neurodegenerative disorders – how to make it work" *Nat. Med.* 2004; 10: S42-S50.

Liu S.Q., Kodama M. "Porous polyurethane vascular prostheses with variable compliances" *J Biomed Mater Res*, 1992, 26: 1489-502.

Livingston T., Kadiyali S., Elkalay M. *et al.*, "Repair of canine segmental bone defects using allogeneic mesenchymal stem cells" Transactions of the 47<sup>th</sup> Annual ORS meeting 2001; 26-49

Locklin R.M., Oreffo R.O., Triffitt J.T. "Effects of TGF $\beta$  and bFGF on the differentiation of human bone marrow stromal fibroblasts" *Cell Biol Int* 23, 185, 1999.

Loebbeck, A., Greene, K., Wyatt S., Culberson C., Austin C., Beiler R., Roland W., Eiselt P., Rowley J., Burg K., Mooney D., Holder W., Halberstadt C. "In vivo characterisation of a porous hydrogel material for use as a tissue bulking agent" *J Biomed Mater Res*, 2001, 57 (4): 575-581.

Lysaght MJ and Reyes J "The Growth of Tissue Engineering" *Tissue Engineering*; 2001; 7(5), 485-493.

Lysaght M.J. and Hazlehurst A.L., "Tissue Engineering: The End of the Beginning" *Tissue Engineering*, 2004; 10(1/2), 309-320.

Ma H.L., Hung S.C., Lin S.Y., Chen Y.L., Lo W.H. "Chondrogenesis of human mesenchymal stem cells encapsulated in alginate beads" *Journal of Biomedical Materials Research*, 64A (2003) 273-281.

Ma T., Yang S.T. and Kniss D.A. "Oxygen tension influences proliferation and differentiation in a tissue-engineered model of placental trophoblast-like cells" *Tissue Eng*, 7: 495-506, 2001.

Mackay A.M., Beck S.C., Murphy J.M., Barry F.P., Chichester C.O., Pittenger M.F. "Chondrogenic differentiation of cultured human mesenchymal stem cells from marrow" *Tissue Eng.*, 1998, 4: 415-428.

Mackie W. Perez S., Rizzo R. Taravel F., Vignon M. "Aspects of the conformation of polyguluronate in the solid state and in solution" *Int. J. Biol. Macromol.*, 1980, 5: 329-341.

Magnusson M.K. and Mosher D.F. "Fibronectin. Structure, assembly and cardiovascular implications" *Arterioscler Thromb Vasc Bio.* 1998; 18: 1363-1370.

Mahler S., Desille M., Fremond B., Chesne C., Guillouzo A., Campion J.-P., Clement B. "Hypothermic storage and cryopreservation of hepatocytes: the protective effect of alginate gel against cell damages" *Cell Transplantation*, 2003, 12(6): 579-592(14).

Majors A.E., Muschler G.F. "Basic FGF enhances proliferation and reversibly inhibits differentiation of osteoblastic progenitors" *Trans. Orth. Res. Soc.* 1996, 21:113.

Majumdar MK, Thiede MA, Mosca JD *et al* "Phenotypic and functional comparison of cultures of marrow-derived mesenchymal stem cells (MSC) and stromal cells", *J. Cell Physiol.*, 1998; 176: 57-66.

Malladi P., Xu Y., Chiou M., Giaccia A.J., Longaker M.T. "Effect of reduced oxygen tension on chondrogenesis and osteogenesis in adipose-derived mesenchymal cells" *Am J Physiol Cell Physiol*, 2005, 290: C1139-C1146.

Marler J.J., Guha A., Rowley J., Koka R., Mooney D., Upton J., Vacanti J.P. "Soft-tissue augmentation with injectable alginate and synergetic fibroblasts" *Plast Reconstr Surg*, 2000, 105: 2049-58.

Markusen J.F., « Growth and characterization of cells used to design a tissue engineered blood vessel » Thesis submitted for the degree of Doctor of Philosophy in Biochemical Engineering, The Advanced Centre for Biochemical Engineering, Department of Biochemical Engineering, University College London, June 2005.

Markusen J.F., Mason C., Hull D. A., Town M.A., Tabor A.B., Clements M., Boshoff C.H. and Dunnill P. "Behaviour of adult human mesenchymal stem cells entrapped in alginate-GRGDY beads" *Tissue Engineering* 2006; 12 (4): 821-830.

Marler J.J., Guha A., Rowley J., Koka R., Mooney D., Upton J., Vacanti J.P. "Soft-tissue augmentation with injectable alginate and syngeneic fibroblasts" *Plast. Reconst. Surg.* 2000; 105: 2049-58.

Martin J.A., Klingelhutz A.J., Moussavi-Harami F. and Buckwalter J.A. "Effects of oxidative damage and telomerase activity on human articular cartilage chondrocyte senescence" *Journal of Gerontology: Biological Sciences* 59A: 324-337 (2004).

Martin I., Muraglia A., Campanile G. *et al.*, "Fibroblast growth factor-2 supports ex vivo expansion and maintenance of osteogenic precursors from human bone marrow" *Endocrinology*, 1997; 138: 4456-4462.

Martin J.A., Klingelhutz A.J., Moussavi-Harami F. and Buckwalter J.A. "Effects of oxidative damage and telomerase activity on human articular cartilage chondrocyte senescence" *Journal of Gerontology: Biological Sciences* 59A: 324-337 (2004).

Martinsen A, Skjak-Braek G, Smidsrod O "Alginate as immobilization material: correlation between chemical and physical properties of alginate gel beads" *Biotech. Bioeng.* 1989, 33 (1): 79-89.

Mason C. "Tissue Engineering" *Biotechnology Investment Today*, 2003a; 2(1), 20-27.

Mason C. "Automated Tissue Engineering: A Major Paradigm Shift in Health Care" *Medical Device Technology*, 2003b; 14, 16-18.

Matsubara T., Tstutsumi S., Pan H., Hiraoka H., Oda R., Nishimura M., Kawaguchi H., Nakamura K. and Kato Y. "A new technique to expand human mesenchymal stem cells using basement membrane extracellular matrix" *Biocehmical and Biophysical Research Communications* 2004, 313: 503-508.

Matsumura G, Miyagawa-Tomita S, Shin'oka T, Ikada Y, Kurosawa H "First evidence that bone marrow cells contribute to the construction of tissue-engineered vascular autografts *in vivo*", *Circulation*, 2003a; 108: 1729-1734.

Matsumura G, Hibino N, Ikada Y, Kurosawa H, Shinoka T "Successful application of tissue engineered vascular autografts: clinical experience", *Biomaterials*, 2003b; 24: 2303-2308.

Mattinger C, Nyugen T, Schafer D, Hormann K "Evaluation of serum-free culture conditions for primary human nasal epithelial cells" *International Journal of Hygiene and Environmental Health*, 2002, vol.205, no.3, pp. 235-238.

Mazurier F, Doedens M, Gan OI and Dick JE "Rapid myeloerythroid repopulation after intrafemoral transplantation of NOD-SCID mice reveals a new class of human stem cells" *Nature Medicine*, 2003; 9: 959-963.

McKee J.A., Banik S.S.R., Boyer M.J., Hamad N.M., Lawson J.H., Niklason L.E. and Counter C.M. "Human arteries engineered *in vitro*" European Molecular Biology Organization (EMBO) Reports, 2003, 4(6): 633-638.

McIntire L.V., Greisler H.P., Griffith L, Johnson P.C., Mooney D.J., MrKsich M., Parentau N.L., and Smith D. "World Technology-WTEC Panel Report on Tissue Engineering", January 2002.

McIntyre A.P. and Bjornson B.H. "Human bone marrow cell colonies: response to hydrocortisone and dependence on platelet-derived growth factor" *Exp Hematol* 14: 833, 1986.

Meirelles L.S., Nardi N.B. "Murine marrow-derived mesenchymal stem cell: isolation, in vitro expansion, and characterization" *BR J Hematol* 2003; 123: 702-11.

Melvik J.E., Kristensen A.H., Dornish M. and Skaugrud O. "Key characterization parameters of alginate for use in biomedical and pharmaceutical applications" Promova Biomedical, Gaustadalleen 21, 0371 Oslo, Norway.

Melvik J.E. and Dornish M. "Alginate as a carrier for cell immobilisation" Book Chapter: "Fundamentals of cell immobilisation Biotechnology", 2004, ISBN 1-4020-1887-8, 33-51; Mohan and Nair, 2005.

Menaschè P, Scorsin M, Hagege A *et al.* "Myoblast transplantation for heart failure" *Lancet* 2001; 357: 279-80.

Merten O.W. "Safety issues of animal products used in serum free media. In: Animal Sera, Animal Sera Derivatives and Substitutes Used in the Manufacture of Pharmaceuticals: Viral Safety and Regulatory Aspects (1999) Editors: Brown F., Cartwright T., Horaud F., Spieser J.M., Developments in Biological Standardization 99, Karger.

Meuleman N., Tondreau T., Delforge A., Dejeneffe M., Massy M., Libertalis M., Bron D., Lagneaux L. "Human marrow mesenchymal stem cell culture: serum-free medium allows better expansion than classical  $\alpha$ -MEM medium" *Eur J Haematol.* 2006; 76: 309-316.

Milnor W.R. (1990) Cardiovascular Physiology, Oxford University Press, Oxford, UK.

Mimeault M. and Batra S.K. "Recent advances on the significance of stem cells in tissue regeneration and cancer therapies" *Stem Cells*, 2006: DOI: 10.1634/stemcell.2006-006.

Minguell J.J., Erices A. And Conget P. "Minireview: mesenchymal stem cells" *Exp. Biol. Med.* 226 (6): 507-520, 2001.

Mohan N. and Nair P.D. "Novel porous, polysaccharide scaffolds for tissue engineering applications" *Trends Biomater. Artif. Organs*, 2005, 28(2): 219-224.

Mooney D.J. and Mikos A.G. "Growing new organs" *Scientific American*, 1997; 10-15.

Mooney D.J., Bouhadir K.H., Wong W.K. and Rowley J.A. "Polymers containing polysaccharides such as alginates or modified alginates" United States Patent, November 4, 2003. Available at: <http://www.freepatentsonline.com/6642363.html>.

Morris C.B. and Warburton S. "Serum-screening and selection" *Cell & Tissue Culture: Laboratory Procedures* (Doyle A., Griffiths J.B., Newell D.G., eds) pp.2B: 1.1-1.5, Wiley; Honn *et al.*, 1975.

Mosahebi A., Simon M., Wiberg M., Terenghi G. "A novel use of alginate hydrogel as Schwann cell matrix" *Tissue Eng.* 2001; 7: 525-34.

Mosmann T. "Rapid colorimetric assay for cellular growth and survival: application to proliferation and cytotoxicity assays" *Journal of Immunological Methods* 1983; 65: 55-63.

Moussavi-Harami F, Duwayri Y, Martin JA, Moussavi-Harami F, Buckwalter J "Oxygen effects on senescence in chondrocytes and mesenchymal stem cells: consequences for tissue engineering" *The Iowa Orthopaedic Journal* 2004; 24: 15-20.

Mulder L. "Cell adhesion on alginate scaffolds for tissue engineering of an aortic valve - a review" Report BMTE 02.40, October 2002.

Mullen Y., Maruyama M., Smith C.V. "Current progress and perspectives in islet transplantation" *Journal of Hepato-Biliary-Pancreatic Surgery*, 2000, 7: 347-357.

Muraglia A., Cancedda R., Quarto R. "Clonal mesenchymal progenitors from human bone marrow differentiate in vitro according to a hierarchical model" *J. Cell Sci.* 2000; 113: 1161-1166.

Murphy J.M., Fink D.J., Hunziker E.B. *et al.*, "Stem cell therapy in a caprine model of osteoarthritis" *Arthritis Rheum* 2003; 48: 3464-3474.

Muschler GF, Midura RJ, and Nakamoto C. "Practical Modeling Concepts for Connective Tissue Stem Cell and Progenitor Compartment Kinetics", *J. Biomed. Biotech.*, 2003, 3: 170-193.

Muschler G.F., Midura R.J. "Connective tissue progenitors: practical concepts for clinical applications" *Clin. Orthop.* 2002, 395: 66-80.

Nagai H., Tsukuda R. Yamasaki H. *et al.*, "Systemic injection of FGF-2 stimulates endocortical bone modelling in SAMP6, a murine model of low turnover osteopenia" *J Vet Med Sci* 1999, 61: 869-875.

Nasseri B.A., Ogawa K. Vacanti J.P. "Tissue engineering: an evolving 21<sup>st</sup> century science to provide biologic replacement for reconstruction and transplantation" *Surgery*, 2001; 130(5), 781-784.

Naughton G. "From Lab Bench To Market. Critical Issues in Tissue Engineering" *Annals of the New York Academy of Sciences*, 2002; 961, 372-385.

Nerem R.M. "Tissue engineering a blood vessel substitute: the role of biomechanics" *Yonsei Med. J.* 41: 6 (2000) 735-739.

Nerem R.M. "Critical issues in vascular tissue engineering" International Congress Series 1262 (2004), 122-125.

Niklason L.E. "Replacement arteries made to order" *Science*, 1999, 286: 1493-1494.

Niklason LE, Gao J, Abbott WM, *et al.* "Functional arteries grown in vitro" *Science* 1999; 284: 489-93.

Noishiki Y, Tomizawa Y, Yamane Y. *et al* "Autocrine angiogenic vascular prosthesis with bone marrow transplantation" *Nat. Med.* 1996; 2: 90-93.

Nugent H.M. and Edelman E. R. "Tissue engineering therapy for cardiovascular disease" *Circulation Research*, 2003; 92: 1068-1078.

Ogura N., Kawada M., Chang W.-J., Lee S.-Y., Kondoh T., Abiko Y. "Differentiation of the human mesenchymal stem cells derived from bone marrow and enhancement of cell attachment by fibronectin" *Journal of Oral Science*, 2004; 46 (4): 207-213.

Oreffo RO, Virdi AS, Triffitt JT "Modulation of osteogenesis and adipogenesis by human serum in human bone marrow cultures" *Eur. J. Cell Biol.* 1997, 74 (3): 251-61.

Orlic D, Kajstura J, Chimenti S, Jakoniuk I, Andersen SM, Li B, Pickel J, McKay R, Nadal-Ginard B, Bodine DM, Leri A, Anversa P "Bone marrow cells regenerate infarcted myocardium" *Nature*, 2001; 410: 701-705.

Orive G., Hernandez R.M., Gascon A.R., Igartua M., Pedraz J.L. "Survival of different cell lines in alginate-agarose microcapsules" *Eur J Pharm Sci*, 2003, 18, p.23-30.

Oswald J, Boxberger S, Jorgensen B, Feldmann S, Ehninger G, Bornhauser M, Werner C. "Mesenchymal stem cells can be differentiated into endothelial cells *in vitro*", *Stem Cells*, 2004; 22: 377-384.

Owen M.E., Cave J., Joyner C.J. "Clonal analysis in vitro of osteogenetic differentiation of marrow CFU-F" *J Cell Science*, 87: 731, 1987.

Ozturk S.S., Thrift J.C., Blackie I.D., Naveh D. "Real-time monitoring and control of glucose and lactate concentration in a mammalian cell perfusion reactor" *Biotech. Bioeng.*, 1997, 53 (4): 372-378.

Palsson B. and Bhatia S., "Tissue Engineering", 2004; Upper Saddle River, New Jersey 07458.

Pangarkar N., Huttmacher D.W., and Huttmacher D.W. "Invention and Business Performance in the Tissue Engineering Industry" *Tissue Engineering*, 2003; 9(6), 1313-1322.

Park J.B. and Lakes R.S. "Biomaterials: and introduction, 2<sup>nd</sup> ed. New York; Plenum Press; 1992.

Park J.K., Chang H.N. "Microencapsulation of microbial cells" *Biotechnol. Adv.*, 2000, 18: 303-19.

Parrinello S, Samper E, Krtolica A, Goldstein J, Melov S, Campisi J "Oxygen sensitivity severely limits the replicative lifespan of murine fibroblasts" *Nat. Cell. Biol.* 2003 Aug; 5 (8): 741-747.

Patterson M.K. « Measurement of growth and viability of cells in culture » *Methods Enzymol.*, 1979, 58: 141-152.

Pedersen RA, "Embryonic stem cells for medicine" *Sci. Am.*, 1997; 18-23.

Pei Y, Ma j, Zhang X, Ji W "Serum-free culture of rhesus monkey embryonic stem cells" *Archives of Andrology*, 2003, vol.49, no.5, pp. 331-342.

Peirone M., Ross C.J.D., Hortelano G., Brash J.L., Chang P.L. "Encapsulation of various recombinant mammalian cell types in different alginate microcapsules" *Journal of Biomedical Materials Research*, 1998, 42(4): 587-596.

Penman A., Sanderson G.R. "A method for the determination of uronic acid sequence in alginates" *Carbohydr. Res.*, 1972; 25: 273-282.

Pereira R.F., Halford K.W., O'Hara M.D. et al., "Cultured adherent cells from marrow can serve as long-lasting precursor cells for bone, cartilage, and lung in irradiated mice" *Proc. Natl. Acad. Sci. USA*, 1995, 92: 4857-4861.

Perkins S., Fleischman R.A. "Stromal cell progeny of murine bone marrow fibroblast colony-forming units are clonal endothelial-like cells that express collagen IV and laminin" *Blood*, 75: 620, 1990.

Pevec WC, Darling RC, L'Italien GJ, Abbott WM, "Femoropopliteal reconstruction with knitted, nonvelour Dacron versus expanded polytetrafluoroethylene" *J. Vasc. Surg.* 1992; 16: 60-65.

Phinney D.G., Kopen G., Righter W. et al. "Donor variation in the growth properties and osteogenic potential of human marrow stromal cells" *J Cell Biochem* 1999; 75:424-436.

Pitaru S., Kotev-Emeth S., Noff D., Kaffuler S., Savion N. "Effect of basic fibroblast growth factor on the growth and differentiation of adult stromal bone marrow cells: Enhanced development of mineralized bone-like tissue in culture" *J. Bone Miner. Res.* 1993, 8: 919-929.

Pittenger M.F., Mackay A.M., Beck S.C., Jaiswal R.K., Douglas R., Mosca J.D., Moorman M.A., Simoneti D.W., Craig S and Marshak D.R. "Multilineage potential of adult human mesenchymal stem cells" *Science*, 1999; 284: 143-7.

Prajapati R.T., Al-Ani S., Smith P.J., Brown R.A. "Fibronectin mats assessed in an *in vitro* model for keratinocyte grafting" *Cellular Engineering*, 1996, 1: 143-149.

Prokop A. and Wang T.G. "Purification of polymers used for fabrication of an immunoisolation barrier" *Annals New York Academy of Sciences*, 1997, 223-231.

Prockop D.J., Sekiya I & Colter D.C. "Isolation and characterization of rapidly self-renewing stem cells from cultures of human marrow stromal cells" *Cytherapy* 2001; 3: 393-396.

Qian L. and Saltzman W.M. "Improving the expansion and neuronal differentiation of mesenchymal stem cells through culture surface modification" *Biomaterials*, 2004; 25: 1331-1337.

Quarto R., Muraglia A., Corsi A. *et al.*, "Cultured bone marrow stromal cells: from bench to the clinic" *Tissue Eng.*, 1998, 4: 473.

Read T.A., Stensvaag V., Vindenes H., Ulvestad E., Bjerkvig R., Thorsen F. "Cells encapsulated in alginate: a potential system for delivery of recombinant proteins to malignant brain tumors" *International Journal of Developmental Neuroscience*, 1999, 6: 653-663.

Read T.A., Sorensen D.R., Mahesparan R., Enger P., Timpl R., Olsen B.R., Hjelstuen M.H.B. Haraldseth O., Bjerkvig P. "Local endostatin Treatment of gliomas administered by micro-encapsulated producer cells" *Nature Biotechnology*, 2001, 19: 29-39.

Reyes M., and Verfaillie C.M. "Turning marrow into brain: generation of glial and neuronal cells from adult bone marrow mesenchymal stem cells" *Blood*, 1999; 94 (suppl 1): 3a.

Reyes M., Lund T., Lenvik T. *et al.*, "Purification and ex vivo expansion of postnatal human marrow mesodermal progenitor cells" *Blood*, 2001; 98: 2615-25.

Riha *et al.*, "Applications of stem cells for vascular tissue engineering" *Tissue Engineering*, Volume 11, Number 9/10, 1535-1552, 2005.

Riley M.R., Muzzio F.J., Reyes S.C., "Experimental and modeling studies of diffusion in immobilized cell systems" *Applied Biochemistry and Biotechnology*, 1999, 80(2): 151-188.

Robertson E.J., "Teratocarcinomas and embryonic stem cells: a practical approach" ed. IRL Press at Oxford University Press, 1987.

Robitaille R., Pariseau J.F., Leblond F.A., Lamoreux M., Lepage Y., Halle J.P. "Studies on small (<350 micron) alginate-poly-L-lysine microcapsules. III Biocompatibility of smaller versus standard microcapsules" *J Biomed Mater Res*, 1999, 44: 116-120.

Rocheffort G.Y., Delorme B., Lopez A., Herault O., Bonnet P., Charbord P., Eder V. and Domenech J. "Multipotential mesenchymal stem cells are mobilized into peripheral blood by hypoxia" *Stem Cells*, 2006, doi:10.1634/stemcells.2006-0164.

Rokstad A.M., Donati I., Borgnagna M., Oberholzer J., Strand B.L., Espevik T., Skiak-Braek G. "Cell-compatible covalently reinforced beads obtained from a chemoenzymatically engineered alginate" 2005, *Biomaterials*, 27(27): 4726-4737.

Romanov Y.A., Svintsitskaya V.A., Smirnov V.N. "Searching for alternative sources of postnatal human mesenchymal stem cells: candidate MSC-like cells from umbilical cord" *Stem Cells*, 2003; 21: 105-10.

Rowley J. A., Madlambayan G., Mooney D.J. "Alginate hydrogels as synthetic extracellular matrix materials" *Biomaterials* 1999; 20: 45-53.



Rowley J.A. and Mooney D.J. "Alginate type and RGD density control myoblast phenotype" *J. Biomed. Mater. Res.* 2002; 60: 217-223.

Ruoslahti E. and Pierschbacher, M.D., *Cell*, 1986, 44, 517.

Ruoslahti E, "Fibronectin and its receptors" *Ann. Rev. Biochem.* 57, 375, 1988.

Ruoslahti E. and Pierschbacher M.D. "New perspectives in cell adhesion: RGD and integrins" *Science*, 1987, vol. 238, 491-497.

Ruoslahti E. "RGD and other recognition sequences for integrins" *Annu. Rev. Cell Dev. Biol.*, 12: 697-715, 1996.

Rutzky C.P., Kaye C.J., Siciliano C., Kahan B.D. "Longitudinal karyotype and genetic signature analysis of cultures human colon adenocarcinoma cell lines LS180 and LS174T" *Can. Res.*, 1980, 40: 1443-1448.

Salim A., Nacamuli R.P., Morgan E.F., Giaccia A.J. and Longaker M.T. "Transient changes in oxygen tension inhibit osteogenic differentiation and Runx2 expression in osteoblasts" *J Biol Chem* 2004, 279: 40007-40016.

Saltzman W.M. "Cell interactions with polymers" In: *Principles of Tissue Engineering*, Second Edition, Lanza R., Langer R., Vacanti J. editors, Academic Press (2000) 221-235.

Sarraf, Harris, McCulloch and Eastwood "Tissue engineering of biological cardiovascular system surrogates", *Heart Lung Circ.* 2002; 11: 142-150.

Sato, (1975) in *Biochemical Actions of Hormones*, G. Litwack (ed.) Academic Press, New York, Vol.3, pp.391-396.

Savion N., Pri-Chen S., Pitaru S. "bFGF enhances the growth and the expression of osteogenic phenotype of dexamethasone treated human bone marrow derived bone-like cells in culture" *J. Bone Miner. Res.* 1996, 11:S347.

Scherping S.C. Jr., Schmidt C.C., Georgescu H.I., Kwoh C.K., Evans C.H., Woo S.L. "Effect of growth factors on the proliferation of ligament fibroblasts from skeletally mature rabbits" *Connect Tissue Res* 36, 1, 1997.

Schnell A.M., Hoerstrup S.P., Zund G., Kolb S., Sodian R., Visjager J.F., Grunenfelder J., Suter A. and Turina M. "Optimal cell source for tissue engineering: venous vs aortic human myofibroblasts" *Thoracic and Cardiovascular Surgeon*, 2001, 49, 221-225.

Schwinger C.; Koch S.; Jahnz U.; Wittlich P.; Rainov N. G.; Kressler J. "High throughput encapsulation of murine fibroblasts in alginate using the JetCutter technology" *Journal of Microencapsulation*, 2002, 19(3): 273-280(8).

Scott J.E. "Oxygen and the connective tissues trends" *Biochem. Sci.* 1992; 17: 340-343.

Sekiya I., Larson B.L., Smith J.R., Pochampally R., Cui J.-G., Prockop D.J. "Expansion of Human Adult Stem Cells from Bone Marrow Stroma: Conditions that Maximize the Yields of Early Progenitors and Evaluate Their Quality" *Stem Cells* 2002;20:530-541.

Sethi K.K., Yannas I.V., Mudera V., Eastwood M., McFarland C., Brown R.A. "Evidence for sequential utilization of fibronectin, vitronectin, and collagen during fibroblast-mediated collagen contraction" *Wound Repair and Regeneration*, 2002, 10(6): 397-408.

Shah, G. "Why do we still use serum in the production of biopharmaceuticals?" *Dev. Biol. Stand.*, 1995, 99: 17-22.

Shahdadfar A., Fronsdal K., Haug T., Reinholt F.P., Brinckmann J.E. "In vitro expansion of human mesenchymal stem cells: choice of serum is a determinant of cell proliferation, differentiation, gene expression and transcriptome stability" *Stem Cells* 2005; 23: 1357-1366.

Shin'oka T. *et al.*, "Transplantation of a tissue-engineered pulmonary artery" *N Engl J Med*, 2001, 344: 532-533.

Shin'oka T. *et al.*, "Midterm clinical result of tissue-engineered vascular autografts seeded with autologous bone marrow cells" *J Thorac Cardiovasc Surg*, 2005, 129: 1330-1338.

Simmons P.J., and Torok-Storb B. "Identification of stromal cell precursors in human bone marrow by a novel monoclonal antibody, STRO-1", *Blood*, 1991, 78: 55-62.

Skjak-Braek, Murano E. and Paoletti S. "Alginate as immobilization material. II: Determination of polyphenol contaminants by fluorescence spectroscopy, and evaluation of methods for their removal" *Biotech. Bioeng.*, 1987, 33 (1): 90-94.

Skjak-Braek G., Grasdalen H. and Smidsrod O. "Inhomogeneous polysaccharide ionic gels" *Carbohydr. Res.* 1989, 10(1): 31-54.

Skjak-Braek G., Grasdalen H., Draget K.I. and Smidsrod O. "Inhomogeneous calcium alginate beads" In: *Biomedical and Biotechnological Advances in Industrial Polysaccharides* (Crescenzi V., Dea I.C.M., Paoletti S., Stivala S.S., Sutherland I.W. Eds.), New York: Gordon and Breach, 1989, 345-363.

Smentana K., "Cell biology of hydrogels" *Biomaterials* 1993; 14: 1046-50.

Smidsrod O. and Haug A., "Properties of poly(1,4hexuronates) in the gel state II. Comparison of gels of different chemical composition" *Acta Chemica Scandinavica*, 1972, 26: 79-88.

Smidsrod O. "Molecular basis for some physical properties of alginates in the gel state" *Faraday discussions on the Chemical Society*, 1974, 57: 263-274.

Smidsrod O and Skjak-Braek G. "Alginate as immobilization matrix for cells" *Trends Biotech.* 1990; 8: 71-8.

Solchaga L.A., Penick K., Porter J.D. *et al.*, "FGF-2 enhances the mitotic and chondrogenic potentials of human adult bone marrow-derived mesenchymal stem cells" *J Cell Physiol*, 2005; 203: 398-409.

Soon-Shiong P., Fedelman E., Nelson R., Heints R., Yao Q., Yao T., Zheng N., Merideth G., Skjak-Braek G., Espevik T., Smidsrod O., Sandford P. (1993) "Long-term reversal of diabetes by the injection of immunoprotected islets" *Proc. Natl. Acad. Sci. USA* 90, 5843-5847.

Soon-Shiong P., Heintz R.E., Merideth N, Yao Q.X., Yao Z.W., Zheng T.L., Murphy M., Moloney M.K., Schmehl M., Harris M., Mendez R., Mendez R., Sandford P.A. (1994) "Insulin independence in a type 1 diabetic patient after encapsulated islet transplantation" *Lancet* 343, 950-951.

Soria B, Roche E, Bernà G, Leon-Quinto T, Reig JA, Martin F "Insulin-secreting cells derived from embryonic stem cells normalize glycemia in streptozotocin induced diabetic mice" *Diabetes* 2000; 49: 157-162.

Sotiropoulou P., Perez S., Salagianni M., Baxevanis C., Papamichail M. "Characterization of the optimal culture conditions for clinical scale production of human mesenchymal stem cells", *Stem Cells*, 2006, 24: 462-471.

Sotiropoulou P.A., Perez S.A., Salagianni M., Baxevanis C.N., Papamichail M. "Cell culture medium composition and translational adult bone marrow-derived stem cell research" *Stem Cells Express*, 2006, doi:10.1634/stemcells.2005-0654.

Spiekermann P., Vorlop K.D., Klein J., *Proc. 4<sup>th</sup> European Congress on Biotechnology*, 1987, 3: 590-593.

Stabler C.L., Sambanis A., Constantidinis I. "Effects of alginate composition on the growth and overall metabolic activity of  $\beta$ TC3 cells" *Annals of the New York Academy of Sciences*, 2002, 961: 103-133.

Stock U.A. and Vacanti J.P. "Tissue engineering: current state and prospects" *Annu. Rev. Med.*, 2001, 52: 443-451.

Stone A. "FDA Issues Felled Advanced Tissue Sciences" *Genetic Engineering News*, 2003; 23(11), 25-28.

Sugiura S., Oda T., Izumida Y., Aoyagi Y., Satake M., Ochiai A., Ohkohchi N. and Nakajima M. "Size control of calcium alginate beads containing living cells using micro-nozzle array" *Biomaterials*, 2005, 26(16): 3327-3331.

Sutherland I.W. "Alginates" In: Byrom. D. (Ed) *Biomaterials; Novel materials from biological sources* Macmillan, New York, 1991, Chapter 7, 309-331.

Syrota A. and Jehenson P. "complementarity of magnetic resonance spectroscopy, positron emission tomography and single photon emission tomography for the in vivo investigation of human cardiac metabolism and neurotransmission" *Eur J Nucl Med*, 1991, 18(11): 897-923.

Takahashi T, Kalka C, Masuda H. et al "Ischemia- and cytokine-induced mobilization of bone marrow-derived endothelial progenitor cells for neovascularization" *Nat. Med.* 1999; 5: 434-438.

Tavassoli M., Friedenstein A. "Hematopoietic stromal microenvironment" *Am J Hematol* 1983, 15: 195-203.

Teebken O.E. and Haverich A. "Tissue engineering of small diameter vascular grafts" *European Journal of Vascular and Endovascular Surgery* 23 (2002) 475-485.

Tie L. "As organ shortage grows, hospitals spar and people die waiting", *Globe Staff*, 3/13/2001, *The Boston Globe*; Health/Science.

TIME Magazine, May 22, 2000.

Thomson A.W. 1991, *The Cytokine Handbook*, Academic Press, London.

Thomson, J.A., Kalishman, J., Golos, T.G., Durning, M., Harris, C.P., Becker, R.A., and Hearn, J.P. "Isolation of a primate embryonic stem cell line" *Proc. Natl. Acad. Sci.* 1995; U. S. A. 92, 7844-7848.

Thomson R.C., Wake M.C., Yaszemski M. J., Mikos A.G. "Biodegradable polymer scaffolds to regenerate organs" *Adv. Polym. Sci.* 1995; 122: 245-74.

Thu B., Gaserod O., Paus D., Mikkelsen A., Skjak-Braek G., Toffanin R., Vittur F. and Rizzo R. "Inhomogeneous alginate gel spheres: an assessment of the polymer gradients by synchrotron radiation-induced X-ray emission, magnetic resonance microimaging, and mathematical modeling" *Biopolymers*, 2000, 53: 60-71.

Tobias C.A., Dhoot N.O., Wheatley M.A., Tessler A., Murray M., Fischer I. "Grafting of encapsulated BDNF-producing fibroblasts into the injured spinal cord without immune suppression in adult rats" *Journal of Neurotrauma*, 2001, 18(3): 287-301.

Trivedi N., Keegan M., Steil G.M., Hollister-Lock J., Hasenkamp W.M., Colton C.K., Bonner-Weir S., Weir G.C. "Islets in alginate macrobeads reverse diabetes despite minimal acute insulin secretory responses" *Transplantation*, 2001, 71: 203-1.

Tsutsumi S., Shimazu A., Miyazaki K., Pan H., Koike C., Yoshida E., Takagishi K. and Kato Y. "Retention of multilineage differentiation potential of mesenchymal stem cells during proliferation in response to FGF" *Biochem Biophys Res Commun*, 2001, 288 (2): 413-9.

Tuan R.S., Boland G. and Tuli R. "Adult mesenchymal stem cells and cell-based tissue engineering" *Arthritis Research and Therapy*, 2002, 5 (1): 32-45.

Tyndall A., Walker U.A., Cope A., Dazzi F., De Bari C., Fibbe W., Guiducci S., Jones S., Jorgensen C., Le Blanc K., Luyten F., McGonagle D., Martin I., Bocelli-Tyndall C., Pennesi G., Pistoia V., Pitzalis C., Uccelli A., Wulffraat N., Feldmann M. "Immunomodulatory properties of mesenchymal stem cells: a review based on an interdisciplinary meeting held at the Kennedy Institute of Rheumatology Division, London, UK, 31 October 2005" Meeting Report, *Arthritis Research & Therapy*, 2007, 9:301.

Ueng, S.W.N.; Lee S.-S.; Lin S.-S.; Chan E.-C.; Hsu B.R.-S.; Chen K.-T. "Biodegradable Alginate Antibiotic Beads" *Clinical Orthopaedics & Related Research*, 2000, 380:250-259.

Uludag H., P. De Vos, and P.A. Tresco, 2000. "Technology of mammalian cell encapsulation" *Advanced Drug Delivery Reviews* 42 (1-2): 29-64.

UNOS, 2001: "Critical Data: U.S. Facts about Organ Transplantation" UNOS. Online. Internet. 2 May 2001.

UNOS, 2002, Annual Report US Scientific Registry of Transplant Recipients and the Organ Procurement and Transplantation Network: Transplant data 1992-2001 Rockville, MD and Richmond, VA: HHS/HRSA/OSP/DOT.

Vacanti J. "Tissue Engineering: current state and prospects" *Annu. Rev. Med.* 2001, 52: 443-51.

van den Bos C., Mosca J.D., Winkles J. *et al.*, "Human mesenchymal stem cells respond to fibroblast growth factors" *Hum. Cell*, 1997; 10: 45-50.

Vandenbossche G.M.R. and Remon J.P. "Influence of the sterilization process on alginate dispersions" *The Journal of Pharmacy and Pharmacology*, 1993, 45(5): 484-486.

van Engeland M. *et al.* "A novel assay to measure loss of plasma membrane asymmetry during apoptosis of adherent cells in culture" *Cytometry*, 1996; 24: 131-139.

van Heerde W.L. *et al.* "The complexity of the phospholipid binding protein Annexin V" *Thrombosis and Haemostasis*, 1995; 73: 172-179.

Vats A, Tolley NS, Polka JM, Buttery LDK "Stem cells: sources and applications" *Clin. Otolaryngol.* Vol 27, pp. 227-232, 2002.

Veckeneer M., van Overdam K., Monzer J., Kobuch K., van Marle W., Spekrijse H. and van Meurs J. "Ocular toxicity study of trypan blue injected into the vitreous cavity of rabbit eyes" *Graefes. Arch. Clin. Exp. Ophthalmol.* 2001, 239: 698-704.

Velema J. and Kaplan D. "Biopolymer-based biomaterials as scaffolds for tissue engineering" *Adv Biochem Engin/Biotechnol*, 2006, 102: 187-238.

Wakitani S., Saito T., Caplan A.I. "Myogenic cells derived from rat bone marrow mesenchymal stem cells exposed to 5-azacytidine " *Muscle Nerve* 1995; 18: 1417-1426.

Wakitani S., Yamamoto T. "Response of the donor and recipient cells in mesenchymal cell transplantation to cartilage defect" *Microsc Res Tech* 2002; 58: 14-18.

Wang L., Shelton R.M., Cooper P.R., Lawson M., Triffitt J.T., Barralet J.E. "Evaluation of sodium alginate for bone marrow cell tissue engineering", *Biomaterials*, 2003, 24: 3475-3481.

Wang Z.-Y., Zhang Q.Z., Konno M. and Saito S. "Sol-gel transition of alginate solution by the addition of various divalent cations: <sup>13</sup>C-NMR spectroscopy study" *Biopolymers*, 1993, 33: 703-711.

Wang Q.-R., Yan Z.-J. and Wolf N.S. "Dissecting the hematopoietic microenvironment" VI. The effects of several growth factors on the *in vitro* growth of murine bone marrow CFU-F" *Exp Hematol*, 1990, 18: 341.

Wang L., Shelton R.M., Cooper P.R., Lawson M., Triffitt J.T., Barralet J.E. "Evaluation of sodium alginate for bone marrow cell tissue engineering", *Biomaterials*, 2003, 24: 3475-3481.

Wang D., Williams C.G., Li Q., Sharma B., Elisseeff J.H. "Synthesis and characterisation of a novel degradable phosphate-containing hydrogel" *Biomaterials*, 2003, 24: 3969-3980.

Wang D.W., Fermor B., Gimble J.M., Awad H.A., Guilak F. "Influence of oxygen on the proliferation and metabolism of adipose derived adult stem cells" *J Cell Physiol.*, 2005, 204: 184-191.

Weber M., Steinert A., Jork A., Dimmler A., Thurmer F., Schutze N., Hendrich C., Zimmermann U. "Formation of cartilage matrix proteins by BMP-transfected murine mesenchymal stem cells encapsulated in a novel class of alginates" *Biomaterials*, 2002, 23: 2003-2013.

Weinberg CB, Bell E "A blood vessel model constructed from collagen and cultured vascular cells" *Science* 1986; 231: 397-400.

West J.L. and Hubbell J.A. "Bioactive polymers" In: Atala A, Mooney D.J., editors: Langer R., Vacanti, J.P., associate editors, Synthetic biodegradable polymer scaffolds. Boston: Birkhauser: 1997. p.83-95.

Wang K. and Healy K.E. "Processing of polymer scaffolds: freeze-drying" In: Methods of tissue engineering (Ed. A. Atala & R.P. Lanza), 2001, pp. 697-704, San Diego, CA: Academic Press.

White S.A., James R.F.L., Swift S.M., Kimber R.M., Nicholson M.L. "Human islet cell transplantation: future prospects" *Diabet. Med.* 2001; 18: 78-103.

Whitworth I.H., Brown R.A., Dore C., Green C.J. Terenghi G. "Orientated mats of fibronectin as a conduit material for use in peripheral nerve repair" *J Hand Surg* (British and European Vol.), 1995, 20B, 4: 429-436.

Widersoe H. and Danielsen S. "Evaluation of the use of  $\text{Sr}^{2+}$  in alginate immobilisation of cells" *Naturwissenschaften*, 2001, 88: 224-228.

Wilkins LM, Watson SR, Prosky SJ, Meunier SF and Parenteau NL "Development of a bilayering skin construct for clinical applications" *Biotechnol. Bioeng.* 1994; 43: 747-756.

Wishart D.S. "Metabolomics in Humans and Other Mammals" in *Metabolomics: Quantitative and Qualitative Analysis of Metabolites* (Editors: Silas Vilas-Boas) John Wiley & Sons, New York, 2006.

Wohlpert D., Gainer J., Kirwan D. 1991, "Oxygen uptake by entrapped hybridoma cells", *Biotechnology Bioengineering*, 37(11): 1050-1053.

Wong W.H. and Mooney D.J. "synthesis and properties of biodegradable polymers used as synthetic matrices for tissue engineering" In: Atala A, Mooney D.J., editors; Langer R., Vacanti J.P., associate editors. "Synthetic biodegradable polymer scaffolds" Boston: Birkhauser: 1997, p.51-82.

Wong M., Siegrist M., Wang X. and Hunziker E. "Development of mechanically stable alginate/chondrocyte constructs: effects of guluronic acid content and matrix synthesis" *Journal of Orthopaedic Research*, 2001, 19: 493-499.

Woodbury D., Schwarz E.J., Prockop D.J. *et al.*, "Adult rat and human bone marrow stromal cells differentiate into neurons" *J Neurosci Res* 2000; 61: 364-370.

[www.altabioscience.bham.ac.uk/services/amacid/](http://www.altabioscience.bham.ac.uk/services/amacid/)

[www.americanheart.org](http://www.americanheart.org) Noteworthy numbers from the 2002 statistical update.

[www.cybercolloids.net/library/alginate/structure.php](http://www.cybercolloids.net/library/alginate/structure.php)

[www.fao.org/docrep/W6355E/w6355e04.htm](http://www.fao.org/docrep/W6355E/w6355e04.htm)

[www.focusonalternatives.org.uk](http://www.focusonalternatives.org.uk)

[www.lsbu.ac.uk/water/hyalg.html](http://www.lsbu.ac.uk/water/hyalg.html)

[www.novamatrix.biz](http://www.novamatrix.biz)

[www.unos.org](http://www.unos.org). 2000 Annual Report of the US Scientific Registry for Transplant Recipients and the Organ Procurement and Transplantation Network: Transplantation Data: 1990-1999. US Department of Health and Human Services, Health Resources and Services Administration, Office of Special Programs, Division of Transplantation, Rockville, MD; United Network for Organ Sharing, Richmond, VA.

[www.yahoo.com](http://www.yahoo.com), October 10, 2002, Advanced Tissue Sciences files for Chapter 11.

Wyllie A.H. "Apoptosis" *Br. J. Cancer*, 1993; 67: 205-208.

Yamamoto N, Isobe M, Negishi A, Yoshimasu H, Shimokawa H, Ohya K, Amagasa T, Kasugai S "Effects of autologous serum on osteoblastic differentiation in human bone marrow cells" *J Med. Dent. Sci.* 2003, 50: 63-69.

Yang, L., Korom S., Welti M., Hoerstrup S.P., Zund G., Jung F.J., Neuenschwander P., Weder W. "Tissue engineered cartilage generated from human trachea using DegraPol scaffold" *European Journal of Cardio-Thoracic Surgery*, 2003, 24: 201-207.

Yannas I.V., Burke J.F., Gordon P.L., *et al.* "Design of an artificial skin. II. Control of chemical composition" *J. Biomed. Mater. Res.*, 1980; 14: 107-32.

Yarden Y. and Ulrich A. 1988 *Annu. Rev. Biochem.* 57; 443-478.

Young J.H., Teumer J., Kemp P.D., Parentau N.L., "Approaches to transplanting engineered cells and tissues" *Principals of Tissue Engineering* Lanza R.P., Langer R., and Chick W.L., editors R.G. Lander Company, Austin TX (1997) 301-304.

Zandstra P.W. and Nagy A. "Stem cell bioengineering" *Annu. Rev. Biomed. Eng.* 2001; 3: 275-305.

Zhang X., Wang W., Xie Y., Zhang Y. "Proliferation, viability and metabolism of human tumor and normal cells cultured in microcapsule" *Applied Biochemistry and Biotechnology*, 2006, 134(1): 61-76.

Zimmermann U., Thurmer F., Jork A., Weber M., Mimietz S., Hillgartner M., Brunnenmeier F., Zimmermann H., Westphal I., Fuhr G., Noth U., Haase A., Steinert A., Hendrich C., "A novel class of amitogenic alginate micorcapsules for long-term immunoisolated transplantation" *Annals of the New York Academy of Sciences* 944 (2001) 199-215.

Zmora S., Glicklis R., Cohen S. "Tailoring the pore architecture in 3D alginate scaffolds by controlling the freezing regime during fabrication" *Biomaterials*, 2002, 23: 4087-4094.

Zund G., Ye Q., Hoerstrup S.P., Schoeberlein A., Schmid A.C., Grunenfelder J., Vogt P. and Turina M. "Tissue engineering in cardiovascular surgery: MTT, a rapid and reliable quantitative method to assess the optimal human cell seeding on polymeric meshes" *European Journal of Cardio-thoracic Surgery* 1999; 15: 519-524.

Zoro B. "Automated biorprocessing of mammalian cells for tissue engineering and cell therapies" Thesis submitted for the degree of Doctor of Engineering, The Advanced Centre for Biochemical Engineering, Department of Biochemical Engineering, University College London, 2005.